

# UC Santa Barbara

## UC Santa Barbara Electronic Theses and Dissertations

### Title

Complexities in crossing membrane barriers: new members of the CdiA and CDI ionophore protein families reveal novel mechanisms for receptor-binding and intoxication of target cells

### Permalink

<https://escholarship.org/uc/item/2d73d052>

### Author

Halvorsen, Tiffany Marie

### Publication Date

2020

Peer reviewed|Thesis/dissertation

University of California  
Santa Barbara

**Complexities in crossing membrane barriers: new members of the CdiA and CDI ionophore protein families reveal novel mechanisms for receptor-binding and intoxication of target cells**

A dissertation submitted in partial satisfaction  
of the requirements for the degree

Doctor of Philosophy  
in  
Biochemistry/Molecular Biology

by

Tiffany Marie Halvorsen

Committee in charge:

Professor Christopher S. Hayes, Chair  
Professor David A. Low  
Professor Kathy Foltz

December 2020

The Dissertation of Tiffany Marie Halvorsen is approved.

---

Professor David A. Low

---

Professor Kathy Foltz

---

Professor Christopher S. Hayes, Committee Chair

December 2020

Complexities in crossing membrane barriers: new members of the CdiA and CDI  
ionophore protein families reveal novel mechanisms for receptor-binding and  
intoxication of target cells

Copyright © 2020

by

Tiffany Marie Halvorsen

For Ida.

## Acknowledgements

This journey was a roller coaster that I only stayed on because of the incredible people that have helped me through it. As they say, your friends are the family you choose for yourself. As such, Santa Barbara will always be a warm place of comfort in my memories. Ben, thank you so much for encouraging me to even be here. You always believed in me more than I did myself. Thank you Lauren, Stephanie, Chelsea, Izzy, Amanda, and Gabi for being the most supportive, incredible friends. Sean, thank you for helping me to change my perspective when it was most necessary to do so. Nicole, I am so grateful to have been able to receive your friendship and support. You were here when it got the hardest and I will always be grateful for that. Kiho - though we may have been a very small cohort (haha) we were indeed a strong one! It was not by chance that we ended up in the same group. You are one of the kindest people I know. Thank you for all of the constant reminders that, in the end, it is all simply OK. :) Thank you Julia, Zach, Docty, Sonya, and Greg for providing constant mentorship while I worked in the lab. Julia - your FNS presentation really drew me in to this research, and I have you to thank for helping me find my niche in this field; you continue to inspire me. Greg - you were always incredibly helpful to talk to about science problems and Chapter 4 would be nonexistent without your brainstorming expertise. You are one of the smartest people I know. Not to mention, you rock at fixing things, and also suggesting better ways of doing, well, mostly everything. Thank you! Allison - thank you for being an encouragement to me these past several years, and for becoming a part of the toxin project! It wouldn't have happened without your help. Quan and Steven, thank you so much for being my lab family up until the very end! I wish you all the very best in your endeavors. Your companionship during this degree made it seem so much more possible. I hope we can re-unite for a celebration soon.

I am so grateful for the committee that I chose. Kathy, you are one of the kindest people I have ever met. My decision to come to UCSB was in part made from the inspiring conversation we had before I even applied to the PhD program here. David, your very authentic enthusiasm for understanding the world around you, and using that information to make the world a better place has been a truly impactful inspiration. I am so happy to have had the honor of working on my PhD with your insightful guidance. Sanna (and the rest of the lab!), coming to Sweden was such an opportunity for growth and a chance to learn more than I would have otherwise – thank you for inviting me into your group and making me feel like a part of the family. With your help, Chapter 4 became a story.

Chris, I walk away from this experience so grateful for your constant guidance during the process of growing into a molecular biologist. Your experimental approach has taught me more than I could have imagined, and your attention to detail has certainly left me a better scientist. I hope that I can emulate this in my career. Thank you for your dedication to the completion of these projects, and for the very helpful and consistent mentorship you have given me.

To my family - I know it's difficult to understand what I've even been through, but thank you for always being there for me through what probably seemed like an unending process.

# Curriculum Vitæ

Tiffany Marie Halvorsen

## Education

- 2020 **Ph.D. in Biochemistry and Molecular Biology** (Expected), University of California, Santa Barbara.
- 2019 **M.S. in Biochemistry and Molecular Biology**, University of California, Santa Barbara.
- 2014 **B.S in Biology**, Chemistry minor, *summa cum laude*, Northern Arizona University, Flagstaff, AZ.

## Research

- 2014 - 2020 **Graduate Student Researcher**, Department of Molecular, Cellular and Developmental Biology, University of California, Santa Barbara
- 2018 **Visiting Researcher**, Uppsala University, Department of Cell and Molecular Biology, Uppsala, Sweden
- 2016 **Participant**, Advanced Bacterial Genetics, Cold Spring Harbor Laboratory, Cold Spring Harbor, New York
- 2015 **Participant**, Water, Ice, and the Origin of Life in the Universe, NASA Astrobiology Institute, Reykjavik, Iceland
- 2012 - 2014 **Undergraduate Student Researcher**, Department of Biological Sciences, Northern Arizona University, Flagstaff, AZ
- 2011 **Wildlife Biology Intern**, Grand Canyon National Park, AZ

## Teaching

- 2020 **Teaching Assistant**, Eukaryotic Molecular Genetics, Department of Molecular, Cellular and Developmental Biology, University of California, Santa Barbara
- 2014-2020 **Teaching Assistant**, General Microbiology, Department of Molecular, Cellular and Developmental Biology, University of California, Santa Barbara
- 2019 **STEM Teaching Assistant**, Research Mentorship Program (RMP), Office of Summer Sessions, University of California, Santa Barbara



## Mentorship

- 2019 **Graduate Research Mentor**, *Contact-dependent growth inhibition in the opportunistic pathogen Klebsiella aerogenes*. Department of Molecular, Cellular and Developmental Biology, University of California, Santa Barbara
- 2019 **Undergraduate Research Mentor**, *Characterization of two new members of the CDI ionophore family*. Department of Molecular, Cellular and Developmental Biology, University of California, Santa Barbara
- 2017 **Undergraduate Research Mentor**, *O-antigen shields target cells from contact-dependent inhibition*, California Alliance for Minority Participation, Department of Molecular, Cellular and Developmental Biology, University of California, Santa Barbara
- 2016 **Summer High School Research Mentor**, *A novel acyltransferase is required for inhibition by Class IV CdiA proteins*, Research Mentorship Program (RMP), Office of Summer Sessions, University of California, Santa Barbara

## Publications

Wäneskog, M., Halvorsen, T., Filek, K., Hammarlöf, D., Low, D., Hayes, C. Poole S. and Koskiniemi, S., 2020. The *E. coli* isolate EC93 uses two class I CDI systems for antagonistic bacterial interactions, *Microbial Genomics*. *In review*

Halvorsen, T., Garza-Sánchez, F., Ruhe, Z, Bartelli, N., Nguyen, J., Low, D., Hayes, C. Lipidation of the CdiA receptor binding domain promotes lipopolysaccharide binding on target bacteria, *Manuscript*

Halvorsen, T., Jones, A., Low, D., Hayes, C. Identification of two CDI ionophore toxins capable of exploiting homologous inner membrane proteins to exert toxicity in target cells, *Manuscript*

## Oral Presentations

- 2019 *Post-translational modification of CdiA facilitates interspecies contact-dependent growth inhibition through the use of lipopolysaccharide as a receptor*, "Diverse Functions of the Bacterial Cell Surface", American Society for Microbiology (ASM) Microbe 2019, San Francisco, CA.

- 2018 *Post-translational modification of CdiA facilitates interspecies contact-dependent growth inhibition in Escherichia coli*, Annual Asilomar Meeting of the West Coast Bacterial Physiologists, Monterey, CA. **Recipient of the Best Graduate Student Oral Presentation Award**
- 2018 *A small protein intoxicates Escherichia coli by parasitizing the multidrug efflux pump AcrB*, Graduate Student Seminar, University of California, Santa Barbara
- 2017 *The increasingly complex behaviors of pathogens: a case study of contact-dependent growth inhibition in Shiga-toxin producing Escherichia coli*, Graduate Student Seminar, University of California, Santa Barbara
- 2017 *The Battle Between Bacteria Begins with a Trojan Horse: Manipulation of bacterial communities using secretion systems*, UC Grad-Slam Competition, University of California, Santa Barbara **Semi-finalist**
- 2017 *The Cell Envelope: bacterial armor*, Guest Lecturer, Cell Physiology, Department of Ecology, Evolution and Marine Biology, University of California, Santa Barbara

### Poster Presentations

- 2018 *Post-translational modification of CdiA facilitates interspecies contact-dependent growth inhibition in Escherichia coli*, Molecular Genetics of Bacteria and Phages Meeting, Madison, Wisconsin. **Winner of Most Outstanding Graduate Student Poster Award**
- 2017 *A contact-dependent inhibition system kills multiple species of Proteobacteria by using lipopolysaccharide as a receptor*, Molecular Genetics of Bacteria and Phages Meeting, Madison, Wisconsin. **Finalist for Most Outstanding Graduate Student Poster Award**
- 2015 *Contact-dependent inhibition in natural isolates of Escherichia coli*, NASA/ESA Nordic-Hawaii Astrobiology Summer School, Reykjavik, Iceland
- 2014 *Investigating the rate of change of the human microbiome*, Undergraduate Research and Design Symposium, Northern Arizona University, College of Engineering, Forestry and Natural Sciences
- 2014 *Genetic relatedness and denning behavior in striped skunk populations of Northern Arizona* Undergraduate Research and Design Symposium, Northern Arizona University, College of Engineering, Forestry and Natural Sciences

### **Competitive Awards**

2018	Most Outstanding Graduate Student Poster, Molecular Genetics of Bacteria and Phages Meeting, Madison, Wisconsin
2018	Best Graduate Student Oral Presentation, West Coast Bacterial Physiologists Meeting, Monterey, California
2017	Finalist for Most Outstanding Graduate Student Poster, Molecular Genetics of Bacteria and Phages Meeting, Madison, Wisconsin
2016	Semi-finalist in UC Grad-Slam elevator pitch competition
2013	1 <sup>st</sup> Place Essay, Louis Agassiz Prize for Excellence in Writing (NAU)
2012	3 <sup>rd</sup> Place Essay, Louis Agassiz Prize for Excellence in Writing (NAU)

### **Scholarships, Fellowships and Travel Awards**

2019	Individual Professional Skills Grant (UCSB CSEP)
2018	Ellen Schamburg Burley Graduate Award (UCSB MCDB)
2017	Doreen J. Putrah Travel Award (UCSB MCDB)
2016	Doctoral Student Travel Grant (UCSB)
2015	Pre-doctoral Travel Grant (UCSB)
2014	Doctoral Scholars Fellowship (UCSB)
2013	Global Opportunities Scholarship (NAU)
2013	Hooper Undergraduate Research Award (NAU)
2013	Jerry O. Wolff Student Enrichment Biological Sciences Scholarship (NAU)
2012	Mildred Fenton and Carol Lane Scholarship (NAU)
2012	Kollis and Opal King Scholarship (NAU)
2011	K.R. and Irene Hafen Forestry Scholarship (NAU)
2011	Joseph C. Dolan Forestry Scholarship (NAU)
2011	Arizona Instruments for Measuring Standards (AIMS) Tuition Scholarship

### **Community Outreach**

2016	Teacher, Family Ultimate Science Exploration (FUSE)
2015 - 2016	Docent, Coal Oil Point Reserve
2015	Volunteer Scientist, Ask a Scientist, Science and Technology MESA Day
2015	Mentor, Women in Science and Engineering Mentorship Program
2015	Instructor, Tech Savvy Conference (AAUW/WiSE)

## **Memberships and Associations**

Women in Science and Engineering (WiSE)

500 Women Scientists

Graduate Students for Diversity in Science

American Society for Microbiology

American Association for the Advancement of Science

Massive Science Consortium

American Alpine Club

## Abstract

Complexities in crossing membrane barriers: new members of the CdiA and CDI ionophore protein families reveal novel mechanisms for receptor-binding and intoxication of target cells

by

Tiffany Marie Halvorsen

Contact dependent inhibition (CDI) systems facilitate antagonistic toxin exchange between closely-related bacteria in a proximity-dependent manner. CDI+ bacteria use the large ( $\sim 300$  kDa) cell surface protein CdiA to intoxicate their neighbors by binding to an outer membrane (OM) receptor. Receptor binding occurs at a central 200-300 amino acids (RBD) and initiates cleavage and translocation of the  $\sim 200$  carboxy-terminal residues of CdiA (CdiA-CT). Delivery of CdiA-CT requires receptor proteins at each stage of membrane transport into the target cell. We have previously identified three OM receptors for CdiA in Enterobacteria: BamA, OmpC/F, and Tsx. Using the CDI locus from *E. coli* STEC\_O31 as a model (*cdiBCAI*), in Chapter 2 I introduce a fourth class of CdiA (CdiA4 or CdiA<sub>4</sub><sup>STECO31</sup>) that exclusively binds to lipopolysaccharide to initiate CdiA-CT translocation. CdiA<sub>4</sub> is also linked to an accessory gene, *cdiC*, which encodes a predicted lysine acyltransferase. Site-directed mutagenesis and HPLC-MS reveals CdiC and its close homologues form a subfamily of bacterial lysine acyltransferases within the toxin-activating acyltransferase (TAAT) family that modify their cognate CdiA proteins to promote LPS binding. In Chapter 3, I use this new CDI system to investigate the interaction between CdiA and O-antigen and find that O-antigen presents a barrier to toxin translocation at the outer membrane of target cells. Finally, in Ch. 4, I identify four new inner-membrane (IM) protein receptors that facilitate toxicity by two new members

of the CDI ionophore family. I demonstrate that the native activity of these receptors is not required for CDI, but their presence in the IM is necessary for ionophore activity both from the periplasm or from the cytosol. Combined with a primary sequence analysis of these CdiA-CTs, the results in Ch. 4 offer a wealth of opportunities to explore the mechanism of CDI ionophore activity further. Together, the results of this work present a new physiological application for bacterial protein lipidation, introduce a new family of accessory acyltransferases, reveal that O-antigen can be a barrier to CdiA-CT delivery, and advance our understanding of the functional diversity of CDI toxins and how they exploit target cell proteins for activity.

# Contents

<b>Title</b>	<b>i</b>
<b>Contents</b>	<b>xv</b>
<b>List of Figures</b>	<b>xvi</b>
<b>List of Tables</b>	<b>xviii</b>
<b>1 Introduction</b>	<b>1</b>
1.1 Overview . . . . .	1
1.2 Bacteriocins . . . . .	3
1.3 Pore-forming toxins . . . . .	5
1.4 Secretion Systems . . . . .	8
1.5 Permissions and Attributions . . . . .	28
<b>2 Lipidation of the CdiA receptor-binding domain promotes recognition of lipopolysaccharide on target bacteria</b>	<b>29</b>
2.1 Abstract . . . . .	29
2.2 Introduction . . . . .	30
2.3 Results . . . . .	32
2.3.1 Class IV CdiA recognizes the core oligosaccharide of LPS as a receptor	32
2.3.2 Class 4 CdiA delivers toxin into closely-related species . . . . .	36
2.3.3 CdiC promotes inhibition activity of class 4 CdiA . . . . .	36
2.3.4 CdiC modifies CdiA at residue Lys1467 with $\beta$ -hydroxydecanoate	37
2.3.5 CdiC acyltransferases are CdiA-specific . . . . .	40
2.4 Discussion . . . . .	40
2.5 Materials and Methods . . . . .	45
2.6 Tables and Figures . . . . .	53
<b>3 CdiA is affected by the presence of O-antigen on targets</b>	<b>80</b>
3.1 Abstract . . . . .	80
3.2 Introduction . . . . .	81

3.3	Results . . . . .	83
3.3.1	<i>E. coli</i> K-12 restored for O-antigen synthesis is fully protected from CDI in liquid broth and partially on solid media . . . . .	83
3.3.2	O-antigen shielding is unidirectional . . . . .	84
3.3.3	CDI systems and O-antigen polymers co-exist on the surface of pathogenic <i>Enterobacteriales</i> . . . . .	85
3.3.4	O-antigen defective <i>S. enterica</i> sv. Typhimurium and <i>C. rodentium</i> are not more susceptible to CdiA4 . . . . .	85
3.3.5	Inhibition by CDI diminishes over long time scales. . . . .	86
3.4	Discussion . . . . .	87
3.5	Materials and Methods . . . . .	90
3.6	Tables and Figures . . . . .	93
<b>4</b>	<b>Identification of two CDI ionophore toxins capable of exploiting homologous inner membrane proteins to exert toxicity in target cells</b>	<b>104</b>
4.1	Abstract . . . . .	104
4.2	Introduction . . . . .	105
4.3	Results . . . . .	109
4.3.1	The mouse enteric isolate NI1076 encodes two CDI loci that encode toxins capable of disrupting the proton motive force in target bacteria	109
4.3.2	NI1076 CT-1 and CT-2 do not require the known ionophore receptor AcrB to exert toxicity . . . . .	110
4.3.3	Transposon mutants are resistant to CT-2 due to mutations not associated with the site of transposon insertion . . . . .	111
4.3.4	UV mutagenesis of target cells reveals that both ionophores can exploit homologous IM proteins as independent receptors . . . . .	112
4.3.5	CT-1 uses the di/tri-nucleotide importers DtpA and DtpB as independent receptors . . . . .	114
4.3.6	CT-2 can exploit both of the putrescine importers PuuP and PlaP as receptors, but with unequal potency . . . . .	115
4.3.7	The native function of DtpA is not required for toxicity of CT-1 .	116
4.4	Discussion . . . . .	118
4.5	Materials and Methods . . . . .	123
4.6	Tables and Figures . . . . .	132
<b>5</b>	<b>Conclusion</b>	<b>169</b>
	<b>Bibliography</b>	<b>178</b>



# List of Figures

1.1	Secretion systems in diderm bacteria . . . . .	12
1.2	CdiA domain architecture . . . . .	17
2.1	Class 4 CdiA binds a unique receptor . . . . .	53
2.2	LPS is the class 4 CdiA receptor. . . . .	54
2.3	LPS mutants are still susceptible to CdiA classes 1-3 . . . . .	55
2.4	CdiA RBD binds to LPS . . . . .	56
2.5	CdiA-4 inhibits closely-related species . . . . .	57
2.6	CdiC contributes to inhibition by CdiA-4 . . . . .	58
2.7	CdiA-4 is modified by CdiC within the RBD . . . . .	59
2.8	Lysine 1467 is the site of modification by CdiA . . . . .	60
2.9	CdiC active site mutations prevent modification . . . . .	61
2.10	Purification of CdiA RBD proteins for HPLC-MS . . . . .	62
2.11	Mutations at Lys1467 disrupt CDI . . . . .	63
2.12	Modification of CdiA-4 only occurs by a cognate acyltransferase . . . . .	64
2.13	Sequence alignment of 3 CdiC homologues . . . . .	65
3.1	CDI+ isolates express CdiA and create O-antigen in the lab . . . . .	93
3.2	Spent media growth curves with EC93 . . . . .	94
3.3	O-antigen shields targets from CDI . . . . .	95
3.4	O-antigen shielding is unidirectional . . . . .	96
3.5	Natural isolates are not inhibited by CdiA-4 in liquid broth . . . . .	97
3.6	Disruption of <i>waaL</i> has off-target effects on <i>Citrobacter rodentium</i> and <i>Salmonella enterica</i> and does not prevent CDI . . . . .	98
3.7	CDI has little effect on population outcomes after 24 hours . . . . .	99
4.1	Alignment of CdiA <sup>536</sup> and CdiA <sup>NI1076-1</sup> . . . . .	135
4.2	Alignment of CdiA <sup>STECO31-2</sup> and CdiA <sup>NI1076-2</sup> . . . . .	138
4.3	NI1976 CT-1 and CT-2 are functional and distinct CDI toxins . . . . .	139
4.4	Both NI1076 toxins are ionophores . . . . .	140
4.5	Neither NI1076 ionophore requires AcrB in targets . . . . .	141

4.6	CT-2 <sup>R</sup> UV mutants carry mutations in PuuP and a large deletion containing PlaP . . . . .	143
4.7	Transposon mutants also carry a deletion specific for CT-2 resistance . . . . .	145
4.8	Sequence alignment of the CT-2 receptors PlaP and PuuP . . . . .	146
4.9	Resistance to either toxin requires deletion of 2 IM receptors . . . . .	147
4.10	PlaP and PuuP are not equivalent CT-2 receptors . . . . .	148
4.11	DtpA/DtpB are equivalent receptors for CT-1, but transport activity is not required for CDI . . . . .	149
4.12	Deletion of both IM receptors protects targets from membrane depolarization . . . . .	150
4.13	Alignment of the di/tr-nucleotide importers in <i>E. coli</i> . . . . .	151
4.14	Alignment of all 4 ionophore toxins . . . . .	152
4.15	Death curve for UV mutagenesis and mutation frequency at chosen dosage . . . . .	153
4.16	Gating approach for flow cytometry . . . . .	154
4.17	Density plots of DiBAC <sub>4</sub> 3-treated targets . . . . .	155
4.18	Density plots of DiBAC <sub>4</sub> 3-treated targets with receptor deletions . . . . .	156
4.19	Density plots comparing uptake of DiBAC <sub>4</sub> 3 in PlaP versus PuuP deletions against CT-2 . . . . .	157
4.20	Alignment of NI1076 CT-1 and CT-2 . . . . .	158
4.21	Hydrophobicity plots of ionophores CT and CdiI pairs . . . . .	159

# List of Tables

2.1	Strains used in Chapter 2. . . . .	66
2.2	Plasmids used in Chapter 2. . . . .	67
2.3	Primers used in Chapter 2. . . . .	73
3.1	Bacterial strains used in Chapter 3. . . . .	100
3.2	Plasmids used in Chapter 3. . . . .	101
3.3	Primers used in Chapter 3. . . . .	103
4.1	<b>Mutations in UV mutants resistant to both NI1076 toxins . . . .</b>	<b>142</b>
4.2	<b>Genes encoded in the CT-2 specific deletion . . . . .</b>	<b>144</b>
4.3	Bacterial strains used in Chapter 4. . . . .	160
4.4	Plasmids used in Chapter 4. . . . .	161
4.5	Primers used in Chapter 4. . . . .	165

# Chapter 1

## Introduction

### 1.1 Overview

It is now well appreciated that bacteria live in extremely complex communities with one another and with their hosts. These host-associated microbial consortia (collectively termed the microbiome) are often temporally stable over long time scales, likely due to their tendency towards mutualism and syntrophy rather than pathogenicity. For example, plant-associated microorganisms collaborate with their hosts to survive in nutrient-limited soil by providing novel adaptations, disease resistance, and increased abiotic stress tolerance [1]. Animals are also extensively colonized by syntrophic microbial communities. Indeed, collaboration between the human body and the microbiome is necessary for maintaining proper health. Therefore, since long-term microbiome stability appears to be a hallmark of healthy individuals, disruption of a healthy microbiome may even be a hallmark of the pathogenic lifestyle [2].

Understanding how pathogens might disrupt healthy bacterial communities is therefore important for the study of infectious microorganisms. In humans, dysbiosis (i.e., disruption to the normal flora/fauna) in the gut is strongly associated with several adverse health effects and diseases [2], suggesting that stable commensal communities directly affect human tissues. In fact, human commensals are known to participate in competitive

exclusion strategies to protect against pathogen invasion, though the molecular details of this so-called colonization resistance are only now becoming fully understood [3, 4]. One example is from the commensal strain *Staphylococcus lugdunensis*, which secretes antibiotics that prevent the invading strain of *S. aureus* from colonizing [5].

Since nearly every surface of the human body is inhabited by bacteria that are important for human health [6, 7], what tools do pathogens harbor which make them such a threat to healthy bacterial communities? At the most fundamental level, at least, we know that the difference between a commensal and a pathogen is the presence of unique accessory (i.e., nonessential) genes, most often encoded on pathogenicity islands. The accessory genome provides pathogens with a competitive advantage over commensals, allowing them to invade in communities in which they are not established [8]. Thus, pathogenicity islands typically encode secretion systems that export adhesins, bactericidal toxins, host effectors, and other proteins to the surface of the cell or extracellular space where they can mediate interactions between the bacterium and its environment. Recent efforts to understand the physiology of bacterial secretion systems have highlighted both how complex their regulation can be [9] but also how dramatically they can affect their environment [10].

In this work, I will focus on a specific secretion system found on pathogenicity islands in the Proteobacteria which mediates inter-bacterial competition. This system, called Contact-Dependent Inhibition (CDI), is harnessed by plant and animal pathogens to directly inhibit the growth of neighboring cells through the delivery of a small toxin. CDI systems are also known to mediate biofilm formation and autoaggregation of sibling cells. Therefore, CDI could play a role in initiating the early stages of pathogen colonization within a host, though this has yet to be shown. Alternatively, as we will see in Ch. 3 and Ch. 4, CDI may also give pathogens a unique tool for communication and ultimately growth regulation in response to some environmental stimuli. The molecular details I

present here expand our interpretation of CDI's physiology, and open up new doors for the engineering of CDI systems for synthetic biology applications.

## 1.2 Bacteriocins

Host-associated bacterial communities can be extremely dense, with an estimated  $10^{11}$  –  $10^{12}$  cells per g within the human colon and feces [11]. In the colon, bacteria form well-mixed micro-communities on every available surface [12], resulting in constant contact with a variety of neighboring cells, both human and bacterial. In an already resource-limiting environment, it is unsurprising that bacteria are in constant competition with neighbors [13, 14, 15], and thus have evolved tools for directly killing neighboring cells.

The first of these bactericidal weapons to be appreciated are the bacteriocins. Bacteriocins are secreted toxins produced by many Gram-negative bacteria that are used to directly kill neighboring cells through the disruption of an essential cellular process [16]. Colicins, which are produced by *Escherichia coli*, are the most thoroughly studied toxins of the bacteriocin family, though other Proteobacteria also secrete their own bacteriocins (including *Pseudomonas pyogens*, *Enterobacter cloacae*, *Yersinia pestis*, *Klebsiella* spp., *Serratia marscescens* and *Photobacterium luminescens*). Intoxication by bacteriocins requires (1) secretion from the producing cell, (2) receptor binding at the recipient cell outer membrane (OM) and (3) translocation through the periplasm to either the inner membrane (IM) or the cytoplasm, resulting in intoxication.

Over 20 different colicins have been identified and split into two groups (A and B) according to which IM translocation machinery they use for cell entry. Group A colicins are synthesized with an associated small lipoprotein (Cxr proteins, for colicin X release proteins) that induces both colicin release and lysis of the producing cell. For intoxication of recipient cells to occur, colicins must unfold and partake in a two-step translocation

pathway at the recipient cell OM [16]. The first step in intoxication involves high-affinity binding to an outer membrane  $\beta$ -barrel protein that normally acts as a nutrient importer or a porin (some examples are: FepA, BtuB, TxC, OmpX, and OmpF) [17]. The structures of three colicins bound to their OM receptors (ColE2 and ColE3 with BtuB, and ColIa to Cir) have revealed that binding does not interfere with nutrient transport, although conformational changes in the bound receptor do occur [18]. Since it therefore appears that colicins cannot enter target cells through their OM receptor, and in their bound conformation colicins are positioned away from the receptor, additional binding steps must occur to enable translocation of the toxin domain. Indeed, colicins require a second OM "translocator" protein to enter target cells. Recruitment of a second translocator OM protein and at least one periplasmic or IM protein is required to form a "translocon" [18]. Some colicins require two OM receptors, with one acting as a translocator, while some can use one OM protein as both a receptor and translocator, such as colicin B which uses FepA [17]. Still some colicins (5, 10 and E1) co-opt the periplasmic export protein channel formed by TolC for cell entry [17].

Though the mechanism of OM receptor binding appears to be common to each colicin for which there is a structure solved of the receptor binding domain (Ia, E2 and E3), periplasmic translocation has been solved in many ways by the colicin family. Whether a colicin uses the Tol or Ton system, both of which are periplasmic-spanning IM embedded, proton motive force (pmf)-dependent export proteins, determines its classification as a Group A or Group B colicin, respectively [18]. The NT domain is completely modular between Group A and B colicins, suggesting that both groups have adapted a general mechanism for cell entry that is dependent on co-opting periplasmic-spanning proteins that utilize the pmf.

Though colicins take many forms, they share in common three modular domains. The central  $\sim 34$  amino acids are responsible for OM receptor recognition, the N-terminal

translocation domain interacts with the Tol/Ton proteins to complete cell entry, and the C-terminal activity domain encodes the toxin itself. Once inside the recipient cell, colicins promote cell death by pore formation in the cytoplasmic membrane, nuclease activity, or disruption of cell wall synthesis [16]. The N-terminal domain appears disordered in all of the colicin structures which have been solved and is likely important for the entry of most colicin proteins [18]. Colicin-producing cells also produce a toxin-specific immunity protein for protection against self-intoxication. The immunity protein binds the toxin in the producing cell, then dissociates upon receptor-binding at the recipient cell surface.

### 1.3 Pore-forming toxins

One class of colicins that are quite relevant to this thesis are the pore-forming colicins. This family of colicins form a class of pore-forming toxins (PFTs) which belong to a much larger family of pore-forming proteins (PFPs) - specialized transmembrane proteins that can depolarize membranes by creating channels [19]. Indeed, due to their prevalence in all domains of life, PFPs are likely an ancient group of proteins. This suggests that membrane depolarization is an effective means of intoxication, and that perhaps the mechanism PFPs use to insert into bilayers may have radiated into other protein families. Thus, PFPs are a valuable source of information about protein-lipid interactions. Understanding the known mechanisms that PFTs use to create pores in lipid bilayers will provide useful context for our exploration of a new family of PFTs that are delivered by CDI systems in Chapter 4.

**$\alpha$ -Pore-forming toxins** PFPs are categorized into two classes ( $\alpha$ -PFTs or  $\beta$ -PFTs) according to the secondary structure that their pore-forming domain adopts (either  $\alpha$ -helical channels or  $\beta$ -barrels). The first structure of a PFP to be solved was that of colicin



A [20], which is a representative member of the  $\alpha$ -PFTs. This structure revealed what is essentially an inside-out membrane protein (i.e., a hydrophobic core within a bundle of amphipathic  $\alpha$ -helices). Additional structures have been solved of other  $\alpha$ -PFTs in their water-soluble form, revealing a shared mechanism of action [21, 22, 23].

$\alpha$ -PFTs must undergo a small state transition, either due to receptor binding or local pH reduction, in order to begin insertion of a hydrophobic core  $\alpha$ -helical bundle into the membrane. In the case of colicins, a core hydrophobic alpha-helical hairpin is sheltered by a bundle of ten  $\alpha$ -helices that together form a globular protein [24]. For colicin E1, specific residues have been identified that can sense a change in local pH. A reduction in pH around these acidic amino acids changes a salt bridge and hydrogen-bonding network that leads to local unfolding at the membrane interface [24]. Following membrane association, insertion of either the hydrophobic core or aromatic residues into the bilayer is thought to lead to irreversible channel formation, ultimately resulting in membrane depolarization and ATP depletion in a recipient cell [16, 17]. Though the exact structure of a membrane-associated  $\alpha$ -PFT is not known, it is thought to adopt an 'umbrella'-like conformation upon bilayer insertion, causing the hydrophobic core to become buried within lipids with the helices electrostatically interacting with lipid headgroups atop the bilayer [25]. Thus, the sequence of events leading to membrane integration are binding, unfolding, reorganization, and hydrophobic anchor insertion. In addition to colicin A, this model has been extended to two more colicins (E1 and Ia) [19], though how this conformation leads to channel formation is unclear; whether oligomerization is required for channel formation remains to be determined.

**$\beta$ -Pore-forming toxins** The insertion mechanism and pore structures of  $\beta$ -pore forming toxins are better understood than those of  $\alpha$ -PFTs. Indeed, combined with the fact that pore size is an alterable feature, this makes  $\beta$ -PFTs good candidates for syn-

thetic biology applications, which is demonstrated by their implementation as engineered nanopores in recent DNA sequencing technologies.  $\beta$ -PFTs are first released as soluble monomers that oligomerize before forming active pores in lipid bilayers. The monomers of a  $\beta$ -PFT oligomerize by donation of individual  $\beta$ -strands to form a completed barrel.

A well-characterized family of  $\beta$ -PFTs are the  $\alpha$ -hemolysins, which are named for their hemolytic activity. Thus, besides being useful in nanopore technology, hemolysins represent major virulence factors produced by many insect and animal pathogens, including *Staphylococcus aureus* and enterohemorrhagic *Escherichia coli* ([26, 27]. *E. coli*  $\alpha$ -hemolysin forms the *hlyCBAD* operon encoding a Type 1 secretion system, along with the pro-toxin and an accessory acyltransferase (*hlyC*) which lipidates HlyA to generate the mature HlyA toxin. Modification to HlyA with heterogenous fatty acids imparts critical hydrophobicity into the toxin, increasing its affinity for membranes to drive channel formation [28, 29].

Other  $\beta$ -PFTs include aerolysin toxins from *Aeromonas hydrophila*, anthrax toxin from *Bacillus anthracis*, and the very large cholesterol-dependent cytolysins (CDCs) that are widespread among Gram-positive bacteria and can form  $\beta$ -barrels with up to 176 strands [24]. In each case, individual monomers each donate one or two (in the case of CDCs) beta strand(s) to form a large, complex barrel structure [24]. Thus, pore-forming toxins represent a great diversity of bacterial proteins that all share the capability of overcoming a common issue: existing in soluble and lipid-associated forms. Achieving both states of existence has led to a radiation of structures and unique mechanisms of adopting alternative conformations.

**Glycine Zipper Channel Proteins** In addition to the thoroughly-studied  $\alpha$ - and  $\beta$ -pore-forming toxins, which can be easily identified by transmembrane alpha helices or beta strands in their secondary structure, a third variety of bacterial pore-forming pro-

teins with more cryptic transmembrane domains are the glycine zipper channel proteins. Glycine zippers are sequence motifs of the pattern (G/A/S)xxxGxxxG or GxxxGxxx(G/S/T). The presence of a repeating GxxxG motif enables close packing of the peptide backbone and, in the low dielectric environment of the lipid bilayer, causes close packing of neighboring helices [30]. The result is an efficient mechanism for homo-multimerization within the bilayer. Indeed, glycine zippers are very common motifs in membrane proteins [31], and are found in a number of proteins that form selective channels in the inner membrane [32]. The glycine zipper motif can also be exploited by secreted pore-forming toxins destined for neighboring lipid bilayers, as has been described for the vacuolating toxin of *Helicobacter pylori* [33], which forms homo-oligomeric protein complexes using helix-helix association.

## 1.4 Secretion Systems

We will now consider the diversity of secretion systems found in Gram-negative bacteria to place CDI within the proper molecular context. Impressively, there are now eight groups of secretion systems that have been identified in diderms. Each unique form of secretion is given an alphanumeric classification based on order of discovery (T1SS - T9SS. The T7SS is found in *Mycobacteria* and therefore will not be discussed here). Secretion across the IM and OM can be accomplished either by a two-step process that relies on the Sec or Tat export machinery in the IM and then uses secretion-specific proteins in the OM (T2SS, T5SS, T9SS), or in a one-step process through the entire envelope (T1SS, T2SS, T3SS, T4SS, T6SS). The ultimate goal of these various systems is to secrete proteins into the extracellular space (T1, T2, T5, T9), to deliver payloads into neighboring bacteria (T5b, T6) or host cells (T3, T6), or to transport surface proteins outside the cell envelope to build of surface structures (T7, T8, T9).

## Type I

The T1SS is comprised of three components: an ATP-dependent ABC transporter in the inner membrane to provide energy for transport, an adaptor protein in the periplasm, and the passive transporter TolC in the outer membrane to which the adaptor is connected [34]. Though this system can export many different adhesins, proteases and toxins outside of the cell, the model for the T1SS is hemolysin from *E. coli*.

Hemolysin is a toxin produced by pathogenic strains of *E. coli* and, as the name suggests, its purpose is the lysis of erythrocytes to release hemoglobin and thus free up iron. HlyA finds its transporter, HlyB, using a C-terminal signal peptide, which induces the formation of a tunnel comprised of HlyB-HlyD-TolC that spans the cell envelope [34]. The cargo traverses the tunnel unfolded, which was shown with a T1SS from *Serratia marcescens* [35]. HlyD is an adaptor anchored in the IM with a large periplasmic domain which it uses to contact TolC when HlyA is bound to HlyB. ATP hydrolysis by HlyB energizes the process of transport; TolC is passively involved but forms an impressive 10 nm long tunnel through which substrate can travel outside of the cell.

## Type II

Type II secretion systems (T2SS) export a wide range of virulence determinants in pathogens. These include enzymatic toxins such as cholera toxin from *Vibrio cholerae* and the heat-labile toxin (LT) of enterotoxigenic *E. coli* [36], and degradative enzymes such as phospholipases [37]. Exoproteins destined for the T2SS encode an N-terminal signal for transport first across the IM using the Sec or Tat machinery. The N-terminal signal peptide is then cleaved following transport, and the cargo protein folds within the periplasm. Finally, the mature periplasmic protein is transported across the OM by a large, 12-16 protein complex called the secreton [38]. The secreton is comprised

of four subcomplexes, including an OM multimeric pore, a periplasmic-spanning channel anchored to the IM, a periplasmic pseudopilus, and an ATPase hexamer in the IM [39, 40]. Though the machinery likely evolved from Type IV pili, T2SSs are thought to function by a pistol-like mechanism where cargo is loaded into to base of the secreton and pushed out by the pilus through the OM pore.

## Type III

The T3SS is our first example of a secretion system designed to achieve one-step export from the producing cell. Additionally, this remarkable apparatus also achieves injection of the cargo directly into a neighboring cell. Understandably, the T3SS has been coined "the injectisome". Unsurprisingly, the T3 system is antagonistic, facilitating host-pathogen interactions. T3SSs have been found in many human pathogens, including *Yersinia* spp., *Salmonella* spp., *Bordetella* spp., *Chlamydia* spp., among others [41]. The T3 system delivers an array of toxic effectors into host cells which are specific to the lifestyle of the pathogen encoding them.

The T3SS apparatus itself is very large, built from 20 - 25 different proteins, with about half of them conserved between most species [41]. The apparatus is built similarly to the bacterial flagella, with two concentric membrane-embedded rings localized to the inner and outer membranes that provide a conduit across the cell envelope. An essential component of the T3SS is the needle - a protein filament that is exported to the cell surface through the basal body and used to deliver effectors directly into host cells [42]. Remarkably, the needle itself is also homologous to the flagellar filament, though the protein sequence lacks apparent similarity [43]. Additional proteins are secreted to the tip of the filament that are thought to be involved in host targeting. After detection of a host cell, a translocon is formed in the host membrane by the activity of hydrophobic

proteins and is thought to cause docking of the filament, though the details of docking and effector translocation are still unclear [42].

Type III effectors are specific to the secreting cell, providing an adaptive benefit to the bacterium's specific niche. In order to be loaded and secreted, T3 effectors encode a T3-specific N-terminal signal sequence and a chaperone binding domain [42]. The T3 chaperones are thought to either keep effector proteins unfolded before export, or to prevent them from prematurely interacting with components of the apparatus prior to export. The effectors are then recruited and unfolded by a T3-associated ATPase [42]. The T3SS is one of the most complex secretion systems discovered, and therefore the coordination of each stage of biogenesis, secretion and delivery is still under investigation.

## Type IV

The T4SS is a multiprotein complex that spans both cell membranes, and harbors a diverse array of functions in bacteria. T4SSs load and transport cargo by the activity of three cytosolic and membrane-bound ATPases. Once cargo is loaded, it enters the core complex of the T4 apparatus, which is built from several protein subunits and located in the IM and periplasm. Finally, two protein subunits comprise the pilus, which is responsible for establishing physical contact with the neighboring cell and, ultimately, the direct transfer of cargo [44].

The range of activities T4 secretion mediates is diverse. In *E. coli*, the T4SS facilitates the transfer of DNA between cells and therefore contributes to the rapid spread of genes located on conjugative plasmids. In other bacteria, the T4SS is involved in the uptake of naked DNA from the environment [45]. Still some bacteria have turned the T4SS into a virulence factor by using the pilus to transport virulent DNA or effectors into host cells. For example, the plant pathogen *Agrobacterium tumefaciens* uses its T4SS

to deliver oncogenic T-DNA into plant cells [46], and the human pathogen *Bordetella pertussis* co-opts its T4SS for export of the pertussis toxin [47]. Finally, the opportunistic pathogen *Stenotrophomonas maltophilia* was recently shown to use the T4SS as a competitive strategy with bacterial opponents, by delivering effectors directly into target cells [48]. Homologues of the bacteria-targeting T4SS may also be widespread in the  $\beta$ -proteobacteria, as evidenced by a bioinformatic survey [49]. Indeed, though T4SSs represent the oldest understood secretion machine, we are still discovering new ways in which bacteria can use it to establish themselves in the environment.

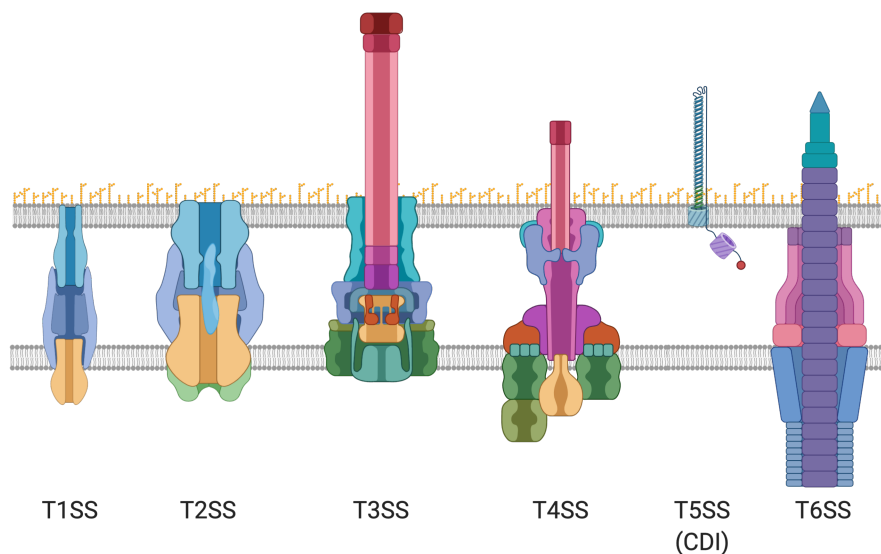


Figure 1.1: **Overview of Type I through Type VI secretion in Gram-negative bacteria.** Cartoon illustration of the protein components of T1SS through T6SS to demonstrate the diversity and complexity of these large complexes, in comparison to CDI. All figures created with Biorender.

## Type V

The Type V family of protein secretion machines, which include the topic under study throughout this thesis, are also the least complex secretory pathways. This family includes autotransporters (Type Va) and two-partner secretion systems (Type Vb) as

well as the more recently described Type Vc system. Proteins within the Type V family share similarities in their sequence and modes of biogenesis.

### **Type Va**

The autotransporters are large proteins built of three domains: an N-terminal Sec-dependent signal peptide, a passenger domain, and a translocation domain. Thus, Type V secretion employs a two-step translocation process, using the Sec machinery to cross the IM and the C-terminal translocation domain for OM export. The size and function of the Sec-dependent signal sequence varies between autotransporters. Typically, the signal sequence is comprised of 20-30 amino acids featuring an N-terminal stretch of basic amino acids, a core region of hydrophobic residues, and a leader peptidase recognition motif. A minority of autotransporters are lipoproteins which encode a lipobox within the signal sequence [50]. An acyltransferase can recognize the signal sequence and add a lipid moiety to the protein. One such autotransporter is NalP of *Neisseria meningitidis*. Lipidation of NalP occurs at an N-terminal cysteine residue within the lipobox on the periplasmic side of the IM, and is required for the function of NalP - which is to cleave and release surface proteins [51]. Other autotransporters encode an extended signal peptide that is thought to prevent misfolding of the passenger domain when inside the periplasm. The unusual extended signal peptide ( $\sim 55$  amino acid) is thought to recruit signal peptidase relatively slowly, thereby transiently anchoring the large autotransporter to the IM to prevent improper folding that would inhibit OM translocation [52]. In addition to lipidation, some autotransporters can be glycosylated by an associated heptosyltransferase. Glycosylated autotransporters typically function as adhesins, such as Ag43, which is found in uropathogenic *E. coli* and functions in adhering to eukaryotic cells [53].

Though the insertion of the C-terminal transport domain into the OM is facilitated by the BAM complex [54], the energy source for translocation of the passenger domain has



remained unresolved. However, an independent system for autotransporter OM secretion has since been discovered in pathogens encoding T5SSa [55]. This envelope-spanning heterodimer (TamA-TamB) is thought to assist in the biogenesis of the passenger domain, possibly solving the issue of an energy source for OM transport since TamB is an IM protein [55]. TamA is also an integral membrane protein yet it is a member of the Omp85 family, and thus has the capacity to actually export cargo via a central pore through the OM. The discovery of an OM export machine to assist in translocation truly turns the name "autotransporter" into a misnomer, yet solidifies its membership in the Type V family since both T5SSs use Omp85 proteins for OM translocation.

### **Type Vb**

The second class of T5SSs are the two-partner secretion (TPS) systems, to which CDI belongs. TPS systems are responsible for many bacterial functions, including aggregation and biofilm formation [56], iron acquisition [57], inhibition of phagocytosis [58], and adherence [59]. As the name suggests, TPS systems encode two proteins: "cargo" proteins (TpsA) and Omp85 transporter proteins (TpsB). TpsA proteins are defined by a conserved  $\sim 250$  amino acid long TPS domain at their N-terminus. Just like the autotransporters, TpsA proteins encode a N-terminal Sec-dependent signal peptide for transport across the cytoplasmic membrane. TpsA then transits through the periplasm and makes contact with the periplasmic domain of its TpsB partner, triggering OM secretion through the channel of TpsB [60]. The folding of TpsA is thought to occur after it is fully exported, and so it is secreted in an extended conformation. The well-studied TpsA protein filamentous haemagglutinin (FHA), which is a model for TpsA export, was shown to cause leakage of intracellular proteins when exported in the absence of a chaperone protein DegP [60]. Therefore, it is likely that TpsA proteins require periplasmic chaperones to traverse the cell envelope in an unfolded state. TpsA proteins are as di-

verse in size and sequence as they are in function - ranging from  $\sim 700$  to  $\sim 5000$  residues in length. Despite their size range, TpsA proteins are mostly predicted to form extended  $\beta$ -helices [61]. Thus, it's likely that the huge size range of TpsA proteins is made possible by increasing the number of structural repeats in the beta-rich filament.

**Discovery of CDI** Contact-dependent growth inhibition (CDI) systems are antagonistic TpsA proteins of the Type Vb secretion system family that participate in toxin exchange between closely related bacteria [62]. CDI was first described in a rat enteric isolate of *Escherichia coli* (EC93) in 2005 [63]. In co-culture with *E. coli* MG1655, EC93 not only exhibits a growth advantage but it is able to prevent MG1655 cells from dividing, causing a reduction in viable MG1655 cells a thousand-fold over the course of 3 hours [63]. Unlike most previously described competition systems, EC93 only inhibits the growth of MG1655 when in close physical contact. Using a genomic library, EC93's contact-dependent growth inhibition phenotype was mapped to a 3-gene locus, *cdiBAI* [63]. Transferring these three genes to MG1655 is sufficient to create a lab strain with the same growth inhibition activity.

CDI was then bioinformatically observed to be widespread within the Proteobacteria, especially in pathogens [64]. CDI systems usually consist of three genes, though different arrangements and additional CDI-linked accessory elements also exist [65, 66, 67]. CDI systems have been most extensively studied in *E. coli* and *Burkholderia thailandensis*, which are distinguished as "*E. coli*"-type and "*Burkholderia*"-type CDI systems, respectively. In *Burkholderia*, the CDI locus is organized as *cdiAIOB* but has been named *bcpAIOB*, and encodes an additional linked gene (*bcpO*, a predicted lipoprotein) whose function in CDI unclear [65]. Growth inhibition is mediated by CdiB, an Omp85  $\beta$ -barrel protein, and CdiA, a very large (300-600 kDa) cell-surface protein. Together they form a Type Vb two-partner secretion system. Growth arrest of target cells is en-

tirely attributable to the carboxy-terminal 200-300 amino acids of CdiA, which comprise a modular effector domain (CdiA-CT) [64]. Inhibitor (CDI+) cells are protected from self-intoxication by expression of CdiI, an internally-expressed immunity protein which neutralizes its cognate CdiA-CT [68].

**Architecture and function of CdiA** CdiA is a multi-domain protein, consisting of both structural domains that appear to provide length and functional domains that are required to achieve growth inhibition (Figure 1.2). CdiA carries large regions of homology to filamentous haemagglutinin (FHA) from *Bordetella pertussis*, called FHA-1 and FHA-2 repeats. The FHA-2 region varies in size and number of repeats, leading to CdiA filaments of differing lengths. For instance, *Acinetobacter baumannii* encodes two CdiA proteins of different length, with the longer protein encoding a much larger FHA region [69]. Indeed, the class 4 CdiA protein introduced in Ch. 2 is also shorter than classes 1-3 because of a shorter FHA-1 domain. It's thought that these amino-terminal FHA-1 repeats form an elongated  $\beta$ -helix that extends CdiA away from the cell surface, perhaps to surpass any surface barriers that might block target cell association [70]. The carboxy-terminal FHA-2 repeats, in contrast, are predicted to form a conduit in the target cell OM to enable toxin translocation, though the conformation they adopt is unclear. In the center of both FHA domains (spanning residues  $\sim$ 1300-1600 in Enterobacteria) resides the receptor-binding domain (RBD) [71], which is most distal from the cell surface when CdiA is presented on the cell surface (Fig. 1.2). The RBD is polymorphic between CdiA proteins, and therefore has been used as a classification metric for CDI systems in *E. coli* [71].

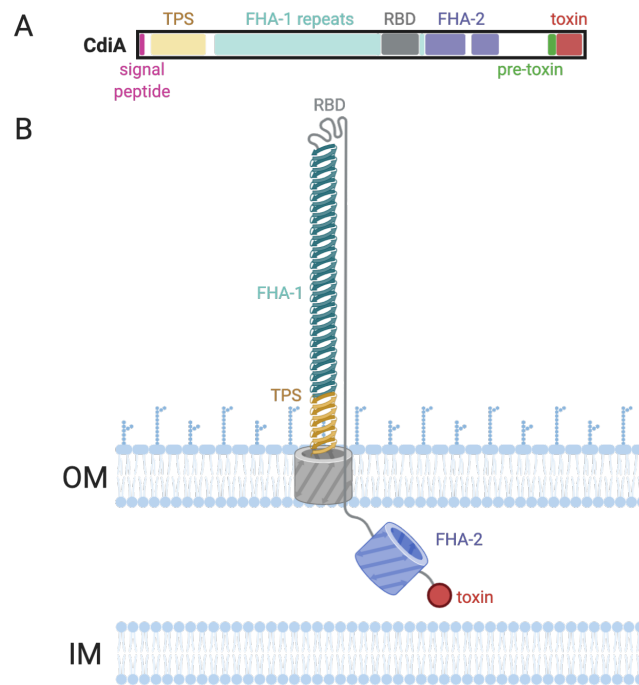


Figure 1.2: **Representative CdiA domain map and predicted surface topology.** (A) Organization of domains within the CdiA amino acid sequence. The class 4 protein from *E. coli* STEC O31–introduced in Ch. 2—is shown as an example. (B) Representative illustration of CdiA topology. The RBD is located at the distal tip, extended by 33 nm due to the presence of FHA-1 repeats, while FHA-2 and CdiA-CT are sequestered within the periplasm.

As previously mentioned, we have used the RBD to group CdiA proteins into classes based on the target cell receptor to which they bind. There are currently three classes of CdiA that have been described within the Proteobacteria. Like most proteins that bind surface receptors, CdiA has so far been observed to bind polymorphic  $\beta$ -barrel proteins, resulting in a restriction on the diversity of target bacteria to which it can inhibit [72]. Class 1 CdiA proteins are represented by CdiA from *E. coli* EC93 (CdiA<sup>EC93</sup>), which recognizes BamA [72]. CdiA from *E. coli* UPEC 536 represents Class 2 CdiA proteins (CdiA<sup>536</sup>), which require the heterotrimeric outer membrane porin proteins OmpC and OmpF for toxin delivery [73]. Finally, Class 3 CdiA binds the nucleoside transporter Tsx, and was isolated from *E. coli* STEC O31 (CdiA<sub>3</sub><sup>STECO31</sup>) [71].

Receptor-binding triggers toxin delivery, which is thought to occur through a  $\beta$ -barrel formed by the FHA-2 domain that is sequestered in the inhibitor cell periplasm until the RBD engages a receptor [70] (Fig. 1.2). This unique mechanism—termed secretion arrest—is supported by electron cryotomography and maleimide-labeling by cysteine scanning, which reveals that the C-terminal half of CdiA is inaccessible to dye labeling and is therefore compartmentalized in the periplasm prior to receptor-binding, resulting in a surface filament that is about half (33 nm) its predicted length [70]. Secretion arrest may be a mechanism used to maintain disorder of the FHA-2 and toxin domains to prevent  $\beta$ -barrel assembly or self-intoxication. Alternatively, receptor-triggered secretion of FHA-2 might exist to energize the process of delivery, since no energy source has yet been described for toxin delivery through the outer membrane of target cells during CDI.

Interestingly, immunoblots have revealed that CdiA in *E. coli* is expressed in its full length form anchored to the cell surface and, sometimes more abundantly by comparison, also as a C-terminal truncation  $\sim$  195 kDa in size which is secreted from the inhibitor cell [63, 74]. Although this secreted fragment contains no inhibitory activity in Enterobacteria, CDI in *Acinetobacter baumannii* appears to be unique; secretion of a 152 kDa fragment of the full  $\sim$  229 kDa protein mediates growth inhibition in a contact-independent manner [75]. Since this CdiA protein shares much of the domain architecture with previously identified CdiA proteins, it will be interesting to determine the physiological and mechanical basis for contact-independent inhibition in *Acinetobacter* and other relevant pathogenic bacteria which encode unique CDI systems.

**Delivery and activity of CDI toxins** With the exception of both toxins deployed by *E. coli* EC93's two CDI systems [68], all of the experimentally characterized CDI toxins to date have endonuclease activity [76, 77, 78, 79, 74, 80]. RNA appears to be the preferred target of CdiA-CTs, with the majority of deployed toxins targeting tRNA

molecules, though ribosomal RNases [81] and general RNases also exist [82]. Interestingly, many CDI toxins prefer to cleave specific tRNA molecules. Indeed, *Burkholderia pseudomallei* contains three CDI systems encoding CdiA-CTs of distinct tRNase activities [76]. Additionally, some CDI toxins also cleave DNA, such as the orphan toxin from *E. coli* EC869, which exhibits  $Zn^{2+}$  or  $Mg^{2+}$ -dependent nickase activity both *in vitro* and *in vivo* [77, 76], or a toxin from *Acinetobacter* which introduces double strand breaks [80]. Only two CDI toxins have been shown to disrupt the proton-motive force [68], and are therefore thought to form membrane pores.

Delivery of CdiA-CTs into target bacteria requires both the OM receptor that initiates translocation of CdiA into the target cell OM through an as-yet undescribed mechanism, but also requires an additional protein receptor in the IM. A single study identified five separate IM protein receptors (also referred to as cytoplasmic-entry proteins [83]) for CdiA-CTs, of which four are known endonucleases [79]. Besides *ycaB*, which appears to be involved in cell envelope biogenesis [84], four of the IM receptors identified are involved in nutrient uptake, including three ABC transporters and a phosphotransferase permease for D-glucose [79]. Presumably, cytoplasmic entry proteins enable CDI toxins to cross the phospholipid bilayer to reach their substrate. Indeed, endonuclease toxins are effective when expressed ectopically within the cytoplasm in the absence of their IM receptor [79]. The native transport activity of these permeases is not required for CdiA-CT delivery [79], though whether or not pore-forming toxins also use their receptor proteins to access the IM, and how they do so, is not known.

Much like colicins, CDI toxins contain modular N-terminal "cytoplasm-entry" domains specific for their IM receptor [79]. Thus, the NT of CdiA-CT is thought to mediate a direct interaction between the CDI toxin and its cytoplasmic-entry protein. Recently, biochemical approaches to studying CdiA-CT function have revealed some of the structural constraints CDI toxins are posed with to maintain function while also remain

amenable to translocation. With the endonuclease toxin from *E. coli* STEC MH1813 as a model, NMR and circular dichroism revealed the modular N-terminus is a molten-globule stabilized by two disulfide pairs that are absent from the enzymatic toxin domain [83]. Such a conformation could enable the entry domain to resist degradation following delivery into the periplasm, while remaining amenable to IM translocation. How the enzymatic toxin reaches its cytoplasmic substrate via the interaction between IM transporter and the cytoplasm entry domain, however, remains unclear since a direct binding interaction has yet to be shown. Thus, there is still much to be learned from how CDI toxins have evolved to exploit IM transporters for membrane transport.

In addition to the knowledge gap we have of CdiA-CT IM transport, there is still very little known of the pore-forming family of CDI toxins. Indeed, Ch. 4 was largely inspired by the mystery of how these unique pore forming toxins function. Before this study, which includes a collaborative investigation of EC93's toxin domains completed with Marcus Wäneskog and Sanna Koskiniemi, only a single CDI ionophore had been described [68]. Both ionophore toxins from EC93 share the same IM receptor - the efflux pump, AcrB [85, 86]. Characterization of CdiA-CT-1 from EC93 as an ionophore was achieved by measuring [<sup>14</sup>C]lactose transport, ATP depletion, ethidium bromide efflux [68], and more recently by uptake of the membrane-potential sensitive dye DiBAC<sub>4</sub>3 [86]. Interestingly, the effects of CdiA-CT-1 EC93 are reversible, since target cells can recover from CDI-induced reduction of steady-state ATP levels within 1.5 hrs [68]. Though nucleases clearly do not require the native activity of their IM receptors, it is unclear if drug binding/extrusion or proton transport activity of AcrB is required for pore-formation by EC93's toxins or if its presence in the IM is enough to facilitate toxicity. Interestingly, in contrast to the endonuclease toxins, pore-forming toxins are entirely ineffective at intoxication when expressed ectopically in the absence of their IM receptor (unpublished data, and also Fig. 4.9 and Fig. 4.10). IM receptor dependency from both the cytosol

and the periplasm is consistent with a receptor requirement for IM insertion, though it is surprising that insertion can be initiated from either face of the cytoplasmic membrane (this topic is explored further in Chapter 4).

Following IM passage, some CdiA-CTs require an additional cytosolic permissive factor for activation [78, 87, 88]. Permissive factors have been identified for the tRNase toxins from uropathogenic *E. coli* 536 (CdiA-CT<sup>536</sup>), which requires the biosynthetic enzyme O-acetylserine sulfhydrylase A (CysK) for activity, and from enterohemorrhagic *E. coli* EC869, which relies on the presence of translation elongation factor Tu (EF-Tu). Interestingly, EF-Tu is dispensable for *in vitro* activity by CdiA-CT<sup>869</sup> [78], possibly suggesting that the binding of CdiA-CT<sup>869</sup> to EF-Tu *in vivo* is physiologically relevant and could serve as a mechanism for cell-cell communication rather than antagonism. CdiA-CT<sup>536</sup>, however, requires CysK for activity even *in vitro*, complicating this interpretation. Since toxin unfolding likely occurs during IM translocation, permissive factors may also be one solution to maintaining thermodynamic stability of the re-folded toxin in the cytoplasm. Given the activity of CdiA-CT<sup>869</sup>, EF-Tu would be the ideal accessory factor for positioning tRNA substrates appropriately for cleavage. However, other CDI tRNase toxins do not require additional factors to achieve similar activities [79], but elucidating their intrinsic stability may clarify this discrepancy.

**Role of CDI in mixed bacterial communities** CDI was first characterized as a competition system, enabling CDI+ cells to directly kill and out-compete neighboring CDI- cells. However, this interpretation has been complicated by the often very specific activity of CDI toxins, the restricted target cell range of CDI, and the complex network of receptors and permissive factors required for toxin delivery, each providing a new opportunity for evolved resistance. The majority of CdiA-CTs target a specific population of tRNA molecules, which seems to be a very ineffective means of cell killing when com-



pared to the diverse effectors delivered by the T6SS. Due to receptor polymorphisms, toxicity can only be exerted on closely-related neighbors [72], and target cells can recover from the metabolic defects exerted by the pore-former CdiA-CT-1 from EC93 [68]. Additionally, each toxin requires a non-essential IM protein for translocation, with some toxins binding to additional cytosolic partners [78, 88]. In contrast with the T6SS, which targets a wider array of bacterial processes, T6 is not restricted by surface receptors, and causes noticeable cell lysis. Importantly, CDI's role in bacterial communities has only been studied under laboratory conditions, so whether or not CDI systems contribute to pathogenicity or host colonization has not been explored. With the data at hand, however, we are finally able to ask the question: do CDI systems mediate interbacterial signaling among siblings to regulate growth?

One clue may come from CDI in *B. thailandensis* strain E264. In the presence of cytosolic immunity, toxin delivery leads to upregulation of genes involved in biofilm formation [89]. The prevailing interpretation of CDI in *B. thailandensis* is that, being immunity-dependent, the benefit of communication via CDI can only be obtained from self-identifying bacteria (CDI+), while non-self bacteria (CDI-) are inhibited by the toxin and excluded. How the toxin-immunity pair mediates gene expression alteration in *B. thailandensis* E264 at a molecular level is not yet understood, but is thought to facilitate gene expression changes as a toxin-immunity complex. In *E. coli*, less work has been done to investigate the target cell response to CDI. That said, the Koskiniemi group has shown that at least 3 distinct toxins with both tRNase activity (from strains *E. coli* EC869 and UPEC 536) and pore-forming activity (from *E. coli* EC93) increase the frequency of persister formation via activation of the stringent response at high cell densities [90]. Moreover, a DNase toxin from *E. coli* EC869 (CdiA-CTo11 EC869) increases the rate of IS element transposition independent of the SOS DNA-damage response in toxin recipients lacking cognate CdiI while inducing filamentation, a hallmark of the DNA damage stress

response [77, 91]. Together, these results demonstrate that CDI systems in both  $\gamma$ - and  $\beta$ -proteobacteria may act as signaling systems that respond to increased cell densities in a contact-dependent manner.

An alternative hypothesis to explain the underwhelming antagonism of CDI systems is the possibility that CDI loci are purely selfish genetic elements that stabilize gene islands. Indeed, the cooperative behavior of CDI-expressing *B. thailandensis* is consistent with this interpretation since CDI+ bacteria receive a benefit from maintaining the locus, while CDI- bacteria are actively excluded from the community. Furthermore, the *bcpAIOB* locus is actually itself a mobilizable transposon, with the ability to circularize as an extrachromosomal element and transfer between self and non-self bacteria [92]. When encoded onto F-plasmid, EC93's CDI locus acts like an addiction system, stabilizing F-plasmid in the population [93]. Curiously, many bacteria encode multiple CDI systems, with most CDI+ genomes encoding at least two. EC93 carries two CDI systems, both of the same CdiA class with the same type of toxin that relies on the same IM receptor (AcrB) (Ch. 4). Though the two EC93 CdiA-CTs are not attached to the same CdiA protein, it would be hard to imagine how the cost of carrying both loci of functional redundancy is beneficial to the CDI+ cell since even the toxins will be competing to gain access to their IM receptor. However, EC93 clearly benefits from carrying this genetic element since it can dominate a co-culture with MG1655 and was found to out-compete all other native *E. coli* flora in the rat from which it was isolated [63]. Taken together, these data could suggest that CDI systems are selfish elements that exert a strong positive selection on their host for continued propagation within bacterial communities.

## Type VI

In addition to secreting effectors into the extracellular milieu, bacteria also carry contact-dependent competition systems to deliver toxins directly into neighboring cells. The Type VI secretion system (T6SS) is one of many protein secretion machines bacteria use to translocate proteins to the outside of the cell, into the extracellular space, and sometimes into eukaryotic cells [94]. The T6SS was first described in *Vibrio cholerae* in 2006 [95] and has now been studied in *Escherichia*, *Burkholderia*, *Agrobacterium*, *Aeromonas*, *Helicobacter* and *Campylobacter*, though bioinformatic evidence suggests it is even more widespread within Gram-negative bacteria [94].

T6 secretion systems are contractile toxin injection systems homologous to the tail spikes T4 phage use to deliver DNA into bacteria [96]. The T6SS, however, has evolved to deliver an array of toxic proteins into neighboring eukaryotic and bacterial cells, enabling the producing cell to directly kill its neighbors in a contact-dependent manner. The T6SS is formed by a complex of 13 conserved proteins and an array of variable toxic effector genes. The conserved structural T6SS proteins form a long contractile sheath which houses an inner tube and spike complex that is anchored in the producing cell's cytosolic membrane by a baseplate complex where contraction initiation occurs [97]. Rearrangement of the baseplate complex opens a pore through which the inner tube can pass, allowing it to physically puncture the target cell's membrane. Baseplate rearrangement causes a wave of conformation shifts of the sheath proteins from that of a high-energy to a lower-energy state which propels the inner tube outward [97]. The outward force from the sheath causes the inner tube to puncture a neighboring cell, delivering an array of toxins which decorate its structural proteins and affect the growth and viability the the target cell. Following toxin delivery, disassembly of the sheath occurs by protease activity of ClpV, which only recognizes the contracted form of the Type VI sheath pro-

tein TssC [98]. Fluorescence imaging of ClpV and T6SS components in *Pseudomonas aeruginosa* revealed that these sheath components can be recycled by the producing cell [98], which may lead to a quicker re-assembly of the sheath for another round of delivery. Indeed, live-fluorescence cell imaging has demonstrated that sheath contraction occurs in less than 5 ms [99].

Type VI effector proteins are diverse in both structure and function, taking the form of single-domain toxins as well as multi-domain proteins fusion proteins comprised of structural portions of the apparatus and effector domains. A thoroughly-studied example of the latter exists in the organism in which the system was discovered. *Vibrio cholerae* uses its Type VI apparatus to deliver an amidase toxin as a carboxy-terminal fusion to the a conserved structural protein VgrG (valine-glycine repeat protein G, VgrG3 in *V. cholerae*), which forms the spike complex that mediates target cell puncturing [100]. Additionally, Type VI loci encode the tip-sharpening PAAR proteins as well as a VgrG chaperone (effector-associated gene, Eag) that may also contain their own effector domains [101]. Since the interactions between the VgrG-PAAR-Eag complex of the apparatus is specific, meaning not all VgrG proteins can interact with all PAAR proteins to form a spike complex, this may allow the producing cell to control the cargo it delivers [102]. It appears that Hcp, the structural protein that self-assembles into hexameric rings to polymerize into the inner tube, may also exist in some species as a fusion protein for effector delivery [101]. Since independent toxins of similar activity can also be delivered to target cells without fusion to VgrG or Hcp, this may suggest that Type VI protein fusions are an outcome of selection for appropriate stoichiometry of effectors to structural proteins during self-assembly. If not delivered as a specialized fusion, toxins can be delivered as "cargo" by interacting with the inside of the hexameric Hcp ring for direct loading into the inner tube [101]. Though it might seem wasteful to load both fusion proteins and single domain toxins that share the same activity, the physical presence of

loaded cargo appears to serve as a checkpoint during Type VI secretion whereas VgrG-PAAR-Eag proteins do not [103].

Regardless of how they are loaded into the apparatus, the activity of Type VI effectors varies, ranging from cell wall and membrane-targeting enzymes such as amidases, lipases and pore-forming toxins to cytoplasmically-localized endonucleases [100]. Each toxin is encoded adjacent to an immunity gene that provides protection in case the producing cell becomes a target, suggesting that delivery of toxins by the T6SS can occur between sibling cells, and might even serve as a self-self recognition mechanism. Indeed, *P. aeruginosa* cells detect delivery events from siblings, since sister cells specifically assemble their T6SS machinery at the site of injection despite being protected from the delivered effectors [98]. A few Type VI toxins can also target eukaryotic cells. Several pathogens (including *V. cholerae*, *P. aeruginosa*, *B. pseudomallei* and *Klebsiella pneumoniae* encode specialized VgrGs that mediate actin cross-linking, fusion to host cell membranes or phospholipase activity that is effective against both eukaryotic and bacterial membrane lipids [101].

Despite being an energetic burden to build, the T6SS confers a fitness advantage to producing cells when grown in co-culture with susceptible bacteria [104, 105, 106, 107]. Since T6 effectors target essential and highly conserved cellular components in a broad range of target bacteria, at times causing rapid lysis of the recipient cell [100], it is likely that the T6SS has evolved as a mechanism to compete for resources and space.

## Type IX

More recently, the T9SS was described in *Bacteroidetes* spp., within the Fibrobacteres-Chlorobi-Bacteroidetes superphylum. The *Bacteroidetes* group is of immense importance for not only in human health, but also in carbon cycling, veterinary science, and agriculture [108, 109]. In contrast with some secretion systems which are specific for a single

cargo protein (e.g., hemolysin), T9 secretion enables its host to secrete an impressive array of cargo proteins outside of the cell. T9 cargo includes cell surface appendages responsible for gliding motility, virulence factors, a multitude of peptidases and proteases, in addition to proteins that have yet to be characterized but were identified as substrates of T9S by analysis of the C-terminal domain which marks a T9 substrate for secretion [110]. The diversity of T9 cargo proteins also means that the T9SS is important for many different lifestyles. Indeed, non-pathogenic *Bacteroidetes* isolates use T9S for gliding and food scavenging [111, 112], whereas pathogens use T9 secretion to for the secretion of virulence factors such as the surface-associated gingipains used by *Porphyromonas gingivalis* to cause chronic periodontitis [113].

Substrates for T9 secretion first pass through the Sec translocon in the IM, and then are deposited in the periplasm where they are transferred to the OM translocon formed by the T9SS. The T9 system contains at least 15 proteins that mediate transport from the IM to the cell surface. A group of four T9 proteins are present in the periplasm and thought to form a motor complex which energizes OM transport via the proton-motive force [114]. The OM translocon represents a novel mechanism for secretion in which the OM channel contains two alternative gates that alternate between open and closed states to shuttle cargo unidirectionally through the transporter [114]. Substrates destined for the T9 translocon carry a C-terminal 100-amino-acid signal domain, which is used not only as a signal for export but also facilitates post-translational modification and OM-attachment of T9 substrates following export [110]. However, the site of modification and cell surface attachment is not the CT signal domain itself. Post-translational modification of T9 substrates with A-LPS enables their incorporation into the OM, a hallmark of T9S, though the mechanism of A-LPS modification is still under study [112].

## 1.5 Permissions and Attributions

1. The content of Chapter 2 contains data collected in collaboration with Dr. Fernando Garza-Sánchez, Dr. Nicholas Bartelli, and Dr. Zach Ruhe.
2. Chapter 3 contains data collected also by Dr. Kiho Song, and is reproduced here with his permission.
3. The data in Chapter 4 was collected and interpreted in collaboration with Dr. Sanna Koskiniemi, Dr. Disa Hammarlöf, and Dr. Allison Jones.
4. Figures were created with BioRender.com.

## Chapter 2

# Lipidation of the CdiA receptor-binding domain promotes recognition of lipopolysaccharide on target bacteria

### 2.1 Abstract

Contact dependent inhibition (CDI) systems facilitate antagonistic toxin exchange between closely related bacteria in a proximity-dependent manner. CDI+ bacteria use the large cell surface protein CdiA to intoxicate their neighbors by binding to an outer membrane (OM) receptor. Receptor binding initiates cleavage and translocation of the ~200 carboxy-terminal residues of CdiA (CdiA-CT). Three OM receptors for CDI systems within the Enterobacteria have been described: BamA, OmpC/F, and TsX. Using the CDI locus from *E. coli* STEC\_O31 as a model, we introduce a fourth class of CdiA that exclusively binds to lipopolysaccharide. Genetic selections for resistant target cells reveal that mutations which disrupt the synthesis of the core oligosaccharide of LPS provide specific resistance to toxin delivery by CdiA<sub>4</sub><sup>STECO31</sup>. CdiA<sub>4</sub> is also linked to an accessory gene, *cdiC*, which encodes a predicted lysine acyltransferase. Site-directed mutagenesis suggests that CdiC and its close homologues form a subfamily of bacterial



lysine acyltransferases within the toxin-activating acyltransferase (TAAT) family. By analyzing peptide maps of the CdiA receptor-binding domain (RBD), we find that CdiC functions to modify CdiA at a lysine residue in the RBD. The modification adds a mass of 170 Da, which corresponds to a lysyl  $\beta$ -hydroxydecanoate moiety. We anticipate that lipidation by CdiC provides hydrophobicity to an otherwise polybasic region of CdiA, which appears to also be important for LPS binding. These findings present a new physiological application for bacterial protein lipidation, introduce a new family of accessory acyltransferases, and advance our understanding of the functional diversity of CDI systems and how they may initiate toxin translocation through the OM.

## 2.2 Introduction

Bacteria have evolved numerous mechanisms to compete for resources within dense, multispecies communities. Contact-dependent growth inhibition (CDI) is a Type Vb secretion system found throughout the  $\alpha$ -,  $\beta$ -, and  $\gamma$ -proteobacteria that is believed to provide a competitive advantage in these mixed communities by enabling a CDI-expressing cell (CDI+) to directly reduce the growth of neighboring cells in a proximity-dependent manner. CDI systems have been most intensively studied in *Escherichia coli* and *Burkholderia thailandensis* [63, 65], though functional CDI systems are widespread throughout the Proteobacteria [66, 67, 115]. CDI loci found within *Enterbacterales* are encoded as the gene cluster *cdiBAI*, differing from the arrangement of CDI genes found within *Burkholderia* spp. (*bcpAIOB* for *Burkholderia*-type CDI), which also contain an additional lipoprotein (BcpO) whose role in CDI is not fully understood [65].

Toxin delivery is achieved by CdiA, a large ( $> 250$  kDa) exoprotein that extends  $\sim 33$  nm away from the outer membrane, where it is anchored by its partner CdiB, an Omp85 outer-membrane  $\beta$ -barrel protein [70]. Deletion analysis of CdiA revealed that

the central  $\sim 300$  amino acids beginning around residue  $\sim 1300$  specify the receptor binding domain (RBD), which is also the most distal portion of CdiA relative to the cell surface [70, 72]. Receptor binding triggers the release of a C-terminal toxin domain (CdiA-CT) from the periplasm of the CDI+ cell (inhibitor) and into the cytoplasm of a neighboring cell (target), which culminates in the disruption of an essential cellular process [68, 77, 81]. Toxin translocation must then occur through the inner membrane as well, and is dependent on the presence of an inner membrane protein receptor that is specified by an amino-terminal cytoplasm-entry domain within the toxin [79, 83]. CdiA-CTs vary widely between CdiA proteins and have been shown to degrade DNA [74], cleave tRNAs [81], or dissipate the proton motive force [68] (see Chapter 4). CDI-expressing cells also carry a toxin-specific immunity protein (CdiI), which binds and inactivates CdiA-CT for protection against auto-inhibition [77].

We have previously described three families of *E. coli*-type CdiA proteins based on the outer membrane receptor to which they bind. Class 1 CdiA proteins are represented by CdiA from *E. coli* EC93 (CdiA<sup>EC93</sup>), which recognizes BamA [72]. CdiA from *E. coli* UPEC 536 represents class 2 CdiA proteins (CdiA<sup>536</sup>), which require the heterotrimeric outer membrane porin proteins OmpC and OmpF for toxin delivery [73]. Finally, class 3 CdiA binds the nucleoside transporter Tsx, and was isolated from *E. coli* STEC\_O31 (CdiA<sub>3</sub><sup>STECO31</sup>) [71]. Being exposed on the cell surface, a common feature of CDI outer membrane receptors is their sequence variability. The extracellular loops to which CdiA binds are divergent even within a species, greatly limiting the susceptible target cell range of CDI. Indeed, class 2 CdiA proteins were demonstrated to have the capability of inhibiting multiple species of *Enterobacteriales*, though inhibition efficiency appears to vary based on receptor divergence [116], further demonstrating that CdiA has a binding preference for receptors in genetically similar cells.

Here, we characterize a second CDI system from *E. coli* STEC\_O31 (*cdiBCAI*<sup>STECO31</sup>)

that is capable of delivering toxin into closely-related species of Enterobacteria by binding the core region of lipopolysaccharide. Intriguingly, the class 4 CdiA protein (CdiA<sub>4</sub>) is linked to an additional gene, *cdiC*, whose role in CDI was previously undescribed [66]. Here, we find that LPS binding by CdiA<sub>4</sub> relies in part on lipidation at a single lysine residue within the RBD, which is added by CdiC. Due to sequence homology and the results of site-directed mutagenesis, CdiC appears to belong to the toxin-activating acyltransferase (TAAT) family of bacterial proteins. We find that CdiC and its close homologues differ from TAAT proteins in that they are likely specific for their cognate CdiA proteins.

## 2.3 Results

### 2.3.1 Class IV CdiA recognizes the core oligosaccharide of LPS as a receptor

We previously reported the existence of a fourth class of CDI from *E. coli* STEC O31 [71], which contains a shorter CdiA protein with a unique RBD as well as an accessory acyltransferase, called CdiC (*cdiBCAI*, CdiA<sub>4</sub>) (Fig. 2.1). To verify the locus from STEC O31 is functional, we cloned the full CDI system onto a plasmid and transformed it into *E. coli* K-12. When in co-culture with wild type K-12 target cells, class 4 CDI inhibitors are evidently more effective than other CDI systems at killing EPI100 target cells (Fig. 2.1). High levels of inhibition are dependent on co-culture conditions, however, since growth inhibition is greatly reduced in liquid media relative to solid media (Fig. 2.1). Since CdiA proteins are classified by OM receptor, it stands to reason that the observed difference in growth inhibition may be due to the receptor CdiA<sub>4</sub> recognizes on target bacteria. Since Class 4 CdiA contains a unique RBD [71], it is unsurprising that target

cells lacking the receptors for CdiA classes 1-3 remain susceptible to CdiA<sub>4</sub> (Fig. 2.1). Thus, class 4 CdiA binds an as-yet unidentified receptor on target cells to deliver toxin.

To identify the outer membrane receptor for CdiA<sub>4</sub>, we performed iterative cycles of co-culture competitions with *mariner* transposon mutant libraries, until the target cell populations were fully resistant. Single colonies were isolated from each of six independent pools enriched for CDI-resistance (CDI<sup>R</sup>) and tested in separate competition experiments. To verify the transposon insertion itself is responsible for target cell resistance rather than a spontaneous mutation elsewhere in the genome, we back-crossed the transposon into the parental strain by transduction. The position of transposon insertions reveal that CDI<sup>R</sup> mutants are defective in biosynthesis of lipopolysaccharide (Fig. 2.2). Each CDI<sup>R</sup> mutant carries a gene-disrupting insertion in either *waaF* or *waaP*, with the exception of one mutant which contains a transposon insertion 235 base pairs upstream of *waaA*, a Kdo transferase and the only essential gene in the core biosynthetic pathway (Fig. 2.2). The *waaF* and *waaP* genes encode LPS heptosyltransferase II and LPS core heptose kinase, respectively [117, 118]. Importantly, no other transposon insertions were observed, despite the fitness cost of obtaining mutations in the LPS biosynthetic pathway.

The glycosyltransferase activity of WaaF results in the addition of Heptose II and subsequent sugar residues to the core, while the activity of WaaP is thought to be required for the addition of two phosphates and possibly Heptose III [119, 120]. Disrupting the activity of either enzyme would result in target cells lacking features of the inner LPS core region. We expect that mutation of *waaC*, which adds Heptose I to the core and would therefore act upstream of WaaF and WaaP in the biosynthetic pathway, should also result in resistance to CdiA<sub>4</sub> [117, 119]. We tested this possibility and also verified that the *waaP* and *waaF* insertions are not resistant due to polar effects on other genes in the LPS operon by creating new deletion strains of each *waa* gene by allelic exchange. As we anticipated, all three mutants (*waaC*, *waaF* and *waaP*) are CDI<sup>R</sup>. While generating the

$\Delta waaC$  strain, we noticed that removal of *waaC* carries a higher fitness cost than either  $\Delta waaF$  or  $\Delta waaP$ , suggesting that *waaC* transposon insertions were selected against in our initial screen.

Inner core LPS mutations result in the so-called "deep-rough phenotype", which has pleiotropic effects on the cell envelope. These include increased membrane permeability, decreased amount of outer-membrane proteins, increased susceptibility to detergents and hydrophobic antibiotics, and an increase in phospholipid content [121]. Therefore, we also removed a kinase from the *waa* locus that does not result in the deep-rough phenotype ( $\Delta waaY$ ) but instead results in the removal of a single phosphate moiety from the core, and found that  $\Delta waaY$  cells phenocopy the wild-type strain in competition with CdiA<sub>4</sub>. Therefore, it is either possible that the heptose region of LPS itself is the antigen for CdiA<sub>4</sub>, or that deep-rough LPS mutants are indirectly resistant to class 4 CdiA due to differences in OMP expression. To differentiate between these possibilities, we analyzed OmpC and BamA expression in each LPS mutant and tested the susceptibility of the  $\Delta waaF$  strain against all classes of CdiA. As anticipated, levels of OmpC and BamA are lower in the core mutants than in wild-type cells (Fig. 2.3), but inhibition by class 1 and class 2 (which recognize BamA and OmpC, respectively) scales with the observed OMP reduction in the *waaF* deletion strain (Fig. 2.3). Together, these results strongly suggest that the inner core region serves as the receptor for class 4 CdiA.

Monocultures of CDI<sub>4</sub><sup>STECO31</sup>-expressing wild-type *E. coli* K-12 produce CdiA in its full length (303 kDa) and  $\Delta$ -CT forms [70]. Therefore, the production of a doublet around  $\sim$  300 kDa indicates that strain is capable of toxin delivery. To test for the ability of each LPS mutant to conduct CdiA-CT cleavage and delivery, which requires an OM receptor to occur, we observed CdiA-CT processing in monocultures of each LPS mutant strain. Since CdiA<sub>4</sub> does not cross-react with antisera raised against previously studied CdiA proteins but contains a single cysteine residue N-terminal to the predicted RBD

(Cys1243, see fig. 4.2), we chose to use the Cys-reactive maleimide dye to monitor CdiA-CT processing by fluorimetry. Though the N-terminus of CdiA contains four Cys residues in addition to our site of labeling, in the absence of Cys1243 CdiA is undetectable by maleimide labeling, suggesting these cysteine pairs must form disulfides (Fig. 2.2). When introduced into each resistant target strain, the production of the CdiA-CT cleavage product is abrogated. Although some CT cleavage occurs in receptor-less monocultures, this phenomenon has also been observed for other CDI systems [70]. Notably, additional accumulation of the  $\Delta$ CT species is present when CdiA is expressed in the *waaP* deletion strain relative to *waaC* and *waaF*, though CT turnover still appears reduced relative to wild type and  $\Delta$ *waaY* (Fig. 2.2). These data suggest that self-delivery is inhibited by the absence of an intact LPS core, again indicating that the inner heptose region of LPS is required by class 4 CdiA for toxin delivery.

Finally, we sought to determine if we could detect a direct and specific binding event between CdiA<sub>4</sub> and LPS. Based on homology to CdiA class 2 from EC93 [71], we anticipate the RBD is encoded from position  $\sim$ Val1328 to  $\sim$ Pro1529 (Fig. 2.4). Under this hypothesis, we cloned the predicted  $\sim$  200 amino acid RBD region into an IPTG-inducible expression plasmid with a C-terminal hexa-histidine tag for purification, as well as an FLAG epitope just upstream of the His<sub>6</sub> tag to allow for detection by immunoblot. Since CdiA<sub>4</sub> binds to LPS, we reasoned that if this region encodes the RBD it should detectably associate with susceptible target cells, but not with LPS mutants that are CDI-resistant. Indeed, though some non-specific binding is detectable prior to washing the cells (data not shown) and remains associated with the  $\Delta$ *waaC* strain following a wash step (Fig. 2.4), only wild type and  $\Delta$ *waaY* target cells remain bound to RBD protein (Fig. 2.4). Taken together, these data indicate the receptor-binding domain of class 4 CdiA is encoded from V1328 - P1529, which binds to the core region of LPS on target cells to deliver toxin.

### 2.3.2 Class 4 CdiA delivers toxin into closely-related species

Since CdiA<sub>4</sub><sup>STECO31</sup> uses lipopolysaccharide as a receptor, we were interested in the possibility that class 4 CdiA proteins could deliver toxins into closely-related bacteria that are predicted to have a similar core oligosaccharide structure. We find that closely-related target species such as *Citrobacter* spp. and *Salmonella enterica* sv. Typhimurium LT2, with structurally similar inner core oligosaccharide regions, are susceptible to CdiA<sub>4</sub><sup>STECO31</sup> (Fig. 2.5), further supporting the conclusion that CdiA-CT delivery depends on the structure of the LPS core. Notably, however, inhibition differs between species: *Salmonella enterica* sv. Typhimurium LT2 is inhibited 10-fold less than *Citrobacter rodentium* DBS100 and *E. coli* MG1655 over the same 3-hour co-culture (Fig. 2.5). This inhibition is likely not due to differences in the core structure itself, however, since we tested *C. freundii* and a second isolate of *S. enterica* Typh. against CdiA<sub>4</sub> and found these additional strains are more susceptible than LT2 and *C. rodentium* (data not shown). We anticipate that other accessory genes, such as the T6SS found in *C. rodentium* or O-antigen on the surface of both of these more "wild-type" strains, may differentially protect these isolates from CdiA<sub>4</sub>.

### 2.3.3 CdiC promotes inhibition activity of class 4 CdiA

Class 4 CDI loci are linked to a putative lysine acyltransferase *cdiC* (Fig. 2.6). Interestingly, we find that deletion of *cdiC* does not completely abrogate inhibition of targets, but instead results in ~ 100-fold loss of growth inhibition activity (Fig. 2.6). CdiC shares 34% identity to members of the toxin-activating acyltransferase (TAAT) family of proteins (Fig. 2.6). Members of the TAAT family activate their substrate toxins by palmitoylation at one or two internal lysine residues using acyl carrier protein (ACP) as the fatty acid donor [122, 123]. Notably, CdiC shares conservation of the established

catalytic residues His23 (His37 in CdiC) and Asp93 (Asp107 in CdiC) required for TAAT activity [124] (Fig. 2.6). To determine if these residues are important for the function of CdiC, we replaced His37 or Asp107 with an alanine residue within the plasmid-encoded CDI locus. Both of the H37A and D107A CdiC mutants phenocopy the *cdiC* deletion strain and can be complemented with a chromosomally-encoded wild-type copy of *cdiC* integrated at *attTn7* under induction by the *araBAD* promoter (Fig. 2.6). Thus, CdiC is a member of the TAAT family and contributes to growth inhibition by class 4 CdiA.

### 2.3.4 CdiC modifies CdiA at residue Lys1467 with $\beta$ -hydroxy-decanoate

Since CdiA makes physical contact with LPS at the RBD, we reasoned that any modification which augments growth inhibition through biochemical alteration would take place within the RBD. To test this hypothesis, we again cloned the RBD region (see figure 2.4) with a C-terminal His<sub>6</sub> epitope tag (pRBD<sub>4</sub><sup>STECO31</sup>) and purified the resulting protein by Ni<sup>2+</sup> affinity chromatography in a *E. coli* K-12 DE3 strain co-expressing pCdiC from a compatible vector. Using reversed phase high-performance liquid chromatography (RP-HPLC), we found that RBD<sub>4</sub><sup>STECO31</sup> is more hydrophobic when co-expressed with CdiC, suggesting CdiA may be acylated (Fig. 2.7). We conducted the same RP-HPLC experiment in cells carrying either CdiC mutant allele and find that the Asp107Ala mutant has no activity in this assay, since there is no shift in polarity of the RBD protein by HPLC (Fig. 2.9). Interestingly, the His37Ala CdiC mutant evidently still has activity when measured by co-expression with RBD protein, though the accumulation of modified RBD is reduced to half (Fig. 2.9).

From our competition and RP-HPLC data, we anticipate the RBD is acylated with a hydrophobic moiety by CdiC. To determine the location and the amount of modifica-



tions within the RBD, we conducted peptide mapping by Arg-C (clostripain) digestion of purified RBD. We observe a single peptide from Arg-C digested CdiA-RBD that is affected by co-expression with CdiC (Fig. 2.7). The mass difference between the unmodified and modified peptide is 170 Da. This same  $\Delta$ mass is also observed with the full modified CdiA-RBD protein, suggesting a single modification is present within the RBD (Fig. 2.7). Intriguingly, the observed mass shift corresponds to a lysyl modification with  $\beta$ -hydroxydecanoate, a medium chain fatty acid. Since there are several lysine residues within the N-terminus of the modified peptide (Fig. 2.7). We first chose to analyze the 3 most proximal to the peptide's N-terminus to determine if any of the first 3 lysines in the modified peptide serve as a substrate for acylation (K1466, K1467 and K1469 in the full length CdiA protein). To test for modification of these candidate lysine residues within CdiA, we created three additional pRBD constructs with alanine substitutions at each lysine residue. When co-expressed in the presence of CdiC, the K1467A mutation completely prevents accumulation of the second HPLC peak, while the K1466A and K1469A mutant RBD proteins are still modified, though to a lesser extent than WT (Fig. 2.8). We also analyzed the mass spectra of each modified mutant RBD protein and verified that the  $\Delta$ mass between unmodified and modified CdiA-RBD is an average of 171 Da, as we observed for the wild type protein. To determine if all three lysines are important for modification in the full length protein or if only the K1467A mutant is relevant in the context of CDI, we introduced all three alanine mutations into CdiA within the full CDI locus and conducted co-culture competitions. From these results it is clear that only lysine 1467 is modified by CdiC in the full length protein, since a K1467A mutant has decreased activity but both K1466A and K1469A mutations phenocopy wild type CdiA (Fig. 2.11).

Surprisingly, inhibition by the K1467A mutant is less effective at inhibiting targets than a *cdiC* deletion (Fig. 2.11). If lack of a modification alone was responsible for this

loss of inhibition, we should observe the same defect in the CdiC null mutant. Since the absence of CdiC does not phenocopy K1467A, however, replacement of lysine with alanine must have a secondary effect on either biogenesis of CdiA or LPS binding. Using maleimide dye to detect surface-exposed CdiA (introduced in Fig. 2.2), we can eliminate the former possibility, since all of the CdiA mutants are expressed and delivered to the OM to similar levels (Fig. 2.11). Therefore, in the absence of a hydrophobic moiety, the presence of alanine instead of lysine appears to disrupt toxin delivery and thus inhibition of targets by CdiA<sub>4</sub>. We then hypothesized that, in addition to a hydrophobic moiety, CdiA<sub>4</sub> might also rely on electrostatic interactions with the core of LPS to establish a productive and specific binding interaction. Indeed, the amino acid neighborhood of lysine 1467 is highly cationic, in contrast with the rest of the protein and in contrast with the RBDs of other CdiA proteins, suggesting that basic residues within the RBD are important for CdiA<sub>4</sub> function (Fig. 2.7C). To test this hypothesis, we constructed two more CdiA mutants, containing either arginine or glutamine at position 1467. Consistent with our reasoning, the K1467R inhibitor strain phenocopies the *cdiC* deletion in co-culture competitions, but a K1467Q mutant inhibits to a similar degree as K1467A (Fig. 2.11). Interestingly, although Lys1466 is one residue upstream from the critical lysine that evidently mediates receptor binding, a K1466A mutant has no defects in inhibition (Fig. 2.11).

In summary, we have determined that the accessory acyltransferase CdiC promotes growth inhibition by CdiA<sub>4</sub><sup>STECO31</sup> through lipidation of the receptor-binding domain at a single lysine residue, which resides within a polybasic region that is likely important for LPS binding, since the absence of both lysine and a lipid moiety reduce growth inhibition to a greater extent than either defect alone.

### 2.3.5 CdiC acyltransferases are CdiA-specific

Since accessory acyltransferases can be found in many predicted class 4 CDI loci, we were interested to know if CdiC proteins have a broad substrate range, or if CdiC proteins are CdiA-specific. By comparison, TAAT proteins can modify non-cognate hemolysins even between species [124]. To explore this possibility, we obtained two different species of Enterobacteriales, both isolated from poison ivy (*Klebsiella* sp. RIT-PI-d and *Pantoea* sp. RIT-PI-b) that encode class 4 *cdiBCAI* loci (Fig. 2.12). CdiC<sup>STECO31</sup> shares 49% sequence identity with CdiC<sup>Pantoea</sup> and 64% with CdiC<sup>Klebsiella</sup> (Fig. 2.13). We used these CdiC proteins to complement our plasmid-based *cdiC* deletion strain via chromosomally-encoded *cdiC* genes at *attTn7*, which is capable of tunable complementation by addition of arabinose (Fig. 2.12).

When competed against wild type K-12 target cells, the only complemented  $\Delta$ *cdiC* strain to reach wild-type (*cdiC*+) levels of growth inhibition is CdiA<sub>4</sub> complemented with its cognate acyltransferase, CdiC<sup>STEC4</sup> (Fig. 2.12). Notably, though Lys1467 is conserved in the receptor binding domains of all three CdiA proteins, there is variability in the surrounding sequence where CdiC might bind (Fig. 2.12). Thus, at least for these three CDI systems, CdiC acyltransferases exhibit substrate specificity.

## 2.4 Discussion

Functional CDI systems have now been studied in several Enterobacteria [63, 64, 66], Burkholderiales [65, 125, 126] and Pseudomonadales [115]. In general, CDI loci contain three genes. They encode an Omp85 family outer membrane  $\beta$ -barrel protein (CdiB), a very large cell surface filamentous protein (CdiA) containing a C-terminal effector domain (CdiA-CT) and small immunity protein that protects against self-delivery (CdiI). Notably, however, CDI loci within *Burkholderia* spp. contain an additional lipoprotein

(BcpO) whose role in CDI is yet to be fully understood [65], and many CDI loci in Enterobacterales contain an additional gene (*cdiC*) that is homologous to accessory acyl-transferases associated with hemolytic toxins that require post-translational lipidation to become activated [66]. In addition to an accessory element, *cdiC*-containing CDI loci encode CdiA proteins with an uncharacterized class of receptor-binding domain. Here, using a combination of genetic and biochemical techniques to study the *cdiBCAI* locus from *E. coli* STEC\_O31 (NCBI 754081), we find that this newly identified receptor-binding domain requires the activity of CdiC to achieve LPS-binding of the target cell. Together, our genetic selection for CDI<sup>R</sup> mutants (Fig. 2.2), decreased CdiA-CT delivery in LPS inner core mutants (Fig. 2.2 and 2.3), cell binding assay with purified CdiA-RBD (Fig. 2.4), and the range of susceptible species to CDI<sub>4</sub><sup>STECO31</sup> (Fig. 2.5) demonstrate that the conserved core region of LPS serves as the outer membrane receptor for CdiA<sub>4</sub>. Additionally, by observing RP-HPLC traces of CdiA-RBD protein purified in the presence of CdiC, we find that CdiC modifies CdiA at a single residue (K1467) within a polybasic region of the RBD with  $\beta$ -hydroxydecanoate (Fig. 2.7 and Fig. 2.8), as indicated by mass spectrometry.

CDI in *Burkholderia pseudomallei* 1026b appears to rely on LPS as well, since CDI<sub>R</sub> transposon mutants carried insertions in a predicted lipopolysaccharide transglycosylase [126]. However, CDI<sup>1026b</sup>-resistant mutants were also isolated with insertions in two other genes of unknown function. At least one of these strains is fully resistant to CDI<sup>1026b</sup>, and neither gene deletion compromises toxin susceptibility when expressed internally, suggesting that there may be additional outer membrane receptors for the *Burkholderia* CDI pathway besides LPS, in contrast to CdiA<sub>4</sub><sup>STECO31</sup>.

Lipidation of CdiA<sub>4</sub><sup>STECO31</sup> occurs via a functional homologue of the TAAT protein family, CdiC. Inhibitor strains lacking *cdiC* exhibit a 100-fold loss of growth inhibition that is not due to a loss of CdiA expression (Fig. 2.11). Rather, this defect is caused by

the loss of  $\beta$ -hydroxydecanoate at K1467 within the RBD, since a K1467R mutant, which is not a substrate for CdiC, phenocopies the  $\Delta cdiC$  strain (Fig. 2.11). K1467 resides in the middle of the RBD, which interfaces directly with the target cell outer membrane (Fig. 1.2). Thus, in the absence of a protein receptor, CdiA<sub>4</sub> may use  $\beta$ -hydroxydecanoate as a hydrophobic anchor in the lipid bilayer, presenting the intriguing possibility that FHA-2 insertion for CdiA<sub>4</sub> begins at position 1467 [70]. Indeed, lipopeptides, amphiphilic peptides modified with a lipid group, disrupt the Gram-negative outer membrane by direct insertion into the bilayer, a mechanism which has been well-studied in polymyxins [127, 128, 129, 130]. Therefore, our findings may contribute to further studies on the CDI toxin delivery process by providing a unique tool to probe both the nature of the OM receptor interaction and receptor-triggered FHA-2 insertion.

Unmodified CdiA<sub>4</sub> is still functional, suggesting lipidation must be coupled to additional LPS-CdiA interactions. Intriguingly, the region around Lys1467 where LPS binding must occur is enriched with basic amino acids and three successive tyrosine residues (Fig. 2.7). The unique sequence around K1467 may indicate that electrostatic interactions also take place between CdiA and the inner core of LPS. In fact, polymyxin antibiotics rely on this same cationic/hydrophobic combination of interactions to disrupt the OM of Gram negative bacteria. Indeed, if FHA-2 eventually inserts itself into the target cell OM, insertion would likely begin adjacent to the site of receptor binding. In fact, the three tyrosine residues upstream of Lys1467 could play a critical role in initiating the insertion of FHA-2 into the bilayer since tyrosine residues are known to become embedded in phospholipid bilayers [131, 132]. Even more intriguing is that polymyxin nonapeptides lacking their N-terminal fatty acid can still associate with the outer membrane [128, 129] and require only a small number of cationic residues to do so [130]. We anticipate, therefore, that the addition of a hydrophobic moiety would cooperate with the surrounding cationic residues to bind the LPS inner core prior to an insertion event.

In support of this possibility, we find that substituting K1467 with alanine or glutamine is more disruptive for CDI than making the same substitution with arginine (Fig. 2.11), which mimics the remaining lysine residue in a CdiC null. Although amide formation with  $\beta$ -hydroxydecanoate would replace the lysyl amino group with a large, hydrophobic moiety, loss of both size and charge of the remaining amine group in the absence of CdiC could disrupt electrostatic interactions with the polybasic region near K1467. Curiously, however, replacement of Lys1466 just upstream of the critical lysine residue has no effect on inhibition or CT processing (Fig. 2.11). The only visible effect of the K1466A mutation is on accumulation of a modified RBD protein by RP-HPLC (Fig. 2.8), but in the absence of physiological evidence for a defect in full length CdiA, these data might indicate that the alanine mutant RBD proteins may either be less stable during over-expression or bind CdiC with less affinity in the cytosol. Since they can be purified to similar levels as WT (Fig. 2.10), the latter hypothesis may be true. Thus, we anticipate that lipidation by CdiC is an adaptation for reaching the inner core of LPS to establish a productive binding and toxin translocation event. It is important to note that a 100-fold defect in growth inhibition due to a lack of lipidation under laboratory conditions may translate to a much greater difference, or even complete loss of efficacy, when CdiA is deployed by pathogens in their natural environment.

Hemolytic toxins from Gram-negative bacteria such as *Bordetella pertussis* (CyaA) and *E. coli* UTI89 (HlyA) rely on a similar lipidation event to increase the unmodified toxins' affinity for erythrocyte cell membranes [133]. Hemolysin modification also occurs by an accessory lysine acyltransferase (e.g., CyaC in *B. pertussis*, HlyC in *E. coli*). Hemolysins maintain some toxicity in the absence of modification, similar to the behavior of unmodified CdiA<sup>STEC4</sup> [122]. Hemolysin acyltransferases form the TAAT protein family, all of which are required to activate their toxin substrates through palmitoylation of internal lysine residues via an amide linkage with acyl carrier protein as the fatty acid

donor [123, 134, 135]. An immediate difference between hemolysins and CdiA is the size of fatty acid added for membrane association - CdiA is modified with a 10-carbon medium chain fatty acid, which is much smaller than the saturated 14-carbon chains added to hemolysins. However, CdiA is destined for the bacterial outer-membrane rather than an erythrocyte phospholipid bilayer. As such,  $\beta$ -hydroxydecanoate mimics the *N*-linked 3-hydroxytetradecanoyl chains attached to the glucosamine groups of lipid A. Thus, the hydrophobic moiety attached to CdiA mirrors the role fatty acids play in insertion of hemolysins into eukaryotic lipid bilayers, further supporting the idea that we may have discovered the position where OM insertion of FHA-2 begins.

Members of the established TAAT family share  $\sim 70\%$  sequence identity and can directly substitute for one another during toxin activation [124]. CdiC shares 34% sequence identity to this family of acyltransferases, including two established active site residues (H37 and D107 in CdiC) as well as a TAAT-specific insertion and deletion (Fig. 2.6), and cannot be substituted for by a homologous CdiC protein (Fig. 2.12). However, CdiC contains a conserved hydrophobic TAAT motif shown to be critical for dimerization of ApxIC (G25/V28/M32 in CdiC and G12/A15/A19 in ApxIC), though the functional relevance of TAAT dimerization is not yet understood and this region is preceded by an N-terminal extension in CdiC which may affect its ability to form dimers (Fig. 2.6). CdiC also differs from TAAT proteins in that it appears to lack two important active site residues conserved in this family of proteins that are functionally important for toxin activation (Arg121 and Asn35), with Arg121 responsible for mediating direct interaction with ACP [124]. Indeed, HlyC from *E. coli* UTI89 (accession: Q1R2T4) cannot substitute for CdiC-mediated lipidation of CdiA<sup>STEC4</sup> (Fig. 2.6), suggesting CdiC and other CdiA-associated acyltransferases form a distinct group of accessory lysine acyltransferases within the established TAAT family. Interestingly, though alanine replacement of His37 phenocopies a *cdiC* null in competitions, consistent with a previous structural

study [124], over-expression of CdiC<sup>H37A</sup> and CdiA-RBD leads to partial modification, in contrast with CdiC<sup>D107A</sup> which completely abrogates modification (Fig. 2.9). Thus, of the two possible mechanisms for toxin activation proposed by Greene et al. [124], our data suggest that the direct attack mechanism, in which Asp107 deprotonates the lysyl amine group and His37 simply serves as a general base which can be substituted for by water, is the most likely.

Two-partner secretion (TPS) proteins contain an N-terminal signal peptide required for Sec-dependent translocation across the inner membrane. In contrast with class 1 – 3 CdiA proteins, CdiA<sup>STEC4</sup> contains an extended signal peptide, which has been observed in other TPS proteins and shown to prolong secretion at the inner membrane to promote proper folding [136, 137]. Compared to RTX toxins, which are exported through the T1SS and therefore must be fully synthesized prior to secretion, CdiA folding and modification may be linked to secretion through the Sec translocon. Indeed, the presence of an extended signal peptide may modulate secretion rate of CdiA<sup>STEC4</sup> to facilitate modification in the cytosol by CdiC.

## 2.5 Materials and Methods

**Growth conditions and competition co-cultures.** All strains were grown at 37 °C in lysogeny broth (LB) or on LB agar unless otherwise noted. Media were supplemented when appropriate with antibiotics at the following concentrations: ampicillin (Amp) 150  $\mu\text{g mL}^{-1}$ ; kanamycin (Kan) 50  $\mu\text{g mL}^{-1}$ ; chloramphenicol (Cm) 66  $\mu\text{g mL}^{-1}$ ; gentamycin (Gm) 15  $\mu\text{g mL}^{-1}$ . For all competition co-cultures, both strains were grown to an optical density at 600 nm ( $\text{OD}_{600}$ ) of 0.6 - 0.9 and mixed at an equal ratio of  $\text{OD}_{600}$  (3.0:3.0), plated in a 15  $\mu\text{L}$  volume on LB agar and incubated 3 hours at 37 °C. Cells were harvested with a sterile swab into 1×M9 salts and ten-fold serial



dilutions were plated on the appropriate antibiotics to enumerate inhibitor and target colony-forming units per milliliter (CFU/mL). Competitive indices were calculated as the ratio of inhibitor to target cells at 3 hrs relative to their starting ratios. Each co-culture was repeated at least three times

**Plasmid and Strain Construction.** The *cdiBCAI* gene cluster (EJK97215 - EJK97218) was amplified from *Escherichia coli* STEC\_O31 (taxid: 754081) genomic DNA using oligonucleotides ZR258 and ZR259, digested with NotI/XhoI, and ligated into pET21b to generate pET21b-*cdiBCAI*<sup>STEC4</sup>. To facilitate genetic manipulation using restriction enzymes within the plasmid-encoded locus, we utilized a previously generated CDI plasmid lacking the multicloning site [70]. The NotI/XhoI fragment from pET21b-*cdiBCAI*<sup>STEC4</sup> was ligated with pET21b-*cdiBCAI*<sup>STEC3</sup> MCS- [70] to create pET21b(MCS-)-*cdiBCAI*<sup>STEC4</sup>, which was used to generate point mutations in CdiA and CdiC. The immunity gene, *cdiI*<sup>STEC4</sup>, was amplified with CH4869/ZR259, digested with KpnI/XhoI and ligated into pTrc99aKX.

The  $\Delta wzb$  mutation was introduced into *E. coli* K - 12 EPI100 by transduction, made possible through the expression of RecA from a modified pSIM6 [138]. The Lambda-Red recombinase genes were replaced with RecA by digesting pSIM6 with BglII/XmaI and ligation with the MG1655 gDNA product of primers CH2131/CH2132. OmpC and Tsx were removed from target cells by phage transduction of lysate originating from the Keio deletion strain [139]. BamA with a deletion of loop 6, the epitope by which class 1 CdiA binds to target cells, was introduced into EPI100 target cells also by transduction from a previously generated strain [72]. LPS biosynthetic mutations were introduced into EPI100  $\Delta wzb$  (CH7175) by recombineering with a kanamycin resistance cassette flanked by regions of sequence homology. The upstream and downstream homology arms were amplified with the following primer pairs: CH4195/CH4196 and CH4197/CH4198 (*waaC*), CH4199/CH4200 and CH4201/CH4202 (*waaP*), CH4203/CH4204 and CH4205/CH4206

(*waaY*) from *E. coli* K-12 MG1655. Upstream homology regions were digested with SacI/BamHI and downstream with EcoRI / KpnI and each ligated into pKAN to flank a kanamycin resistance cassette. The resulting plasmid was PCR amplified with the outer primer pair, DpnI digested, and recombined onto the chromosome of CH7175, carrying pSIM6. Recombinants were selected for on Kan-supplemented LB agar. The *waaF::kan* allele was amplified with primers CH4299/CH4300 from the Keio deletion strain [139] and directly recombined into CH7175 carrying pSIM6. For complementation of LPS deletion mutants, the following primers were used to amplify each gene: CH4387/CH4388 (*waaC*), CH4207/CH4208 (*waaF*), and CH4209/CH4210 (*waaP*), digested with NcoI/XhoI, and ligated into pCH450.

To generate a *cdiC* deletion mutant, we took advantage of unique restriction sites within pET21b(MCS-)-*cdiBCAI*<sup>STEC4</sup>. A fragment was generated with primers ZR258 and ZR253, digested with AscI/NotI, and ligated to remove the majority of *cdiC* from the locus. The resulting plasmid (pET21b(MCS-)-*cdiBCAI*<sup>STEC4</sup>  $\Delta$ *cdiC*) contains 81 bp of *cdiC*. OE-PCR was used to generate CdiC point mutations within pET21b(MCS-)-*cdiBCAI*<sup>STEC4</sup>. Two PCR products were generated from the native locus with either ZR258/CH4177 and CH4176/CH4088 (for mutation of His37) or ZR258/CH4175 and CH4174/CH4088 (for Asp107). Each pair was combined into a single fragment by OE-PCR, digested with NotI/XhoI and ligated into pKAN. The resulting shuttle vector was then digested with AscI/NotI-HF and ligated back into pET21b(MCS-)-*cdiBCAI*<sup>STEC4</sup>. For complementation of CdiC deletion or point mutants, *cdiC*<sup>STEC4</sup> (EJK97216) and *hlyC*<sup>UTI89</sup> (ABE10330), and either *cdiC* homologue from *Pantoea* sp. RIT-PI-b and *Klebsiella* RIT-PI-d were cloned first onto the arabinose-inducible plasmid pCH450 and then sub-cloned onto the mobilizable plasmid pUC18R6k-miniTn7T for insertion onto the chromosome with P<sup>BAD</sup>. CdiC was amplified from pET21b(MCS-)-*cdiBCAI*<sup>STEC4</sup> with primer pair CH4087/CH4088. *HlyC*<sup>UTI89</sup> (taxid: 754081), CdiC<sup>Pantoea</sup> and CdiC<sup>Klebsiella</sup>

were amplified by colony PCR, and digested either with NcoI/XhoI (*HlyC*) and ligated into pCH450 or with KpnI/XhoI (CdiC<sup>Pantoea</sup>/CdiC<sup>Klebsiella</sup>) and ligated into pCH450kpn. After we determined plasmid burden was an issue during complementation with CdiC in trans from pCH450 itself, each plasmid was then digested with NsiI/XhoI and ligated into pUC18R6k-miniTn7T-Gmr to generate mobilizable plasmids with each acyltransferase linked to P<sup>BAD</sup> and a gentamycin resistance cassette that could be integrated at the *attTn7* site at *glmS* [140]. Using these constructs, integration of the acyltransferase was accomplished biparentally with the MFD<sub>pir+</sub> mating strain. Equal ratios of the two donors (CH14478 and either CH4873 for *cdiC*, CH7787 for *hlyC*, CH7389 for CdiC<sup>Pantoea</sup> RIT-PI-b, or CH7379 for CdiC<sup>Klebsiella</sup> RIT-PI-d) and MC1061 were mixed from overnight cultures in 100  $\mu$ L, plated on a 25 mm 0.22  $\mu$ m filter and incubated at 37 °C for 4 hours. The resulting integrants were selected on Gm15 and the insertion site verified by colony PCR with primer pairs CH4672/CH4616.

In order to generate CdiA point mutations within the plasmid-encoded CDI locus, the following primers were paired with CH4802 or CH4761 (K1467A and K1466A) to create a megaprimer carrying each mutation, to be used in a second PCR reaction: CH4841 (K1466A), CH4647 (K1467A), CH4648 (K1469A), CH4888 (K1467R), and CH5186 (K1467Q). Each megaprimer was paired with CH4803 or CH4760 (K1466A and K1467A) in a second PCR reaction with the wild type locus as a template and the resulting fragment digested with NotI-HF/XhoI and ligated back into pET21b(MCS-)-*cdiBCAI*<sup>STEC4</sup>.

For protein purification, *cdiC*<sup>STEC4</sup> was amplified from pET21b(MCS-)-*cdiBCAI*<sup>STEC4</sup> WT as well as pET21b(MCS-)-*cdiBCAI*<sup>STEC4</sup> CdiC [H37A] and pET21b(MCS-)-*cdiBCAI*<sup>STEC4</sup> CdiC [D107A] with oligos CH4087/CH4088. All 3 PCRs were digested with NcoI/XhoI, and ligated into pET21b to generate three CdiC clones (WT, H37A and D107A) that could be co-expressed with pCdiA-RBD. The delineated RBD was then am-

plified from either the WT locus (pET21b(MCS-)-*cdiBCAI*<sup>STEC4</sup>) or each mutant derivative (i.e., K1466A, K1467A, K1469A, K1467R, K1467Q) with primers CH4358/CH4359, digested with NcoI/XhoI and ligated into pACYC-DUET to generate 5 RBD constructs for co-expression with pET21b-*cdiC*. For purification of an epitope-tagged RBD construct for cell binding assays, the reverse forward was replaced with CH5468, which encodes a FLAG epitope, to generate a RBD protein with an N-terminal FLAG tag and a C-terminal his<sub>6</sub> tag.

**Transposon mutagenesis to identify CDI-resistant mutants.** The mariner transposon was introduced into CH7175 by conjugation with MFDpir cells carrying pSC189 [141, 142]. Donors were supplemented with 30  $\mu$ M diaminopimelic acid in shaking liquid LB and grown to mid-log at 37 °C. Donors and recipients were mixed and plated on LB agar at 37 °C for 5 hrs. Cell mixtures were harvested with a sterile swab, collected in 1×M9 media, and plated on Kan-supplemented LB agar for selection of transposon integrants. Each of six mutant pools were harvested into 1mL 1×M9 media for selection and subjected to selection by co-culture with MC1061 carrying pET21b(MCS-)-*cdiBCAI*<sup>STEC4</sup>. The surviving colonies of each pool were collected again into 1mL 1×M9 media and subjected to two more rounds of co-culture selection. After three rounds, presumptive CDI-resistant clones were randomly selected from each independent transposon mutant pool. Transposon insertion sites were determined by rescue cloning. Chromosomal DNA from each resistant mutant was digested overnight with NspI at 37 °C followed by a 20 min inactivation step at 65 °C. Each reaction was supplemented with ATP and T4 Ligase and incubated overnight at 16 °C. The reactions were electroporated into *E. coli* DH5 $\alpha$  *pir*+ cells. Plasmids from the resulting kanamycin-resistant colonies were isolated and transposon insertion junctions identified by sequencing using primer CH2260.

**Lipopolysaccharide purification and gel electrophoresis.** To purify LPS from EPI100 deep-rough mutants, *C. rodentium* and *S. Typhimurium*, 2 mL portions of over-

night cultures were normalized to OD<sub>600</sub> 2.0 and their LPS collected using a LPS Extraction Kit (iNtRON Biotechnology). Approximately 9  $\mu$ g of LPS from each sample was loaded onto a 13% polyacrylamide gel and run for 1 hr at 110 V. The gel was stained with Pro-Q Emerald 300 Lipopolysaccharide Gel Stain Kit (ThermoFisher) and imaged on a Kodak 200 Gel Logic UV trans-illuminator.

**Protein Purification, HPLC and ESI-MS analysis.** His<sub>6</sub>-tagged CdiA<sup>RBD</sup> constructs were overproduced in CH2016 [143] in 150 mL LB with aeration from overnight cultures supplemented with the appropriate antibiotics (220 rpm, 37 °C). Expression of CdiC was allowed to accumulate in the absence of inducer due to inefficient repression by LacI on pTrc99a. Once the cultures reached OD<sub>600</sub> 2.5, 1 mM isopropyl- $\beta$ -D-thiogalactosidase was added to allow expression of CdiA<sup>RBD</sup> from pACYC-Duet. After 60 mins of induction, pellets were collected and resuspended in 12 mL denaturing buffer (6 M guanidine-HCl/10 mM Tris-HCl, pH 8.0) then frozen overnight at -80° C. Lysates were prepared by quickly thawing the cultures and pelleting insoluble material by centrifugation at 15,000 rpm for 15 min. Soluble lysates were supplemented with 10 mM imidazole, treated with 300  $\mu$ L Ni<sup>2+</sup>-nitrilotriacetic acid (NTA) (Qiagen) and prepared for RP-HPLC by rinsing 3 times in wash buffer (8M urea/10 mM imidazole), 2 times in 8M urea only, and finally eluted with 8M urea/200 mM acetic acid. Total protein concentration was calculated by absorbance at 280 nm with a NanoDrop Spectrophotometer (Thermo Fisher). Equal volumes of eluent were observed by separation by SDS-PAGE and staining with Coomassie R-250. Finally, normalized concentrations of protein were injected into a Vydac 15 $\times$ 300 mm C4 column and separated by a 65 min reversed-phase high performance liquid chromatography gradient of 0.01% trifluoroacetic acid and 80% acetonitrile (v/v) using a Waters 1525 binary pump, monitored at 214 nm. The mass of RP-HPLC-purified proteins was determined by electrospray ionization on a Waters Xevo Gz-XS Time-of-Flight Mass Spectrometer, and MassLynx was used for computation.

**Co-sedimentation assay to measure RBD-cell binding.** To assay RBD association with whole cells, FLAG-RBD-his<sub>6</sub> was natively purified from an *E. coli* DE3 strain over-expressing pET21-RBD<sup>STEC4</sup>-FLAG-his<sub>6</sub> with Ni-NTA. For cell binding, strains were grown as overnight cultures with the appropriate antibiotics. Overnight cultures were then normalized to OD<sub>600</sub> 10.0 by centrifugation at 10,000 RCF for 1 min and by re-suspension in the appropriate volume 1×LB. A protease inhibitor cocktail was added to each cell suspension (0.1 mM Leupeptin, 0.01 mM Pepstatin, 1 mM PMSF, and 0.1 mM TLCK) before the addition of 5.1 μM FLAG-RBD-his<sub>6</sub> protein. Samples were then incubated at RT for 5 mins, washed once with 1 mL LB to remove excess RBD protein, centrifuged at RT at 100,000 RPM for 5 min, and the supernatant was removed. The remaining pellet was suspended in 100 μL 1×LB. Samples were treated with SDS load dye, heated for 10 mins at 95 °C and loaded onto a 12% SDS-PAGE gel for separation and visualized with either immunoblotting or staining of total protein by Coomassie R-250 Brilliant Blue. Detection of FLAG-tagged RBD was accomplished with a mouse anti-FLAG primary and a 800CW secondary antibody which was visualized with a LI-COR Odyssey infrared imager.

**Immunoblotting.** To detect outer-membrane proteins in LPS mutants, 2 mL cultures in Kan supplemented LB media were grown to stationary phase (> OD600 1.5) at 37° C. Approximately  $3.2 \times 10^9$  cells were harvested from each culture and frozen at -80 °C. Frozen cell pellets were resuspended in 75 μL urea lysis buffer and frozen a second time. The frozen suspension was quickly thawed at 42 °C and spun at 14,000 rpm at 4 °C for 20 minutes to remove insoluble material. The remaining urea-soluble lysate was analyzed by Bradford reagent and the same amount of protein was loaded for all samples onto three separate 10% SDS-PAGE gels for separation at 100 V for 2 hrs. To observe total protein content, one gel was treated with Coomassie R-250 for 60 mins and de-stained overnight. Protein from the remaining two gels was transferred to

polyvinylidene difluoride (PVDF) membranes (1 hr at 17 V) and analyzed with anti-BamA or anti-OmpC antisera. The 800CW secondary antibody was visualized with a LI-COR Odyssey infrared imager.

## 2.6 Tables and Figures

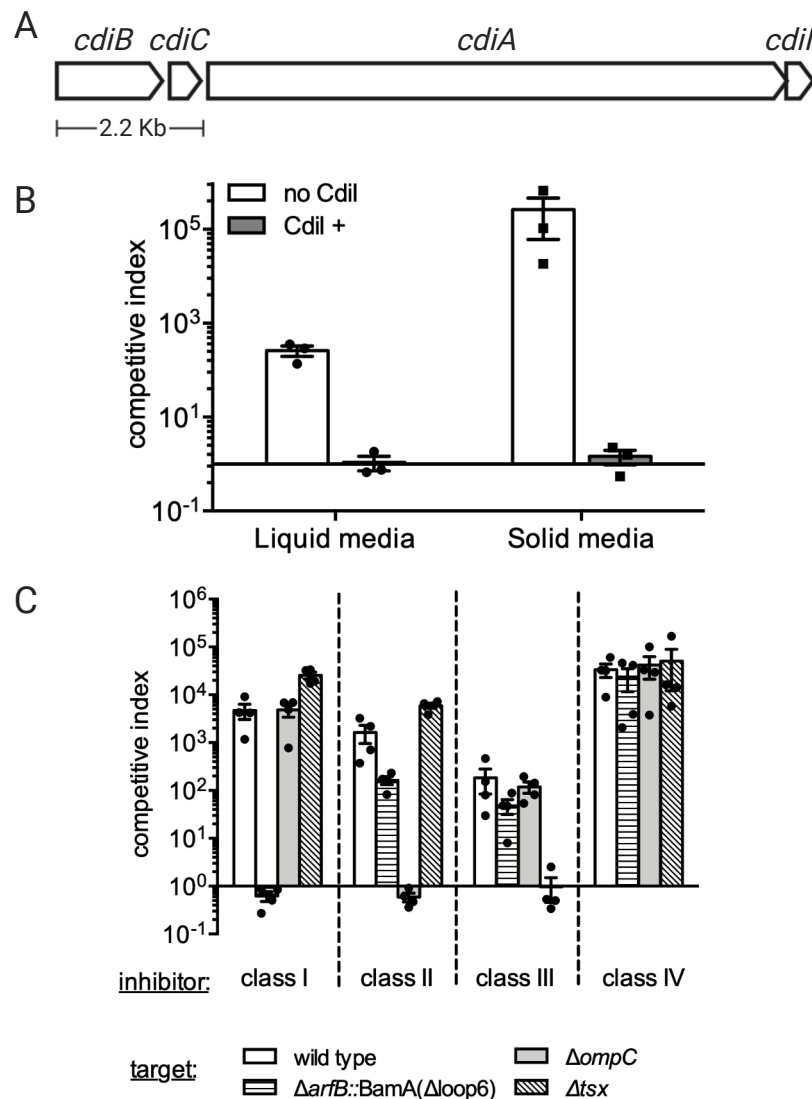
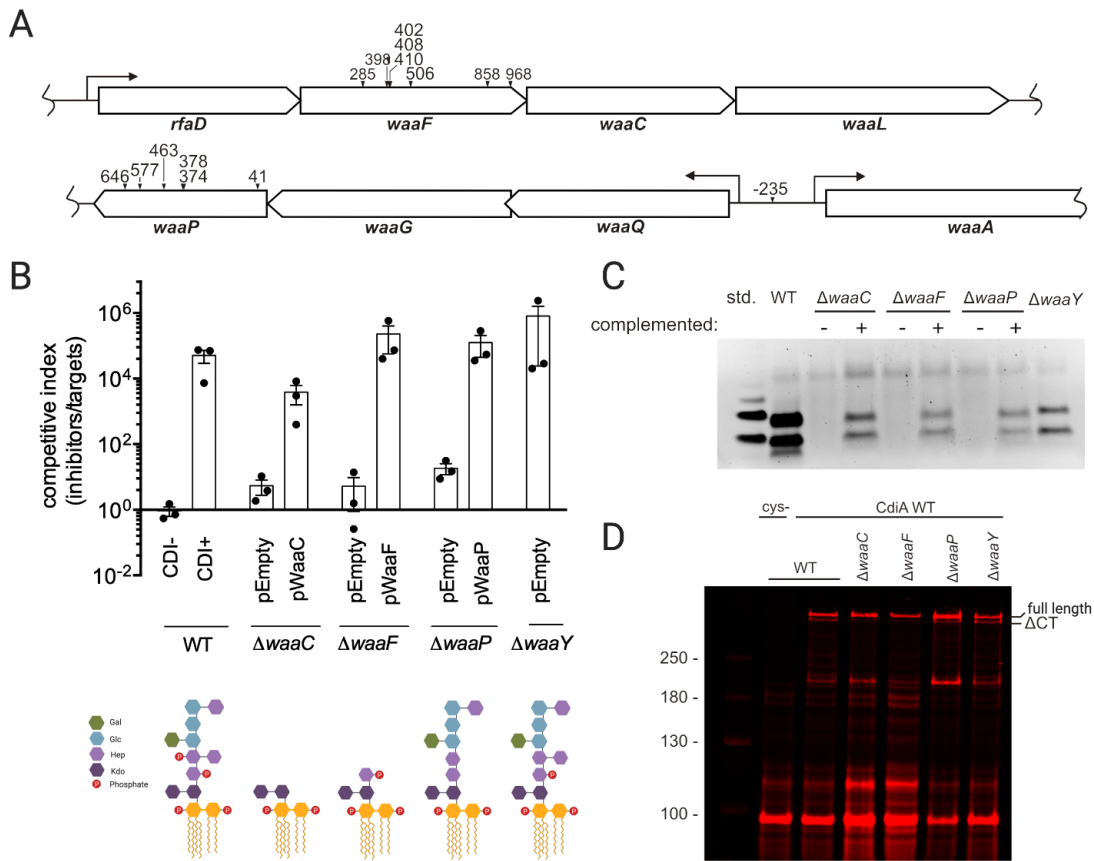


Figure 2.1: **Class 4 CDI from *Escherichia coli* STEC O31 recognizes a unique target cell receptor.** (A) Class 4 CDI locus to scale. (B) Co-culture competitions. Class 4 CDI inhibits *E. coli* EPI100 target cells in a CdiI-dependent manner, and is more effective on solid media than in shaking liquid broth. (C) Co-culture competitions between the indicated inhibitor and target strains. Target cells lacking the receptors for class 1-3 CdiA are still susceptible to CdiA<sub>4</sub>. Competitive Index (CI) is the ratio of viable colony-forming units per milliliter (CFU/mL) of inhibitors to targets at 3 hours relative to their starting ratios. CI values are represented as the average of at least 3 independent experiments  $\pm$ SEM.





**Figure 2.2: Deep-rough LPS mutants are resistant to class 4 CdiA** (A) Map of *mariner* transposon insertions rendering target cells resistant to CdiA<sub>4</sub>. (B) Competition co-cultures. Top: Mutations that disrupt LPS core biosynthesis result in CDI-resistance. Bottom: diagram of the predicted LPS core structures for the indicated mutants. The average  $\pm$ SEM is presented for three independent experiments. (C) LPS gel (ProQ Emerald, Invitrogen) of the indicated target strains. (D) Total protein from the indicated strains carrying CdiA<sub>4</sub> visualized with cysteine-reactive maleimide dye. CDI-resistant LPS mutants accumulate less CdiA  $\Delta$ CT than wild-type, indicating a defect in toxin delivery.

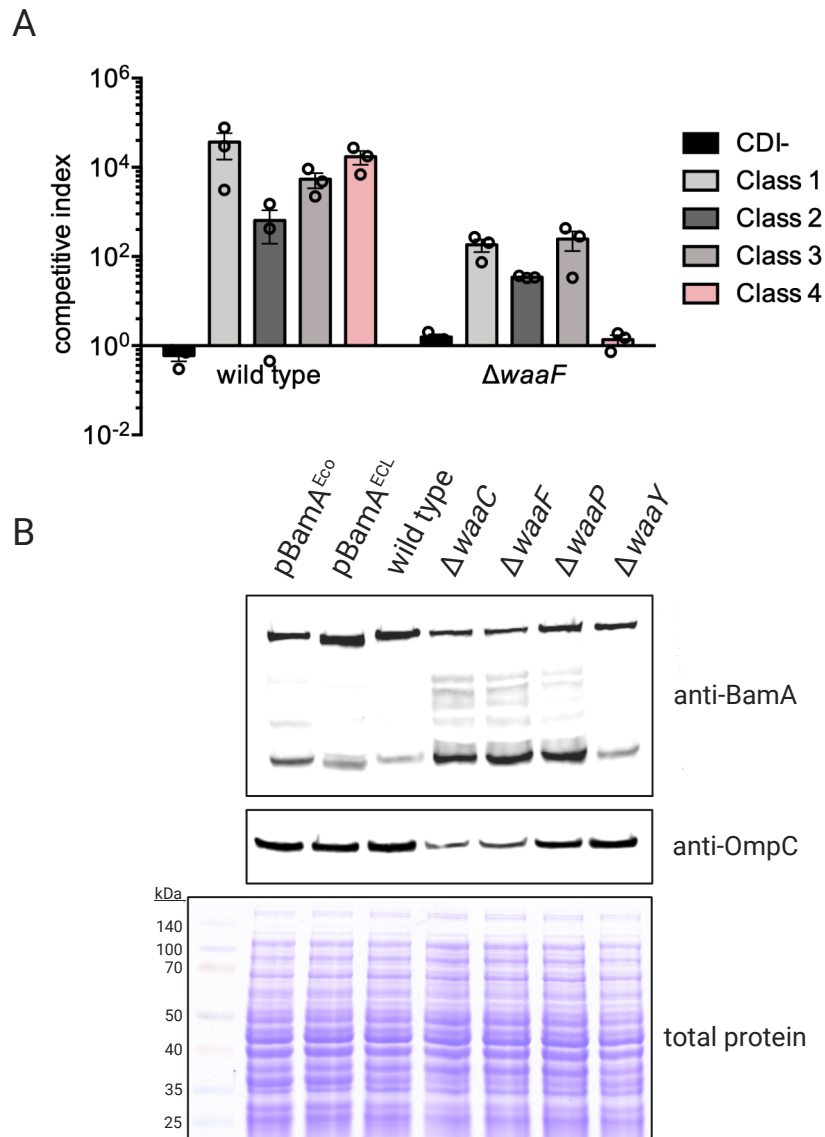


Figure 2.3: **Deep-rough LPS mutants are specifically resistant to Class 4 CdiA.** (A) Co-culture competitions. The indicated inhibitor strain was co-cultured with a  $\Delta waaF$  target strain to test for cross-resistance. The  $waaF$  mutant is fully resistant to CdiA<sub>4</sub>, and partially resistant to class 1 and 2 CDI. The average  $\pm$ SEM is presented for three independent experiments. (B) (Top) Anti-BamA immunoblot. (Middle) Anti-OmpC immunoblot. Partial resistance to class 1 and 2 CDI is due to a reduction in BamA and OmpC in the  $waaF$  deletion strain relative to wild type. (Bottom) Coomassie R-250 Brilliant Blue stained SDS-PAGE gel of whole cell lysates from the samples used for immunoblotting.

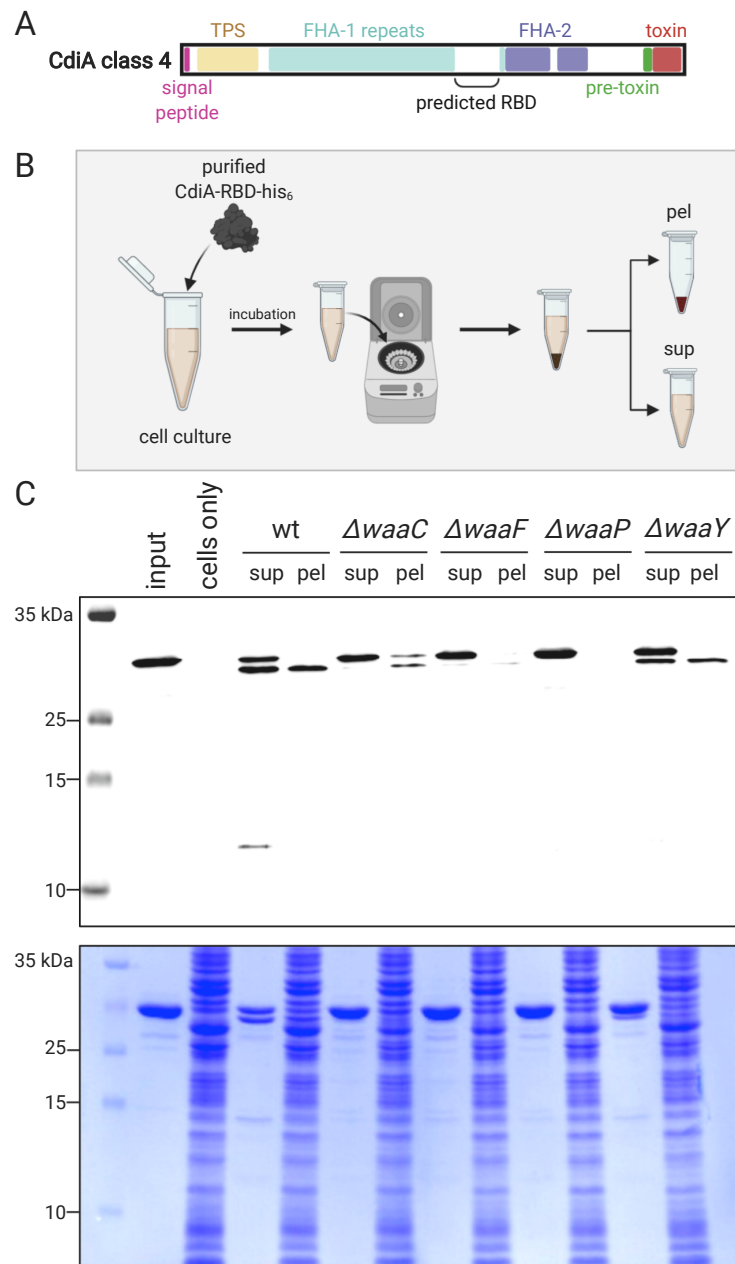


Figure 2.4: **Purified CdiA receptor-binding domain associates with whole cells containing intact LPS but not inner core mutants.** (A) Domain map of class 4 CdiA from *E. coli* STEC O31 showing the bounds of the RBD used for binding experiments. (B) Experimental approach for RBD-cell binding assay. (C) Top: Anti-FLAG immunoblot of total protein from cell pellets (pel) or supernatant (sup) from whole cells incubated with purified RBD protein, using assay outlined in (B). Bottom: Coomassie stained SDS-PAGE protein gel of the same samples used for immunoblotting.

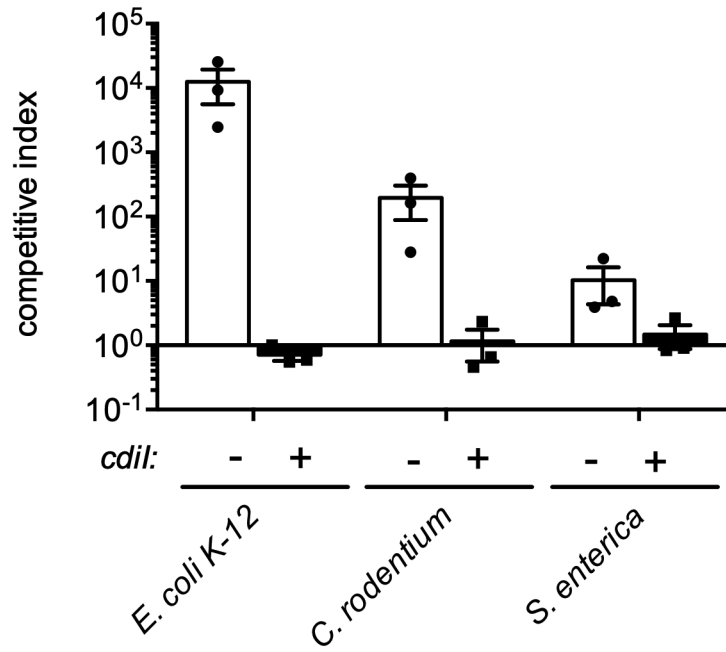


Figure 2.5: **Class 4 CdiA inhibits closely-related Enterobacteriales.** Competition co-cultures between wild-type CdiA<sub>4</sub> inhibitor cells and the indicated target species, with either empty plasmid or plasmid-encoded immunity (CdiI) against CdiA-CT<sup>STECO31</sup>. The average of three separate experiments ±SEM is presented.

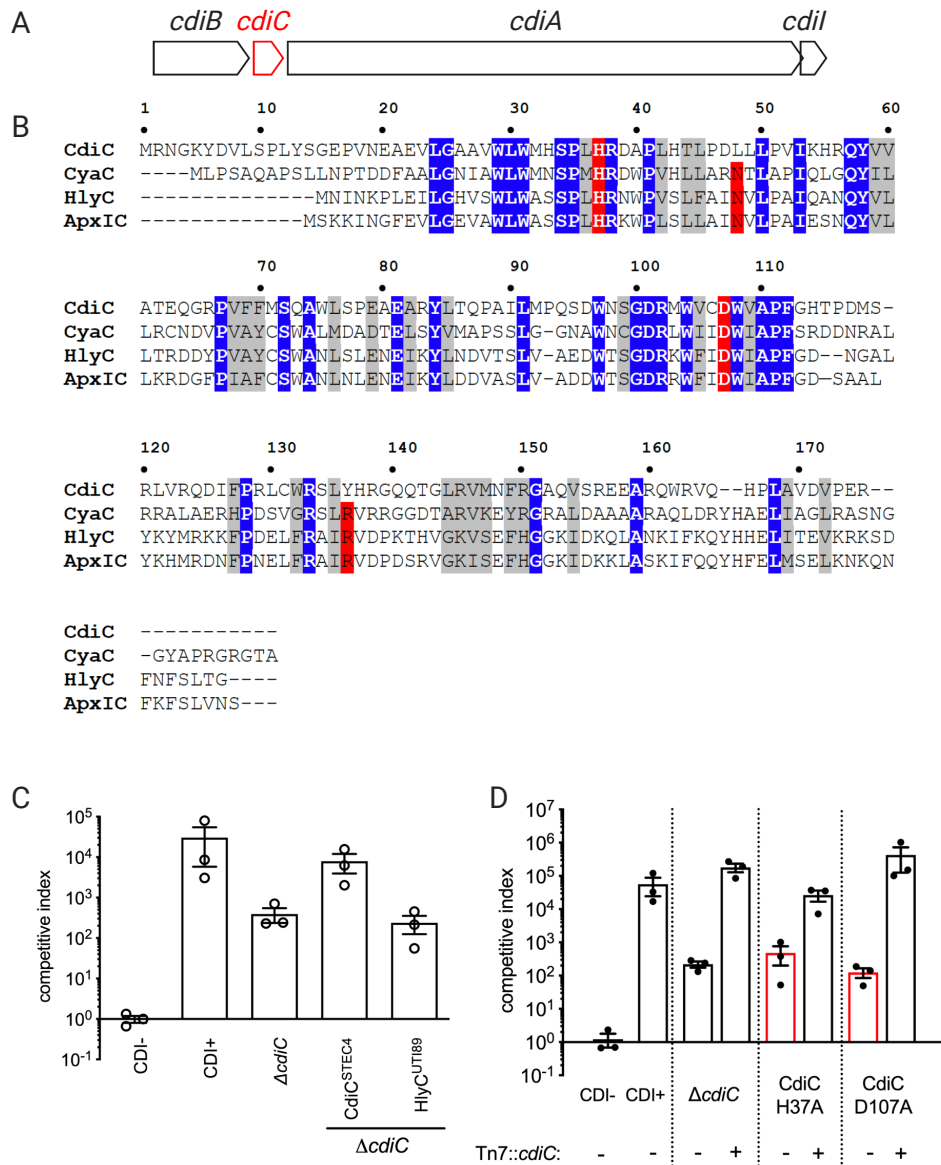
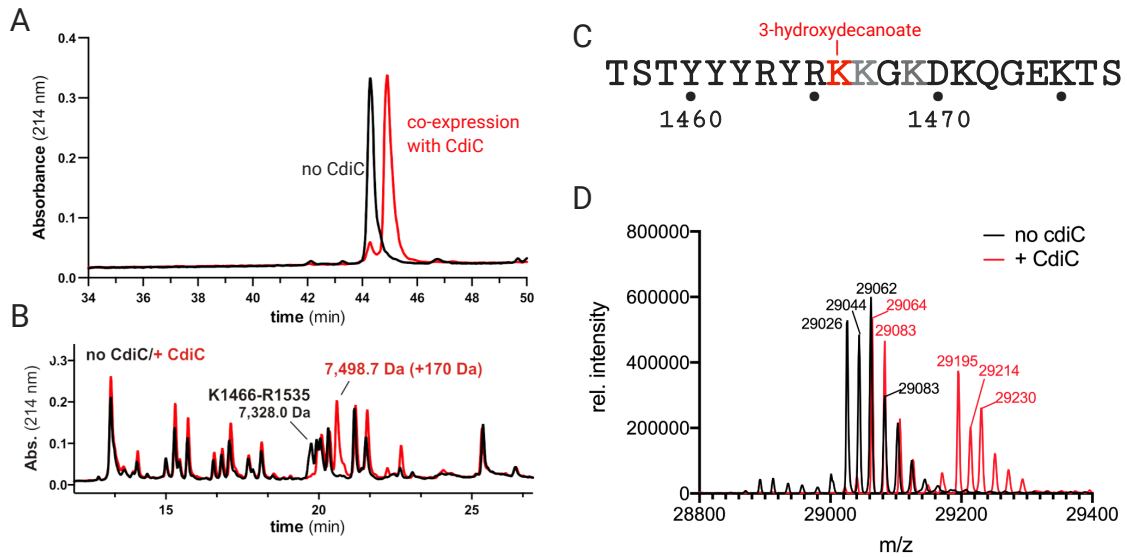


Figure 2.6: **CdiC is required for wild type growth inhibition by class 4 CDI.** (A) The STEC O31 class 4 CDI locus to scale. (B) Clustal Omega alignment of CdiC and other TAAT proteins. Conserved residues are highlighted in blue, with known active site residues in red. (C) and (D) Competition co-cultures between the indicated inhibitor strain and wild-type K-12 target cells. CDI- is an empty plasmid. Complementation was achieved with a single copy of *cdiC* under arabinose-inducible control inserted on the chromosome at the *attTn7* site. Therefore, all cultures were treated with 0.4% arabinose before and during the competition. The indicated CdiC mutants in (D) were constructed in the *cdiBCAI* locus, and complemented with wild-type CdiC. The average of three separate experiments  $\pm$ SEM is presented.



**Figure 2.7: CdiA RBD is modified in the presence of CdiC.** (A) RP-HPLC chromatogram of purified RBD proteins co-expressed with CdiC (red) or an empty plasmid (black). (B) RP-HPLC chromatogram of RBD proteins digested with Arg-C to generate a peptide map. The resulting HPLC-purified peptides from each experiment were analyzed by electrospray ionization mass spectrometry to obtain a delta mass for the modification, which was 170 Da for both the full RBD and the single modified peptide. (C) Amino acid sequence of the CdiA-RBD beginning at residue 1457. Lys1467 (red) is modified by CdiC with 3-hydroxydecanoate. K1466 and K1469 (analyzed in Fig. 2.11 and 2.8) are in gray. (D) Electrospray ionization mass spectrum of CdiA RBD protein purified in the absence of CdiC (black) or during co-expression with CdiC (red).

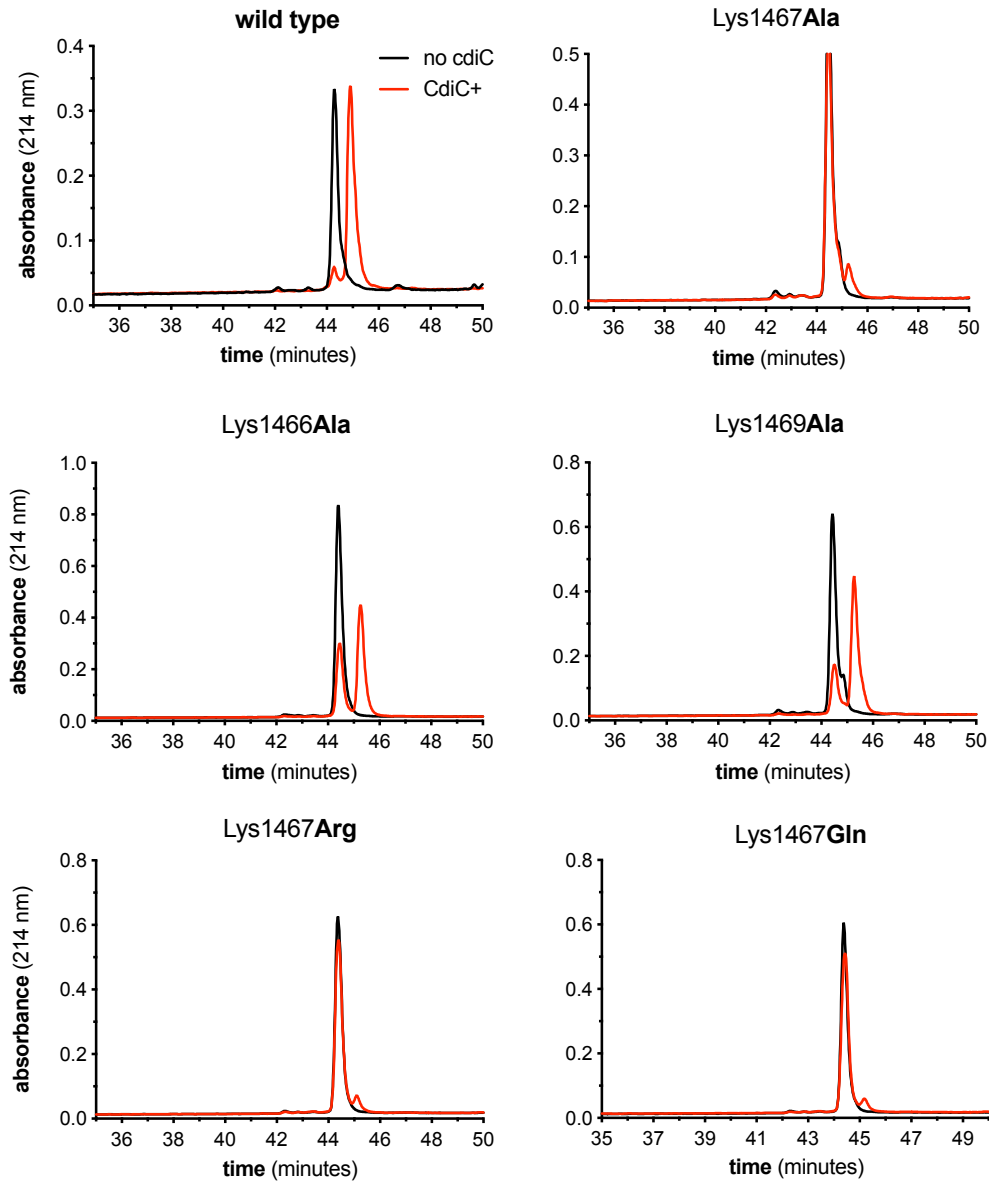


Figure 2.8: **Mutations at lysine 1467 within the receptor-binding domain prevent modification of CdiA.** HPLC chromatograms. Purified RBD protein was purified with  $\text{Ni}^{2+}$ -NTA and analyzed by RP-HPLC for changes in solubility during co-expression with CdiC. Top row: wild type RBD is fully converted to a modified species in the presence of CdiC, whereas alanine replacement of Lys1467 is completely blocked from modification. Second row: Alanine replacement of surrounding lysine residues (Lys1466, left and Lys1469, right) reduce the final amount of modified RBD protein but do not prevent modification. Bottom row: Additional mutations at Lys1467 (Arg, left, and Gln, right) all completely block modification of RBD protein. A representative graph for each construct is presented, but each experiment replicated 3 times.

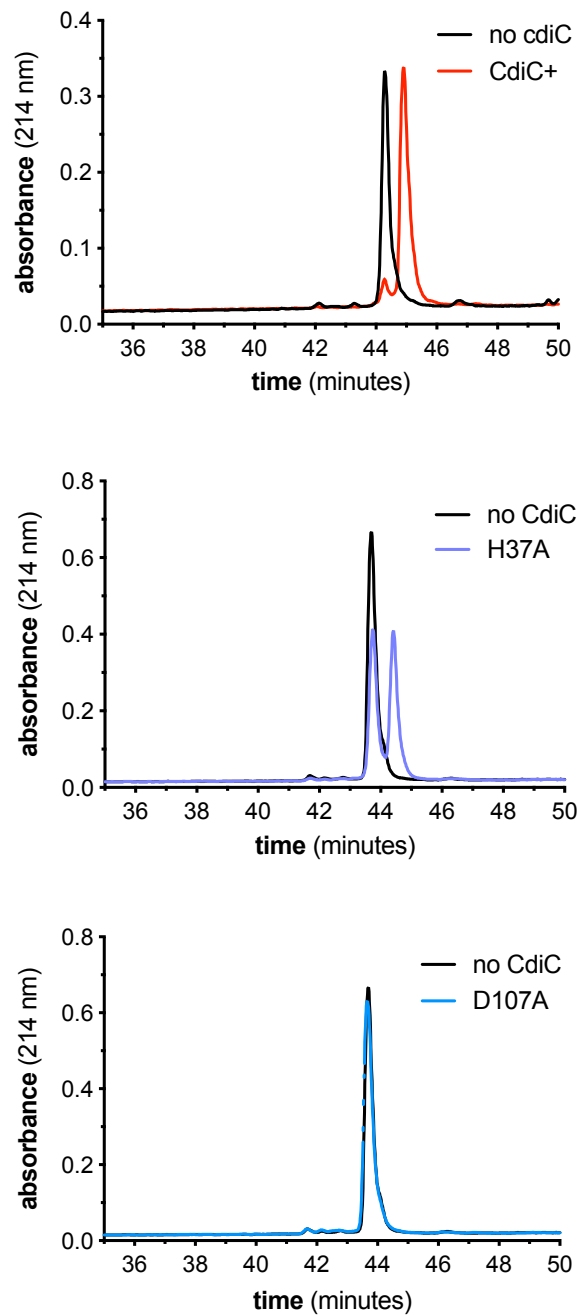


Figure 2.9: **Mutations at predicted active site residues in CdiC also abrogate modification of the CdiA receptor binding domain.** HPLC chromatograms. Purified RBD protein was co-expressed with wild type (top) or mutants of CdiC (His37Ala, middle and Asp107Ala, bottom), purified with Ni<sup>2+</sup>-NTA and analyzed by RP-HPLC. A representative graph for each construct is presented, but each experiment replicated 3 times.



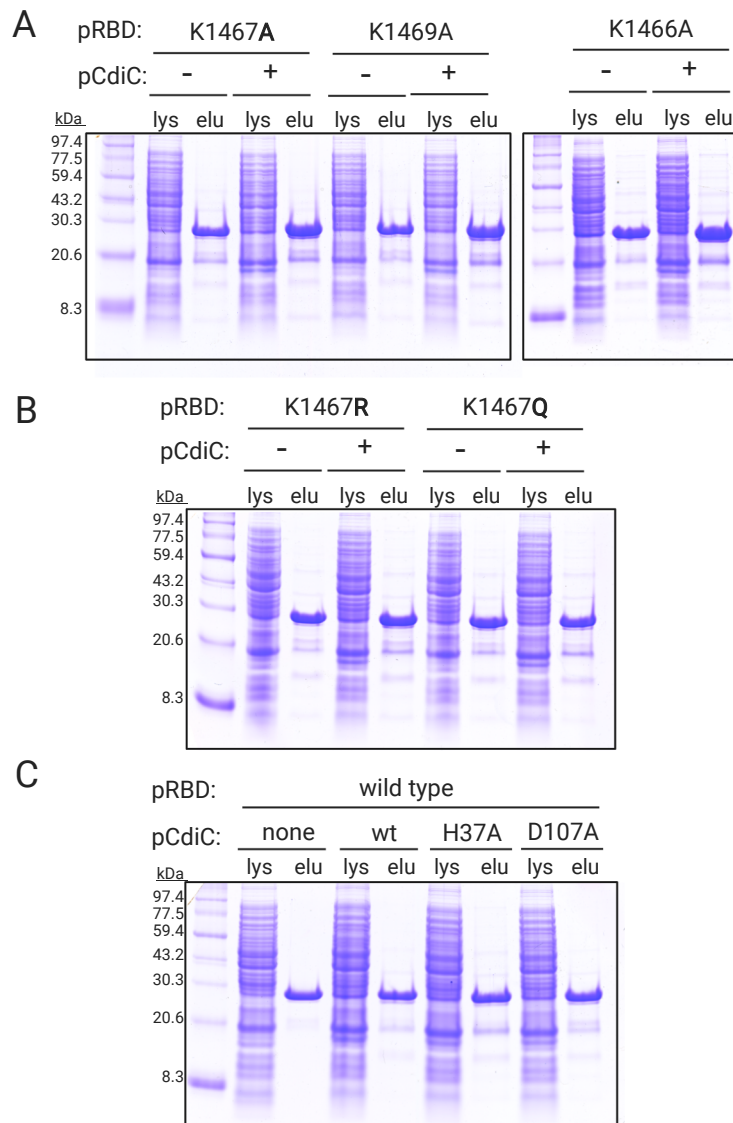


Figure 2.10: **Purified CdiA receptor-binding domain protein constructs used for analysis of the RBD by RP-HPLC and mass spectrometry.** Coomassie stained SDS PAGE protein gels of each RBD construct used for HPLC-MS analysis. (A) RBD alanine mutants purified with Ni<sup>2+</sup>-NTA (elu) from total protein (lys) in the absence or presence of CdiC. (B) Coomassie stained SDS-PAGE protein gel from two additional Lys1467 mutants. (C) Wild type RBD protein purified in the presence of no CdiC, wild type CdiC (STEC O31) or in the presence of active site mutant variants of CdiC.

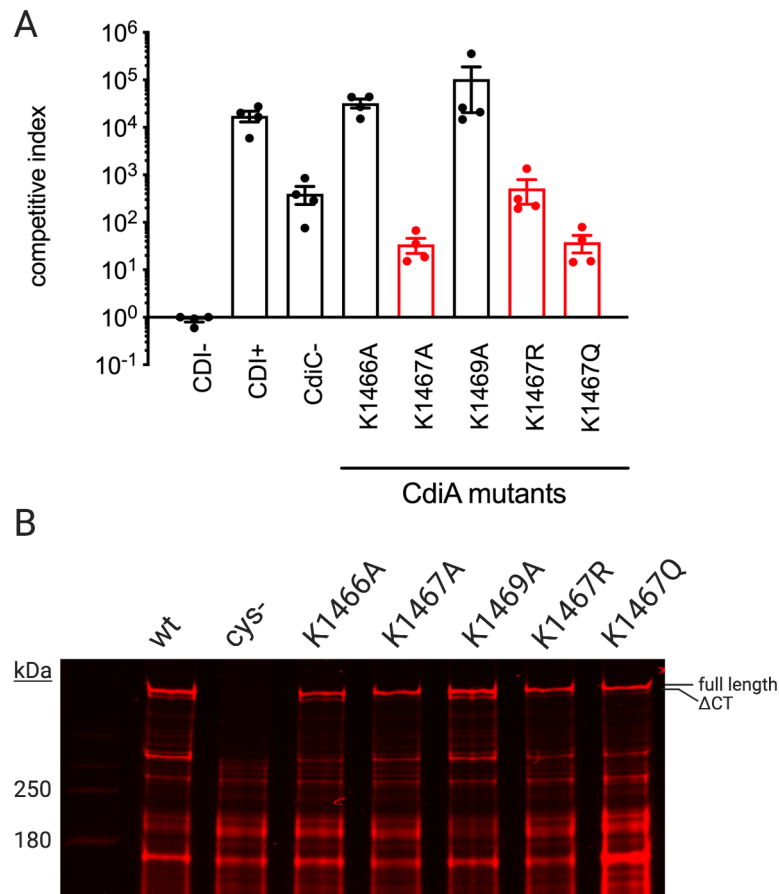


Figure 2.11: **Mutations at Lys1467 disrupt the process of CdiA-CT delivery.** (A) Co-culture competitions reveal mutations at Lys1467 disrupt CDI. Only Lys1467Arg phenocopies a *cdiC* null mutant. Co-cultures were conducted by mixing the indicated inhibitor strains with equal density wild type target cells for 3 hours. The resulting viable cell counts were enumerated for both populations, and the ratio inhibitors:targets presented as CI. The average of 3 independent experiments  $\pm$ SEM is presented. (B) Fluorimetry analysis of total protein from all CdiA mutants. Each protein is expressed and present on the cell surface. Mutations at Lys1467 disrupt toxin delivery, evidenced by decrease in CdiA- $\Delta$ CT. Monocultures of the indicated inhibitor strain were treated with maleimide dye, separated by SDS-PAGE, and imaged at 700 nm by a LI-COR Odyssey imaging system. The second lane is wild type CdiA<sub>4</sub> with the only dye-accessible cysteine (Cys1243) residue replaced with serine as a control. The top band of the doublet is full-length CdiA, and the lower band is a processed  $\Delta$ CT band, which has undergone toxin cleavage and is indicative of receptor-binding activity in a monoculture. A representative protein gel is presented, but was replicated at least three times.

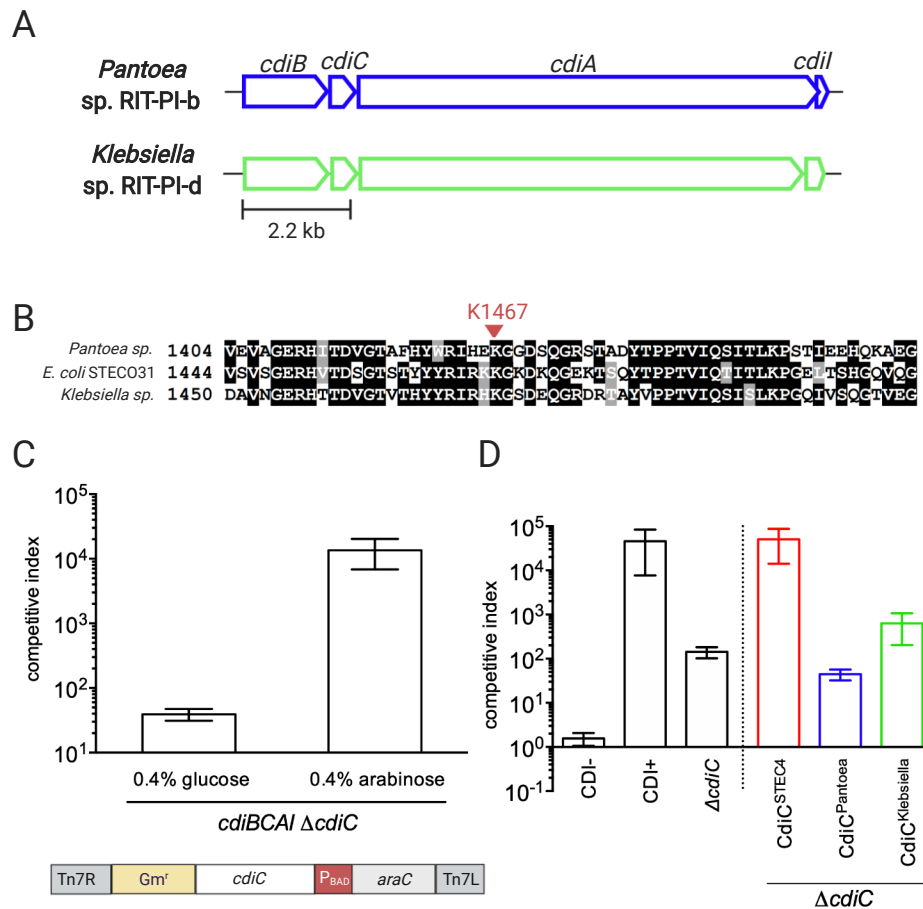


Figure 2.12: **CdiC acyltransferases exhibit substrate specificity.** (A) CDI loci to scale from two different isolates of Enterobacteriales. (B) Clustal Omega alignment of homologous class 4 CdiA proteins, showing the center of the receptor binding domain with lysine 1467 indicated with an arrow. (C) Bottom: diagram of the genomic arrangement of *cdiC* under arabinose control integrated at *attTn7*, used in complementation experiments. Top: Competition co-cultures with identical *cdiC* deletion strains, conducted in the presence of either arabinose or glucose. (D) Competition co-cultures conducted in the presence of 0.4% arabinose between wild type K-12 target cells and the indicated inhibitor strain. The average of three independent replicates  $\pm$ SEM is presented.

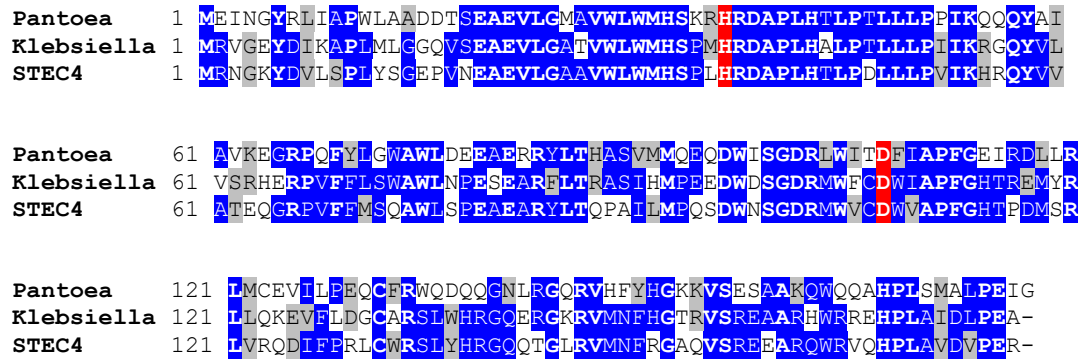


Figure 2.13: Alignment of CdiC<sup>STECO31</sup> and closely-related homologues from two other CDI systems. Obtained using Clustal Omega. Active site residues shared with other TAAT proteins are highlighted in red. Conserved residues are highlighted blue.

Table 2.1: Strains used in Chapter 2.

Strain	Description	Source
EPI100	F- <i>mcrA</i> $\Delta(mrr-hsdRMS-mcrBC)$ <i><math>\phi</math>80dlacZ<math>\Delta</math>M15 <math>\Delta</math>lacXcZ<math>\Delta</math>M15<math>\Delta</math>lacX <i>recA1 endA1</i> <i>araD139 <math>\Delta</math>(ara, leu)7697 galU galK<math>\gamma</math> -rpsL</i> <i>nupGStrR</i></i>	Epicentre
CH7175	EPI100 $\Delta$ <i>wzb</i> StrR	[74]
MG1655	WT strain	-
MFDpir	MG1655 RP4- 2-Tc::( $\Delta$ Mu1::aac(3)IV $\Delta$ <i>aphA-<math>\Delta</math>nic35-<math>\Delta</math>Mu2::zeo) dapA::(erm-pir) <math>\Delta</math>recA</i>	[142]
CH2016	X90 (DE3) $\Delta$ <i>rna <math>\Delta</math>slyD::kan</i> RifR KanR	[143]
CH5775	EPI100 $\Delta$ <i>wzb <math>\Delta</math>ompC::kan</i>	This study
CH5776	EPI100 $\Delta$ <i>wzb <math>\Delta</math>arB::kan-BamA (<math>\Delta</math>2014-2043)</i>	This study
CH5777	EPI100 $\Delta$ <i>wzb <math>\Delta</math>tsx::kan</i>	Zach Ruhe
CH13815	EPI100 $\Delta$ <i>wzb <math>\Delta</math>waaC::kan</i>	This study
CH13816	EPI100 $\Delta$ <i>wzb <math>\Delta</math>waaF::kan</i>	This study
CH13817	EPI100 $\Delta$ <i>wzb <math>\Delta</math>waaP::kan</i>	This study
CH13818	EPI100 $\Delta$ <i>wzb <math>\Delta</math>waaY::kan</i>	This study
CH14482	<i>Citrobacter rodentium</i> DBS100 <i>attTn7::Spm, SpmR</i>	This study
CH4448	<i>Salmonella enterica</i> sv. Typhimurium LT2 <i>attTn7::SpmR</i>	This study
CH4449	<i>Klebsiella aerogenes</i> ATCC 13048, RifR	This study
CH100	<i>Klebsiella</i> sp. RIT-PI-d	Michael Savka
CH15056	<i>Pantoea</i> sp. RIT-PI-b	Rochester Institute of Technology
CH7381	MC1061 <i>attTn7-pBAD</i> CdiC WT ( <i>Klebsiella</i> sp. RIT-PI-d)-- GmR	This study
CH7512	MC1061 <i>attTn7-pBAD</i> CdiC WT ( <i>Pantoea</i> sp. RIT-PI-b)-- GmR	This study

Table 2.2: Plasmids used in Chapter 2.

Plasmid	Description	Source
pSIM6	Heat-inducible expression of the phage $\Lambda$ Red recombinase proteins on a temperature-sensitive plasmid. AmpR	[138]
pSIM6-recA	$\Lambda$ Red recombinase proteins replaced by RecA. Ampr	This study
pKAN	pBluescript derivative with FRT-flanked kanamycin resistance cassette. KanR	This study
pSC189	Mobilizable plasmid with R6K $\gamma$ replication origin; carries the mariner transposon containing kanamycin resistance cassette; AmpR KanR	[141]
pCH450	pACYC184 derivative with <i>E. coli araBAD</i> promoter for arabinose-inducible expression. TetR	[72]
pUC18R6k-miniTn7T-Gmr	For integration at <i>attTn7</i> when mated biparentally with pTNS2. Carries gentamycin resistance cassette between Tn7 homology arms. AmpR, GmR	[140]
pUC18R6k-miniTn7T-pBADcdiC <sup>STECO31</sup> –GmR	Mobilizable plasmid encoding <i>cdiC</i> from <i>E. coli</i> STEC O31 under control of <i>araBAD</i> promoter, linked to a gentamycin resistance cassette, for integration at <i>attTn7</i> . AmpR, GmR	This study
<i>Ch. 2 plasmids, cont'd.</i>		

Plasmid	Description	Source
pUC18R6k-miniTn7T- pBAD <i>hlyC</i> <sup>UTI89</sup> -GmR	Mobilizable plasmid encoding <i>hlyC</i> from <i>E. coli</i> UTI89 under control of <i>araBAD</i> promoter, linked to a gentamycin resistance cassette, for integration at <i>attTn7</i> . AmpR, GmR	This study
pTNS2	Carries the <i>tnsABCD</i> operon for recombination with sequences cloned onto pUC18R6k-miniTn7T at <i>attTn7</i> . AmpR	[140]
pET21b(MCS-)	Derivative of pET21b lacking XbaI-NheI-BamHI-EcoRI to facilitate cloning. AmpR	[70]
pMF19	Expresses the <i>wbbL</i> (rhamnosyltransferase) gene for O16 polysaccharide biosynthesis constitutively. SpmR	[144]
pTrc99a	IPTG-inducible expression plasmid. AmpR	GE Health-care
pTrc99aKX	Derivative of pTrc99a that contains a KpnI, SpeI and XhoI sites to facilitate cloning. AmpR	[81]
pTrc99aKX- <i>cdiI</i> <sup>STEC4</sup>	Immunity gene from <i>E. coli</i> STECO31 class 4 locus under IPTG induction.	This study
pKAN- <i>waaC</i> US + DS	Carries 500 bp homology arms to replace <i>waaC</i> in <i>E. coli</i> K12 with a kanamycin resistance cassette by Red-mediated recombination. KanR	This study

*Ch. 2 plasmids, cont'd.*

Plasmid	Description	Source
pKAN- <i>waaP</i> US + DS	Carries 500 bp homology arms to replace <i>waaP</i> in <i>E. coli</i> K12 with a kanamycin resistance cassette by Red-mediated recombination. KanR	This study
pKAN- <i>waaY</i> US + DS	Carries 500 bp homology arms to replace <i>waaY</i> in <i>E. coli</i> K12 with a kanamycin resistance cassette by Red-mediated recombination. KanR	This study
pCH450- <i>waaC</i>	<i>waaC</i> gene from <i>E. coli</i> K12 under control of <i>araBAD</i> promoter. TetR	This study
pCH450- <i>waaF</i>	<i>waaF</i> gene from <i>E. coli</i> K12 under control of <i>araBAD</i> promoter. TetR	This study
pCH450- <i>waaP</i>	<i>waaP</i> gene from <i>E. coli</i> K12 under control of <i>araBAD</i> promoter. TetR	This study
pET21b(MCS-)- <i>cdiB-CAI</i> <sup>STEC4</sup>	<i>cdiBCAI</i> (class 4) locus from <i>E. coli</i> STECO31 on pET21b, with expression driven by native promoter. AmpR	This study
pET21b(MCS-)- <i>cdiBAI</i> <sup>STEC3</sup>	<i>cdiBAI</i> (class 3) locus from <i>E. coli</i> STECO31 on pET21b, with expression driven by native promoter. AmpR	[70]
pET21(MCS-)- <i>cdiBCA</i> <sup>STEC4</sup> -Chimera	NheI site introduced in pre-toxin domain of pET21b(MCS-)- <i>cdiBCAI</i> <sup>STEC4</sup> to facilitate cloning of new toxin-immunity pairs onto the STEC4 CdiA protein.	This study
<i>Ch. 2 plasmids, cont'd.</i>		



Plasmid	Description	Source
pET21b(MCS-)-cdiBCA <sup>STEC4</sup> -CT/cdiI <sup>STEC3</sup>	The toxin-immunity pair from CdiA <sup>STEC3</sup> is fused at the modular (V)ENN motif of CdiA <sup>STEC4</sup> , resulting in a chimeric CdiA-CT protein with the cognate CdiI downstream. AmpR	This study
pET21b(MCS-)- <i>cdiB</i> -CAI <sup>STEC4</sup> $\Delta$ <i>cdiC</i>	An internal 442 bp of <i>cdiC</i> was removed from the WT locus on pET21b, leaving the first 26 bp and the last 55 bp of <i>cdiC</i> intact. AmpR	This study
pET21b(MCS-)-cdiBCAI STEC O31 CdiC [H37A]	STEC4 locus with CdiC His37Ala mutation. AmpR	This study
pET21b(MCS-)-cdiBCAI STEC O31 CdiC [D107A]	STEC4 locus with CdiC Asp107Ala mutation. AmpR	This study
pET21b(MCS-)-cdiBCAI STEC O31 CdiA [K1466A]	STEC4 locus with CdiA Lys1466Ala mutation. AmpR	This study
pET21b(MCS-)-cdiBCAI STEC O31 CdiA [K1467A]	STEC4 locus with CdiA Lys1467Ala mutation. AmpR	This study
pET21b(MCS-)-cdiBCAI STEC O31 CdiA [K1469A]	STEC4 locus with CdiA Lys1469Ala mutation. AmpR	This study
pET21b(MCS-)-cdiBCAI STEC O31 CdiA [K1467R]	STEC4 locus with CdiA Lys1467Arg mutation. AmpR	This study
pET21b(MCS-)-cdiBCAI STEC O31 CdiA [K1467Q]	STEC4 locus with CdiA Lys1467Gln mutation. AmpR	This study
<i>Ch. 2 plasmids, cont'd.</i>		

Plasmid	Description	Source
pACYC-Duet-CdiA <sup>STEC4</sup> (V1328-P1529)-His <sub>6</sub>	The presumptive receptor-binding domain (region encompassing V1328-P1529 of CdiA) cloned on pACYC-Duet as an open-reading frame with a hexahistidine tag for co-expression with CdiC and biochemical analyses. CmR	This study
pACYC-Duet-CdiA <sup>STEC4</sup> (V1328-P1529)-His <sub>6</sub> [K1466A]	CdiA RBD cloned as ORF with hexahistidine tag from K1466A mutant full length protein. CmR	This study
pACYC-Duet-CdiA <sup>STEC4</sup> (V1328-P1529)-His <sub>6</sub> [K1467A]	CdiA RBD cloned as ORF with hexahistidine tag from K1467A mutant full length protein. CmR	This study
pACYC-Duet-CdiA <sup>STEC4</sup> (V1328-P1529)-His <sub>6</sub> [K1469A]	CdiA RBD cloned as ORF with hexahistidine tag from K1469A mutant full length protein. CmR	This study
pACYC-Duet-CdiA <sup>STEC4</sup> (V1328-P1529)-His <sub>6</sub> [K1467R]	CdiA RBD cloned as ORF with hexahistidine tag from K1467R mutant full length protein. CmR	This study
pACYC-Duet-CdiA <sup>STEC4</sup> (V1328-P1529)-His <sub>6</sub> [K1467Q]	CdiA RBD cloned as ORF with hexahistidine tag from K1467Q mutant full length protein. CmR	This study
pET21-RBD <sup>STEC4</sup> -FLAG-His <sub>6</sub>	CdiA RBD cloned as ORF with FLAG epitope upstream of C-terminal hexahistidine tag. AmpR	This study
pTrc99aKX- <i>cdiC</i> [H37A]	CdiC histidine mutant from locus under IPTG control for co-expression. AmpR	This study

*Ch. 2 plasmids, cont'd.*

Plasmid	Description	Source
pTrc99aKX- <i>cdiC</i> [D107A]	CdiC aspartic acid mutant from locus under IPTG control for co-expression. AmpR	This study
pET21b(MCS-)- <i>cdiB-CAI</i> <sup>STEC4</sup> CdiA [C1243S]	Cys1243 removed from wild type CdiA to control for maleimide labeling.	This study
pCH450KX- <i>cdiC</i> <i>Klebsiella</i> sp. RIT-PI-d	CdiC homologue cloned onto pCH450KX to pair it with arabinose-inducible promoter before cloning onto mobilizable plasmid.	This study
pCH450KX- <i>cdiC</i> <i>Pantoea</i> sp. RIT-PI-b	CdiC homologue cloned onto pCH450KX to pair it with arabinose-inducible promoter before cloning onto mobilizable plasmid.	This study
pUC18R6k-miniTn7T- pBADCdiC WT ( <i>Klebsiella</i> sp. RIT-PI-d)-GmR	CdiC homologue from <i>Klebsiella</i> sp. RIT-PI-d on mobilizable plasmid for biparental mating at <i>attTn7</i> .	This study
pUC18R6k-miniTn7T- pBADCdiC WT ( <i>Pantoea</i> sp. RIT-PI-b)-GmR	CdiC homologue from <i>Pantoea</i> sp. RIT-PI-b on mobilizable plasmid for biparental mating at <i>attTn7</i> .	This study
<i>Ch. 2 plasmids, cont'd.</i>		

Table 2.3: Primers used in Chapter 2.

Primer	Sequence	Source
CH2131 (recA-BgIII)	5' - TGC AGA TCT TGT GGC AAC AAT TTC TAC - 3'	This study
CH2132 (recA-Xma)	5' - GCG ACC CGG GTG TAT CAA ACA AGA CG - 3'	This study
ZR258 (J2ELL3 CDI-Not-for)	5' - TTT GCG GCC GCT CAG GAG ACT GAG TTT CCT GAT G - 3'	This study
ZR259 (J2ELL3 CDI-Xho-rev)	5' - TTT CTC GAG CAC AAG CTC AGA CAG CGC - 3'	This study
ZR253 (cdiB J2ELL3-Asc-rev)	5' - TTT GGC GCG CCA GAA CGT CAT ATT TCC CGT TAC G - 3'	This study
CH4869 (STEC4-cdiI-Kpn-for)	5' - TTG GTA CCA TGA TTT TAA ATG ATT TTT TTT TAT TAA TGC TTG C - 3'	This study
CH4195 (waaC-KO-Sac-for)	5' - TTT TGA GCT CGC TTT CAT CAG AAC GTC CGA TG - 3'	This study
CH4196		
<i>Ch. 2 primers, cont'd.</i>		

Primer	Sequence	Source
(waaC-KO-Bam-rev)	5' - TTT TGG ATC CGT AAC AAT AGC GCG TTG AGT TCT TCC - 3'	This study
CH4197 (waaC-KO-Eco-for)	5' - TTT TGA ATT CAG GTA AAA CAT GCT AAC ATC CTT TAA AC - 3'	This study
CH4198 (waaC-KO-Kpn-rev)	5' - TTT TGG TAC CAA CGC CAC TAA CTA TCC CTA TTA GC - 3'	This study
CH4199 (waaP-KO-Sac-for)	5' - TTT TGA GCT CGC TTT GGC ATC GTT ACC GG - 3'	This study
CH4200 (waaP-KO-Bam-rev)	5' - TTT TGG ATC CCC AAA GTG TGG CAA GCG G - 3'	This study
CH4201 (waaP-KO-Eco-for)	5' - TTT TGA ATT CGA GCG AAC ACA ACG CAA AGG - 3'	This study
CH4202 (waaP-KO-Kpn-rev)	5' - TTT GGT ACC GGA AAA AAC ATA TTG GCT GGC TG - 3'	This study
CH4203 (waaP-KO-Sac-for)	5' - TTT TGA GCT CGA AAG GGA TGA CAT TAT TTT TGC CTC G - 3'	This study
CH4204		
<i>Ch. 2 primers, cont'd.</i>		

Primer	Sequence	Source
(waaP-KO-Bam-rev)	5' - TTT TGG ATC CCC AGT TAA ATG TTA TTT ACG GTA ATA TTT TC - 3'	This study
CH4205 (waaP-KO-Eco-for)	5' - TTT TGA ATT CCC ACA ATT ACA TGT CTT CAC CAG G - 3'	This study
CH4206 (waaP-KO-Kpn-rev)	5' - TTT GGT ACC CCC GAC GGT AAA AGG ACC G - 3'	This study
CH4299 (waaF-Sac-for)	5' - TTT GAG CTC CCT GCC TGA AGC GAA CTC G - 3'	This study
CH4300 (waaF-Kpn-rev)	5' - TTT GGT ACC GCG ATA GCA TAA TCG CCC TGG - 3'	This study
CH4387 (waaC-Kpn-for)	5' - TTT GGT ACC ATG CGG GTT TTG ATC GTT AAA AC - 3'	This study
CH4388 (waaC-Xho-rev)	5' - TTT CTC GAG TTA TAA TGA TGA TAA CTT TTC CAA AAC TGC - 3'	This study
CH4207 (waaF-Not-for)	5' - TTT GCG GCC GCA ATC GCG ACG CAT AAG AGC - 3'	This study
CH4208		
<i>Ch. 2 primers, cont'd.</i>		

Primer	Sequence	Source
(waaF-Xho-rev)	5' - TTT CTC GAG TCC GTC AGC TTC CTC TTG - 3'	This study
CH4209 (waaP-Not-for)	5' - TTT GCG GCC GCG GAT ATC ATT ACA GGT GG - 3'	This study
CH4210 (waaP-Xho-rev)	5' - TTT CTC GAG TTA TAA TCC TTT GAG TTG TGT TCG - 3'	This study
CH4174 (cdiC-D107A-for)	5' - CCG GAT GTG GGT CTG TGC CTG GGT TGC CCC TTT TG - 3'	This study
CH4175 (cdiC-D107A-for-complement)	5' - CAA AAG GGG CAA CCC AGG CAC AGA CCC ACA TCC GG - 3'	This study
CH4176 (cdiC-H37A-for)	5' - GAT GCA CTC CCC CCT GGC GCG TGA TGC GCC ACT G - 3'	This study
CH4177 (cdiC-H37A-for-complement)	5' - CAG TGG CGC ATC ACG CGC CAG GGG GGA GTG CAT C - 3'	This study
CH4087 (cdiC-Kpn-for)	5' - GAA GGT ACC ATG CGT AAC GGG AAA TAT - 3'	This study
CH4088		
<i>Ch. 2 primers, cont'd.</i>		

Primer	Sequence	Source
(cdiC-Xho-rev)	5' - AAA CTC GAG TTA TCT CTC CGG CAC ATC - 3'	This study
CH4760 (STEC4-N1326-Eco-for)	5' - TTT GAA TTC TGT CAA TGA CCA TTT CAC CAC G - 3'	This study
CH4761 (STEC4-S1564-Bam-rev)	5' - GAT GGA TCC CTG AGG TGC GCT GAC - 3'	This study
CH4771 (UTI89-hlyC-Kpn-for)	5' - GAG GGT ACC ATG AAT ATG AAC AAT CCA TTA GAG - 3'	This study
CH4772 (UTI89-hlyC-Xho-rev)	5' - AAT CTC GAG TTA ACC TGT TAA TGA AAA ATT GAA ATC TG - 3'	This study
CH4672 (GlmS-for)	5' - GAG ATG CCG CAC GTT GAG G - 3'	This study
CH4616 (Tn7R-screen-rev)	5' - CAC AGC ATA ACT GGA CTG ATT TC - 3'	[140]
CH4802 (STEC4-N1229-Eco-for)	5' - CTG ACG AAT TCC GGT ACC GGG CGA ATC - 3'	This study
CH4803 (STEC4-S2159-Xba-rev)	5' - CCT GCA GGG CTT CAA GTC TAG AGT TTC CGG CAG ATT TCG - 3'	This study

*Ch. 2 primers, cont'd.*



Primer	Sequence	Source
CH4841 (STEC4-K1466A-rev)	5' - GCT TAT CCT TTC CTT TTG CCC TGA TAC GGT AAT AAT AC - 3'	This study
CH4647 (RBR4-K141A-for)	5' - TAC CGT ATC AGG AAA GCA GGA AAG GAT AAG CA - 3'	This study
CH4648 (RBR-K143A-for)	5' - ATC AGG AAA AAA GGA GCG GAT AAG CAG GG - 3'	This study
CH5186 (STEC4-K1467Q-rev)	5' - GCT TAT CCT TTC CTT GTT TCC TGA TAC GGT AAT AAT AC - 3'	This study
CH4888 (STEC4-K1467R-rev)	5' - GCT TAT CCT TTC CTC TTT TCC TGA TAC GGT AAT AAT AC - 3'	This study
CH4358 (STEC4-V1328-Nco-for)	5' - TTT CCA TGG TCA ATG ACC ATT TCA CCA CGG AGC - 3'	This study
CH4359 (STEC4-P1589-Xho-rev)	5' - TTT CTC GAG TTA GTG GTG ATG ATG ATG ATG TGG CAC ATT CAC TGC CGG - 3'	This study
CH5468		
<i>Ch. 2 primers, cont'd.</i>		

Primer	Sequence	Source
(STEC4-P1589-FLAG-Xho-rev)	5' - TTT CTC GAG TTT GTC ATC ATC ATC TTT ATA ATC TGG CAC ATT CAC TGC CGG - 3'	This study
CH2260 (mariner-rev-seq)	5' - CAA GCT TGT CAT CGT CAT CC - 3'	This study
CH4876 (RIT-PI-d-CdiC-Kpn-for)	5' - TTT GGT ACC ATG CGC GTT GGC GAG TAT GAC - 3'	This study
CH4877 (RIT-PI-d-CdiC-Xho-rev)	5' - ATT CTC GAG TTA AGC TTC CGG CAG ATC TAT CG - 3'	This study
CH4957 (RIT-PI-b-CdiC-Kpn-for)	5' - GAG GGT ACC ATG GAG ATT AAT GGT TAC C - 3'	This study
CH4958 (RIT-PI-b-CdiC-Xho-rev)	5' - CAT CTC GAG TCC TTA TCC GAT TTC GG - 3'	This study
<i>Ch. 2 primers, cont'd.</i>		

# Chapter 3

## CdiA is affected by the presence of O-antigen on targets

### 3.1 Abstract

With the identification of a CDI system that can be deployed against a variety of natural isolates (CdiA<sub>4</sub>), we have observed lower levels of growth inhibition of more wild-type isolates (*Salmonella enterica* sv. Typhimurium and *Citrobacter rodentium* DBS100) relative to *E. coli* K-12. In this chapter, we investigate the potential role of O-antigen in blocking the LPS-binding function of CdiA<sub>4</sub>. We find that O-antigen is capable of shielding targets from not only class 4 CdiA, but also a Tsx-binding (class 3) CdiA protein in liquid media. We observe diverse O-antigen polymers in natural isolates that also express CdiA proteins under laboratory conditions, suggesting that the O-antigen shielding phenomenon must also be applicable to natural isolates. Furthermore, we have found that over longer time scales, CDI+ strains delivering CdiA-CT<sub>4</sub><sup>STECO31</sup> are not capable of dominating a culture, especially when the competing strain has a growth advantage. Lastly, though insertional mutagenesis of O-antigen ligase in *Salmonella* and *Citrobacter* does prevent O-antigen biosynthesis, the *waaL*::Cm mutation does not protect these isolates from CDI but instead appears to result in compensatory mutations which

further prevent CDI intoxication. Thus, future studies should investigate the role of O-antigen in natural isolates further in an attempt to determine the extent to which CdiA might have evolved to overcome this natural barrier to OM contact. Together, the data in this chapter strongly indicates that CDI systems have evolved to target neighboring bacteria only in sessile communities in the natural environment.

## 3.2 Introduction

In Chapter 2 I introduced a new kind of CDI system that is equipped to bind the core of lipopolysaccharide for the initiation of toxin delivery into neighboring bacteria. These findings offer new opportunities to investigate the physiology of CDI in bacterial communities. For example, because CdiA<sub>4</sub> has a broader target range due to its receptor preference, it can be used to target a variety of more wild-type isolates as well as important pathogens such as *Citrobacter* spp. and *Salmonella* spp., which also are mouse models of infection. Thus, CdiA<sub>4</sub> provides an opportunity to explore the effect CDI would have on both commensal and pathogen colonization and virulence. In this chapter, we have begun to explore the physiological role of CdiA<sub>4</sub> in mixed bacterial communities through an investigation of the interaction between class 4 CdiA and O-antigen. These initial experiments pave the way for future work with class 4 CDI and its effect on host-associated microbial communities.

All classes of CDI systems are predominantly found within opportunistic or virulent pathogens [64] with a notable exception found in the probiotic strain *E. coli* Nissle 1917 [145]. The lifestyle of human pathogens demands they evolve mechanisms for dealing with exogenous stressors, such as antimicrobial peptides [146], antibiotics [147], and other host defenses [148]. One major outcome of the arms race between host and bacteria is the complex structure and rapid evolution of the bacterial cell envelope, which is a

likely target for the mammalian immune response. Most notable among the components of the cell envelope is a unique class of glycoconjugate called lipopolysaccharide (LPS). LPS is attached to lipid A by a core oligosaccharide, which is the most conserved region of LPS between species. The exposed and most distal portion of LPS relative to the cell surface, and therefore the most variable region, is O-antigen. Together, the core oligosaccharide and O-antigen form an amphiphilic molecule (roughly 10 kDa, though the molecular weight varies widely) that provides a permeability barrier to large, negatively charged or hydrophobic molecules. Despite their prevalence in pathogens, O-side chains evidently contribute to host colonization by symbionts as well and are therefore function as mediators of general host-bacteria interactions [149]. Since O-side chains are multifunctional surface antigens distributed across the bacterial cell surface, their relevance to CdiA structure and function has likely been overlooked. Indeed, with the receptor-binding domain (RBD) being the most distal portion of CdiA relative to the inhibitor cell surface, the class 4 RBD that actually binds to the core of LPS could be sequestered by nonspecific interactions with the sugar residues in O-antigen. It is therefore important to consider the barrier O-antigen presents in the context of CdiA structure and function.

In this chapter, we show that at least two different RBDs (class 3 and class 4) are efficiently blocked by *E. coli* K-12 targets restored for O-antigen synthesis. This so-called O-antigen shielding is completely effective in liquid broth, and partially effective on solid media. Additionally, O-antigen shielding is unidirectional, with no effect on toxin delivery when inhibitors carry O-antigen as well. We also find that *S. enterica* and *C. rodentium* actually out-compete CDI inhibitor cells over longer time-scales, which brings in to question the effect CDI would have on their growth *in vivo*. Though we succeeded in removing O-antigen from these species, our gene disruptions had unintended effects on both strains that complicate our interpretation of their phenotype. However, additional resistance to CdiA<sub>4</sub> is observed in the *S. enterica waaL::Cm* O-antigen defective strain

when compared to wild type, and these mutants also appear more opaque, possibly due to secretion of capsule polysaccharide. Taken together, we find that the cell surface can be effectively manipulated by a target cell to overcome CDI, resulting in different population outcomes when studied over longer time scales than we have typically considered during the study of CDI.

### 3.3 Results

#### 3.3.1 *E. coli* K-12 restored for O-antigen synthesis is fully protected from CDI in liquid broth and partially on solid media

Though we can detect CdiA expression in natural isolates (Fig. 3.1), detecting growth inhibition specifically due to CdiA is complicated by their accessory genome. For example, when grown in the spent media from *E. coli* NI1076 (introduced in Ch. 4), the natural isolate *E. coli* EC93—which carries two CDI systems—is inhibited, likely by iron scavenging siderophores secreted by NI1076 (Fig. 3.2). Even if CDI has an immediate effect in a co-culture assay which can be observed over short time scales, the question remains as to how effective CDI actually is between natural populations of bacteria in the environment over longer periods of time.

To circumvent the issues of using natural isolates to investigate the interaction between CDI+ and CDI- bacteria in the presence of O-antigen, we restored O-antigen biosynthesis in *E. coli* K-12 using the O16 serotype from pMF19 [144]. We then equipped the O-antigen producing K-12 strain (O-Ag+) a plasmid-encoded copy of either the class 4 LPS-binding CDI system from *E. coli* STECO31, which was introduced in Chapter 2, or the class 3 Tsx-binding CdiA protein also from *E. coli* STECO31 [70]. Thus, this K-12

strain will produce O-antigen as well as many copies of either CdiA, mimicking what we expect would occur in wild-type CDI+ strains 3.3.

In co-culture competitions between inhibitor and target strains producing O-antigen, competitive indices are reduced to  $\sim 1$  when competitions are conducted in liquid broth (Fig. 3.3). Even on solid media, which would increase the frequency and time of cell-cell contacts, we observe partial protection of target cells relative to O-Ag- competitions (Fig. 3.3). Thus, O-antigen reduces toxin delivery by CdiA in general, but most effectively when co-cultures are conducted in liquid media.

### 3.3.2 O-antigen shielding is unidirectional

Since it is possible that O-antigen extends farther than CdiA from the cell surface, or presents a barrier to proper biogenesis in the inhibitor cell, we conducted competitions with both smooth and rough strains in both combinations (i.e., either inhibitors or targets carry O-Ag). We found that CdiA is effectively blocked by smooth LPS in targets, but is unaffected by smooth LPS in the inhibitor (Fig. 3.4). Therefore, O-antigen shielding specifically disrupts CdiA access to the target cell surface, presumably through occlusion of the CdiA receptor.

Interestingly, CdiA proteins containing the class 4 receptor-binding domain (RBD), which recognizes the core of LPS, are much worse at inhibiting target cells in liquid media than a class 3 protein that binds to the outer-membrane protein Tsx (Fig. 3.3). Indeed, both the wild-type CdiA<sub>4</sub> and a chimeric CdiA<sub>4</sub>-CT/I<sub>3</sub> which contains the class 3 CdiA-CT domain have a 100 to 1000-fold defect in liquid broth. These results suggest that, even in the absence of O-antigen, binding to the core of LPS to initiate CdiA-CT translocation is extremely unlikely in shaking broth, where cell-cell contact is a function of time and cell density.

### 3.3.3 CDI systems and O-antigen polymers co-exist on the surface of pathogenic *Enterobacteriales*

CDI systems are often carried by plant and animal pathogens [64, 115, 125], which are under selection to maintain intact O-antigen chains on the cell surface for survival and virulence in the host [150, 151, 152]. Indeed, we find different O-antigen polymers are present in purified LPS samples of various CDI+ isolates (Fig. 3.1). Surprisingly, full length and truncated CdiA proteins are detectable in whole cell lysates from these CDI+ isolates grown in rich media (including *Klebsiella aerogenes* ATCC 13048, *Enterobacter cloacae* ATCC 13047, *E. coli* UPEC 93, *Enterobacteri hormaechei* ATCC 49162 and *Yersinia frederiksenii* ATCC 33641), revealing that translation of CdiA under laboratory conditions is not repressed in many cases (Fig. 3.1). Therefore, since CdiA is present, expressed and functional in O-antigen carrying isolates [81] (including data not shown for *E. cloacae* and *K. aerogenes*), we anticipate that CDI must be capable of activity even in the presence of O-side chains. Since our data with O16 suggests that CDI cannot occur in the presence of O-antigen in liquid broth, this further suggests that CDI only occurs on solid surfaces.

### 3.3.4 O-antigen defective *S. enterica* sv. Typhimurium and *C. rodentium* are not more susceptible to CdiA4

Since *E. coli* K-12 with O-antigen is resistant to CdiA in liquid broth, we reasoned that naturally occurring O-antigen polymers in *S. enterica* sv. Typhimurium (STy) and *C. rodentium* (Crod), which are both targets for CdiA<sub>4</sub> 2 would be resistant to inhibition in liquid broth as well. As anticipated by the presence of O-antigen in these strains (Fig. 3.5), both STy and Crod are completely resistant to CdiA<sub>4</sub><sup>STECO31</sup> in liquid but not on solid media (Fig. 3.5). Consistent with our observation in Chapter 2, a *cdiC* deletion



strain inhibits less than a wild type class 4 inhibitor, though appears to inhibit both species equally (a competitive index of 1-5).

To determine if STy and Crod are protected from CdiA<sub>4</sub> in liquid media solely due to O-antigen, we disrupted the O-antigen ligase gene (*waaL*) in both species using an insertional mutagenesis approach. However, we anticipate that the insertion has caused other physiological responses that also affect CDI. For instance,  $\Delta waaL$  STy appears to have upregulated capsule polysaccharide, since it creates thicker, more opaque colonies and is more resistant to CdiA<sub>4</sub> than the wild type, and Crod  $\Delta waaL$  colonies appear to have a fitness defect when compared to wild type (Fig. 3.6). Future studies to investigate the O-antigen shielding of natural isolates will improve on this approach to determine if a non-pleiotropic *waaL* deletion can improve inhibition of natural isolates by CdiA<sub>4</sub><sup>STECO31</sup>.

### 3.3.5 Inhibition by CDI diminishes over long time scales.

Since we have already observed that growth of the CDI+ natural isolate *E. coli* EC93 is inhibited presumably by siderophore secretion by another murine isolate, I was curious to know if CDI-dependent inhibition of STy and/or Crod becomes insignificant when analyzed over longer time scales. Thus, we conducted 24-hour co-culture competitions at a 1:1 ratio between *E. coli* K-12 CDI+ strains and either K-12, Sty or Crod targets. Indeed, over the course of 24 hours, all target cells begin to grow once more and competitive indices fall towards an even ratio inhibitor:target (Fig. 3.7). CDI+ cells even begin to lose their growth advantage over susceptible K-12 targets of the same strain background (Fig. 3.7). Interestingly, after 24 hours, Crod actively inhibits the growth of its competitor despite the presence of a CDI system in that strain, resulting in a patchy lawn when the CDI+ inhibitor is plated on selective media post-competition (Fig. 3.7). In conclusion, these results reveal that CDI does not have a dramatic effect on popula-

tion outcomes over long time scales, and that other antagonistic interactions may drive community structure more than inhibition by CdiA.

### 3.4 Discussion

In this chapter, I demonstrate that toxin delivery by CdiA is blocked at the target cell surface by the presence of O-antigen (Fig. 3.3.1). *E. coli* K-12 restored for O16 biosynthesis is fully resistant to two different CDI systems when co-cultured in liquid broth and is partially protected on solid LB agar. The same phenomenon is observed when K-12 target cells are replaced by more wild-type targets like *S. enterica* sv. Typhimurium and *C. rodentium*, which both produce different O-antigens (Fig. 3.5).

O-antigen shielding by receptor occlusion has also been reported for other proteins such as colicins, antibodies, and phage tail spikes, all of which require access to OM proteins for cell surface adsorption [153, 154, 155]. The specific composition of O-antigen appears to be less important than its presence alone in shielding the bacterial cell surface. Indeed, it appears that what may be capsule coated *S. enterica* is also more resistant to CdiA<sub>4</sub> (Fig. 3.6). Even though the composition does not seem to matter, the amount of O-antigen produced can determine the extent of protection in some cases [153], which might explain the difference in inhibition between Crod and STy when competed against CDI<sub>4</sub><sup>STECO31</sup>. Similar to our suspicions of *waaL::kan* *S. enterica* targets, capsular polysaccharide has been reported to be an effective cell surface shield in many other cases, even preventing T3SS-mediated attachment to human cells in pathogenic strains of *E. coli* [156]. Indeed, CdiA-CT genetic selections often result in mucoid colonies that have acquired surface-altering mutations (such as a transposon mutant isolated with resistance to CDI in Ch. 4) which suggests that the effect is from the target cell surface. Thus, the composition of the target cell envelope is crucial during CDI. Indeed, specific Pap

pili in *E. coli* target cells were long ago shown to provide almost complete protection from growth inhibition by a class 1 CDI system [63]. Although it is still unclear how CDI systems are regulated in the environment, CDI is primarily deployed by pathogens and is known to be involved in collective behaviors such as biofilm formation [157, 158]. Therefore, expression of CDI systems is likely coordinated with the expression of other cell surface antigens. After all, we now know that CdiA-CT delivery can increase alarmone production in sibling cells [90], which is a major mechanism for stress adaptation and thus gene expression regulation.

A curious observation in CDI biology is the large variation in size of CdiA proteins. CdiA length is primarily controlled by the number and size of FHA-1 repeats, which correlates with the size of the variable RBD [70, 159]. It is possible that the length of FHA-1 is actually tuned to the O-antigen length in the bacteria it has evolved to target. Indeed, FHA-1 truncation mutants are still capable of delivering toxin (unpublished data, Kiho Song), suggesting that the FHA-1 repeats do not play a role in toxin delivery or biogenesis. However, as the CdiA filament is shortened by progressively larger deletions in FHA-1, inhibition of targets is reduced. These results suggest a second possible role of FHA-1 in addition to overcoming barriers on the target cell surface: extending far enough away from the inhibitor cell to prevent auto-delivery. Future studies should therefore investigate the role of FHA-1 length to differentiate between these hypotheses.

*E. coli* K-12 producing O16 antigen is partially protected on solid LB agar (Fig. 3.3), and other species that produce their own O-antigen polymers (*C. rodentium* and *S. enterica* sv. Typhimurium) are much more resistant to inhibition than lab strains of *E. coli* (Fig. 3.5). Taken together, these results suggest that the levels of growth inhibition observed for CDI systems in the lab are inflated by orders of magnitude. Combined with recent insights into the complex physiological effects CdiA-CTs have on target bacteria [90, 89], the data presented here suggest that CDI systems likely only deliver a very small

number of toxins into neighboring bacteria in the environment to cause physiological outcomes. Furthermore, we have also learned that liquid broth differentially inhibits toxin delivery by CdiA proteins with variable RBDs. Class 4 CdiA which binds LPS has a 100-1000 fold defect over a class 3 Tsx-binding protein even in the absence of O-antigen, indicating that LPS binding is highly dependent on the increased time for cell-cell interactions that occurs on solid media. Even though CDI inhibition is effective when monitored over short ( $\sim 3$  hr) time scales, target cells escape from CDI even on solid media if given enough time (here, 24 hrs). Indeed, even in the absence of other antagonistic genes, a target cell population identical to the inhibitor strain except for the presence of *cdiBCAI* is only slightly out-competed over 24 hours (Fig. 3.7). These data agree with earlier studies that indicate the expression of CDI alone can reduce growth rate [93, 160]. Thus, the fitness defect associated with CDI expression likely reduces the success of the CDI+ strain over time even in the environment. These results suggest either that the effect of CdiA-CT delivery must be relevant for only a short period of time, or as discussed previously and in Ch. 4, toxin delivery is not meant to eradicate a population but instead mediate communication.

The mechanism for CDI escape by target cells over time under our conditions can likely be explained by population segregation within the co-culture, which is also a function of toxin potency. Previous studies have reported the formation of discrete communities at the initial culture boundary when a CDI+ strain is present, with a greater proportion of monoculture sectors at the boundary comprised of targets when co-cultured with a less potent CdiA-CT [160]. As we have seen here in Figure. 3.7, the outcome of this culture border segregation can sometimes enable the target population to actually outgrow the inhibitors if given enough time [160]. Interestingly, we also find that a CDI+ *E. coli* K-12 strain is inhibited visibly over 24 hrs by wild-type Crod, revealing patches in the CDI+ *E. coli* population when plated on media selecting against Crod growth

following the co-culture (Fig. 3.7). Thus, in conclusion, not only is expressing CDI disadvantageous in itself for growth rate as other studies have found, if given enough time other antagonistic interactions may become more relevant for shaping community structure. In light these facts, it will be fascinating to learn how and when CdiA is deployed by natural isolates in a host setting and if CDI expression is modulated in response to the production of other cell surface structures.

### 3.5 Materials and Methods

**Growth conditions and competition co-cultures.** All strains were grown at 37 °C in lysogeny broth (LB) or on LB agar. Media were supplemented when appropriate with antibiotics at the following concentrations: ampicillin (Amp) 150  $\mu\text{g mL}^{-1}$ ; kanamycin (Kan) 50  $\mu\text{g mL}^{-1}$ ; gentamycin (Gm) 15  $\mu\text{g mL}^{-1}$ ; spectinomycin (Spm) 100  $\mu\text{g mL}^{-1}$ . For all competition co-cultures, both strains were grown to an optical density at 600 nm ( $\text{OD}_{600}$ ) of 0.6-0.9 and mixed at an equal ratio of  $\text{OD}_{600}$  (3.0:3.0), plated in a 15  $\mu\text{L}$  volume on LB agar and incubated 3 hours at 37 °C. Cells were harvested with a sterile swab into 1×M9 salts and ten-fold serial dilutions were plated on the appropriate antibiotics to enumerate inhibitor and target colony-forming units per milliliter (CFU/mL). Liquid competitions were conducted in addition to plate competitions at an  $\text{OD}_{600}$  0.3:0.3 for 3 hrs at 220 rpm and 37 °C in 10 mL pre-warmed LB using baffled flasks. Competitive indices were calculated as the ratio of inhibitor to target cells at 3 hrs relative to their starting ratios. Each co-culture was repeated at least three times

**Strain and plasmid construction.** For O-antigen competition co-cultures, MG1655 WT cells were given either gentamycin or kanamycin resistance using biparental mating and integration of the appropriate cassette at *attTn7* as previously described [140]. Equal ratios of the two donors (MFDpir cells carrying the helper plasmid pTNS2 and MFDpir

with either pUC18R6K-miniTn7T-GmR or pUC18R6K-miniTn7T-KanR) were mixed with MG1655 recipient cells from overnight cultures in 100  $\mu$ L, plated on a 25 mm 0.22  $\mu$ m filter and incubated at 37 °C for 4 hours. The resulting *att*Tn7 integrants were selected on gentamycin (CH15163) or kanamycin (CH15164) and the insertion site verified by colony PCR with primer pairs CH4672/CH4616. Both of the selectable MG1655 derivatives were then transformed with pMF19 [144]. CH15164 cells were used as inhibitors, while CH15163 served as targets.

O-antigen ligase deficient targets were created using an insertional mutagenesis approach. A 685 bp portion of *waaL/rfaL* from *C. rodentium* DBS100 (CH14482) was amplified with oligonucleotides CH5371/CH5372, and a 471 bp portion also from *S. enterica*'s *waaL* gene with oligos CH5374/CH5375 using colony PCR. Both products were ligated into pRE118 lacking the counter-selectable *pheS\** marker (pCH110/pCAT-KAN) with SacI/KpnI and resulting plasmids were sequenced to verify the correct insertion and transformed into the mating strain *E. coli* MFD*pir*+. Equal ratio *C. rodentium* or *S. enterica* was mixed with MFD*pir*+ cells containing the appropriate plasmid on LB agar for a minimum of 4 hours, and a portion of the co-culture was spread onto Cm media with a sterile loop to select for conjugates.

A chimeric CdiA<sub>4</sub>-CT<sub>3</sub> protein was created (with the class 4 CdiA protein and the toxin-immunity pair from the class 3 *cdiBAI*<sup>STECO31</sup> locus) to control for potential toxin potency differences when comparing cell-cell binding efficiencies of CdiA classes in the presence of O-antigen. To facilitate cloning of CdiA-CT/I pairs, a NheI site was introduced in the pretoxin domain of pET21b(MCS-)-*cdiBCAI*<sup>STEC4</sup> using a XbaI/XhoI fragment. The resulting plasmid (pET21b(MCS-)-*cdiBCA*<sup>STEC4</sup>-Chimera) was digested with NheI/XhoI and ligated to a CdiA-CT/I fragment from the Tsx-binding class 3 CDI locus in *E. coli* STEC\_O31 to produce pET21b-*cdiBCA*<sup>STEC4</sup>-CT/I<sup>STEC3</sup>.

**Lipopolysaccharide purification and gel electrophoresis.** LPS was purified

from *E. coli* K-12, *C. rodentium* and *S. Typhimurium* using 2 mL portions of overnight cultures were normalized to OD<sub>600</sub> 2.0. LPS was collected using a LPS Extraction Kit (iNtRON Biotechnology). Approximately 9 μg of LPS from each sample was loaded onto a 13% polyacrylamide gel and run for 1 hr at 110 V. The gel was stained with Pro-Q Emerald 300 Lipopolysaccharide Gel Stain Kit (ThermoFisher) and imaged on a Kodak 200 Gel Logic UV trans-illuminator.

### 3.6 Tables and Figures

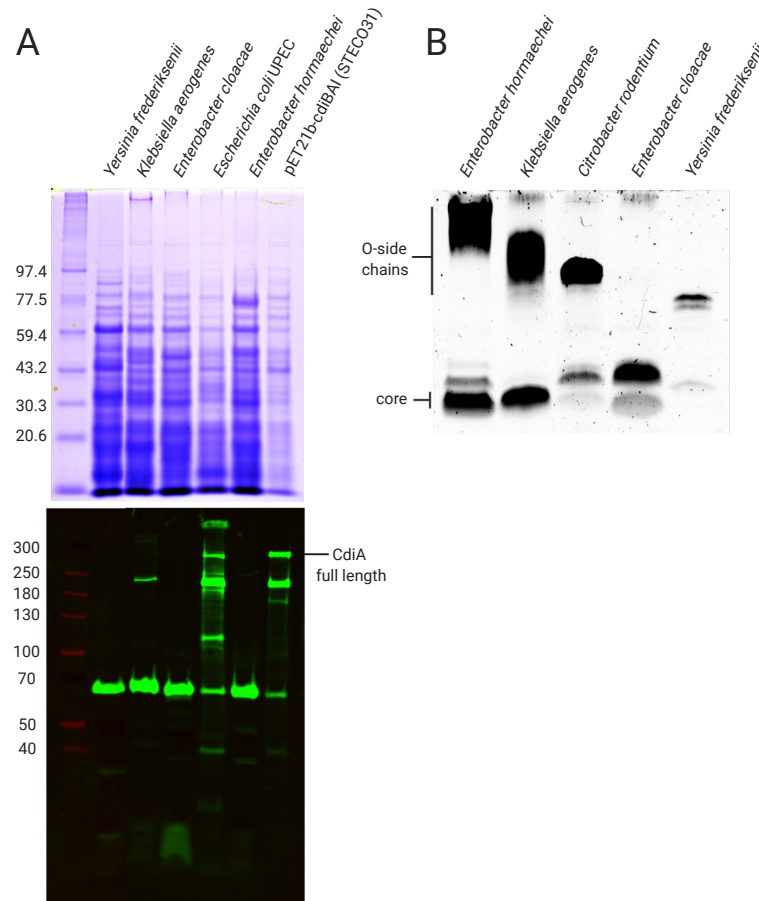


Figure 3.1: **Natural isolates express CdiA and synthesize O-antigen.** (A) Upper panel: Coomassie Blue-stained SDS-PAGE gel of whole cell lysates from the indicated strain. Molecular weight markers (kDa) are on the left. Lower panel: Anti-N-terminal CdiA antibody reactive against FHA-1 domain of class 1-3 CdiA was used to probe whole cell lysates from above. Positive control for CdiA expression and reactivity in the last lane is from plasmid-expressed CdiA<sub>3</sub><sup>STECO31</sup>. (B) SDS-PAGE LPS gel (Pro-Q Emerald, Invitrogen) demonstrating that CDI+ natural isolates which express CdiA also produce unique O-antigens.



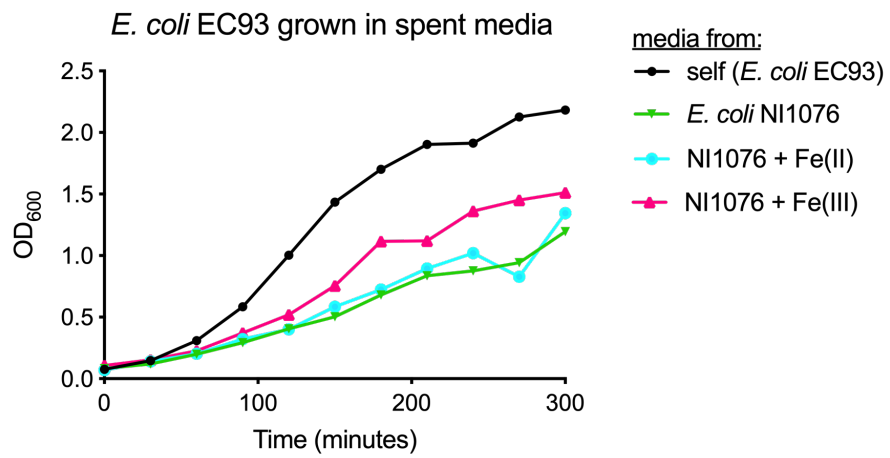


Figure 3.2: **CDI+ isolates can be out-competed independently of CDI, which complicates co-culture assays between wild type bacteria.** Growth curve of *E. coli* EC93 in its own spent media, or filtered spent media from the growth of the murine isolate *E. coli* NI1076 (see Ch. 4) either supplemented with iron or not.

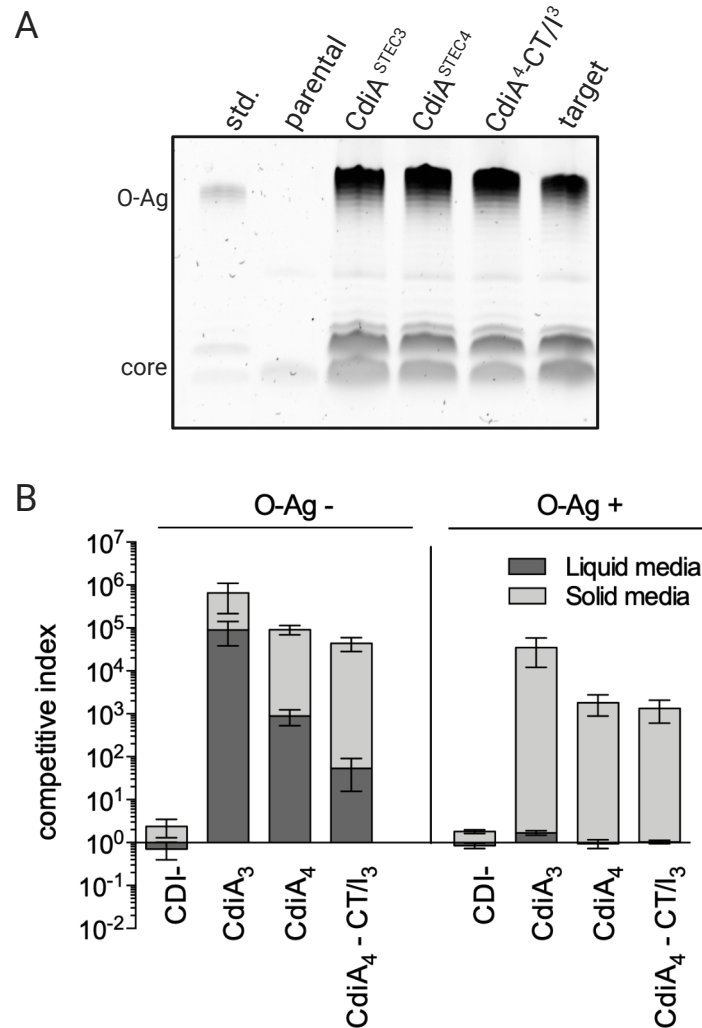


Figure 3.3: **O-antigen fully blocks CDI in liquid broth and partially on solid media.** (A) SDS-PAGE LPS gel of purified LPS of the indicated strains, stained with Pro-Q Emerald (Invitrogen). (B) O-antigen shielding is extremely effective in shaking liquid broth. Competition co-cultures of target cells containing O-antigen (right) or not (left) against three different CDI+ inhibitors on solid media (light gray) or in liquid media (dark gray). Competitive index is the ratio between viable cells collected from inhibitors:targets at 3 hours relative to their starting ratio. The average  $\pm$ SEM for three separate experiments is presented.

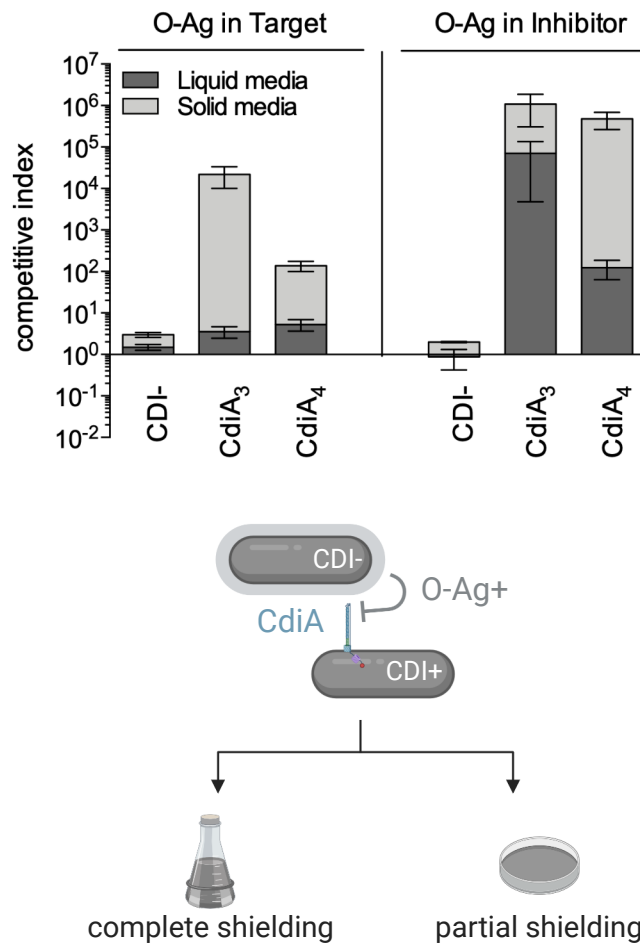
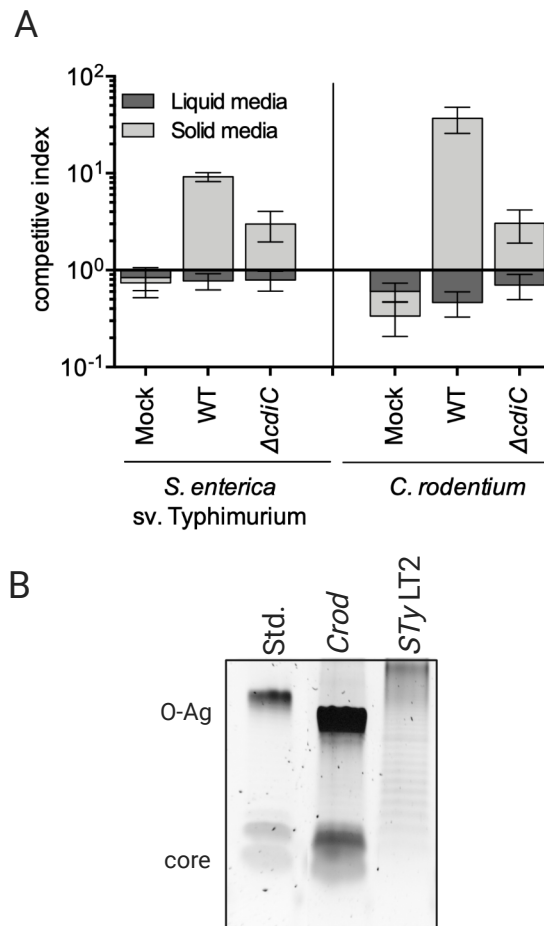


Figure 3.4: **O-antigen blocks CdiA only when present in target cells.** Top: Competition co-cultures between the indicated inhibitor strains and K-12 targets either with O-antigen in the inhibitor (right) or in the target (left). The average  $\pm$ SEM for three separate experiments is presented. Bottom: illustration summarizing the effect of O-antigen on target cells during CDI.



**Figure 3.5: Natural isolates are CDI-resistant in liquid co-cultures.** (A) Competition co-cultures between *Salmonella enterica* LT2 (left) or *Citrobacter rodentium* DBS100 (right) and the indicated inhibitor either in liquid media (dark gray) or solid media (light gray). Mock inhibitors carry an empty plasmid only. The average  $\pm$ SEM is presented for three independent experiments. (B) Purified LPS from *S. enterica* and *C. rodentium* separated by SDS-PAGE and stained with Pro-Q Emerald (Invitrogen).

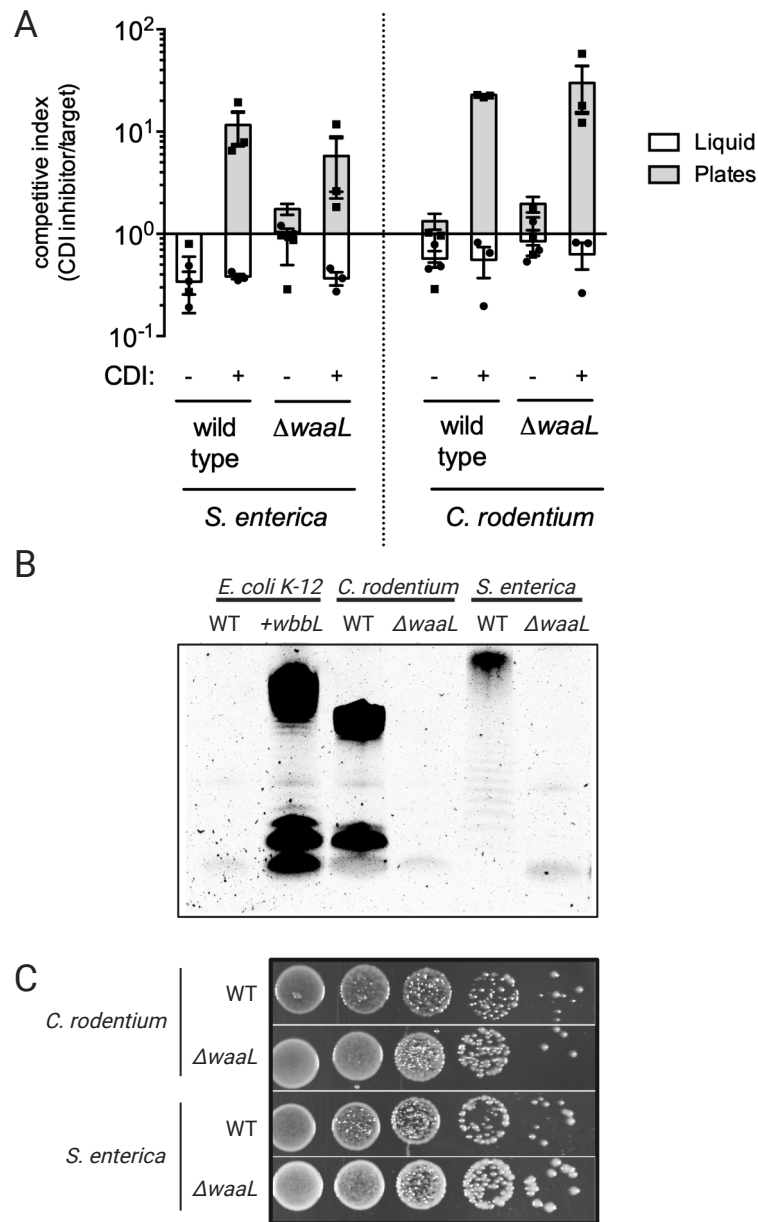


Figure 3.6: **Insertional mutagenesis of *waaL* in *C. rodentium* and *S. enterica* does not result in increased CDI susceptibility under the chosen conditions but instead has unintended phenotypic effects.** (A) 3-hour, equal ratio competition co-cultures with CDI- (empty plasmid) or CDI+ ( $CdiA_4^{STE\text{CO}31}$ ) inhibitors and the indicated targets. The average  $\pm$ SEM is presented for three independent experiments. (B) Pro-Q Emerald stain of purified LPS from the target strains used in (A), plus *E. coli* K-12 with and without O-antigen for comparison. (C) Dilutions on selective media of *C. rodentium*  $\Delta waaL$  and *S. enterica*  $\Delta waaL$  revealing that their colony size and morphology differs unexpectedly from wild-type.

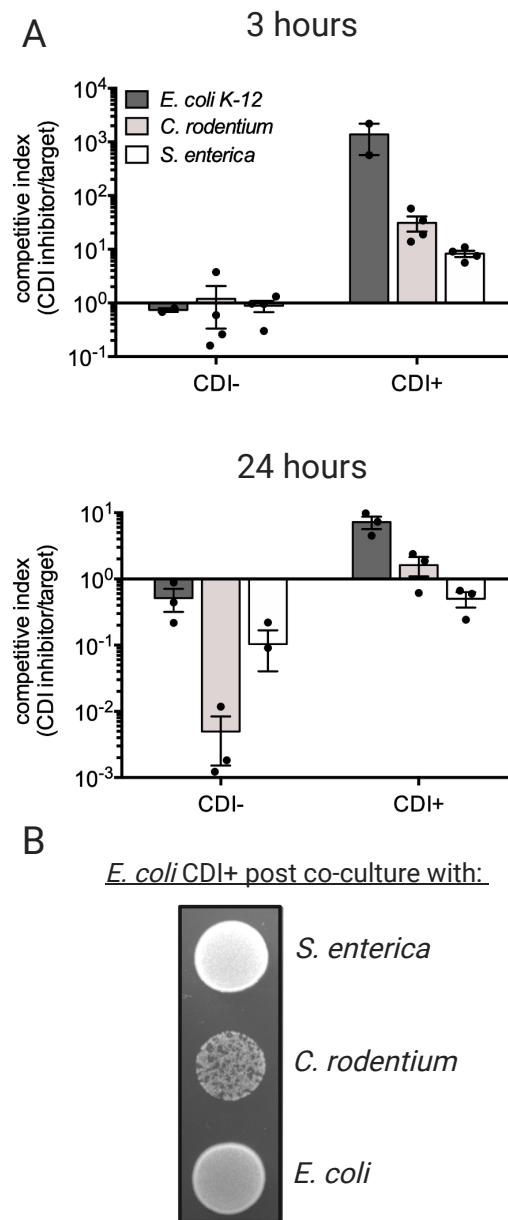


Figure 3.7: **CDI diminishes over long time scales, other inhibition mechanisms become more influential.** (A) Competition co-cultures conducted on solid media for either 3 hrs (top) or 24 hrs (bottom) at a 1:1 ratio inhibitors:targets between the indicated targets and *E. coli* inhibitors (either CDI- or CDI+). The average  $\pm$ SEM is presented for three independent experiments. (B) *E. coli* CDI+ cells plated on selective media (20  $\mu$ L) following the 3-hr co-culture in (A).

Table 3.1: Bacterial strains used in Chapter 3.

Strain	Description	Source
MG1655	WT Strain (5 (F- $\lambda$ - <i>ilvG</i> - <i>rbf</i> -50 <i>rph</i> -1)	Dan Anderson
DL8698	MG1655 $\Delta wzb$	[78]
DL8705	MG1655 $\Delta wzb$ <i>araBAD</i> ::spec, SpcR	[78]
MFDpir	MG1655 RP4- 2-Tc::( $\Delta$ Mu1::aac(3)IV $\Delta$ aphA]- $\Delta$ nic35- $\Delta$ Mu2::zeo) <i>dapA</i> ::(erm-pir) $\Delta$ recA Aprr Zeor Ermr	[142]
CH13163	MG1655 <i>attTn7</i> ::Gm <sup>r</sup> , GmR	This study
CH13164	MG1655 <i>attTn7</i> ::Kan <sup>r</sup> , KanR	This study
CH87	<i>Citrobacter rodentium</i> DBS100 WT strain	Andy Goodman
CH14482	<i>Citrobacter rodentium</i> DBS100 <i>attTn7</i> ::Spm, SpmR	This study
CH4448	<i>Salmonella enterica</i> sv. Typhimurium LT2 <i>attTn7</i> ::SpmR	This study
CH4449	<i>Klebsiella aerogenes</i>	ATCC 13048
CH88	<i>Yersinia frederiksenii</i> WT strain	ATCC 33641
CH13882	<i>Enterobacter hormaechei</i> WT strain	ATCC 49162
CH7839	<i>Enterobacter cloacae</i> WT strain	ATCC 13047

Table 3.2: Plasmids used in Chapter 3.

Plasmid	Description	Source
pUC18R6k-miniTn7T-Gm <sup>r</sup>	For integration at <i>attTn7</i> when mated biparentally with pTNS2. Carries gentamycin resistance cassette between Tn7 homology arms. AmpR, GmR	[140]
pTNS2	Carries the <i>tnsABCD</i> operon for recombination with sequences cloned onto pUC18R6k-miniTn7T at <i>attTn7</i> . AmpR	[140]
pMF19	Expresses the <i>wbbL</i> (rhamnosyltransferase) gene for O16 polysaccharide biosynthesis constitutively. SpmR	[144]
pET21b(MCS-)	Derivative of pET21b lacking XbaI-NheI-BamHI-EcoRI to facilitate cloning. AmpR	Ch. 2
pET21b(MCS-)- <i>cdiB-CAI</i> <sup>STEC4</sup>	<i>cdiBCAI</i> (class 4) locus from <i>E. coli</i> STECO31 on pET21b, with expression driven by native promoter. AmpR	Ch. 2
pET21b(MCS-)- <i>cdiBAI</i> <sup>STEC3</sup>	<i>cdiBAI</i> (class 3) locus from <i>E. coli</i> STECO31 on pET21b, with expression driven by native promoter. AmpR	[70]
pET21(MCS-)- <i>cdiBCA</i> <sup>STEC4</sup> -Chimera	NheI site introduced in pre-toxin domain of pET21b(MCS-)- <i>cdiBCAI</i> <sup>STEC4</sup> to facilitate cloning of new toxin-immunity pairs onto the STEC4 CdiA protein.	This study
<i>Ch. 3 plasmids, cont'd.</i>		



Plasmid	Description	Source
pET21b(MCS- )-cdiBCA <sup>STEC4</sup> - CT/cdiI <sup>STEC3</sup>	The toxin-immunity pair from CdiA <sup>STEC3</sup> is fused at the modular (V)ENN motif of CdiA <sup>STEC4</sup> , resulting in a chimeric CdiA-CT protein with the cognate CdiI downstream. AmpR	This study
pCAT-KAN- <i>pheS</i> *	Mobilizable plasmid with R6K origin used for counter selection.	This study
pCAT-KAN	Derivative of pCAT-KAN-PheS* lacking the counter selective marker for insertional mutagenesis.	This study
pCAT-KAN- <i>waaL</i> <i>C. rodentium</i>	A 685 bp fragment of <i>waaL</i> (O-antigen ligase) from <i>C. rodentium</i> ligated into a mobilizable plasmid for insertional mutagenesis.	This study
pCAT-KAN- <i>waaL</i> <i>S. enterica</i> LT2	A 685 bp fragment of <i>waaL</i> (O-antigen ligase) from <i>S. enterica</i> LT2 ligated into a mobilizable plasmid for insertional mutagenesis.	This study
<i>Ch. 3 plasmids, cont'd.</i>		

Table 3.3: Primers used in Chapter 3.

Strain	Description	Source
CH4672 (GlmS-for)	5' - GAG ATG CCG CAC GTT GAG G - 3'	Ch. 2
CH4616 (Tn7R-screen-rev)	5' - CAC AGC ATA ACT GGA CTG ATT TC CG - 3'	[140]
CH5371 (Crod- <i>waaL</i> -KO-sac-for)	5' - TTT GAG CTC GGA AGC CCT ACT GGA ACA GAG C - 3'	This study
CH5372 (Crod- <i>waaL</i> -KO-kpn-rev)	5' - TTT GGT ACC GTG GCG GCA AAC AGG ATG G - 3'	This study
CH5373 (LT2- <i>waaL</i> -KO-sac-for)	5' - TTT GAG CTC GGA CTT CGC TGC CTT GCA GAG AG - 3'	This study
CH5374 (LT2- <i>waaL</i> -KO-kpn-rev)	5' - 5' - TTT GGT ACC GCC GTA GCC CTT GAT CGG G - 3'	This study

# Chapter 4

## Identification of two CDI ionophore toxins capable of exploiting homologous inner membrane proteins to exert toxicity in target cells

### 4.1 Abstract

CDI systems are widespread throughout the Proteobacteria and have been implicated in both competition and the initiation of collective behaviors such as biofilm and persister formation [90, 157, 161]. Toxin delivery by CdiA is mediated by the large CdiA exoprotein, which encodes a modular toxin domain in its C-terminus (CdiA-CT). CdiA-CTs harbor a variety of activities, including DNA or RNA degradation or dissipation of the proton motive force, presumably through formation of an inner membrane (IM) pore [161]. To reach their substrate, endonuclease CdiA-CTs exploit a variety of IM proteins for translocation to the cytosol [79]. By contrast, only a single IM receptor (AcrB) has been identified for the ionophore family [86]. It is unknown if AcrB is required for insertion into the bilayer, or if its proton transport function is hijacked. Here we characterize two more ionophore toxins (CT-1 and CT-2 from *E. coli* NI1076) and identify

their IM receptors. Interestingly, in contrast to all previous reported CDI toxins, both NI1076 ionophores are capable of independently exploiting two homologous IM proteins in target cells (DtpA/DtpB and PuuP/PlaP, respectively). By virtue of their promiscuity, obtaining resistance to these ionophores is extremely difficult, which likely points to their importance in mediating competition. Furthermore, we find that the native transport activity of DtpA is not required for CT-1 activity, suggesting that IM receptors may serve as a scaffold for ionophore toxins to enter the membrane. These results are an important step in characterizing the mechanism of CDI pore formation as well as the physiology of CDI systems in bacterial communities.

## 4.2 Introduction

Contact-dependent inhibition (CDI) systems facilitate the delivery of toxins between bacteria. As introduced in Chapter 2, CDI is a member of the Type Vb family of two-partner secretion systems (see section 1.4) and therefore includes an Omp85  $\beta$ -barrel protein (CdiB) and its partner, a large ( $> 200$  kDa) exoprotein (CdiA). CdiA encodes a modular toxin domain in its carboxy-terminus (CdiA-CT) that is responsible for growth arrest when translocated into target bacteria. CDI systems are found widespread within the Proteobacteria, but the mechanism of toxin delivery and activation has been extensively studied in *E. coli* and *Burkholderia* spp. (*cdiBAI/cdiBCAI* from *E. coli* and *bcpAIOB* from *Burkholderia* spp.) [63, 64, 65, 125]; see Chapter 2 for *cdiBCAI*)

CdiA biogenesis and toxin delivery have been investigated by expressing the *cdiBAI* system in *E. coli* K-12 [70]. By using this plasmid system, we have found that toxin delivery is controlled by a series of discrete steps. CdiA must first bind to an OM receptor in the target cell. Receptor binding is controlled by a central 200-300 amino acids of CdiA (receptor-binding domain (RBD), see Ch. 2) and is flanked on both sides

by beta-rich structural domains (FHA-1 and FHA-2) homologous to those of filamentous hemagglutinin (FHA) from *Bordetella pertussis* (Figure 2.4). Receptor binding initiates a series of dramatic changes in CdiA. First, half of CdiA containing FHA-2 and CdiA-CT is released from within the CDI+ cell periplasm, which requires unfolding of CdiA-CT from a degradation-resistant state [83]. Then, FHA-2 is thought to facilitate the delivery of CdiA-CT. Secondary structure predictions suggest FHA-2 could conceivably form a  $\beta$ -barrel in the OM of the recipient cell to facilitate toxin translocation [70]. Multiple membrane translocation steps demand that CDI toxins harbor plasticity to unfold and refold during transport. To facilitate this, CdiA-CT enzymatic toxins encode an N-terminal translocation domain [79] with a disulfide pair necessary for protease resistance in the periplasm of the inhibitor cell [83]. Once the toxin arrives in the target cell periplasm, it parasitizes an inner-membrane protein to gain access to the cytosol [91] through a third stage of membrane transport that is still under study.

Structural and functional studies of CdiA-CTs, in addition to highlighting toxin diversity, also present a new perspective on the physiological role of CDI in bacterial communities. These studies have shown, for instance, that the activity of some tRNase toxins can be highly specific, in some cases differentiating between acylated and de-acylated tRNA substrates [162]. If CDI toxins are non-discretionary bactericidal weapons, deployment of a toxin that can only deplete a single pool of tRNAs appears counter intuitive. However, evolving highly restricted effectors that are not bactericidal suggests CDI systems could potentially act as a form of collective growth regulation rather than as weapons for direct competition. This model, termed “contact-dependent signaling” (CDS), is also supported by the finding that CdiA RBDs bind to highly divergent OMPs, sometimes limiting their effective range to the same species [71]. Even the broadest-range CdiA proteins are quite limited (Figure. 2.5 and [116]). The CDS hypothesis first arose, however, from observations that *Burkholderia thailandensis* uses CdiA to initiate biofilm

formation in a CdiA-CT-dependent manner [89]. In fact, early observations that *E. coli* targets can recover from CDI intoxication by a pore-former may also support the CDS model [68]. Recently, investigations have also revealed that target cells do in fact activate stress responses upon receipt of CDI toxins, which suggests that CdiA-CT exchange could strategically induce growth arrest in sibling cells, providing an interpretation of the CDS model [90]. Indeed, by expanding our understanding of CDI toxin activities and their effect on target cell growth and gene expression, we stand to gain a better appreciation for the larger picture of CDI's role in the environment.

In addition to displaying limited toxicity in target cells in some cases, CDI toxins also require the presence of specific IM and sometimes cytosolic proteins (termed "permissive factors") in target bacteria. Of course, the requirement of target cell proteins for activity further limits the effective range of CdiA-CTs. Though cytosolic-acting toxins clearly must pass the IM to gain access to substrates, pore-forming toxins do not share this barrier yet still curiously require a translocation protein in the IM [85]. Even among enzymatic CDI toxins, some are inactive unless target cells express a second cytosolic permissive factor [88, 78]. For example, of two tRNase toxins that have identical activity and structure, only one requires EF-Tu and EF-Ts for activity while the other is autonomous [162]. Though permissive factors may be a deliberate checkpoint to limit delivery to siblings, they might also represent a requirement specific to the constraints of CdiA-CT structure and function. For instance, in attempting to balance the structural requirements of unfolding and refolding that are associated with CdiA-CT delivery, a RNase toxin from *Yersinia kristensenii* shares 3D structural homology with the RNase A superfamily yet has substituted conserved cysteine disulfides with alternative interactions that favor plasticity over rigidity [163]. Another clear example of the constraints of CdiA-CT plasticity is demonstrated by another tRNase toxin from *E. coli* 536 which binds a permissive factor (CysK) specifically for stability in the cytosol [88]. Addition-

ally, the native activity of neither the IM cytoplasmic entry protein nor the permissive factor is required for toxicity of CDI nucleases, which seems to also support the notion that these protein partners serve as scaffolds to aid in folding of the disorder-prone toxin domain [74, 83, 87]. Taken together, it seems that CdiA-CTs are either rapidly diversifying with selection for target cell recognition, or that CdiA-CT structural constraints necessitate co-factors to ensure stability or sub-cellular localization following delivery.

To shed some light on the mechanism of pore-forming CDI toxins, we have characterized the receptor dependence of two new members of the CDI ionophore family. Both CdiA-CTs originate from the same strain of *E. coli* (*Escherichia coli* NI1076) and share sequence-level similarities that may point to a shared mechanism of pore-formation. Indeed, we find that both toxins have evolved to exploit two different yet homologous inner-membrane proteins for their activity. Interestingly, during genetic selections to enrich for CDI-resistant (CDI<sup>R</sup>) targets against CdiA-CT<sup>NI1076-2</sup>, we observed the same ~34.5 Kb deletion in nine separate pools of MG1655 K-12 target cells that were mutagenized using two different approaches. Six of these mutants were verified by whole genome sequencing, while the remaining three screened positive for the removal of at least some of the genes in the same region. Indeed, the CT-2 specific deletion is flanked by IS5 elements that removed not only one of the IM receptor proteins for this toxin but also 38 other open-reading frames. In selections against CdiA-CT<sup>NI1076-1</sup>, by contrast, only a single transposon mutant and two UV-mutagenized target cell pools became resistant. By sequencing the CT1<sup>R</sup> UV mutants, we find that CT-1 can similarly exploit two independent IM proteins as receptors in target bacteria, making CDI-resistance difficult to obtain. Additionally, as a first step in understanding the interaction between these toxins and their receptors, we introduced structure-based functional mutations into a receptor for CdiA-CT<sup>NI1076-1</sup> and find that, similar to observations of other CDI toxins, receptor function is not required for the toxicity of CdiA-CT<sup>NI1076-1</sup>.

## 4.3 Results

### 4.3.1 The mouse enteric isolate NI1076 encodes two CDI loci that encode toxins capable of disrupting the proton motive force in target bacteria

*E. coli* NI1076 (a murine isolate) contains two CDI loci, predicted to encode an OmpC/F-binding class 2 CdiA protein (CdiA-1) and a lipopolysaccharide - binding class 4 CdiA protein (CdiA-2) (Fig. 4.1 and 4.2). To study these toxins, we constructed chimeric CdiA proteins using a plasmid-encoded class 1 BamA-binding CDI system from *E. coli* EC93 (CdiA-1 EC93) by replacing the C-terminal toxin domain, demarcated by a conserved VENN motif, with the desired toxin, as previously described [77]. The resulting chimeras (CdiA<sup>EC93</sup>-CT/I<sup>NI1076-1</sup> and CdiA<sup>EC93</sup>-CT/I<sup>NI1076-2</sup>, referred to as CT-1 and CT-2) are functional for growth inhibition, since susceptible MG1655 target cells lose viability when in co-culture with inhibitor cells expressing either chimera (Fig. 4.3). Furthermore, both toxins can only be neutralized by plasmid expression of their cognate immunity gene, demonstrating that inhibition is specifically due to CdiA-CT delivery and that each toxin is likely structurally unique (Fig. 4.3).

Based on sequence homology, we predict that NI1076 CT-1 and CT-2 belong to a previously identified yet understudied class of CDI ionophore toxins (Fig. 4.14) [68]. Indeed, only two CdiA-CT domains with ionophore activity have been previously described [68, 86]. We chose to test this possibility by treating CDI co-cultures with the membrane potential dye bis(1,3-dibutylbarbituric acid) trimethine oxonol (DiBAC<sub>4</sub>(3)), which enters depolarized membranes and can be detected by excitation at 516 nm [164]. Whereas a known endonuclease has no effect on dye uptake, both NI1076 toxins disrupt the membrane potential in target cells to the same degree as the known pore-forming



toxin CdiA-CT<sup>EC93-1</sup> (Fig. 4.4). An average of  $\sim 96\%$  of target cells across three separate experiments were positive for dye uptake when in competition with either NI1076 toxin as well as EC93 CT, and the accumulation of DiBAC<sub>4</sub>(3) is fully prevented by internal expression of the cognate *cdiI* gene (Figs. 4.4 and 4.17). We can therefore conclude that NI1076 encodes two CDI loci that contain unique ionophore CdiA-CT toxin domains.

Endonuclease toxins delivered by CDI systems are toxic when expressed in the cytoplasm in the absence of a cytoplasmic entry protein [83, 91, 162]. To see if NI1076 CT-1 and CT-2 behave similarly, we expressed both toxin domains from an arabinose-inducible plasmid (pCH450) in the wild-type *E. coli* K-12 cells used in competitions. When plated on selective media containing 0.2% arabinose, CT-1 is not toxic. However, no colonies grow when transformed with CT-2 (Fig. 4.3). Interestingly, neither toxin is toxic when expressed with the conserved VENN motif (data not shown). Thus, only VENNless CT-1 is toxic to wild-type K-12 cells by ectopic expression.

### 4.3.2 NI1076 CT-1 and CT-2 do not require the known ionophore receptor AcrB to exert toxicity

Both of the previously described ionophore toxins also originate from a murine isolate (strain *E. coli* EC93; Fig. 4.14) and, interestingly, though many different inner membrane CDI receptors have been identified for the nuclease family of CDI toxins [79], both EC93 toxins require AcrB to depolarize target cell membranes (Fig. 4.5) [86]. As reported previously by the Koskiniemi group [86], we find that EC93 CT-1 is a less potent toxin than EC93 CT-2, since there is a 10-fold reduction in competitive index when CT-1 is delivered from the same CdiA protein (Fig. 4.5). Since EC93 CT-1 and CT-2 can only disrupt the membrane potential in the presence of AcrB, it is possible that AcrB might be required for bilayer entry and pore formation. However, here we find that neither

NI1076 CT-1 and CT-2 require AcrB to inhibit target cells (Fig. 4.5). Thus, AcrB is not a requirement for pore-formation by CDI toxins.

### 4.3.3 Transposon mutants are resistant to CT-2 due to mutations not associated with the site of transposon insertion

Since the NI1076 CTs do not require AcrB for toxicity, they either exploit a different inner membrane protein to achieve membrane depolarization or they are autonomous. To differentiate between these possibilities, we conducted genetic selections on mutagenized target cells in an attempt to identify IM proteins required for toxin delivery. In a first attempt, we mutagenized 6 separate pools of target cells for each toxin using the *mariner* transposon (as previously described [79]), then subjected the mutant pools to iterative cycles of liquid co-culture competitions with either CdiA-CT chimera, seeking to enrich until the target cell populations became fully resistant (CDI<sup>R</sup>, Fig. 4.6). After three rounds of co-cultures, 3 pools enriched for CT-2 resistance, and 1 pool became resistant to CT-1. Interestingly, single colonies from all 4 toxin resistant pools carry insertions in *puuP*, which encodes a putrescine importer present in the IM and therefore represents a possible cytoplasmic-entry protein (Fig. 4.7) [165]. However, deletion of *puuP* does not render the wild type strain resistant to either toxin, and neither does transduction of P1 lysate made from any of the 4 transposon-resistant mutants (Fig. 4.7). These results suggest that the CDI-resistant transposon mutants must carry additional mutations that arose spontaneously outside of the transposon insertion which are responsible for rendering them CDI<sup>R</sup>. We therefore conclude that the selection pressure applied during enrichments for CDI-resistance was strong enough to obtain the desired mutants, but the receptors for either toxin may be too difficult to obtain using transposon insertions that will not affect essential genes.

#### 4.3.4 UV mutagenesis of target cells reveals that both ionophores can exploit homologous IM proteins as independent receptors

Since our co-culture selection was strong enough to enrich for CDI<sup>R</sup> mutations, but transposon insertions were not an efficient approach for finding those mutants, we repeated the enrichments with target cells mutagenized instead by ultraviolet light. Using this method, 2 of 6 pools became fully resistant to CT-1 after 3 rounds of enrichment, while all 6 pools became resistant to CT-2. These results are consistent with the trend in our transposon mutant pools; enrichment for CT-1<sup>R</sup> was much harder to achieve than resistance to CT-2. Whole genome sequencing of one colony from each resistant pool reveals that the two pools with CT-1 resistance carry loss of function mutations in at least two di/tri-peptide importers, namely DtpA and DtpB (Table 4.1). Interestingly, one of the two CT-1<sup>R</sup> mutants also carries a LOF mutation in DtpC, though our mutagenesis and competition results using deletion strains suggest that loss of DtpA/DtpB is sufficient for CT-1<sup>R</sup> (Table 4.1 and 4.9). Notably, neither CT-1<sup>R</sup> mutant contains a mutation in *puuP*. Thus, it appears that inactivation of *puuP* is irrelevant for CT-1 and must have arisen in the transposon mutant by chance, which may contain relevant mutations outside of the transposon insertion itself though we did not investigate that mutant further.

We performed co-culture enrichments with the same starting pools of UV-mutagenized target cells also against CT-2. Of all 6 pools that enriched for resistance to CT-2, each mutant carries a mutation in the putrescine importer PuuP (Table 4.1), suggesting PuuP is critical for CT-2 activity. This is consistent with our selections against transposon-mutagenized target cells receiving this same toxin, since 3 of 6 CT-2<sup>R</sup> pools all contain transposon insertions in *puuP* (Fig. 4.7B). However, because we tested a *puuP*

deletion strain against CT-2 after finding three mutants with *puuP*::Tn-KanR insertions, we already knew that deletion of *puuP* is not sufficient to protect target cells from CT-2 intoxication. Informed by our selection with CT-1, we perused the genome for a homologue of *puuP* and were delighted to discover exactly that: another putrescine importer (*plaP*, formerly *yeeF*) that shares 63% amino acid sequence identity with PuuP (Fig. 4.8). Remarkably, *plaP* is encoded within a region that has been deleted in every CT-2<sup>R</sup> mutant selected for by UV mutagenesis. This ~ 34.5 Kb deletion spans nucleotide position 2,064,549 - 2,098,995 in *E. coli* MG1655 (Fig. 4.6; parental strain and reference genome from Dan Andersson). All 6 CT-2<sup>R</sup> mutants carry this same deletion, while the CT-1<sup>R</sup> colonies do not. Therefore, because we conducted our selections on the same parental mutant pools which were subsequently split for selections against either toxin domain, the large deletion rendering targets resistant to CT-2 arose independently six times.

The deletion region is flanked on either end by *insH1* sequences encoding the transposase for the IS5 element bordered by inverted repeats. This suggests that the removal of the large intervening region could have been RecA-mediated. The CT-2-specific deletion also encodes the biofilm-promoting Ag43 autotransporter and one gene involved in colanic acid biosynthesis (*ugd*; UDP-glucose dehydrogenase) (Table 4.2 and Fig. 4.6). Though we used a *wzb* deletion strain for selections, which should also lack the ability to make capsule polysaccharide, *ugd* also produces a compound (UDP-4-amino-4-deoxy-L-arabinose) that can modify lipid A to produce polymyxin resistance [166, 167]. Therefore, it is possible that loss of Ag43 and *ugd* could provide additional positive selection for the observed deletion in competition with a CDI inhibitor strain, since cell surface changes are known to affect access to the target cell surface [153] (see Ch. 3). Only in combination with selection for loss of *plaP*, however, do we see this deletion arise during enrichments for CDI<sup>R</sup>.

Since all six UV mutant pools became resistant through the same independent deletion encompassing *plaP* that may be RecA-mediated, this same deletion could explain the resistance observed in our transposon mutants that are also CT-2 resistant and contain additional mutations outside of the transposon insertion in *puuP* (Fig. 4.7A). To determine if the transposon mutants have lost both *plaP* and *puuP*, we conducted PCR reactions with primers that anneal exclusively to either gene and verified that the *puuP*::Tn-Kan mutants carry a transposon in *puuP* by band shift as expected, but do not have detectable *plaP* in their genome (Fig. 4.7D). Finally, because the deletion found in each UV mutant includes the entire histidine biosynthesis operon (Fig. 4.6D), we plated the CT-2-resistant transposon mutants on M9 minimal media (MM) with or without histidine. As anticipated, none of the CT-2<sup>R</sup> transposon mutants are able to grow on MM media in the absence of supplemented histidine, like a *hisB* deletion strain and the two CT-2<sup>R</sup> UV mutants (Fig. 4.7E). Taken together, these results indicate that deletion of *plaP* arose spontaneously nine independent times and therefore was an efficient means of gaining CDI-resistance. These data also indicate that, like CT-1, CT-2 is also capable of exploiting two homologous IM proteins (PlaP and PuuP) independently for toxicity.

### 4.3.5 CT-1 uses the di/tri-nucleotide importers DtpA and DtpB as independent receptors

*E. coli* K-12 has four Proton-dependent Oligopeptide Transporter (POT) proteins: DtpA - D [168]. As expected from the CT-1<sup>R</sup> UV mutants, DtpA/B (51% identity) and DtpC/D (56% identity) are more closely related to each other than the two groups are together (~ 27% identity; Figure 4.13). However, one of two CT-1<sup>R</sup> mutants does have a frameshift mutation in *dtpC* as well (Table 4.1). To determine how many Dtp proteins can serve as receptors for CT-1, we created deletions of each di/tri-nucleotide importer

within the family (DtpA, DtpB, DtpC, DtpD), either alone or in combination with DtpA (which was inactivated in both CT-2<sup>R</sup> mutants), and conducted co-culture competitions. As anticipated, a deletion of *dtpA* or *dtpB* alone is insufficient for protection from CT-1 toxicity, but a combined *dtpA/dtpB* deletion strain is fully resistant to CT-1 by both viable cell counts and DiBAC<sub>4</sub>(3) uptake (Fig. 4.9 and Fig. 4.12 or Fig. 4.18). Since the only strain resistant to CT-1 is  $\Delta dtpA \Delta dtpB$ , and deletion of *dtpC* in combination with *dtpA* is insufficient for CT-1 resistance, only DtpA or DtpB serve as IM receptors for CT-1. Moreover, plasmid-encoded DtpA or DtpB can restore wild-type susceptibility to a resistant  $\Delta dtpA \Delta dtpB$  strain (Fig. 4.11A).

### 4.3.6 CT-2 can exploit both of the putrescine importers PuuP and PlaP as receptors, but with unequal potency

Mirroring the behavior of NI1076 CT-1, only a double deletion of both *plaP* and *puuP* can produce a fully CT-2 resistant target strain when challenged with CT-2 in co-culture competitions (Fig. 4.9B). Interestingly, however, we find that a *plaP* deletion strain is partially resistant to CT-2, which would presumably indicate that the remaining PuuP is less productive at facilitating intoxication by CT-2. However, pPlaP unexpectedly produces a less potent response from CT-2 compared to complementation with PuuP during competitions (Fig. 4.10). One interpretation of these conflicting data is that expression levels of *puuP* and *plaP* are very different, and thus more PlaP may be present in a  $\Delta puuP$  strain than vice versa. Therefore, when we control for protein abundance by expressing either putrescine importer from the same promoter (leaky expression of the *lac* repressor) to separate expression from toxin affinity, we then find that PlaP elicits much lower inhibition in target cells, indicating CT-2 may bind PlaP with lower affinity.

To explore the difference in receptor-dependent CT-2 potency further, we then ex-

pressed just the CT-2 toxin domain from a plasmid under control of the *araBAD* promoter and conducted transformations of the complemented deletion strains with empty plasmid or pCT-2. Again, we observe partial resistance to CT-2 when only *plaP* is expressed, as can be seen by the presence of very small colonies which are obvious after several days of growth on 0.2% L-arabinose (Fig. 4.10B). These results again suggest that CT-2 may have higher affinity for PuuP than it does for PlaP.

To see if a *plaP* deletion strain is also partially resistant to membrane depolarization, we once more used the membrane potential-sensitive dye DiBAC<sub>4</sub>(3) to assay the sensitivity of receptor-less target cells to CDI. Consistent with our inhibition data, a double deletion of *plaP/puuP* is completely resistant to dye uptake, whereas individual deletion strains are not (Fig. 4.12). Again, the *plaP* deletion is slightly resistant to dye uptake as well, in contrast to a  $\Delta$ *puuP* strain. In summary, both pore-forming toxins can exploit two homologous inner-membrane nutrient transporters (DtpA/DtpB by CT-1 and PuuP/PlaP by CT-2) to intoxicate target bacteria by disruption of the proton-motive force. Since CT-2 displays lower toxicity in the presence of PlaP when compared to PuuP, this may suggest that CT-2 binds PlaP/PuuP with different affinities.

### 4.3.7 The native function of DtpA is not required for toxicity of CT-1

Little to nothing is known of the mechanism by which CdiA-CT ionophore toxins disrupt the proton-motive force in target cells. Indeed, only two pore-forming toxins have been characterized (EC93 CT-1 and CT-2), and only one inner membrane protein receptor is known to support pore-forming activity (AcrB) [86]. Both EC93 toxins were classified as ionophores using the same dye uptake assay we have used here, as well as by measuring the accumulation of ethidium bromide due to inactivity of pmf-dependent

efflux pumps [68]. However, a complicating factor is that both EC93 toxins happen to exploit the cell's main efflux pump (AcrB) as an IM receptor, and it is unclear if the ionophores themselves would disrupt AcrB's native activity during CDI. AcrB is also a large trimer of functionally integrated subunits, making it a more difficult target for probing toxin-receptor interactions. By contrast, DtpA and DtpB are monomeric POT proteins that are widely distributed from humans to bacteria and so have been thoroughly characterized, providing an alternative approach to investigating the ionophore-receptor interaction [168, 169].

To determine if the native activity of DtpA is important for toxicity of NI1076 CT-1 when delivered into target cells, we introduced mutations into a plasmid-encoded DtpA in a *dtpA/dtpB* deficient strain to test mutant variants against wild-type complementation during co-culture competitions. We introduced alanine residues in place of Y38 and Y156, which are substrate-binding residues conserved with the human POT homologue hPepT1, and known to participate in binding the antiviral valganciclovir and, at least for Y156, to alafosfalin as well [169, 170]. Using two time points to assay target cell sensitivity to CT-1, our results reveal that substrate-binding mutations have no noticeable effect on toxicity of CT-1 during CDI (Fig. 4.11). This is not due to changes in protein expression, however, since both DtpA variants are tagged with a viral epitope and appear to be expressed at the same level and properly localized when probed by immunoblot (Fig. 4.11). Notably, though functional mutations do not affect CDI, the presence of a VSV epitope tag does appear to partially disrupt CDI in competitions (Fig. 4.11A). We also tested the possible dependency of CT-1 on the proton binding activity of DtpA by replacing E56 with Arg, which should prevent its ability to relay protons as part of the periplasmic gate [170]. Though this mutant also supports CT-1 mediated inhibition, suggesting it is properly expressed and localized, DtpA E56R is not visible by immunoblot against the VSV epitope (Fig. 4.11C). Thus, we have determined that CT-1 toxicity is



unaffected by functional mutants of DtpA, but a C-terminal VSV tag appears to partially disrupt CDI in competition co-cultures.

## 4.4 Discussion

In this study, we identify two new members of the CdiA-CT family of ionophore toxins (CdiA-CT<sup>NI1076-1</sup> and CdiA-CT<sup>NI1076-2</sup>) and also the inner membrane proteins they exploit for toxicity (DtpA/DtpB and PuuP/PlaP, respectively). We find that each toxin can use either IM protein independently as a receptor, presumably to enter and depolarize the IM. Interestingly, for CT-2, the two alternative putrescine importers PlaP and PuuP do not complement a  $\Delta plaP \Delta puuP$  strain to the same degree; PlaP elicits a  $\sim 1000$ -fold defect in inhibition when expressed from the same plasmid as PuuP (Fig. 4.10). Therefore, CT-2 might have lower affinity for PlaP. Interestingly, because a *plaP* deletion strain is actually partially resistant to CT-2 in co-culture competitions compared to either a  $\Delta puuP$  or wild type target strain, lower affinity for PlaP might have arisen due to differential expression levels of both IM proteins. Indeed, if there is much more PlaP expressed in a  $\Delta puuP$  target strain, the abundance of receptor could overcome imperfect association with CdiA-CT. Likewise, if much less PuuP exists in the *plaP* deficient strain but it associates with CT-2 with much higher affinity, when we normalize expression levels PuuP should facilitate greater inhibition than PlaP, which is consistent with our observations. In *Proteus mirabilis* and *Dickeya zaeae*, PlaP orthologues mediate collective behaviors such as swarming motility, biofilm formation, and invasion of host cells in response to environmental putrescine availability, which it binds with low affinity in order to serve as a surveillance importer [171, 172]. Therefore, putrescine will only accumulate in the cytosol if enough of it is present to overcome PlaP's low binding affinity, which then leads to downstream gene expression changes [171, 173]. Our data

suggest that *plaP* is expressed to higher levels than *puuP* in *E. coli*, possibly indicating a similar role for PlaP as a putrescine sensor in the Enterobacteria. It will be interesting to study this interaction further in the future, possibly supplementing target cells with polyamines to affect expression levels of PlaP/PuuP and adding epitope tags to both proteins. Additionally, with the option for exploiting two different receptors that may undergo differential expression due to a signaling molecule, these data introduce the intriguing possibility that CT-2 can selectively exert different potencies in target cells based on environmental conditions such as polyamine availability, if those conditions lead to differential expression of PuuP/PlaP.

Prior studies to identify receptor proteins for CdiA-CTs have thus far only identified single receptor-toxin pairs. However, many uncharacterized CDI toxins may exist that can similarly exploit more than one IM protein and simply have yet to be described. Indeed, by evolving receptor promiscuity, the NI1076 ionophores are more capable of evading target cell resistance than other toxins, which is clearly demonstrated by our genetic selections; we were unable to enrich for multiple transposon insertions in DtpA/B and, even when mutagenized by ultraviolet light, only two of six pools became resistant to this toxin. CT-2 resistance was much easier to select for: three of six transposon mutant pools and all six UV mutant pools became CT-2 resistant, even though this required removal of two putrescine importers. Intriguingly, the ease at which *plaP* and *puuP* became doubly inactivated in CT-2<sup>R</sup> target cells is explained by a  $\sim 34.5$  Kb deletion encompassing *plaP* (formerly *yeeF*). Since the deletion is flanked at each end by an insertion sequence element (*insH1*) surrounded by inverted repeats, it's possible that the removal of intervening sequence was RecA-mediated.

Most studies of CDI toxins have been conducted on the abundant diversity of nucleases deployed by CdiA, which are diverse in activity and receptor preference. Interestingly, some CdiA-CT nucleases also require cytosolic permissive factors for activity,

which likely aid in maintaining thermodynamic stability following the translocation process [79, 87, 162]. In contrast, only two pore-forming toxins have been characterized that both exploit the multidrug efflux pump AcrB. Since EC93's toxins both use AcrB but are differentially potent (Fig. 4.5), it has been suggested that the two redundant CdiA proteins may be expressed at different times during cell growth to modulate inhibition and prevent competition for receptor access [86]. *E. coli* NI1076 also encodes two CDI loci, but in contrast to those of EC93, both of NI1076's CdiA-CTs are similarly potent (Fig. 4.5). These toxins, however, use unique IM receptors to inhibit targets. Thus, at least in NI1076, both CDI systems could be used at the same time to deliver a higher dose of toxins. Indeed, if pore-forming toxins require oligomerization, a high dose of toxin would facilitate channel formation. Future studies should consider this when analyzing CDI regulation in natural isolates.

Since we have now identified four new IM proteins recognized by ionophore toxins, it is clear pore-formation does not exclusively require AcrB during CDI. However, in contrast to the variety of transporter families exploited by nucleases that can use a variety of energy sources [79], the 5 pore-forming receptors now identified are all proton-coupled substrate transporters. This raises the possibility that the ionophore toxins might parasitize the proton relay activity of their receptor proteins. However, arginine replacement of the periplasmic gating residue Glu56 did not disrupt CDI in our study, suggesting that the toxin itself is disrupting the pmf rather than parasitizing the native proton shuttling activity of its receptor (Fig. 4.11). Importantly, however, though the E56R variant complemented a resistant receptor deletion strain, we could not detect DtpA E56R in whole cell lysates by immunoblot as we could other DtpA mutants expressed from the same plasmid, possibly indicating that the epitope is inaccessible or cleaved. Alternatively, DtpA E56R could be remaining in the insoluble pellet even after extraction with sarkosyl. Why this would occur for only the periplasmic gating mutant is not clear.

We also tested the possibility that CT-1 could mimic a peptide substrate and utilize the same residues known to coordinate peptides in the binding cavity of DtpA. However, since alanine replacement of two conserved and critical tyrosine residues did not prevent CDI, we conclude that the native substrate transport and proton binding activity of DtpA is not important for CdiA-CT function (Fig. 4.11) [169, 170]. We anticipate that because pore-formation requires coupling of an energy source to the unfavorable thermodynamics of bilayer entry, interacting with a transmembrane protein may enable the toxin to refold at the interface of the bilayer and the protein itself. In this case, disrupting localization or abundance of the receptor but not substrate transport would affect CDI, which is consistent with our observations. Future work should elaborate on these findings, since investigating how ionophores exploit their IM receptors will help in understanding how they disrupt the membrane potential, which is yet unknown.

Colicins, many of which are pore-forming toxins, are bacteriocins that are secreted by *E. coli* into the extracellular space to mediate interbacterial cell killing [16]. Much like CDI toxins, colicins are either enzymatic (nucleases) or ionophoric (pore-formers). The pore-forming colicins are essentially inside-out membrane proteins in solution that bind to lipid bilayers and reorganize upon membrane insertion, acting as polyvalent cations driven to interact with lipid headgroups [174]. In vitro experiments with liposomes revealed that colicin insertion into the bilayer progresses through four stages: electrostatically driven membrane binding, unfolding at the membrane surface, elongation of two hydrophobic helices to form an anchor, and insertion of the anchor into the bilayer - the so-called “umbrella” model of insertion [175]. However, in contrast to colicins, CDI ionophores lack obvious transmembrane domains and are overall less hydrophobic than expected for a membrane protein (Fig. 4.21 and 4.20). Although the minimal cytotoxic portion of CdiA-CT responsible for pore-formation is not known, it likely begins just downstream of the conserved VENN motif, since CT2<sup>NI1076</sup> is toxic ectopically only when VENN is removed

(Fig. 4.10). We also know that other CdiA-CTs with tRNase activity are inactive if expressed internally with VENN (Nick Bartelli, unpublished data), so this is not strictly a feature of ionophore CTs and may indicate the delivered fragment of CdiA itself includes only residues downstream of VENN. Likewise, the modular cytoplasmic entry domains found in endonuclease CTs [79, 83] appear to be present within pore-forming toxins as well; an alignment of CdiA-CT<sup>NI1076-1</sup> and CdiA-CT<sup>NI1076-2</sup> suggests that the cytoplasmic entry domain of ionophores is much smaller than that of nucleases (Fig. 4.20). In addition to lacking alpha-helical transmembrane domains, the CT sequence following these putative entry domains seems too small to function similarly to self-assembling colicin pores by comparison. But despite a lack of similarity between CdiA-CT ionophores and colicins, a close observation of the shared features of the putative toxic domain of CdiA-CT ionophores reveals a great overrepresentation of small nonpolar amino acids, with 16% of both NI1076 CT sequences comprised of glycines and a combined 20% represented by alanine and serine residues. In fact, an alignment of all four characterized CDI ionophores (from *E. coli* EC93 and NI1076, Fig. 4.14) reveals the existence of putative glycine zipper motifs (GxxxG) with the most well-conserved motif flanked on either side by conserved prolines in both NI1076 toxins (Fig. 4.20). In the VacA toxin, which relies on glycine zippers to form pores by oligomerization, prolines flanking the glycine zipper domain are critical for toxicity [176]. Glycine zippers in general are a prevalent structural motif that drive helix-helix interactions of single-pass membrane integrated alpha helices [177], and are known to facilitate channel formation by both eukaryotic and bacterial proteins [31, 176]. Thus, ionophore CDI toxins could conceivably use these motifs for channel formation. However, as glycine zippers are associated with self-assembly of large oligomeric complexes, if the same mechanism is responsible for CdiA-CT channel formation, it is difficult to imagine how these toxins could achieve such high levels of potency without oligomerizing. Furthermore, the glycine repeats we observe

here are shorter (GxxxGxxxG) than typical glycine zippers, and the toxin itself is less hydrophobic than would be expected for a membrane protein (Fig. 4.21). Similar to the unique structural constraints imposed on endonucleases by CDI, we anticipate that pore-forming toxins embody these same constraints in the form of imperfect transmembrane motifs.

Interestingly, in contrast to the cryptic functional domains in ionophore CdiA-CTs, ionophore immunity proteins are extremely hydrophobic and likely to contain transmembrane alpha helices (Fig. 4.21). Therefore, although the mechanism of pore formation is less obvious, ionophore immunity proteins are likely pre-localized to the IM in anticipation of CdiA-CT delivery. Indeed, an immunity protein that has greater stability within the bilayer than its cognate toxin would be an efficient means of preventing self-intoxication, especially if CDI pores are extremely effective. This idea is supported by our observation that over-expression of ionophore immunity proteins is itself toxic (data not shown), which would be expected from over-expression of an integral membrane protein. Thus, how exactly pore-forming CdiA-CTs are neutralized by their cognate immunity proteins will be an intriguing topic to explore further.

## 4.5 Materials and Methods

**Bacterial strain and plasmid construction.** To study the activity of CdiA-CT<sup>NI1076-1</sup> and CdiA-CT<sup>NI1076-2</sup>, we constructed chimeric CdiA proteins using a recombineering approach as previously described [77]. Three PCR products were generated and fused by overlap-extension (OE) PCR, resulting in a fragment encoding the toxin of interest flanked by regions of homology to the desired CdiA protein. To build the fragments for recombineering, *cdiA*-CT1/*cdiI* and *cdiA*-CT2/*cdiI* were first amplified with primer pairs CH3953/CH3954 and CH4127/CH4128, respectively. Next, upstream and

downstream homology regions were amplified from the *cdiA*<sup>EC93-1</sup> gene using primer pairs DL1527/DL2470 and DL1663/DL2368, respectively. All three fragments were fused by OE-PCR with the outer primers DL1527/DL2368. The resulting OE-PCR product was electroporated with pCH10163 into *E. coli* DY378 cells as previously described [77]. The resulting recombinants were selected on yeast extract glucose agar containing 33  $\mu\text{g}/\text{mL}$  chloramphenicol and 10 mM D/L-p-chlorophenylalanine and sequenced with oligonucleotides CH4070/CH4071 to verify.

Immunity genes were amplified from *E. coli* NI1076 genomic DNA with primer pairs CH4058/CH4059 (locus 1) and CH4060/CH4061 (locus 2). The resulting fragments were digested with KpnI/XhoI and ligated into pTrc99aKX [91]. For complementation, each membrane protein was amplified with the following primer pairs from MG1655 genomic DNA: *dtpA* (CH5141/CH5144, which adds a viral VSV epitope tag), *dtpB* (CH5366/CH4885), *puuP* (CH4529/CH5085), and *plaP* (CH5095/CH5096). Each PCR fragment was digested with the appropriate enzymes (EcoRI/XbaI for *dtpA*, KpnI/XhoI for *dtpB* and *plaP*, NcoI/XbaI for *puuP*) and the purified fragments ligated into pTrc99aKX, except for *dtpA*-VSV which was ligated into pTrc99a. Mutations were introduced into plasmid-encoded *dtpA*-VSV using megaprimer PCR, in which only a segment of the gene is amplified in the first round with a reverse oligo encoding the desired change. To build the megaprimers, fragments from primer pairs CH5141/CH5142 (Y38A), CH5141/CH5365 (Y156A), and CH5141/CH5166 (E56R) were generated from pTrc99a-*dtpA*-VSV. In a second PCR reaction, these megaprimers were paired with a single reverse primer (CH5144) to generate the final mutant *dtpA* fragments. These products were then digested with EcoRI/XbaI, ligated into pTrc99a, and sequenced to verify the point mutation was successfully introduced.

To study CdiA-CT toxicity by internal expression, both toxins were amplified first with primer pairs CH4108/CH4236 (CT-1) and CH4110/CH4111 (CT-2), digested with

NcoI/XhoI and ligated into pCH450 for arabinose-inducible expression. After determining that neither toxin construct inhibited growth when induced, both CTs were then cloned with a new forward primer (CH4235 for CT-1 and CH4237 for CT-2) to skip the conserved VENN motif, which is likely cleaved and separated from CdiA-CT during delivery. The new VENNless toxin domains were digested with KpnI/XhoI and ligated into pCH450KX.

Target strains used for all assays in this work are derived from wild-type MG1655 originally obtained from Dan Andersson (Uppsala University), who also provided a complete genome sequence. Wild-type MG1655 was transduced with a  $\Delta wzb::kan$  deletion from the Keio collection [139] to inhibit colanic acid synthesis during competitions. Target cells were cured of the kanamycin resistance cassette with pCP20, but also carry a *araBAD::spm* deletion. EPI100 cells also with a cured  $\Delta wzb$  deletion were used for inhibitors. Because the CDI cosmids confer Cm resistance, inhibitor strains were tracked on chloramphenicol and targets on spectinomycin.

All deletions ( $\Delta dtpA/B/C/D$ ,  $\Delta puuP/plaP$ , and  $\Delta acrB$ ) were constructed by P1 transduction. Fresh lysates were prepared by treating the appropriate Keio deletion strain (grown in 1 mL LB supplemented with 0.4 % glucose, 10 mM MgSO<sub>4</sub>, and 5 mM CaCl<sub>2</sub>) with 100  $\mu$ L phage lysate while in early log phase. Once the culture cleared, it was vortexed with 400  $\mu$ L chloroform and spun for 2 min at 15,000 rpm to separate. For transduction, target cells were grown overnight in 2 mL LB, collected in 1 mL, and resuspended in 300  $\mu$ L LB supplemented with 10 mM MgSO<sub>4</sub> and 5 mM CaCl<sub>2</sub> then treated with a 1:10 dilution of the appropriate P1 lysate. After 30 minutes, transductants were treated with 240 mM sodium citrate in LB and recovered for 1-4 hrs. Presumptive deletion strains were selected on Kan and screened by PCR with a nested Kan cassette primer (CH3832 or CH3833) paired with a locus-specific reverse primer. Where necessary, the Kan cassette was cured with pCP20 and these mutants were also screened by PCR,



by monitoring a band shift.

Wild type target cells and each mutant derivative that exhibited any amount of CDI resistance ( $\Delta dtpA \Delta dtpB$ ,  $\Delta puuP$ ,  $\Delta plaP$ ,  $\Delta puuP \Delta plaP$ ) were subjected to another round of transduction with P1 lysate from SK2873, to insert the *galK::dTomato-cat* marker used for separation of targets and inhibitors during flow cytometry. The resulting transductants (CH6757 – CH6762) were selected for on Cm and screened for fluorescence against the nonfluorescent wild type strain at 580 nm by a MACSQuant flow cytometer (Miltenyi Biotech).

**Competitions and growth conditions.** All strains were grown at 37 °C in lysogeny broth (LB) or on LB agar except where noted for certain assays (ts plasmid curing, recombineering selections). Media were supplemented when appropriate with antibiotics at the following concentrations: ampicillin (Amp) 150  $\mu\text{g mL}^{-1}$ ; kanamycin (Kan) 50  $\mu\text{g mL}^{-1}$ ; spectinomycin (Spm) 100  $\mu\text{g mL}^{-1}$ ; chloramphenicol (Cm) 33  $\mu\text{g mL}^{-1}$ ; rifampicin (Rif) 200  $\mu\text{g mL}^{-1}$ ; tetracycline (Tet) 15  $\mu\text{g mL}^{-1}$ . For all competition co-cultures, inhibitor and target strains were grown to an optical density at 600 nm ( $\text{OD}_{600}$ ) of 0.6-0.9 and mixed at an equal ratio ( $\text{OD}_{600}$  1.0:1.0), plated in a 15  $\mu\text{L}$  volume on LB agar and incubated at 37 °C for the indicated time. Except for the time course, all competitions were conducted for 2 hours on pre-warmed LB agar plates. The zero time point was taken from the same mixture. The final time point was obtained from harvesting the plated cells with a sterile swab into 600  $\mu\text{L}$  1 $\times$ M9 salts. The diluted pellet was then subjected to ten-fold serial dilutions again in 1 $\times$ M9 salts, which were plated on the appropriate antibiotics to enumerate CFU/mL of both populations.

**Transformation assays.** To test for toxicity by plasmid-expression, TSS competent cells were prepared for transformation by growing to  $\text{OD}_{600}$  0.3, then cooled on ice for 15 min. Cell pellets were collected by centrifugation at 4 °C at 6000 rpm for 3 min. Pellets were resuspended in TSS solution (10% polyethylene glycol (PEG-8,000), 30 mM  $\text{M}_g\text{Cl}_2$ ,

5% dimethylsulfoxide) at 1/100th the original culture volume. Next, approximately 60 ng of plasmid DNA from pCH13925 and CH14011 (CT-1 and CT-2, respectively) was mixed with the TSS competent cells and transformed by briefly heat-shocking the cells at 42 °C for 60 seconds. Heat-shocked transformants were cooled on ice also for 60 seconds, resuspended in 1 mL LB, and allowed to recover at 37 °C for 2 hours. After recovery, cells were plated at a volume of 100  $\mu$ L per 8.5 cm agar plate (i.e., 33  $\mu$ L per 1/3 of plate). If transformants contained a plasmid already, antibiotics were included during each step of the assay to ensure selection for the pre-existing plasmid, and the recovered cell culture was concentrated at 2 $\times$  the original OD before plating.

**Mutagenesis and selections for CDI-resistance.** To select for target cells resistant to CdiA-CT<sup>NI1076-1</sup> and CdiA-CT<sup>NI1076-2</sup> MG1655 cells were mutagenized and selected for as previously described [79]. The mariner transposon was introduced into MG1655 Rif<sup>r</sup> by conjugation with MFD $pir$  cells carrying pSC189. Donors were supplemented with 30 $\mu$ M diaminopimelic acid in shaking liquid LB and grown to mid-log at 37°C. Donors and recipients were mixed and plated on LB agar at 37°C for 5 hrs. Cell mixtures were harvested with a sterile swab, collected in 1 $\times$ M9 media, and plated on Kan-supplemented LB agar for selection of transposon integrants. Each transposon library was harvested directly from Kan plates into 1 mL 1 $\times$ M9 media for selection. Six pools were mutagenized for each toxin chimera.

Prior to mutagenesis using ultraviolet light, a survival curve was first established to determine the proper irradiation dose for 0.1-1% bacterial survival. 25 mL cultures of SK3300 cells were grown to OD<sub>600</sub>  $\sim$  0.4 and resuspended in 0.1 M MgSO<sub>4</sub>. Cells were UV irradiated in 8.5 cm petri plates at 0, 2, 6, 8, 10, 12, and 18 mJ/cm<sup>2</sup> in a Stratalinker 1800. Viable cell counts were performed from ten-fold serial dilutions pre- and post-irradiation by plating cells on LB agar and agar containing both streptomycin or rifampicin to obtain mutation frequencies (Fig. 4.15).

Selections for CDI<sup>R</sup> mutants were conducted with pDAL879-*cdiA*<sup>EC93</sup>-CT/*cdiI*<sup>NI1076</sup> constructs for each toxin. Inhibitor cells with each CDI chimera were grown to mid-log phase and mixed with each of 6 mutant pools for 3 hours in liquid co-culture at a ratio of 2:1 (targets:inhibitors) to minimize bottle-necking during the initial selection. Target cells were added to the competitions by harvesting from plates into 1 mL of 1×M9 media, which was used to seed 25 mL liquid LB. Following each 3-hour co-culture, targets were plated on Kan at multiple ten-fold serial dilutions to enumerate viable cells and to separate them from inhibitors. Two additional competitions were performed to enrich for CDI<sup>R</sup> mutants using these Kan-selected colonies from the previous round. After the third enrichment, single colonies were isolated, checked for CDI<sup>R</sup>, and the location of the transposon was determined by rescue cloning. Briefly, resistant colonies were grown overnight, their genomic DNA extracted by phenol-chloroform, and approximately 1 μg was digested by incubation with NspI overnight. The enzyme digest was stopped by incubation at 65 °C for 25 mins, 2 μL Cutsmart buffer containing 10 mM ATP (NEB) and 1 μL T4 DNA ligase was added and incubated overnight at 4 °C. The mixture was transformed into *E. coli* DH5α *pir*+ competent cells. Plasmid DNA from the resulting transformants was prepped and sequenced with primer CH2260 to identify the chromosomal insertion site.

Since 12 mJ/cm<sup>2</sup> resulted in ~ 5% survival and 18 mJ/cm<sup>2</sup> < 1% survival, we conducted mutagenesis on SK3300 cells in the middle of that range, at 15 mJ/cm<sup>2</sup>. Mutagenized target cells (10 mL of each) were added to a 500 mL flask filled with 90 mL LB (supplemented with Kan to maintain the presence of pZS21-*bamA*) and allowed to recover overnight in the dark. Selections were performed by mixing each mutant pool at a 2:1 ratio with inhibitors (SK2972 and SK2973 grown to OD<sub>600</sub> ~ 0.7), so as to minimize bottlenecking while facilitating toxin delivery into most mutants. All 6 mutant pools were split between the two inhibitor strains, so that each pool for selection by either

inhibitor strain started off with the same library prior to selections. Co-cultures were performed by concentration large cultures of inhibitors and targets into a total OD<sub>600</sub> of 33, and 100  $\mu$ L of the dense mixture was plated on pre-warmed 8.5 cm LB agar plates. After 3 hrs, the mixture was harvested into 1 mL 1 $\times$ PBS and serially diluted to obtain viable cell counts for target cells, while 100  $\mu$ L of two dilutions was reserved for plating on full Kan plates to seed the next enrichment. After 3 rounds of co-culture competitions with all 12 pools (6/toxin), single colonies were isolated from pools that appeared to be enriching for CDI<sup>R</sup>. Each colony was competed with CdiA-CT<sup>EC93</sup> to rule out mutations in *bamA* and its growth rate measured against wild type with a Tecan Infinite 20-0 Pro.

**Flow cytometry to measure pmf dissipation.** To assess the integrity of the proton motive force in target cells receiving CdiA-CTs, we conducted liquid co-culture competitions with wild type or CDI<sup>R</sup> target cells (including *cdiI+*) marked with *galK::dTomato-cat*. Both inhibitor and target strains were mixed at a 1:1 ratio with a starting OD<sub>600</sub> of 1.0. After 1 hr of shaking, 150  $\mu$ L aliquots were moved to 1.5 mL Eppendorf tubes and treated with 10  $\mu$ g mL<sup>-1</sup> bis(1,3-dibutylbarbituric acid) trimethine oxonol (DiBAC<sub>4</sub>(3)), which enters depolarized cells [164]. After 30 mins of incubation in the dark, the dye-treated cell mixtures were rinsed in 1 $\times$  PBS twice and 2  $\mu$ L of the final resuspended pellet was diluted into 2 mL 1 $\times$  PBS for analysis by flow cytometry (MACSQuant). To normalize the data collected from these competitions, a stop gate was applied to each sample based on the fluorescence intensity of a monoculture of wild type red (channel: FITC) target cells (SK4210) and 100,000 events were recorded in the gated population for each sample. Next, these 100,000 events that represent the target cell population were analyzed for fluorescence intensity in the GFP channel, which detects DiBAC<sub>4</sub>(3). The histograms are a representative experiment from at least three separate replicates, which we plotted as the percent GFP+ cells of the entire FITC+ (target cell) population.

**Protein Extraction and Immunoblotting.** To detect DtpA in target cells, cell

lysates containing total protein were prepared by treating from 1 mL of stationary phase ( $\sim OD_{600}$  1.5) cultures of MG1655  $\Delta dtpA \Delta dtpB$  cells expressing each DtpA-VSV variant from pTrc99a. Cell pellets were resuspended in 5  $\mu$ L BugBuster (Sigma) per mg of cell mass. Lysozyme and Dnase I were added to the resuspension and the samples were incubated on a rotisserie for 40 min at room temperature. Cell lysates were spun at 4 °C for 60 mins at 13,000 rpm and the soluble fraction was removed and stored at - 20 °C. The remaining insoluble material was resuspended in the same volume of BugBuster used previously with the addition of 1% Sarkosyl to extract IM proteins. This second resuspension was then spun again for 60 mins at 4 °C and 13,000 rpm. The supernatant containing IM proteins was removed and also stored at - 20 °C. Protein extracts were quantified by Bradford and equal amounts of protein were loaded onto a 10% SDS-PAGE gel and separated at 110 V for 1 hr. Proteins were transferred to a PVDF membrane for 1 hr at 17 V, which was treated with anti-VSV antisera. The 800CW secondary antibody was visualized using a LI-COR Odyssey infrared imager. To visualize total protein, a second gel was loaded with the same quantities of total protein and stained with Coomassie Brilliant Blue R-250 for 60 mins at RT and destained overnight.



## 4.6 Tables and Figures

UPEC536_CdiA	1	MHQPVRFTYRLLSYLISTIIAGQPLLPAVGAVITPQNGAGMDKAANGVPVVNIATPNGA
NI1076_CdiA1	1	MHQPVRFTYRLLSYLISTIIAGQPLLPAVGAVITPQNGAGMDKAANGVPVVNIATPNGA
UPEC536_CdiA	61	GISHNRFDTYNVGKEGLILNNA TGKLNPTQLGGLIQNNPNLKAGGEAKGIINEVTGGNRS
NI1076_CdiA1	61	GISHNRFDTYNVGKEGLILNNA TGKLNPTQLGGLIQNNPNLKAGGEAKGIINEVTGGNRS
UPEC536_CdiA	121	LLQGYTEVAGKAANVMVANPYGITCDGCGFINTPHATLTTGRPVMNADGSLQALEVTEGS
NI1076_CdiA1	121	LLQGYTEVAGKAANVMVANPYGITCDGCGFINTPHATLTTGRPVMNADGSLQALEVTEGS
UPEC536_CdiA	181	ITINGAGLDGTRSDAVSI IARATEVNAALHAKDLTVTAGANRITADGRVSALKGEGDVPK
NI1076_CdiA1	181	ITINGAGLDGTRSDAVSI IARATEVNAALHAKDLTVTAGANRITADGRVSALKGEGDVPK
UPEC536_CdiA	241	VAVDTGALGGMYARRIHLTSTESGVGVNGLNYARDGDIITLSSAGKLVKNSLAGENTTV
NI1076_CdiA1	241	VAVDTGALGGMYARRIHLTSTESGVGVNGLNYARDGDIITLSSAGKLVKNSLAGENTTV
UPEC536_CdiA	301	TGTDVSLSGDNKAGGNLSVITGTGILINPRLVTDKNI VLSSSGQIVQNGGELTAGONAM
NI1076_CdiA1	301	KQGGVILIGDHKAGGNLSVSRSDIVLSNGTILNSDKNLSLLAGGRITQONEKLTAGRDVT
UPEC536_CdiA	361	LSAQHINNOTSG-TVNAAEVTLTTINDTLKGRSIAGKTLTVSSGSLNNGGTLVAGRDAT
NI1076_CdiA1	361	LAAKNITQDTASQINAARDIVTVASDITLTCGQITAGQNLTA SATILITDGLLAKSHAG
UPEC536_CdiA	420	VKTGTFSNIGTVQCNGLKVTATDITLSTGSLKSGSTLDTISARNAITLSSGDAGAKDSARVTVS
NI1076_CdiA1	421	LNAGTLNNSGAVQGATLITGSLTILNSGSLLSGGPITVNTREDFITQSGRTGAKGKVDITAS
UPEC536_CdiA	480	GITENRGRLVSDVLTLSATQINNSGTLSSGAKELVASAPLITTEKSVTNSDGNIMLDSA
NI1076_CdiA1	481	GKLTSTGSLVSDDALVLAQDVTQNGVLSGGKGLTVSACTLSSGKKSVDHSDAAMTLNVT
UPEC536_CdiA	540	SSTLAGETSAGGTIVSVKNSLKTITTTACT-CGNSVSVVDVQNAQLDGTQAARDITLTVNASE
NI1076_CdiA1	541	IVALDGETSAGDTLRVQADRLSIAAGACLQSGKNLSINARDARLAGTQAQQITVTVNASE
UPEC536_CdiA	599	KLTHSGKSSAPSLSLSAPELTSSGVLVGSALNTQSQTLTNSGLLQCEASLTVNTQRLDNQ
NI1076_CdiA1	601	KLTHSGKSSAPSLSLSAPELTSSGVLVGSALNTQSQTLTNSGLLQCKASLTVNTQRLDNQ
UPEC536_CdiA	659	QNGTLYSAADLTLDIPDIRNSGLITGDNGLMLNAVSLSNPGKIIADTILSVRATTLDGDGL
NI1076_CdiA1	661	QNGTLYSAADLTLDIPDIRNSGLITGDNGLMLNAVSLSNPGKIIADTILSVRATTLDGDGL
UPEC536_CdiA	719	LQGAGALALAGDTLSQGSNCRWLTADDLILRGKTLNNTAGTTQGNITVQADRWANSGSVL
NI1076_CdiA1	721	LQGAGALALAGDTLSQGSNCRWLTADDLILRGKTLNNTAGTTQGNITVQADRWANSGSVL
UPEC536_CdiA	779	ATGNLTASATGQLTSTGDIMSQGDITLKAATTDNRGSLLSAGTSLDGNSLDMSGTVQGD
NI1076_CdiA1	781	ATGNLTASATGQLTSTGDIMSQGDITLNAATTDNRGSLLSAGTSLDGNSLDNRGTVQGN
UPEC536_CdiA	839	HVTIRQNSVTNSGTLTGIAALT LAARM---VSPQALMNNGGSLTSGDLTITAGS-----
NI1076_CdiA1	841	HVTIRQNSVTNSGTLTGIAALT LAARMDMA SPQALMNNGGSLTSGDLTITAGSITSSG
UPEC536_CdiA	893	-----VNSGAIQAADSLTARLTGELVSTAGSKVTSNGEMALSALNLSNSGG
NI1076_CdiA1	901	HWQGKQVLITADSLANSGAIQAADSLTARLTGELVSTAGSKVTSNGEMALSALNLSNSGG
UPEC536_CdiA	939	WIAKNLTLKANSITSAGDITGVDTLTLTVNQTLLNQANGKLLSAGVLTALKADSVTNDGQL
NI1076_CdiA1	961	WIAKNLTLKANSITSAGDITGVDAITLTLTVNQTLLNHSAGKLLSAGVLTALKADSVKNDGQL

UPEC536\_CdiA 999 QGNATTITAGQLTNGGHLQGETLTLAASGGVNNRFGGVLMsrNALNVSTATLSNQGTIQG  
 NI1076\_CdiA1 1021 QGNATTITAGQLTNGGHLQGETLTLAASGGVNNRSGGVLMsrNALNVSTATLSNQGTIQG

UPEC536\_CdiA 1059 GGGVSLNVTDRLQNDISKILSGSNLTLTAQVLANTGSGLVQAATLLLDVVNTVNGGRVLAT  
 NI1076\_CdiA1 1081 GGGVSLNVTDRLQNDISKILSGSNLTLTAQVLANTGSGLVQAATLLLDVVNTVNGGRVLAT

UPEC536\_CdiA 1119 GSADVKGTTLNNGTGTLQGADLLVNYHTFNSGTLTGLTSGLVKGSLLQHGTRGLYSAGN  
 NI1076\_CdiA1 1141 GSADVKGTTLNNGTGTLQGADLLVNYHTFNSGTLTGLTSGLVKGSLLQHGTRGLYSAGN

UPEC536\_CdiA 1179 LLLDAQDFSGQGQVVATGDVTLKLI AALTNHGTLAAGKTL SVTSONAITNGGVMQGDAMV  
 NI1076\_CdiA1 1201 LLLDAQDFSGQGQVVATGDVTLKLI AALTNHGTLAAGKTL SVTSONAITNGGVMQGDAMV

UPEC536\_CdiA 1239 LGAGEAFTNNGMLTAGKGNsvfSAQRFLFNAPGSLQAGGDVSLNSRSDITISGFTGTAGS  
 NI1076\_CdiA1 1261 LGAGEAFTNNGMLTAGKGNsvfSAQRFLFNAPGSLQAGGDVSLNSRSDITISGFTGTAGS

UPEC536\_CdiA 1299 LTMNVAGTLLNSALIYAGNNLKFtdRLHNQHGDILAGNSLWVQKDASGGANTEIINTSG  
 NI1076\_CdiA1 1321 LTMNVAGTLLNSALIYAGNNLKFtdRLHNQHGDILAGNSLWVQKDASGGANTEIINTSG

UPEC536\_CdiA 1359 NIETHQGDIVVRtGHLLNqREGFSATTTTRtNPSSIQGMGNALVDIPLSLLPDGSYGyFT  
 NI1076\_CdiA1 1381 NIETHQGDIVVRtGHLLNqREGFSATTTTRtNPSSIQGMGNALVDIPLSLLPDGSYGyFT

UPEC536\_CdiA 1419 REVENQHGTpCNGHGACNITMDtLYYYAPFADsATQRFLSSQNIITtVTGADNPAGRIASG  
 NI1076\_CdiA1 1441 REVENQHGTpCNGHGACNITMDtLYYYAPFADsATQRFLSSQNIITtVTGADNPAGRIASG

UPEC536\_CdiA 1479 RNLSAEAEERLENRASfILANGDIALSGRELSNQSWQtGENEYLvYRYDPKtFYGSyATG  
 NI1076\_CdiA1 1501 RNLSAEAEERLENRASfILANGDIALSGRELSNQSWQtGENEYLvYRYDPKtFYGSyATG

UPEC536\_CdiA 1539 SLDKlPLlLSPeFENNTIRfSLdGREKDYtPGKtYYSVIQAGGDVKtRfTtSSINNGtTtAH  
 NI1076\_CdiA1 1561 SLDKlPLlLSPeFENNTIRfSLdGREKDYtPGKtYYSVIQAGGDVKtRfTtSSINNGtTtAH

UPEC536\_CdiA 1599 AGSVSPVVSAPVLNtLSQQtGGDSLtQtALQqYEPVVVGSQWHDelAGALKNIAGGSPL  
 NI1076\_CdiA1 1621 AGSVSPVVSAPVLNtLSQQtGGDSLtQtALQqYEPVVVGSQWHDelAGALKNIAGGSPL

UPEC536\_CdiA 1659 TGQtGISDDWPLPSGnNGYLVPStDPDSpYLItVnPKLDGLGQVDShLFAGLYELLGAKF  
 NI1076\_CdiA1 1681 TGQtGISDDWPLPSGnNGYLVPStDPDSpYLItVnPKLDGLGQVDShLFAGLYELLGAKF

UPEC536\_CdiA 1719 GQAPREtAPSYtDEKQfLGSSyFLDRLGLKPEKDYRFLGDAVFDtRYVSNVLSRtGSRY  
 NI1076\_CdiA1 1741 GQAPREtAPSYtDEKQfLGSSyFLDRLGLKPEKDYRFLGDAVFDtRYVSNVLSRtGSRY

UPEC536\_CdiA 1779 LNLGSDtEQMRyLMDNAArQqKGLGLeFGVAlTAEQIAQLDGSILWwESAtINgQTVmV  
 NI1076\_CdiA1 1801 LNLGSDtEQMRyLMDNAArQqKGLGLeFGVAlTAEQIAQLDGSILWwESAtINgQTVmV

UPEC536\_CdiA 1839 PKLYLSPEDITLHNGSVISGNNVQLAGGNITNSGSSINAQNDLSLDSStGYIDNLNAGLIS  
 NI1076\_CdiA1 1861 PKLYLSPEDITLHNGSVISGNNVQLAGGNITNSGSSINAQNDLSLDSStGYIDNLNAGLIS

UPEC536\_CdiA 1899 AGGSLDLSAIGDISNIRSVISGktVQLESVSGNISNITRRQqWAGSDSRYGGVHLsGtD  
 NI1076\_CdiA1 1921 AGGSLDLSAIGDISNIRSVISGktVQLESVSGNISNITRRQqWAGSDSRYGGVHLsGtD



UPEC536\_CdiA 1959 TGPVATIKGTDSLSDAGKNIDITGATVSSGGT LGM SAGNDINIAANLISGSKSQSGFWH  
 NI1076\_CdiA1 1981 TGPVATIKGTDSLSDAGKNIDITGATVSSGGT LGM SAGNDINIAANLISGSKSQSGFWH

UPEC536\_CdiA 2019 TDDNSASSTTSQGSSISAGGNLAMAAGHNLVDVTASSVSAGHSALLSAGNDLSLNAVRESK  
 NI1076\_CdiA1 2041 TDDNSASSTTSQGSSISAGGNLAMAAGHNLVDVTASSVSAGHSALLSAGNDLSLNAVRESK

UPEC536\_CdiA 2079 NSRNGRSESHESHAAVSTVTAGDNLLLVAGRDV ASQAAGVAAENNVVIRGGRDVNLVAES  
 NI1076\_CdiA1 2101 NSRNGRSESHESHAAVSTVTAGDNLLLVAGRDV ASQAAGVAAENNVVIRGGRDVNLVAES

UPEC536\_CdiA 2139 AGAGDSYTSKKKKEINETVRQQGTEIASGGDTTVNAGRDI TAVASSVTATGNISV NAGR D  
 NI1076\_CdiA1 2161 AGAGDSYTSKKKKEINETVRQQGTEIASGGDTTVNAGRDI TAVASSVTATGNISV NAGR D

UPEC536\_CdiA 2199 VALTTATESDYHYLETKKKS GGF LSKKTTHTI SEDSASREAGSLLSGNRVTVNAGDNLT V  
 NI1076\_CdiA1 2221 VALTTATESDYHYLETKKKS GGF LSKKTTHTI SEDSATREAGSLLSGNRVTVNAGDNLT V

UPEC536\_CdiA 2259 EGS D V V A D R D V S L A A G N H V D V L A A T S D T S W R F K E T K K S G L M G T G G I G F T I G S S K T T H D R  
 NI1076\_CdiA1 2281 EGS D V V A D R D V S L A A G N H V D V L A A T S D T S W R F K E T K K S G L M G T G G I G F T I G S S K T T H D R

UPEC536\_CdiA 2319 REAGTTQSQSASTIGSTAGNVSITAGKQAHISGSDVIANRDISITGDSVVVDPGHRRRTV  
 NI1076\_CdiA1 2341 REAGTTQSQSASTIGSTAGNVSITAGKQAHISGSDVIANRDISITGDSVVVDPGHRRRTV

UPEC536\_CdiA 2379 DEKFEQKKSGLTVALSGTVGSAINNAV TSAQETKESSDSRLKALQATKTALS G V Q A G Q A A  
 NI1076\_CdiA1 2401 DEKFEQKKSGLTVALSGTVGSAINNAV TSAQETKESSDSRLKALQATKTALS G V Q A G Q A A

UPEC536\_CdiA 2439 TMASATGDPNATGVSLSLTTQKSKSQHSESDTVSGSTLNAGNNLSVVATGKNRGDNRGD  
 NI1076\_CdiA1 2461 TMASATGDPNATGVSLSLTTQKSKSQHSESDTVSGSTLNAGNNLSVVATGKNRGDNRGD

UPEC536\_CdiA 2499 I V I A G S Q L K A G G N T S L D A A N D I L L S G A A N T Q K T T G R N S S S G G G V G V S I G A G G N G A G I S V F  
 NI1076\_CdiA1 2521 I V I A G S Q L K A G G N T S L D A A N D I L L S G A A N T Q K T T G R N S S S G G G V G V S I G A G G N G A G I S V F

UPEC536\_CdiA 2559 A G V N A A K G S E K G N G T E W T E A T T D S G K T V T I N S G R D T V L N G A Q V N G N R I I A D V G H D L L I S S  
 NI1076\_CdiA1 2581 A G V N A A K G S E K G N G T E W T E A T T D S G K T V T I N S G R D T V L N G A Q V N G N R I I A D V G H D L L I S S

UPEC536\_CdiA 2619 Q Q D T S K Y D S K Q T S V A A G G S F T F G S M T G S G Y I A A S R D K M K S R F D S V A E Q T G M F A G D G G F D I  
 NI1076\_CdiA1 2641 Q Q D T S K Y D S K Q T S V A A G G S F T F G S M T G S G Y I A A S R D K M K S R F D S V A E Q T G M F A G D G G F D I

UPEC536\_CdiA 2679 T V G R H T Q L D G A V I A S T A T P D K N H L D T G T L G F S D L H N E A D Y K V S H S G I S L S G G G S F G D K F Q  
 NI1076\_CdiA1 2701 T V G R H T Q L D G A V I A S T A T P D K N H L D T G T L G F S D L H N E A D Y K V S H S G I S L S G G G S F G D K F Q

UPEC536\_CdiA 2739 G N M P G G M I S A G G H S G H A E G T T Q A A V A E G T T T I R D R D N Q K Q N L A N L S R D E A H H N D S I S P T F  
 NI1076\_CdiA1 2761 G N M P G G M I S A G G H S G H A E G T T Q A A V A E G T T T I R D R D N Q K Q N L A N L S R D E A H H N D S I S P I F

UPEC536\_CdiA 2799 D K E K E Q R R L Q T V G L I S D I G S Q V A D I A R T Q G E L N A L K A A Q K Y C - P V P A D A T E E Q R Q A Y L A  
 NI1076\_CdiA1 2821 D K E K E Q R R L Q T V G L I S D I G S Q V A D I A R T Q G E L N A L K A A K E A T G E T L P A N A T E R Q R Q E Y L A

UPEC536\_CdiA 2858 K L R D T P E Y K E Q K Y G T G S D M Q R G I Q A A T A A L Q G L V G G N M A G A L A G A S A P E L A N I I G H H A  
 NI1076\_CdiA1 2881 K L R D T Q A Y R N E M A K Y G T G S E I Q R G I Q A A T A A L Q G L A G D N L A G A L A G A S A P E L A H L I K S T -

UPEC536\_CdiA 2918 G I D N T A A R A I A H A I L G G V T A A I Q G N S A A A G A T G A C T G E W I A S A I A K S L Y P G V D P S K L I E  
 NI1076\_CdiA1 2940 --K D F A V N A I A H A I L G G A V A A M O G N N V A A G A A G A T G E L A A R A I A G M L Y P G V K Q S D L S E

```

UPEC536_CdiA 2978 DQKQTVSTLATV SAGMAGG IASGDVAGAAAGAGAGKNV VENNALSLVAR-----C-
NI1076_CdiA1 2998 EQKQTVSTLATV SAGMAGG I TGNSTASAAVGAQSGKNA VENNLLGGSEW LQTEKTRHGA

UPEC536_CdiA 3028 ----CA---VAAPCR TKVABQL-----LEI GARAGVAGLA-----GAAVVKDMADRMTSD
NI1076_CdiA1 3058 DVLSCSDNFSCEACR RGAENKAYAAALATG SVALPGSAQAMWLLGACTNAGMQYADSG

UPEC536_CdiA 3070 EIEH-----LITLQMGND EITTKMLSS LHDKYISGAASNPNI CKDLTD EKVELGGS
NI1076_CdiA1 3118 EENPVNSVAAGW NVITMGQG-----KGT IAWNTAGGALINAINGDDPLTCAITNGAGA

UPEC536_CdiA 3123 GSGTGT----PPSENDPKQNEKTVDKLNKQESAIKKIDNITKNALKDHDIIGTLKIM
NI1076_CdiA1 3173 GVCYGVGNVYVKEAANTIGK---WITGGWNPK-----FDPILLKYTEVKGQLCLSKEM

UPEC536_CdiA 3179 DGKPVFKENGGYWDHICEMQNTLRGLRNHADTLKNVNNPEQAAYGRATDAINKIESAIK
NI1076_CdiA1 3223 VPSKLESAVGNAGGSIS-----SERGSS--ITQKKKDAIE

UPEC536_CdiA 3239 GYCI
NI1076_CdiA1 3256 ACGK
    
```

Figure 4.1: Alignment of OmpC-binding CdiA from *E. coli* UPEC 536 and CdiA of locus 1 from *E. coli* NI1076. Sequences diverge at both the TPS domain (residues 280 - 596) and at VENN, which demarcates the toxin domain (highlighted in red). Generated with Clustal Omega.

Identification of two CDI ionophore toxins capable of exploiting homologous inner membrane proteins to exert toxicity in target cells

STECO31\_CdiA2 1 MNRNCYRIFFNKARGMLMVVADIARSGRAGTSLSSRTGYPRRQRCRVTPLEFSLWLASG  
 NI1076\_CdiA2 1 MNRNCYRIFFNKARGMLMVVADIARSGRAGSSPSSRTGYPRRQRCRVTPLEFSLWLASG

STECO31\_CdiA2 61 MVHSVNAAGIADHGAPGHQQPTITOTASGIPOVNIQTSPAGGVSHNTYSQFDVGNKGV  
 NI1076\_CdiA2 61 MVHSVSAAGIADHGAPGHQQPTITOTASGIPOVNIQTSPAGGVSHNTYSQFDVGNKGV

STECO31\_CdiA2 121 LNNAHNNVQTLQGGMVAGNPWLAKGEARIILNEVNSRNPSQLNGFVEVAGKKAQVVIANP  
 NI1076\_CdiA2 121 LNNAHNNVQTLQGGMVAGNPWLAKGEARIILNEVNSRNPSQLNGFVEVAGKKAQVVIANP

STECO31\_CdiA2 181 AGISCDGCGFINANRATLTTGQPQMKNGSLTGFSVERGEIQITGKMDASRTDYTDIAR  
 NI1076\_CdiA2 181 AGISCDGCGFINANRATLTTGQPQMKNGSLTGFSVERGEIQITGKMDASRTDYTDIAR

STECO31\_CdiA2 241 SVKINAGIWAQDLKVTTRGNVVDIAHGQTEKKAADASSCPQVALDVSLGGMYAGKIRLV  
 NI1076\_CdiA2 241 SVKINAGIWAQDLKVTTRGNVVDIAHGQTEKKTGDASSIQVALDVSLGGMYAGKIRLV

STECO31\_CdiA2 301 GTETGVGVRNAGHIGAQAGAVTLTADGRIENSGSISAKTDVHLATRELHNSGSVYAGQD  
 NI1076\_CdiA2 301 GTETGVGVRNAGHIGAQAGAVTLTADGRIENSGSISAKTDVHLATRELHNSGSVYAGQD

STECO31\_CdiA2 361 TQIQSNGVFTHTGVSARRNTRIQTARLTGGERSLLAAGVKDDGRLAAAGNLTVSATGEL  
 NI1076\_CdiA2 361 TQIQSDGAFSHTGVSARRNTRIQTARLTGGERSLLAAGVKDDGRLAAAGNLTVSATGEL

STECO31\_CdiA2 421 AAHQVLSGGDMQLKGQGLDLSNSRIQGQHTELDATSGNLSIQNVQLSAGTLSARTAGHF  
 NI1076\_CdiA2 421 AAHQVLSGGDMQLKGQGLDLSNSRIQGQHTELDAGSGNLSIQNVQLSAGTLSARTAGHF

STECO31\_CdiA2 481 SNNGGTINADTLQISAQSLSNRERGLIQTGTGDFSLNLPGGVDNREGLLAANGAVRLDAL  
 NI1076\_CdiA2 481 SNNGGTINADTLQISAQSLSNRERKGLIQTGTGDFSLNLPGGVDNREGLLAANGAVRLDAL

STECO31\_CdiA2 541 SLDNRRGKVAWQSGSLQVKTGAVDNOQGSILASRDVRLINLQALNNDNGLISAAGTGR  
 NI1076\_CdiA2 541 SLDNRRGKVAWQSGSLQVKTGAVDNOQGRILLASRDVRLINLQALNNDNGLISAAGTGR

STECO31\_CdiA2 601 IKTQQAVSNTEGRMESAGRLDTSAGSLNNHQGTVVSDGLSVTLDGALDNTSGRLLSQKTL  
 NI1076\_CdiA2 601 IKTQQAVSNTEGRMESAGRLDTSAGSLNNYQGTVVADGLSVTLDGALDNTSGRLLSQKTL

STECO31\_CdiA2 661 SVSGSELVSDGLIQSGSDMTLDVQDGVLSNRNTRKTRGGISSAGTLTVRAGMLNNQQGFI  
 NI1076\_CdiA2 661 SVSGSELVSDGLIQSGSDMTLDVQDGVLSNRNTRKTRGGISSAGTLTVRAGMLNNQQGFI

STECO31\_CdiA2 721 VGQKDMTLNAGTLDNRQGVLSQASLQSSGTLMNQKALKAGTDMLLSGGDVSNQEGTL  
 NI1076\_CdiA2 721 VGQKDMTLNAGTLDNRQGVLSQASLQSSGTLMNQKALKAGTDMLLSGGDVSNQEGTL

STECO31\_CdiA2 781 AAGRDLNAHLNVLENQOQGTVVSNNGNSRLDVTRFDNQGGRLLVAQOSLTLSSDTIINDASGL  
 NI1076\_CdiA2 781 AAGRDLNAHLNVLENQOQGTVVSNNGNSGLDVTRFDNQGGRLLVAQOSLTLSSDTIINDASGL

STECO31\_CdiA2 841 IQSGASLNLRADTSLNRNSGDRGGVISQGPITLNACTLDSIAGVLLSCEALSLTAGVVNN  
 NI1076\_CdiA2 841 IQSGASLNLRADTSLNRNSGDRGGVISQGPITLNACTLDSIAGVLLSCEALSLTAGVVNN

STECO31\_CdiA2 901 TSGQVVANGLLGWNSQALNNQSGLIQGRGISINTAGQTLNRRGTLNLSLQELTVSTGAMD  
 NI1076\_CdiA2 901 TSGQVVANGLLGWNSLVLNNQSGLIQGRGISINTAGQTLNRRGTLNLSLQELTVSTGAMD

STECO31\_CdiA2 961 NRGGTVGAKTADLSTTSLDNREGGRLVSEGELRLHTGGLQNSHGQIQSVGDMILNSVRG  
 NI1076\_CdiA2 961 NRGGTVGAKTKVLDLSTTSLDNREGGRLVSEGELRLHTGGLQNSHGQIQSVGDMILFDSVRG

STECO31\_CdiA2 1021 VVDNVSGLIRSGSAITLNALQFINRHTQNTGQGLEAQTTHITTDQLDNDQEGSILADRALT  
 NI1076\_CdiA2 1021 VVDNVSGLIRSGSAITLNALQFINRHTQNTGQGLEAQTTHITTDQLDNDQEGSILADRALT

STECO31\_CdiA2 1081 VMADRTLSNNDGVLISGATLSVSGRQLAFSNRDGVVKAGQSVSVDAAGQLGGDGKLLSLGN  
 NI1076\_CdiA2 1081 VMADRTLSNNDGVLISGATLSVSGRQLAFSNRDGVVKAGQSVSVDAAGQLGGDGKLLSLGD

STECO31\_CdiA2 1141 MTLKSNTTFSNSGQTIANGNLTLVNGDVSNTGSLLAGSRDLNLSIRLENTBKGEISAGO  
 NI1076\_CdiA2 1141 MTLKSNTTFSNSGQTIANGNLTLVNGDVSNTGSLLAGSRDLNLSIRLENTBKGEISAGO

STECO31\_CdiA2 1201 TWLNVTDTLNLRGLIDGKYTRLQANTLTNSGTGRIYGDVAVGCAATFNNLEENGVAATLA  
 NI1076\_CdiA2 1201 TWLNVTDTLNLRGLIDGKYTRLQANTLTNSGTGRIYGDVAVGCAATFNNLEENGVAATLA

STECO31\_CdiA2 1261 GRERVDLGVQTLNNRTHSLIYSAGDMHTGGMLDANGIATGKAGVLNNSHATIEAAGYVVL  
 NI1076\_CdiA2 1261 GRERVDLGVQTLNNRTHSLIYSAGDMHTGGMLDANGIATGKAGVLNNSHATIEAAGSITL

STECO31\_CdiA2 1321 SAGQINNVDHFETERVVVSTEKVTEYQLSGSDKRWSAGEPGVYVNDSSNSLKKLHTPE  
 NI1076\_CdiA2 1321 SAGQINNVDHFETERVVVSTEKVTEYQLSGSDKRWSAGEPGVYVNDSSNSLKKLHTPE

STECO31\_CdiA2 1381 GARDKFTQYDYTRTVEETRVKESDPGKILSGAGMTIVADKLFNDKSQVVAGGLTIPSGS  
 NI1076\_CdiA2 1381 GARDKFTQYDYTRTVEETRVKESDPGKILSGAGMTIVADKLFNDKSQVVAGGLTIPSGS

STECO31\_CdiA2 1441 VENVSVSGERHVTDSGSTSYVYRIRKKGKDKQGEKTSQYTPPTVIQTTITLPGELTSHGQ  
 NI1076\_CdiA2 1441 VENVSVSGERHVTDSGSTSYVYRIRKKGKDKQGEKTSQYTPPTVIQTTITLPGELTSHGQ

STECO31\_CdiA2 1501 PQGSHVTLSPKPGQTDVQTELTGNVDATVAGTDRIPIRPFVVSAGEPVILLPGQQFEVSA  
 NI1076\_CdiA2 1501 PQGSHVTLSPKPGQTDVQTELTGNVDATVAGTDRIPIRPFVVSAGEPVILLPGQQFEVST

STECO31\_CdiA2 1561 PQGSIHVAGPDVRLPDSSLFKTNPVAVNYPYLVEVDPRFTNQKRWLGSYMQKAFSONGDN  
 NI1076\_CdiA2 1561 PQGSIHVAGPDVRLPDSSLFKTNPVAVNYPYLVEVDPRFTNQKRWLGSYMQKAFSONGDN

STECO31\_CdiA2 1621 MLKRLGDGFYEQRLIREQVVALTGQRYLDGYSNDEEQFKALMDAGITFGKQYNLTPGVAL  
 NI1076\_CdiA2 1621 MLKRLGDGFYEQRLIREQVVALTGQRYLDGYSNDEEQFKALMDAGITFGKQYNLTPGVAL

STECO31\_CdiA2 1681 TAEQMALLTGDIVVWLVNTTVLTPDGSTQTVQVPQVYARVKPGDVNSAGALIAGRDMVMKL  
 NI1076\_CdiA2 1681 TAEQMALLTGDIVVWLVNTTVLTPDGSTQTVQVPQVYARVKPGDVNSAGALIAGRDMVMKL

STECO31\_CdiA2 1741 DGDLFNSGKLAGKQTVQLSADNIHNQAGTVQGANVSLTARTDINSTGGCLQASDSSLAMA  
 NI1076\_CdiA2 1741 DGDLFNSGKLAGKQTVQLSADNIHNQAGTVQGANVSLTARTDINSTGGCLQASDSSLAMA

STECO31\_CdiA2 1801 GRDISLTTTTRTAQRDAGQNHFERTRIDSVAGVYVQNDQGRVLVQAGRDMNLTAATVVNQ  
 NI1076\_CdiA2 1801 GRDISLTTTTRTAQRDAGQNHFERTRIDSVAGVYVQNDQGRVLVQAGRDMNLTAATVVNQ

STECO31\_CdiA2 1861 GKDSLTLQLSAGRDMTLSTVTTSAQDNITWDKNNRLSQGVTTQSTGSTLACNGDPVTLTAGRD  
 NI1076\_CdiA2 1861 GKDSLTLQLSAGRDMTLSTVTTSAQDNITWDKNNRLSQGVTTQSTGSTLACNGDPVTLTAGRD

STECO31\_CdiA2 1921 MTSQAASLSAQKGLALMAEHDVTLTGAQNTSSLDEYHKVTGSSGMLSKTTHHVDVSDRR  
 NI1076\_CdiA2 1921 MTSQAASLSAQKGLALMAEHDVTLTGAQNTSSLDEYHKVTGSSGMLSKTTHHVDVSDRR

STECO31\_CdiA2 1981 TMTGSELNGDVTVSIAGHNLNVTGSSVAGDNRVSLVAGNNLNIQMLTESNRETHLKOEKK  
 NI1076\_CdiA2 1981 TMTGSELNGDVTVSIAGHNLNVTGSSVAGDNRVSLVAGNNLNIQMLTESNRETHLKOEKK

```

STECO31_CdiA2 2041 SGLMSSGGVGFVSVGSQSLKVRDTATDTTQKGSTVGSVHGDVSLQAGNRLTVNGSDLIAGR
NI1076_CdiA2 2041 SGLMSSGGVGFVSVGSQSLKVRDTATDTTQKGSTVGSVHGDVSLQAGNRLTVNGSDLIAGR

STECO31_CdiA2 2101 DMALSGKEVSIITAATDQHVQHTVVEQKTSGLTLALSCTVGSALNTTVETVQAAKSAGNSR
NI1076_CdiA2 2101 DMALSGKEVSIITAATDQHVQHTVVEQKTSGLTLALSCTVGSALNTTVETVQAAKSAGNSR

STECO31_CdiA2 2161 LEALQGVKAALSQAQAVQAGRLADAQGADAGNNTVGVLSYGSQSSKSEQQSEQTVAKG
NI1076_CdiA2 2161 LEALQGVKAALSQAQAVQAGRLADAQGADAGNNTVGVLSYGSQSSKSEQQSEQTVAKG

STECO31_CdiA2 2221 SALTAGNNLSIQATGSGVKGVGDGLTIQGSQIKAGNNVLLQANRDVNLVSAENTSGLLEGK
NI1076_CdiA2 2221 SALTAGNNLSIQATGSGVKGVGDGLTIQGSQIKAGNNVLLQANRDVNLVSAENTSGLLEGK

STECO31_CdiA2 2281 NTSSGGSVGVGVGSGGWGISVSASANQKGGSEKNGTTHTEITVDAGNRLTIISGRDT
NI1076_CdiA2 2281 NTSSGGSVGVGVGSGGWGISVSASANQKGGSEKNGTTHTEITVDAGKHLTIISGRDT

STECO31_CdiA2 2341 TLTGALASGEMVVKVDAGRHLTLTSEQSDRYDSKQONASAGGSFTFGSMGSASVNLSRD
NI1076_CdiA2 2341 TLTGALASGEMVVKVDAGRHLTLTSEQSDRYDSKQONASAGGSFTFGSMGSASVNLSRD

STECO31_CdiA2 2401 KMHSNYDSVQAQTGIFAGRGGFDVTTGQHTQLNGAVIASTATADKNRLDTGLGFSDIEN
NI1076_CdiA2 2401 KMHSNYDSVQAQTGIFAGRGGFDVTTGQHTQLNGAVIASTATADKNRLDTGLGFSDIEN

STECO31_CdiA2 2461 RADFKTEHQSAGLSTGGSVAGNFLGNMANNLLVGANHEGHADSTTQSAVSDGNIITIRDTK
NI1076_CdiA2 2461 RADFKTEHQSAGLSTGGSVAGNFLGNMANNLLVGANHEGHADSTTQSAVSDGNIITIRDTK

STECO31_CdiA2 2521 SQKQDMADLNRDAAHANQTLSPIFDREKEHQRLQQAQLIGEIGNQVADIARTEGQIAGEK
NI1076_CdiA2 2521 SQKQDMADLNRDAAHANQTLSPIFDREKEHQRLQQAQLIGEIGNQVADIARTEGQIAGEK

STECO31_CdiA2 2581 AKRDPAAALNQAARAELEAAGKPFTEQDVVQRAYNNGMAASGFGTGGKYQQAIAATAAVQG
NI1076_CdiA2 2581 AKRDPAAALNQAARAELEAAGKPFTEQDVVQRAYNNGMAASGFGTGGKYQQAIAATAAVQG

STECO31_CdiA2 2641 LAGGNLSAALAGGAAPYIAEVVKMTTDPVTVGEVVKAAVNTAHAVVNAALAVAQGNLALA
NI1076_CdiA2 2641 LAGGNLSAALAGGAAPYIAEITKNNTPD-----GAEVAAHAVVNAALAVAQGNLALA

STECO31_CdiA2 2701 GAAGAATGEMVGMIAIOMYCKKSVSGLSETEKQTVSTLATVAAGLAGGLVGNVSGASAVAGA
NI1076_CdiA2 2694 GAAGAATGEMVGMIAIEMDKKFSVSETEKQTVSTLATVAAGLAGGLVGNVSGASAVAGA

STECO31_CdiA2 2761 QSGKTTIENNSMSGLVPPRVQDASL--AFDPSQQKSAEE-----ISDAICASHMGPSP
NI1076_CdiA2 2754 QSGKTTVENNSIAHVLAIAEANKPGTITSSSTKEQQAAIKKACSGNTPVSCQLAVAAMGTV

STECO31_CdiA2 2813 WGTTYKVHPIVQAG---GDVSEFIRGYTINGTIDDNHISVNQGDIYSIGAHGGASLGLSF
NI1076_CdiA2 2814 MSGGILPEAMVAVAGVISAGAVG-SVDLAWNGSVDPKNI-----I

STECO31_CdiA2 2869 GPYFPGLINT-----NNDYISNGGFCVCSAGITMCKDGV
NI1076_CdiA2 2852 AAYNSCALTRYTGFEFSTVLLINAGSSAIVSYIDGKNPFLYGTIGGLCG-AIYGVGNKFIIE

STECO31_CdiA2 2905 FTF--GVGFSWGSATEIKGVDPVNGTS-----TNEIIRYDFK-----
NI1076_CdiA2 2911 PILGIVNPTWKALQWDIGCMGMSQPSRLSLPIPGIAGSFLGGTASEGNNVLDVDPNSVSH

STECO31_CdiA2 -----
NI1076_CdiA2 2971 GEKSK

```

Figure 4.2: Alignment of lipopolysaccharide-binding CdiA from *E. coli* STEC O31 (introduced in Ch. 2) and CdiA of locus 2 from *E. coli* NI1076. Sequences diverge at VENN, which demarcates the toxin domain (highlighted in red). Generated with Clustal Omega.

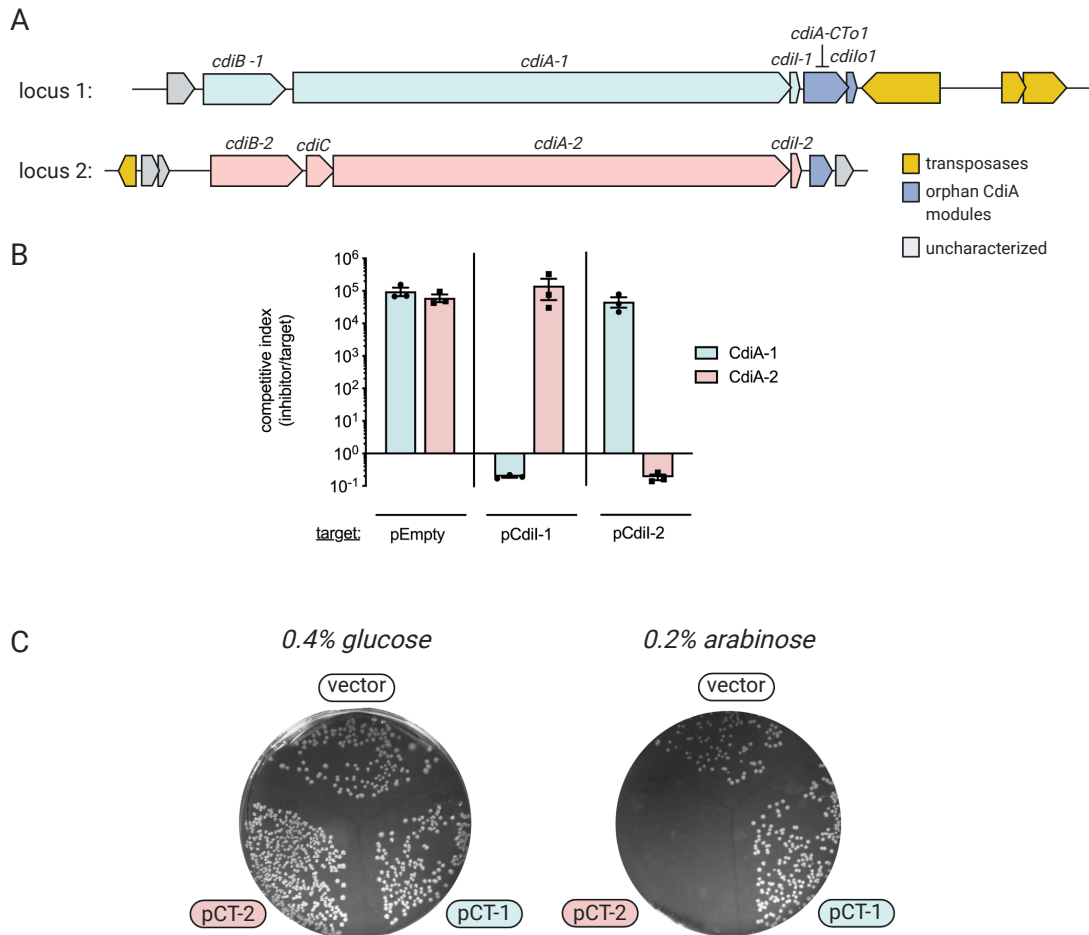


Figure 4.3: *E. coli* NI1076 encodes two CDI loci with functional and distinct toxin domains. (A) Diagram of locus 1 (upper) and locus 2 (lower) to scale. CdiA-1 is homologous to OmpC/F Class II CdiA proteins (see figure 4.1) and CdiA-2 is homologous to Class IV LPS-binding CdiA proteins (Fig. 4.2). (B) Competition co-cultures. The indicated target strain was mixed with an *E. coli* EPI100 inhibitor strain carrying a chimeric EC93-1 CdiA-CT protein with the toxin-immunity gene replaced with either NI1076 CT/CdiI pair (see Methods 4.5) [77]. Competitions were conducted at an equal ratio for 2 hours on solid media. Competitive Index is the ratio of viable inhibitor colony-forming units per milliliter (CFU/mL) to viable target cell CFU/mL at the end of the co-culture relative to their starting ratios. (C) Transformation assay. *E. coli* K-12 targets were transformed with an empty plasmid (pCH450) or plasmid-encoded CT-1 or CT-2 and plated on selective media with glucose or arabinose to suppress or induce CT expression, respectively. Toxins are cloned without the conserved VENN motif, under the control of the P<sup>BAD</sup> arabinose-inducible promoter.

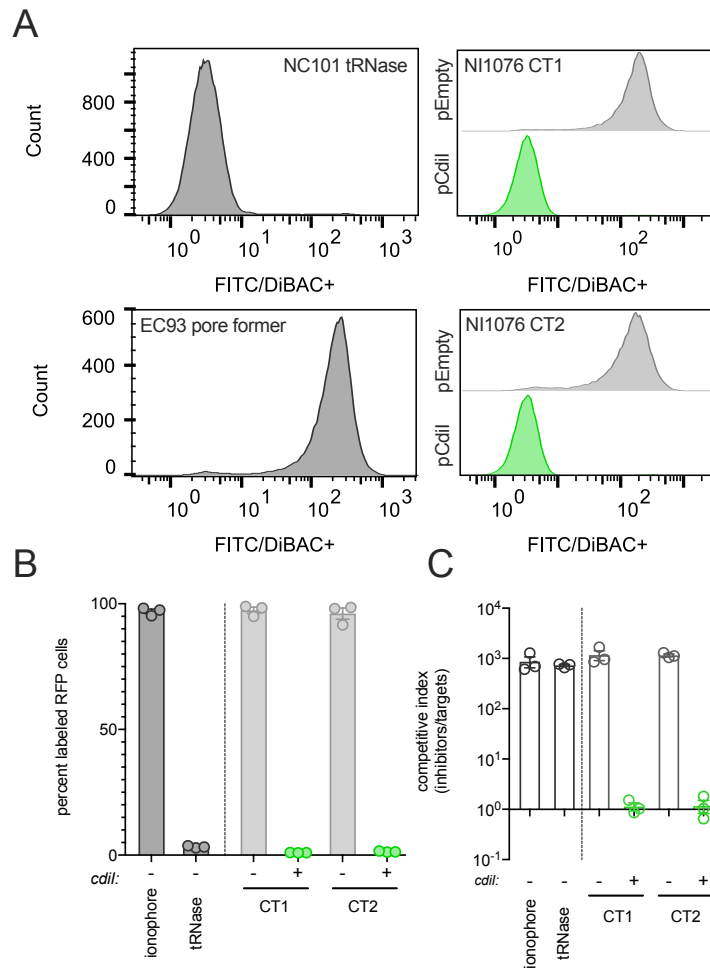


Figure 4.4: **Both CdiA-CTs from *E. coli* NI1076 disrupt the proton motive force in target cells.** (A) Total cell count histograms from flow cytometry of co-cultures between CDI+ inhibitors (unlabeled) and wild type or CdiI+ targets (RFP+) treated with DiBAC<sub>4</sub>(3). Left: a known pore-forming toxin (CdiA-CT<sup>EC93</sup>) and tRNase (CdiA-CT<sup>NC101</sup>) against wild type targets. Right: either toxin from NI1076 in co-culture with targets carrying vector or the cognate *cdiI*. Plots are representative of three separate experiments. All toxins are delivered via the CdiA-1<sup>EC93</sup> stick. (B) Percent DiBAC<sub>4</sub>(3) positive target cells from three independent experiments between the indicated inhibitor and target strains plotted as the average  $\pm$ SEM for three replicates. (C) Competition co-cultures between inhibitor and target strains used for flow cytometry experiments. Results are presented as the average  $\pm$ SEM for three separate experiments.

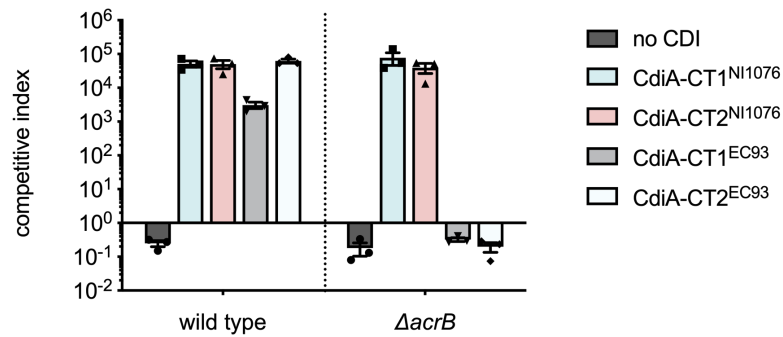


Figure 4.5: **AcrB is not required for the activity of NI1076 CT-1 or NI1076 CT-2.** Co-culture competitions between the indicated inhibitor and target strain. Each inhibitor strain uses the same CdiA protein (EC93 CdiA-1) with the toxin domain swapped for that of the indicated CdiA-CT. CdiA-CT1 EC93 is the native protein for EC93 locus 1, and no CDI is the same cosmid with a deletion of CdiA and thus has no CDI activity.



Table 4.1: **CDI-specific mutations in UV mutagenized target cells resistant to NI1076 CT-1 and CT-2.** Two colonies were verified and sequenced from each pool enriched for resistance to the indicated toxin. Only 1 pool resulted in two different CT2-specific CDI-resistance mutations (Pool 1). Those mutations that resulted in a frameshift are denoted by "fs" and the resulting stop codon type is indicated without the specific location.

	Source of Mutant Colony	Allele	Result
CT1	Pool 2	<i>dtpA</i> *-1	Thr61fsTer (amber)
		<i>dtpB</i> *-1	Lys43Ter (ochre)
		<i>dtpC</i> *-1	Trp66Ter (amber)
	Pool 5	<i>dtpA</i> *-2 <i>dtpB</i> *-2	Glu397fsTer (opal) Val40fs (opal)
CT2	Pool 1	<i>puuP</i> *-1	Lys92fsTer (opal)
		$\Delta$ <i>plaP</i>	Complete deletion (2,064,549-2,098,995)
	Pool 1	<i>puuP</i> *-2	$\Delta$ 20bp (+1348)
		$\Delta$ <i>plaP</i>	Complete deletion (2,064,549-2,098,995)
	Pool 2	<i>puuP</i> *-3	Ser228Ter (amber)
		$\Delta$ <i>plaP</i>	Complete deletion (2,064,549-2,098,995)
	Pool 3	<i>puuP</i> *-4	Tyr248Ter (ochre)
		$\Delta$ <i>plaP</i>	Complete deletion (2,064,549-2,098,995)
Pool 4	<i>puuP</i> *-5	P405L	
	$\Delta$ <i>plaP</i>	Complete deletion (2,064,549-2,098,995)	
Pool 5	<i>puuP</i> *-6	P405L	
	$\Delta$ <i>plaP</i>	Complete deletion (2,064,549-2,098,995)	
Pool 6	<i>puuP</i> *-7	Trp104Ter (opal)	
	$\Delta$ <i>plaP</i>	Complete deletion (2,064,549-2,098,995)	

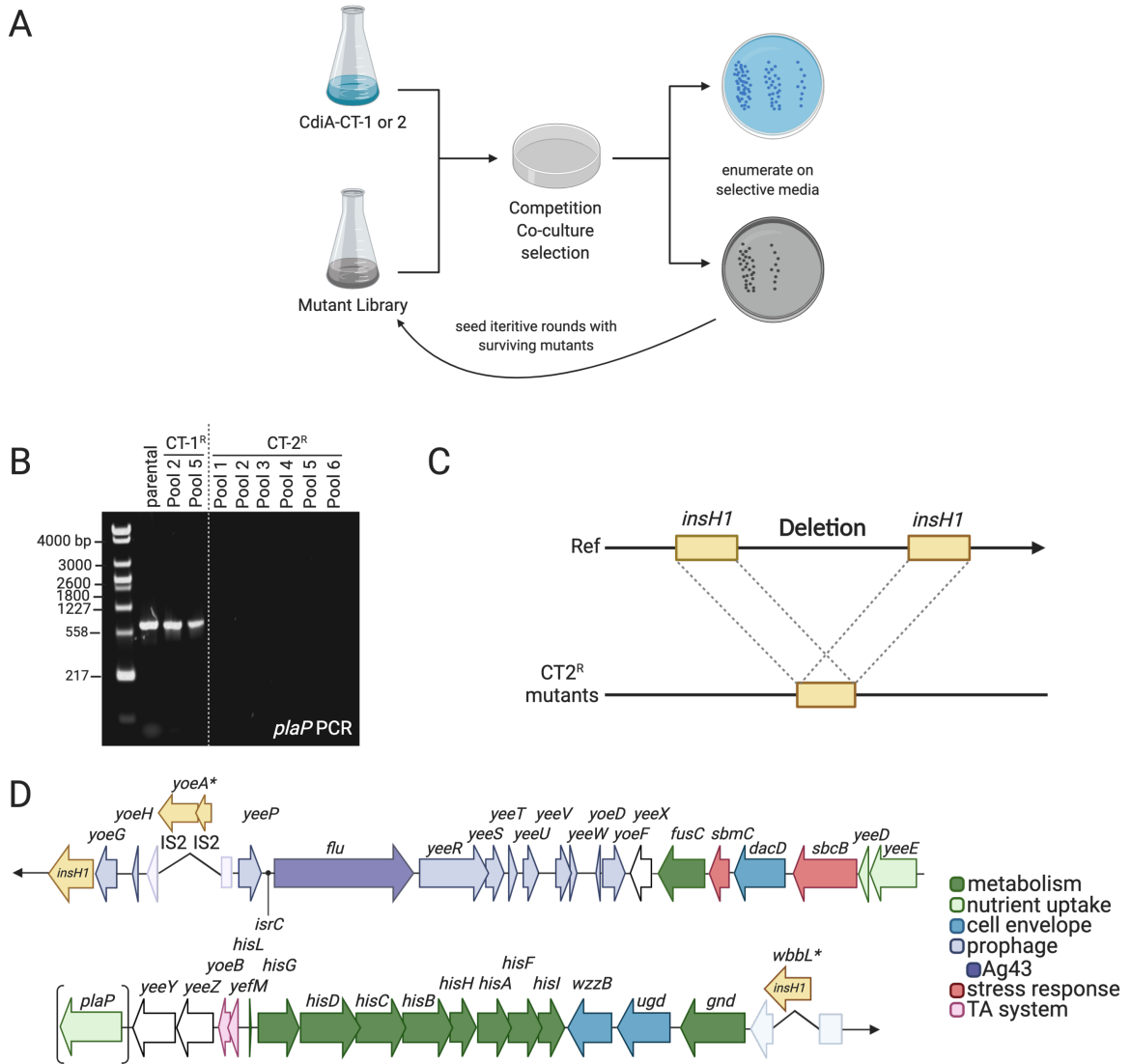


Figure 4.6: Selections against NI1076 CT-2 with UV-irradiated target cells enriches for a ~34 Kb deletion in each of six CDI-resistant target cell pools. (A) Schematic of the workflow for co-culture genetic selections used to obtain CDI-resistant mutants. (B) Ethidium-bromide stained DNA gel of *plaP* amplified from wild-type MG1655 (lane 1) as well as both mutants resistant to NI1076 CT-2 (lanes 2 and 3) and all 6 colonies isolated from separate UV-mutagenized pools resistant to CT-2 (lanes 4 - 9). (C) Schematic of possible RecA-mediated mechanism for deletion in CT-2 resistant mutants. (D) Diagram of the *insH*-flanked bounds and all ORFs included in deletion region, with *plaP* indicated with brackets.

Table 4.2: **Open reading frames absent from CT-2<sup>R</sup> mutants due to deletion of a ~ 34 Kb region encompassing *plaP*.**

Genes located within deletion region in CT-2 resistant mutants			
category	# of ORFs	gene(s)	function
Nutrient uptake and metabolism	14	<i>fusC</i> (formerly <i>yeeA</i> )	Fusaric acid exporter. Aromatic acid exporter family
		<i>yeeD</i>	Putative sulfurtransferase
		<i>yeeE</i>	Putative IM protein. Possibly responds to aromatic compounds.
		<b><i>plaP</i></b> (formerly <i>yeeF</i> )	Putrescine uptake.
		<i>hisL-hisG-hisD-hisC-hisB-hisH-hisA-hisF-hisl</i>	Histidine biosynthesis
		<i>gnd</i>	6-phosphogluconate dehydrogenase, oxidative branch of pentose phosphate pathway.
Cryptic Prophage CP4-44	10	<i>yeeP-flu-yeeR-yeeS-yeeT-yeeU-yeeV-yeeW-yoeD-yoeF</i>	Encodes Ag43, promoter of biofilm formation.
Defective putative cryptic prophage	3	<i>yoeG, yoeH, yoeA (insD insC insertion)</i>	
Stress response genes	3	<i>sbcB</i>	Exonuclease I
		<i>sbmC</i>	DNA gyrase inhibitor
Uncharacterized	2	<i>yeeY</i>	Putative transcriptional regulator
		<i>yeeZ</i>	Putative epimerase
TA system	2	<i>yoeB-yifM</i>	Ribosome-dependent mRNA interferase toxin/antitoxin pair
Peptidoglycan biosynthesis/ beta-lactam resistance	1	<i>dacD</i>	D-alanyl-D-alanine carboxypeptidase
O-antigen length	1	<i>wzzB (cld)</i>	Regulator of O-antigen chain length
Colanic acid production	1	<i>ugd</i>	UDP-glucose 6-dehydrogenase
Pseudogene	1	<i>wbbL</i>	IS5-interrupted rhamnosyltransferase (3' end of deletion)
Genes of unknown function	1	<i>yeeX</i>	

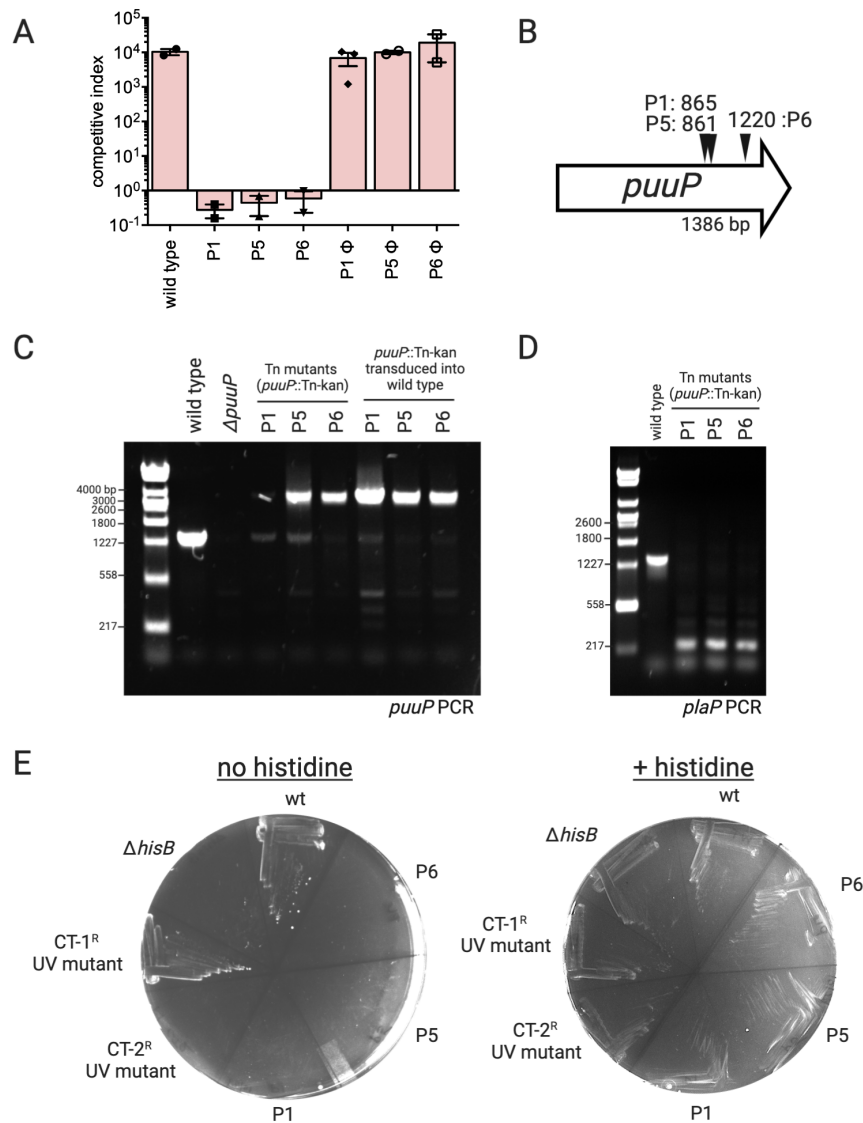


Figure 4.7: Selection for target cells resistant to CT-2 using the *mariner* transposon results in insertions into *puuP* and another deletion encompassing *plaP* and the histidine biosynthetic operon. (A) Competition co-cultures. Three of six transposon mutant pools enriched for resistance to CT-2 (P1/P5/P6 = single colony from Pool 1, Pool 5, or Pool 6), but a parental strain transduced with phage lysate prepared from each mutant (*puuP*::Tn-Kan<sup>R</sup>) is not resistant. (B) Locations of transposon insertions in *puuP*. (C) DNA gel of colony PCR performed on the indicated strains using primers specific for *puuP*. (D) Colony PCR using primers specific for *plaP*. (E) Growth assay on M9 minimal media in the absence (left) or presence (right) of histidine.

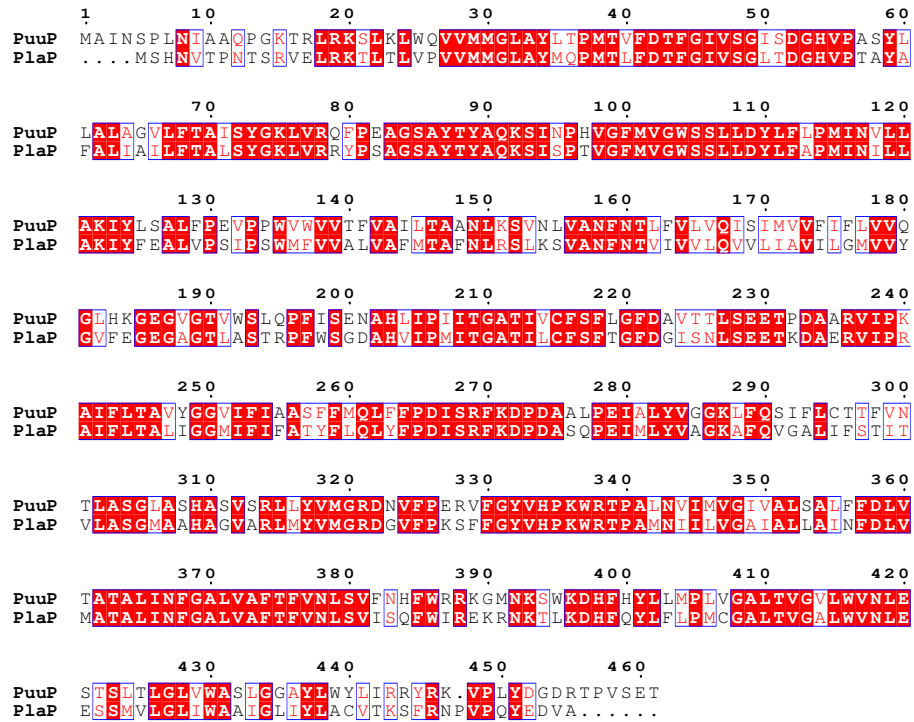


Figure 4.8: Alignment of *E. coli* MG1655 putrescine importers PuuP and PlaP. Generated with Clustal Omega, graphic created with ESPrnt [178].

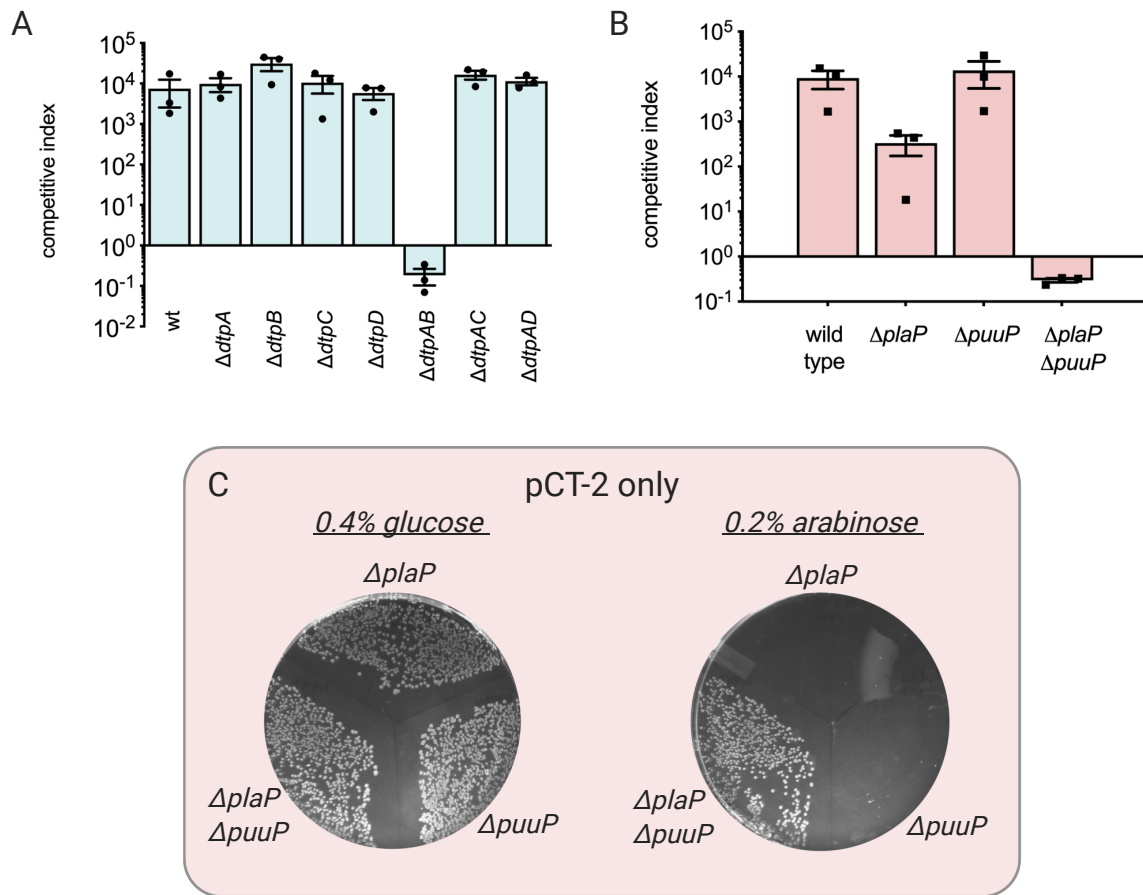
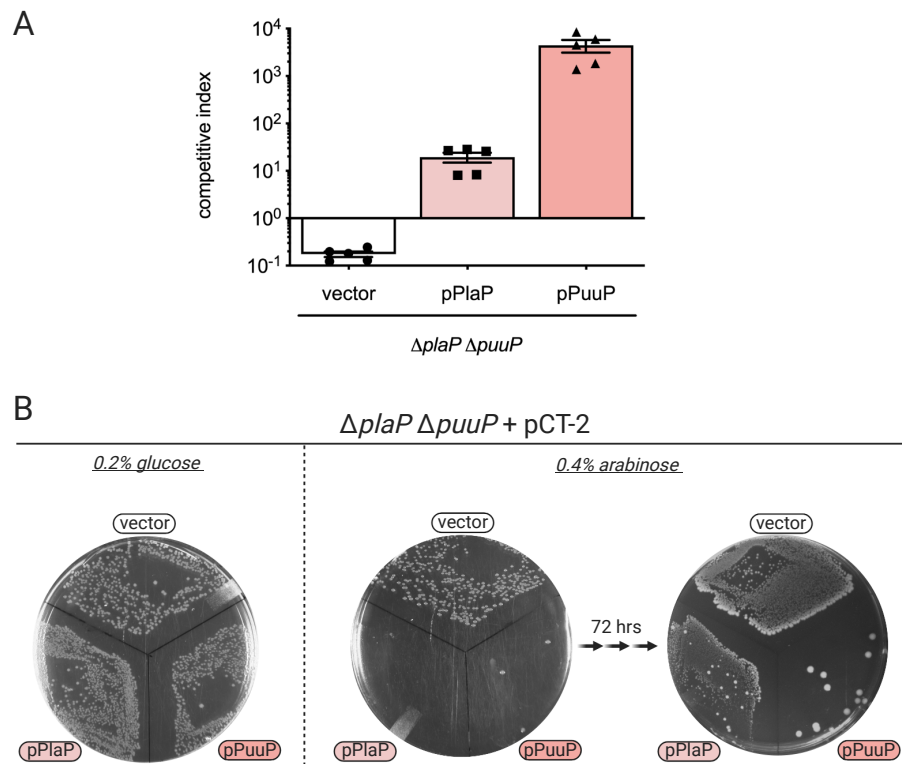


Figure 4.9: **Both NI1076 ionophore toxins exploit multiple homologous IM proteins independently to exert toxicity on target cells.** Competition co-cultures. Inhibitor cells carrying either CdiA-CT1 (A) or CdiA-CT2 (B) were cultured at an equal ratio with the indicated target cells. Data is presented as the average  $\pm$ SEM for at least three separate experiments. (C) Transformation assay. The indicated *E. coli* K-12 deletion strain was transformed with pCT-2 and plated on glucose to repress toxin expression or arabinose for induction. Only a double  $\Delta plaP \Delta puuP$  deletion strain resists intoxication by internal expression of CT2.



**Figure 4.10: PlaP and PuuP are not equivalent receptors for CT-2.** (A) Competition co-cultures between a CT-1 inhibitor strain and a  $\Delta plaP \Delta puuP$  target strain carrying empty plasmid (vector) or plasmid-encoded PuuP and PlaP (expressed from imperfect LacI repression). (B) Transformation assay. The same complemented target strains from (A) transformed with plasmid-encoded CT-2 (beginning just after the conserved VENN motif) and plated on selective media with the indicated inducible. In this assay, PlaP also partially protects targets from intoxication relative to PuuP: after 3 days at room temperature, the small surviving colonies carrying pPlaP on inductive media that were present at 24 hours are now clearly visible. Despite being plated on both antibiotics, the large colonies growing in the PuuP sector are no longer resistant to both ampicillin and tetracycline when inoculated into liquid media.

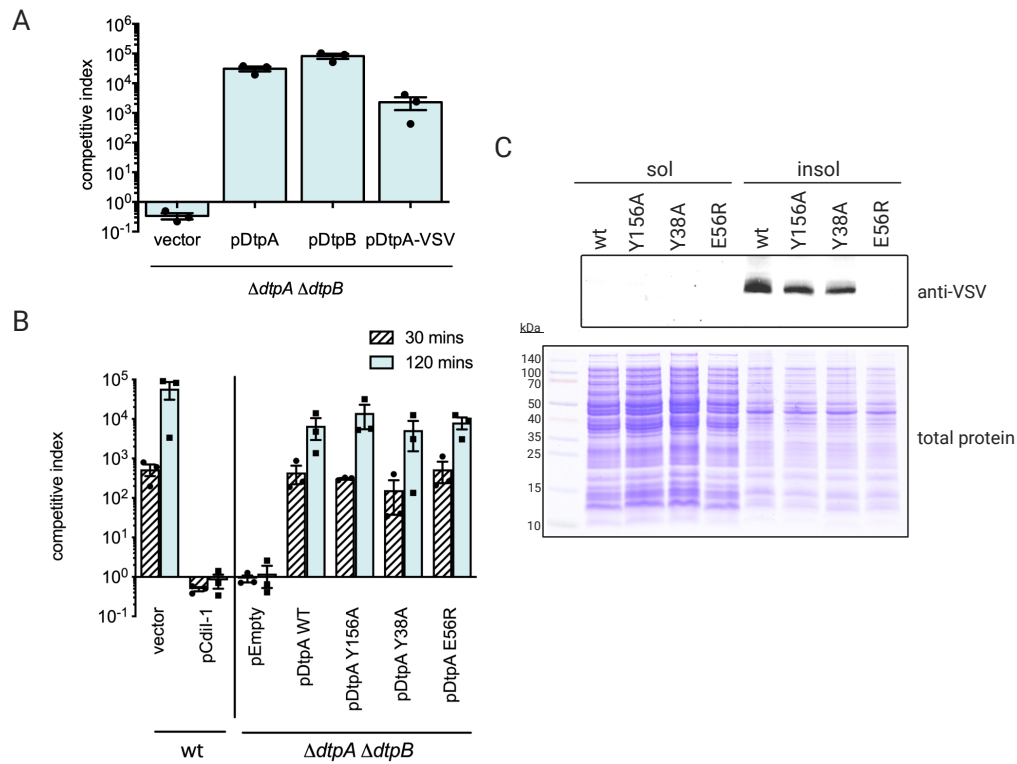


Figure 4.11: **DtpA** and **DtpB** are equivalent receptors for **CT-1**, and **substrate-binding activity of DtpA is not required for CDI**. (A) Co-culture competitions between CdiA-CT-2 expressing inhibitor cells and  $\Delta dtpA \Delta dtpB$  target cells complemented with empty plasmid (vector) or the indicated IM protein. (B) Same as in (A) except complemented strains are also compared to wild type targets or targets expressing cognate immunity. (C) (Top) Anti-VSV Western Blot against the soluble or insoluble material from whole cell lysates of the indicated strains, which are the same as in (B). (Bottom) The same amount of protein was loaded as above and separated by SDS-PAGE, but stained with Coomassie R-250 Brilliant Blue to compare load levels.



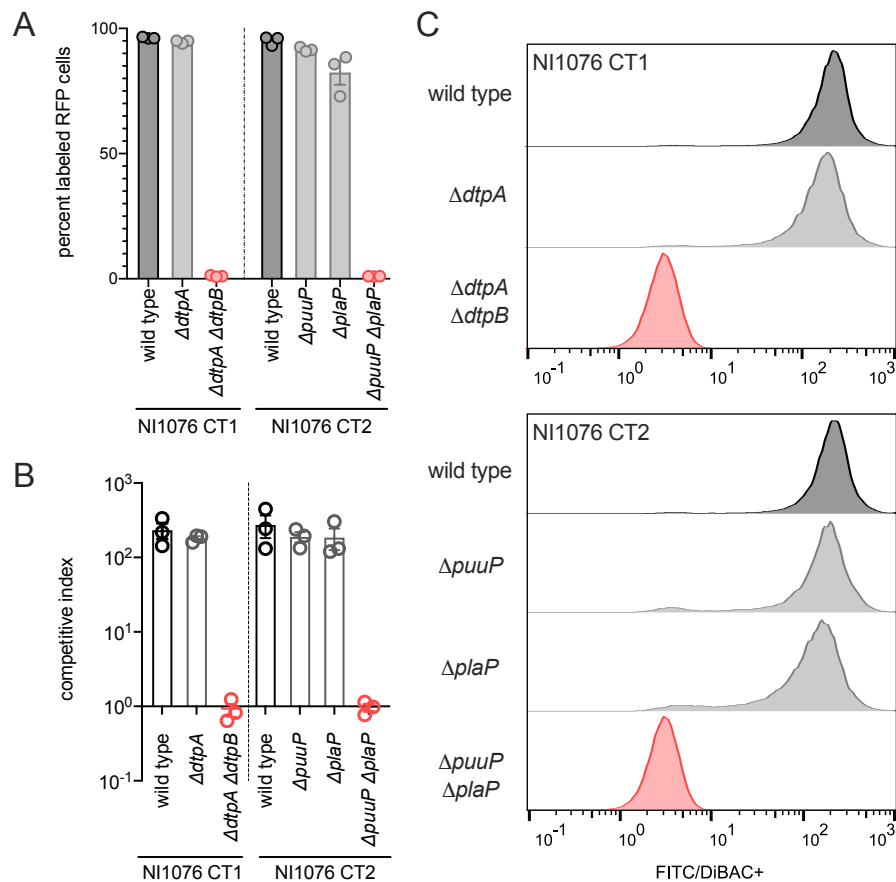


Figure 4.12: **Both ionophore CdiA-CTs require at least one inner-membrane protein receptor to cause membrane depolarization in target cells.** (A) Fraction of target cells from competition co-cultures with the indicated CDI+ inhibitor strain that were positive for DiBAC<sub>4</sub>3 uptake. Three separate experiments are presented  $\pm$  SEM. (B) The same competition co-cultures used to conduct flow cytometry experiments presented as competitive indices, which is the ratio of viable inhibitor:target cells at the end of the experiment relative to their starting ratio. The average of three independent experiments  $\pm$  SEM is presented. (C) Flow cytometry histograms with total cell count on the Y-axis of competition co-cultures between the indicated inhibitor and RFP+ target strain treated with DiBAC<sub>4</sub>(3) (x-axis). The histograms are representative of three separate experiments.

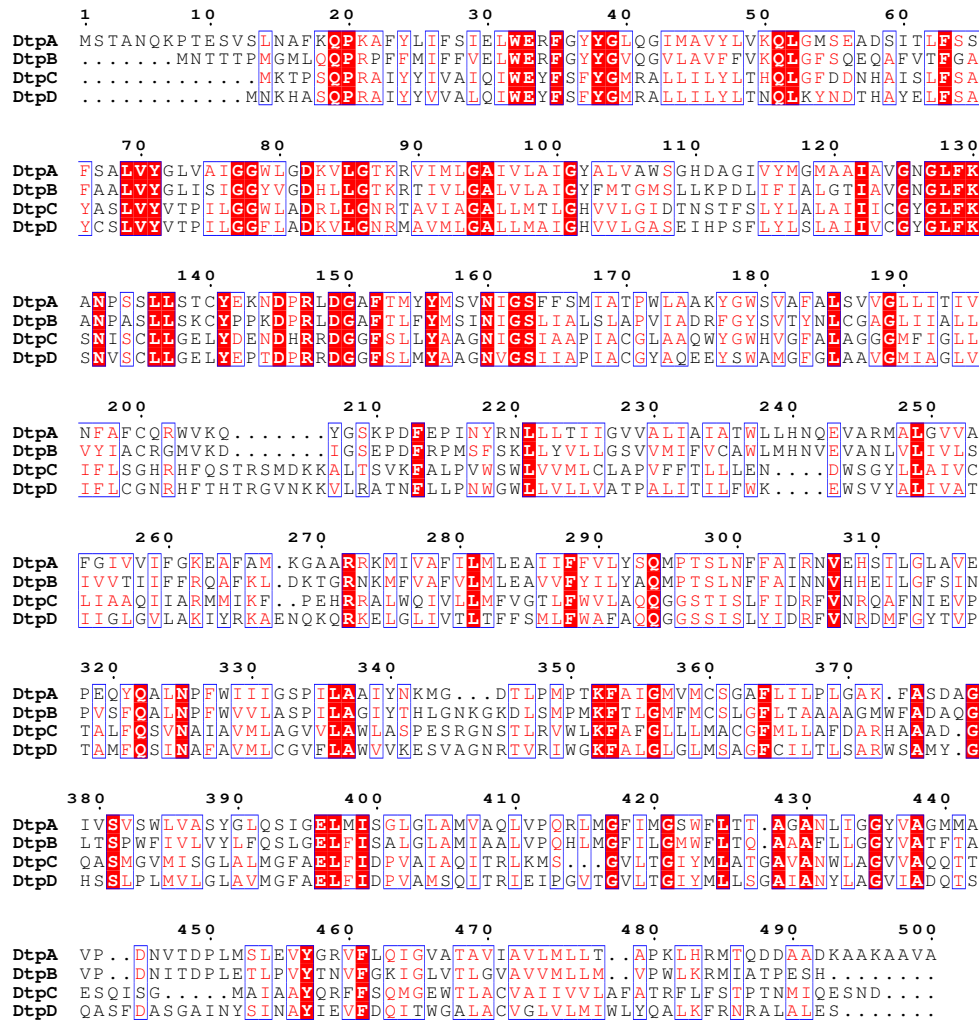


Figure 4.13: Alignment of *E. coli* MG1655 di/tri-nucleotide importers DtpA/B/C/D. Generated with Clustal Omega and formatted with ESPript [178]. Conserved residues highlighted in red, while functionally conserved residues are written in red.

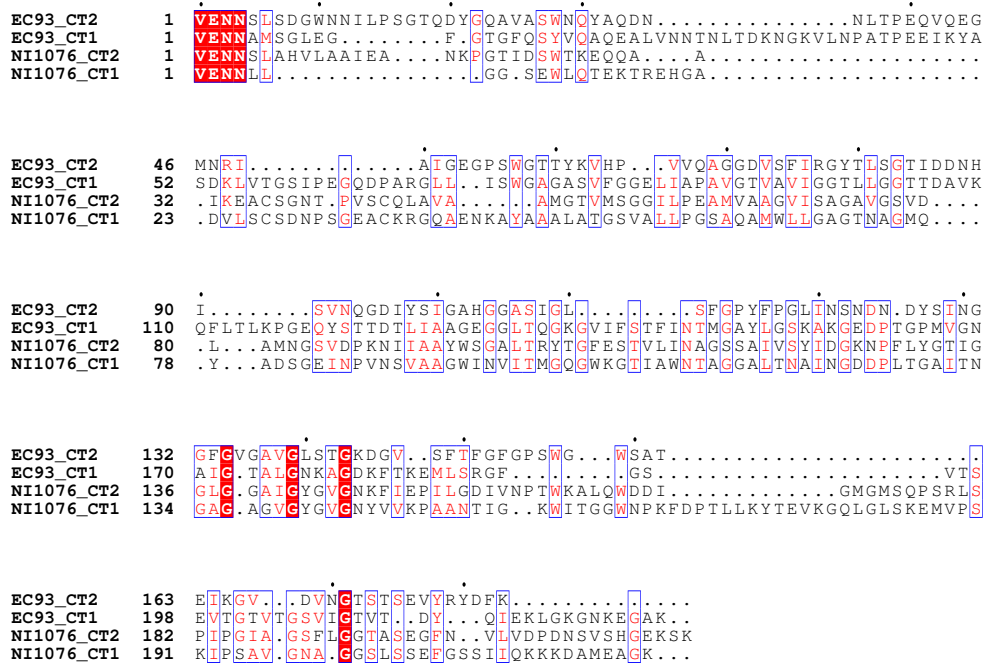


Figure 4.14: **Alignment of all 4 CDI ionophore toxins.** Clustal Omega multiple sequence alignment of ionophore toxins from EC93 and the two toxins identified in this study from *E. coli* NI1076. Alignment begins at conserved VENN motif. Conserved glycine residues that are part of at least 1 putative glycine zipper motif are highlighted in red, with one conserved glycine present in a seemingly less well-conserved motif. Formatted with ESPript [178].

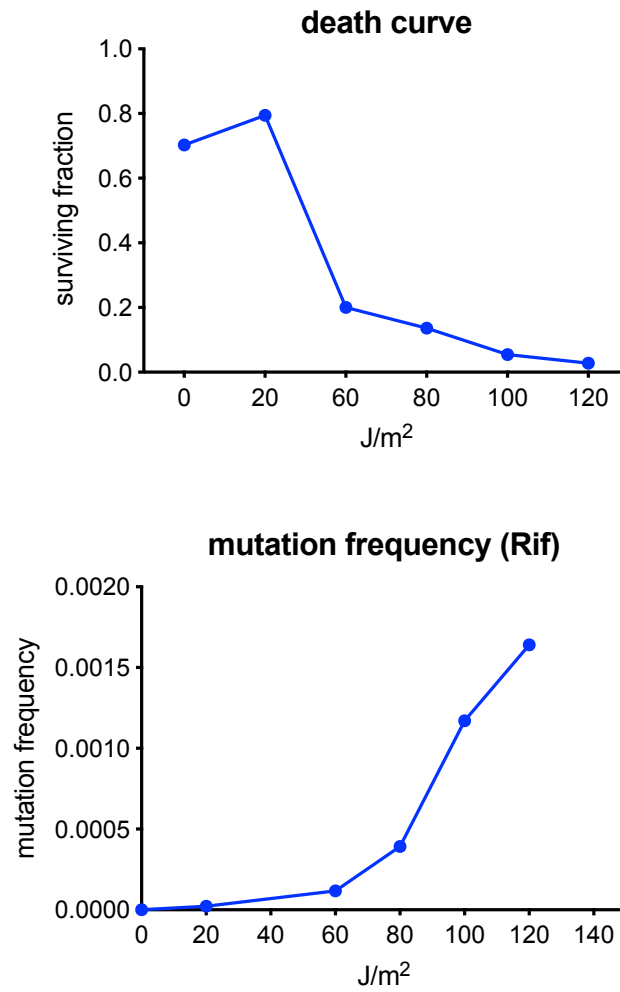


Figure 4.15: **Percent survival at increasing doses of ultraviolet light and the corresponding frequency of rifampicin-resistant mutations.** Top: viable cells recovered from ultraviolet light irradiation at the indicated dosage. Bottom: frequency of rifampicin-resistant target cells arising from the indicated UV irradiation dosage.

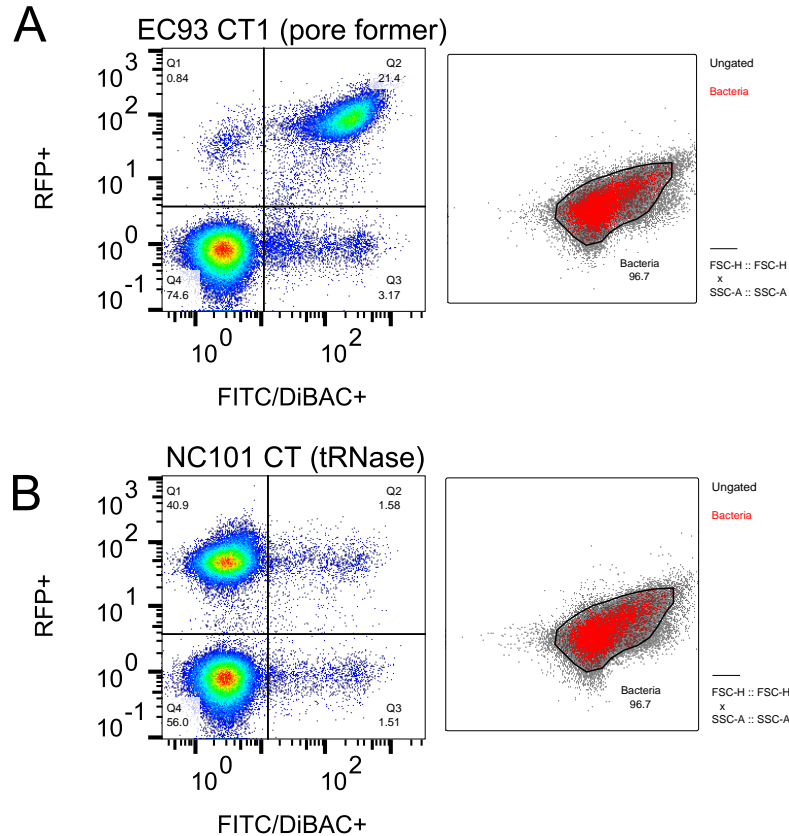


Figure 4.16: **Gating approach for flow cytometry experiments.** Density plots of flow cytometry co-culture experiments showing both inhibitor (unlabeled) and target (RFP+) cell populations following treatment with DiBAC<sub>4</sub>3. (A) Positive control for ionophore activity, known pore-former from *E. coli* EC93. (B) Negative control, known endonuclease toxin from *E. coli* NC101. To generate histograms of target cell populations, a gate was applied to the entire sample in the FSC x SSC window (right, red population) and then RFP-positive cells were analyzed for FITC signal within that population by breaking the sample into quadrants of RFP +/- and DiBAC<sub>4</sub>3 +/- cells (left). Thus, histograms in figures 4.4 and 4.12 show the RFP population only.

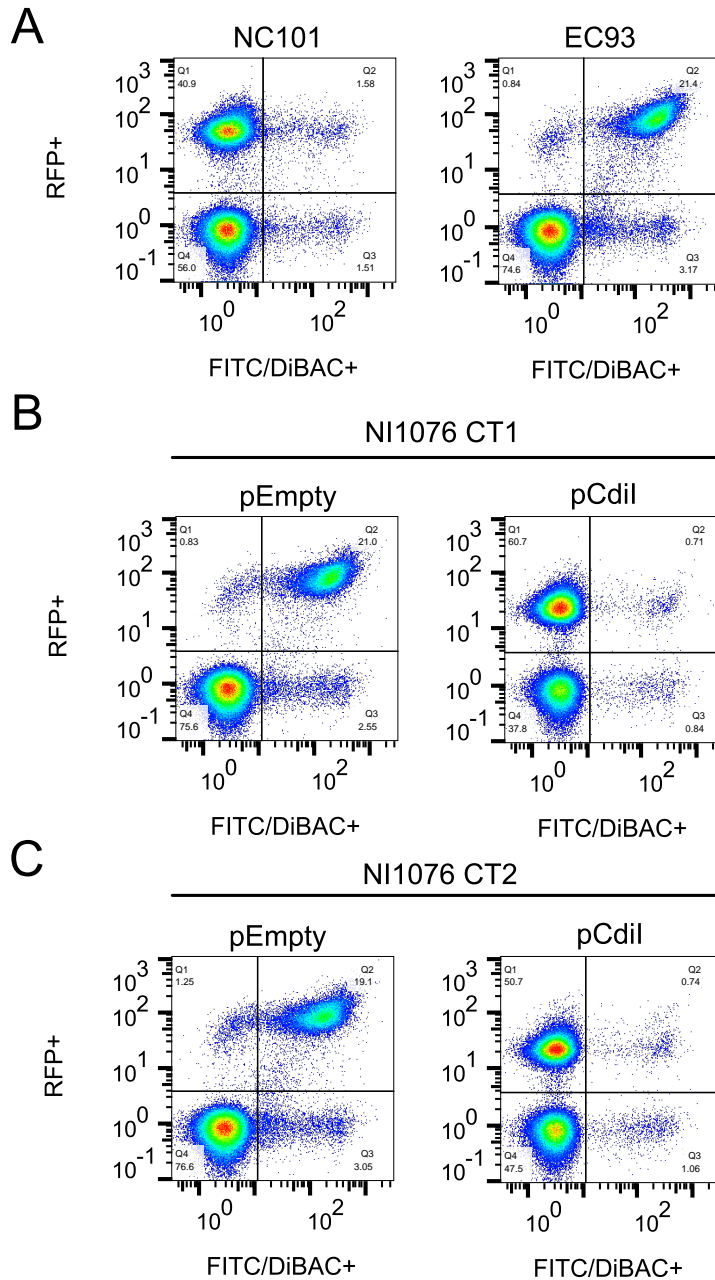


Figure 4.17: **Flow cytometry analysis of DiBAC<sub>4</sub>3-treated co-cultures of immunity-protected, RFP-labeled target strains and the cognate inhibitor strain.** Quadrants are the same as in Fig. 4.16, but provide entire populations used to generate histograms in Fig. 4.4. (A) Controls: a known tRNase (left) and known pore-former (right). (B) and (C) CT-1 and CT-2 from NI1076 cause uptake of the membrane-potential dye DiBAC<sub>4</sub>3 much like the characterized pore-former from EC93 in (A). CdiI expression protects targets from membrane depolarization in both cases.

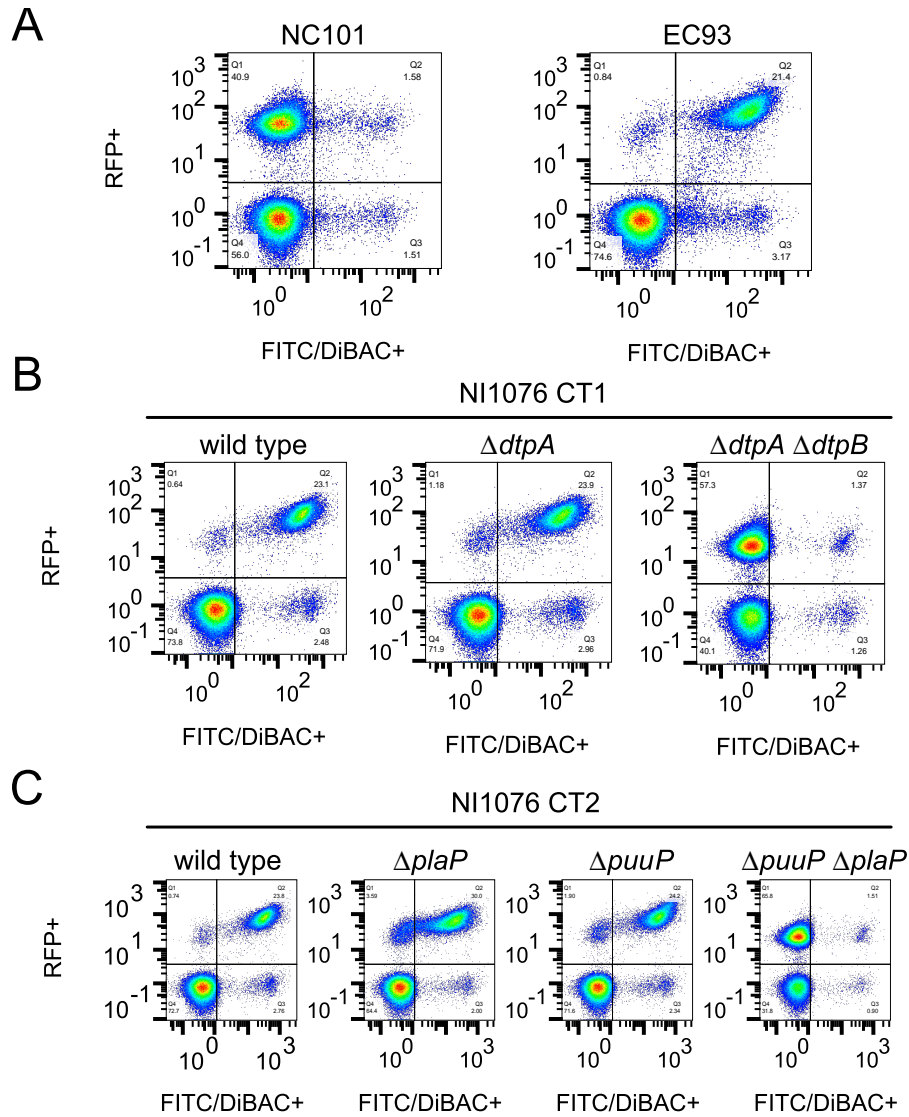


Figure 4.18: **Flow cytometry analysis of DiBAC<sub>4</sub>3-treated co-cultures of receptor-less, RFP-labeled target strains with the cognate inhibitor strains.** Quadrants are the same as in Fig. 4.16 and 4.17 but here represent the entire population from the samples used to generate histograms in Fig. 4.12). (A) Controls: NC101 is a known tRNase and EC93 is a known pore-former. (B) Analysis of co-culture competitions by flow cytometry between the indicated red-fluorescent target strain and CT-1. (C) Analysis of co-culture competitions by flow cytometry between the indicated red-fluorescent target strain and CT-2.

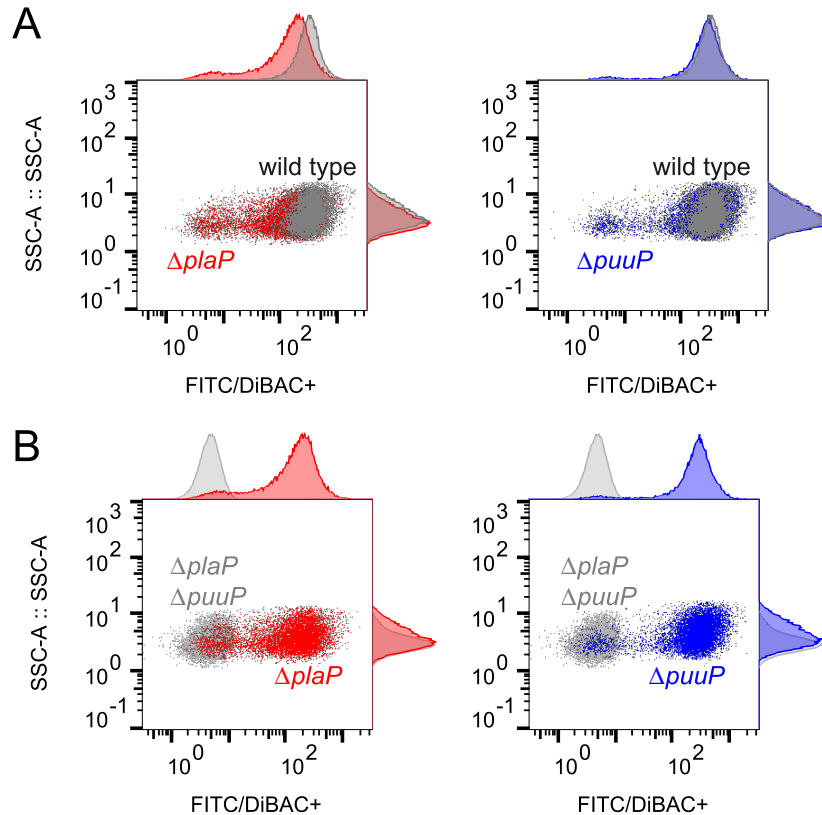


Figure 4.19: **Comparison of target cell populations from DiBAC<sub>43</sub>-treated co-culture competitions with CdiA-CT<sup>NI1076-2</sup>.** Overlay of red-fluorescent target cell populations as in Figure 4.18C, but without inhibitor populations present. Thus, the RFP+ target population from two co-culture experiments is plotted only as FITC+ cells on the x-axis to analyze DiBAC<sub>43</sub>- uptake in two target strains. (A) Single receptor deletions (either  $\Delta plaP$  or  $\Delta puuP$  compared to wild-type). The  $\Delta plaP$  target strain is partially resistant to membrane depolarization in this assay when compared to  $\Delta puuP$ . (B) The same single receptor deletions from (A) overlaid with a double deletion of both  $\Delta plaP$   $\Delta puuP$ . Histograms of the corresponding target populations are plotted above each axis to show target cell count as a function of either SSC or FITC signal. Thus, histograms on top of each graph represent FITC+ cells in each population indicated on the density plot.



```

NI1076 CT1   1  ---LLG-----GSEWLQTEKTREHGADVLSCSDNPSGEACKRQOAENKAYAAALA
NI1076 CT2   1  SLAHVLAAAEANKPGTIDSWTKEQQA---AIKEACSGNT-PVSCQLAV-----AAMGT

NI1076 CT1   48  TGSVAILPGSAQAMWLLGAGTNAGMQYADSCETINPVNSVAAGWINVITMGQGNKGTIAWN
NI1076 CT2   50  VMSGGILPEAMVAAGVISAGAVCSVDLAMNGSVDPKNILAAYWSGALTRYTCHESTVLIN

NI1076 CT1  108  TAGGALTNAINGDDPLTGAITNGAGAVGYGVGNYVVKPAANTIG--KWITGGWNPKFDP
NI1076 CT2  110  AGSSAIVSYIDGKNPFLYCTIGLGGAIGYGVGNKFIEPILGDIVNPTWKALQWDDI---

NI1076 CT1  166  TLLKYTEVKGQIGLSKEMVPSKIPSAVGNA-GSLSSEFGSSIIQKKDAMEAGK---
NI1076 CT2  167  -----GMGSQPSRLSPLPGIACSFLGGTASEGFN--VLVDPDNSVSHGEKSK

```

Figure 4.20: **Alignment of *E. coli* NI1076 CdiA-CT1 and CdiA-CT2.** Generated with Clustal Omega. Predicted glycine zipper motifs in red. Conserved prolines that might also be functionally important are also highlighted in red. Predicted N-terminal cytoplasmic entry domain underlined. In comparison to alignment of all 4 characterized pore-forming toxins in Fig. 4.14 which share conservation of a singly glycine zipper motif, both toxins from NI1076 appear to share two glycine zippers.

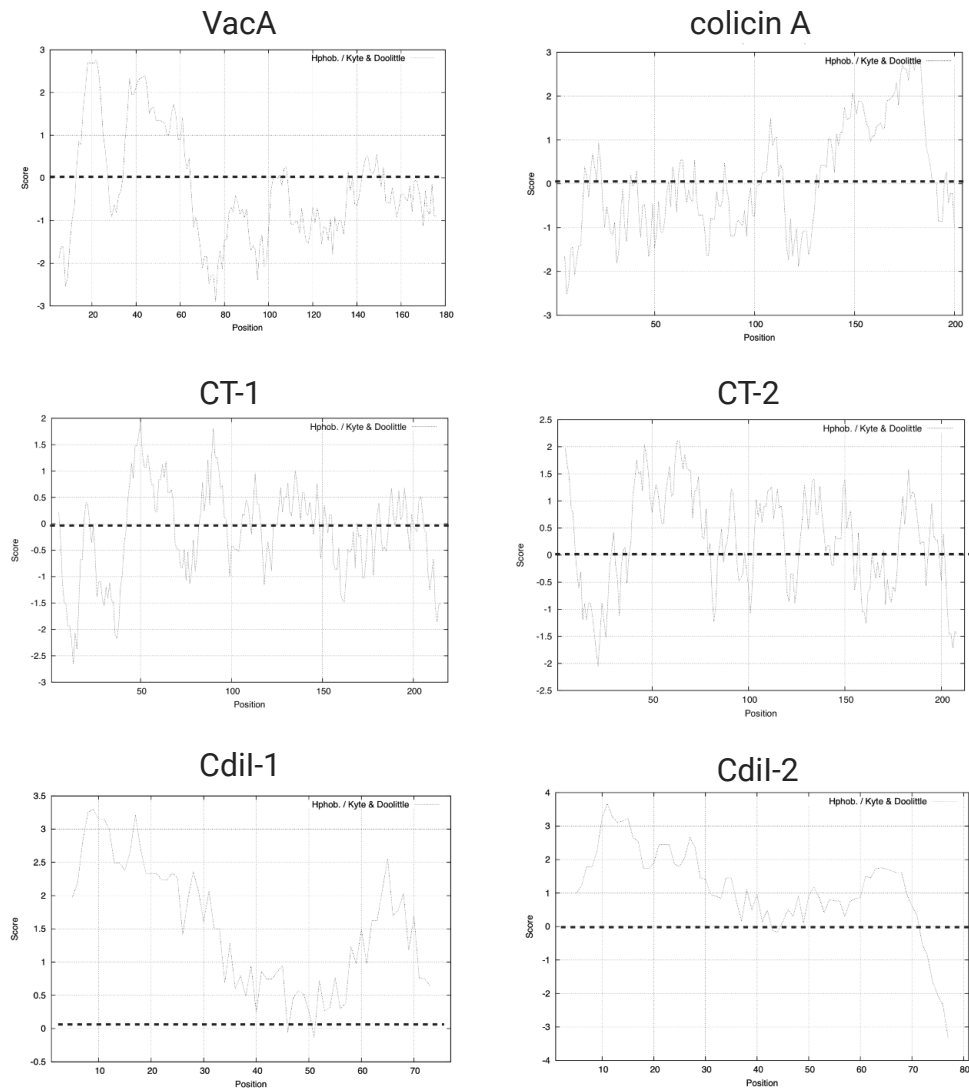


Figure 4.21: **Hydrophobicity plots of NI1076 toxins and their cognate immunity proteins reveal ionophore immunity proteins are hydrophobic and likely transmembrane proteins, in contrast to the ionophore toxins themselves.** Top row is the first ~ 180 residues of the glycine zipper toxin VacA (Q9KJA6) and the pore-forming colicin A (Q47108) for comparison. Second row shows each ionophore from NI1076, and third row is the respective immunity protein. Plots were generated with ExPASy ProtScale.

Table 4.3: Bacterial strains used in Chapter 4.

Strain	Description	Source
EPI100	F- <i>mcrA</i> $\Delta$ ( <i>mrr</i> - <i>hsdRMS</i> - <i>mcrBC</i> ) <i><math>\phi</math>80dlacZ<math>\Delta</math>M15 <math>\Delta</math>lacXcZ<math>\Delta</math>M15<math>\Delta</math>lacX <i>recA1 endA1</i> <i>araD139</i> <math>\Delta</math>(<i>ara</i>, <i>leu</i>)7697 <i>galU galK<math>\gamma</math> -rpsL</i> <i>nupG</i>StrR</i>	Epicentre
CH7176	EPI100 $\Delta$ <i>wzb</i> ::kan, KanR, StrR	[74]
DY378	W3110 $\lambda$ <i>cI857</i> $\Delta$ ( <i>cro</i> - <i>bioA</i> )	[77]
MFDpir	MG1655 RP4- 2-Tc::( $\Delta$ Mu1::aac(3)IV $\Delta$ aphA- $\Delta$ nic35- $\Delta$ Mu2::zeo) <i>dapA</i> ::(erm-pir) $\Delta$ recA Aprr Zeor Ermr	[142]
SK2873	MG1655 $\Delta$ <i>araFGH</i> $\Delta$ <i>araBAD</i> PJ23106- <i>araE</i> <i>rpoSdel galK</i> ::dTomato- <i>cat</i> , CmR	Sanna Koskiniemi
MG1655	WT Strain	Dan Anders- son
DL8698	MG1655 $\Delta$ <i>wzb</i>	[78]
DL8705	MG1655 $\Delta$ <i>wzb ara</i> ::spec	[78]
CH4942	MG1655 $\Delta$ <i>wzb ara</i> ::spec $\Delta$ <i>plaP</i>	This study
CH4946	MG1655 $\Delta$ <i>wzb ara</i> ::spec $\Delta$ <i>puuP</i>	This study
CH6756	MG1655 $\Delta$ <i>wzb ara</i> ::spec $\Delta$ <i>plaP</i> $\Delta$ <i>puuP</i>	This study
CH4141	MG1655 $\Delta$ <i>wzb ara</i> ::spec $\Delta$ <i>dtpA</i>	This study
CH4147	MG1655 $\Delta$ <i>wzb ara</i> ::spec $\Delta$ <i>dtpB</i> ::kan	This study
CH4166	MG1655 $\Delta$ <i>wzb ara</i> ::spec $\Delta$ <i>dtpC</i> ::kan	This study
CH4146	MG1655 $\Delta$ <i>wzb ara</i> ::spec $\Delta$ <i>dtpD</i> ::kan	This study
CH4143	MG1655 $\Delta$ <i>wzb ara</i> ::spec $\Delta$ <i>dtpA</i> $\Delta$ <i>dtpB</i>	This study
CH4168	MG1655 $\Delta$ <i>wzb ara</i> ::spec $\Delta$ <i>dtpA</i> $\Delta$ <i>dtpC</i> ::kan	This study
CH4169	MG1655 $\Delta$ <i>wzb ara</i> ::spec $\Delta$ <i>dtpA</i> $\Delta$ <i>dtpD</i> ::kan	This study
CH6757	MG1655 $\Delta$ <i>wzb ara</i> ::spec <i>galK</i> ::dTomato- <i>cat</i>	This study
CH6758	MG1655 $\Delta$ <i>wzb ara</i> ::spec $\Delta$ <i>plaP galK</i> ::dTomato- <i>cat</i>	This study
CH6759	MG1655 $\Delta$ <i>wzb ara</i> ::spec $\Delta$ <i>puuP galK</i> ::dTomato- <i>cat</i>	This study
CH6760	MG1655 $\Delta$ <i>wzb ara</i> ::spec $\Delta$ <i>plaP</i> $\Delta$ <i>puuP</i> <i>galK</i> ::dTomato- <i>cat</i>	This study
CH6761	MG1655 $\Delta$ <i>wzb ara</i> ::spec $\Delta$ <i>dtpA galK</i> ::dTomato- <i>cat</i>	This study
CH6762	MG1655 $\Delta$ <i>wzb ara</i> ::spec $\Delta$ <i>dtpA</i> $\Delta$ <i>dtpB</i> <i>galK</i> ::dTomato- <i>cat</i>	This study

Table 4.4: Plasmids used in Chapter 4.

Plasmid	Description	Source
pTrc99a	IPTG-inducible expression vector. AmpR	GE Health-care
pTrc99aKX	Derivative of pTrc99a that contains a KpnI, SpeI and XhoI sites, AmpR	[81]
pCH450	pACYC184 derivative with <i>E. coli araBAD</i> promoter for arabinose-inducible expression, TetR	[179]
pSC189	Mobilizable plasmid with R6K $\gamma$ replication origin; carries the mariner transposon containing kanamycin resistance cassette; AmpR KanR	[141]
pCH10163	Cosmid pCdiA-CT/pheS* that carries a <i>kan-pheS*</i> cassette in place of the <i>E. coli</i> EC93 <i>cdiA-CT/cdiI</i> coding sequence. Used for allelic exchange and counter selection. CmR KanR	[77]
pCP20	Heat-inducible expression of FLP recombinase. CmR AmpR	[180]
pZS21- <i>bamA</i> <sup>Eco</sup>	pZS21 derivative that expresses <i>bamA</i> from <i>E. coli</i> , KanR	[72]
pDAL660 $\Delta$ 1-39	Constitutive expression of <i>cdiA</i> <sup>EC93</sup> and <i>cdiI</i> <sup>EC93</sup> genes, CmR AmpR	[63]
pDAL660 $\Delta$ 2-63:: <i>cat</i>	pDAL660 deletion with the entire <i>cdiABI</i> insert deleted CmR AmpR	[63]

*Ch. 4 plasmids, cont'd.*

Plasmid	Description	Source
pCH13533	Constitutive expression of chimeric <i>cdiA</i> <sup>EC93</sup> - <i>CT</i> <sup>EC93-2</sup> and <i>cdiI</i> <sup>EC93-2</sup> genes. (pDAL879- <i>cdiA</i> <sup>EC93</sup> - <i>CT</i> / <i>cdiI</i> <sup>EC93-2</sup> ), CmR	This study
pCH13531	Constitutive expression of chimeric <i>cdiA</i> <sup>EC93</sup> - <i>CT</i> <sup>NI1076-1</sup> and <i>cdiI</i> <sup>NI1076-1</sup> genes. (pDAL879- <i>cdiA</i> <sup>EC93</sup> - <i>CT</i> / <i>cdiI</i> <sup>NI1076-1</sup> ), CmR	This study
pCH13532	Constitutive expression of chimeric <i>cdiA</i> <sup>EC93</sup> - <i>CT</i> <sup>NI1076-2</sup> and <i>cdiI</i> <sup>NI1076-2</sup> genes. (pDAL879- <i>cdiA</i> <sup>EC93</sup> - <i>CT</i> / <i>cdiI</i> <sup>NI1076-2</sup> ), CmR	This study
pCH5766	pTrc99aKX:: <i>cdiI-1</i> (NI1076), IPTG-inducible expression of <i>cdiI</i> immunity gene from <i>E. coli</i> NI1076 locus 1, AmpR	This study
pCH5766	pTrc99aKX:: <i>cdiI-2</i> (NI1076), IPTG-inducible expression of <i>cdiI</i> immunity gene from <i>E. coli</i> NI1076 locus 2, AmpR	This study
pCH5779	pTrc99a:: <i>plaP</i> , IPTG-inducible expression of <i>E. coli</i> K-12 <i>plaP</i> gene, AmpR	This study
pCH5780	pTrc99a:: <i>puuP</i> , IPTG-inducible expression of <i>E. coli</i> K-12 <i>puuP</i> gene, AmpR	This study
pCH6337	pTrc99a:: <i>dtpB</i> , IPTG-inducible expression of <i>E. coli</i> K-12 <i>dtpB</i> gene, AmpR	This study
pCH6361	pTrc99a:: <i>dtpA-VSV</i> , IPTG-inducible expression of <i>E. coli</i> K-12 <i>dtpA</i> gene with a C-terminal VSV viral epitope tag, AmpR	This study

*Ch. 4 plasmids, cont'd.*

Plasmid	Description	Source
pCH6339	pTrc99a:: <i>ctpA</i> -VSV [Y156A], IPTG-inducible expression of <i>E. coli</i> K-12 <i>ctpA</i> gene carrying a substrate binding mutation with a C-terminal VSV viral epitope tag, AmpR	This study
pCH6342	pTrc99a:: <i>ctpA</i> -VSV [Y38A], IPTG-inducible expression of <i>E. coli</i> K-12 <i>ctpA</i> gene carrying a substrate binding mutation with a C-terminal VSV viral epitope tag, AmpR	This study
pCH6343	pTrc99a:: <i>ctpA</i> -VSV [E56R], IPTG-inducible expression of <i>E. coli</i> K-12 <i>ctpA</i> gene carrying a peripasmic gate mutation with a C-terminal VSV viral epitope tag, AmpR	This study
pCH13269	pCH450:: <i>CT-1</i> (NI1076), arabinose-inducible expression of CdiA-CT toxin domain from <i>E. coli</i> NI1076 locus 1. TetR	This study
pCH13270	pCH450:: <i>CT-2</i> (NI1076), arabinose-inducible expression of CdiA-CT toxin domain from <i>E. coli</i> NI1076 locus 2. TetR	This study
pCH13925	pCH450KX:: <i>CT-1</i> ΔVENN (NI1076), arabinose-inducible expression of CdiA-CT toxin domain beginning just after the conserved (V/I)ENN motif from <i>E. coli</i> NI1076 locus 1. TetR	This study
<i>Ch. 4 plasmids, cont'd.</i>		

Plasmid	Description	Source
pCH14011	pCH450KX:: <i>CT-2</i> ΔVENN (NI1076), arabinose-inducible expression of CdiA-CT toxin domain beginning just after the conserved (V/I)ENN motif from <i>E. coli</i> NI1076 locus 2. TetR	This study
<i>Ch. 4 plasmids, cont'd.</i>		

Table 4.5: Primers used in Chapter 4.

CH2260 (mariner-rev-seq)	5' - CAA GCT TGT CAT CGT CAT CC - 3'	Ch. 2
CH3953 (NI1076-CT17-mid-for)	5' - CAG GTA GGA ACT CGG TTG AGA ATA ATC TGC TGG GTG GCA GTG AAT GG - 3'	[140]
CH3954 (NI1076-CT17-mid-rev)	5' - GGT CTG GTG TCT AAC CTT TGG TCA GAA CCC CTT AAC TTT CAT GAT ATG - 3'	This study
CH4127 (NI1076-CT21-mid-for)	5' - CAG GTA GGA ACT CGG TTG AGA ATA ATA GCC TGG CGC ATG TTC TGG - 3'	This study
CH4128 (NI1076-CT21-mid-rev)	5' - GGT CTG GTG TCT AAC CTT TGG CTA TCT GTT CCT TCT GTC ATT TTG G - 3'	This study
DL1527	5' GAA CAT CCT GGC ATG AGC G - 3'	[77]
DL2470	5' - ATT ATT CTC AAC CGA GTT CCT ACC TG - 3'	[77]
DL1663	5' - CCC AAA GGT TAG ACA CCA GAC C - 3'	[77]
DL2368	5' - GTT GGT AGT GGT GGT GCT G - 3'	[77]
CH4070 (CDI-204-nested)	5' - CAC AGT TGC GGG AGA C - 3'	This study
CH4071		
<i>Ch. 4 primers, cont'd.</i>		



Primer	Description	Source
(CDI-205-nested)	5' - GGC GCT TTT ATC CGG C - 3'	This study
CH4058 (NI1076- <i>cdiI1</i> -Kpn-for)	5' - GGC GGT ACC ATG AAG AGA CTC CTT ATT G - 3'	This study
CH4059 (NI1076- <i>cdiI1</i> -Xho-rev)	5' - AAC CTC GAG TTA GAA CCC CTT AAC TTT CAT - 3'	This study
CH4060 (NI1076- <i>cdiI2</i> -Kpn-for)	5' - AAA GGT ACC ATG ACT TTC GGA AGA TG - 3'	This study
CH4061 (NI1076- <i>cdiI2</i> -Xho-rev)	5' - AAT CTC GAG CTA TCT GTT CCT TCT GTC - 3'	This study
CH4108 (NI1076-CT1-Nco-for)	5' - AAA CCA TGG TTG AGA ATA ACC TGC TGG G - 3'	This study
CH4236 (NI1076-CT1-Xho-rev2)	5' - AAA CTC GAG TCA TTT CCC AGC CTC CAT TGC - 3'	This study
CH4110 (NI1076-CT2-Nco-for)	5' - TTT CCA TGG TTG AGA ATA ACA GCC TGG C - 3'	This study
CH4111		

*Ch. 4 primers, cont'd.*

Primer	Description	Source
(NI1076-CT2-Xho-rev)	5' - TTT CTC GAG TTA TTT TGA TTT TTC CCC ATG - 3'	This study
CH4235 (NI1076-CT1-VENNless-Kpn-for)	5' - AAA GGT ATG CTG CTG GGT GGC AGT GAA TGG - 3'	This study
CH4237 (NI1076-CT2-VENNless-Kpn-for)	5' - AAA GGT ACC ATG AGC CTG GCG CAT GTT CTG G - 3'	This study
CH5141 ( <i>ctpA</i> -Eco-for)	5' - AAA GAA TTC GAA AGC ACC CCC GTT AAT ATG GG 3'	This study
CH5144 ( <i>ctpA</i> -VSV-Eco-rev)	5' - TTC TAG ATT ATT TGC CAA GAC GAT TCA TTT CAA TAT CAG TAT ACG CTA CGG CTG CTT TCG - 3'	This study
CH5142 ( <i>ctpA</i> -Y38A-rev)	5' - CCT TGT AGG CCG GCA TAA CCA AAA CGT TCC C - 3'	This study
CH5143 ( <i>ctpA</i> -E56Q-rev)	5' - GGT GAT TGA ATC CGC TTg AGA CAT ACC C - 3'	This study
CH5365 ( <i>ctpA</i> -Y156A-rev)	5' - CCG ATG TTG ACG GAC ATG GCG TAC ATG GTG AAT GC - 3'	This study
CH5366		

*Ch. 4 primers, cont'd.*

Primer	Description	Source
( <i>ctpB</i> -Kpn-for)	5' - TTT GGT ACC CTT ACG CGT TCA TAC TTT TCA GG - 3'	This study
CH4885 ( <i>ctpB</i> -Xho-rev)	5' - AAA CTC GAG GCA AGA ATA ATT AAT GGC TTT CCG GCG - 3'	This study
CH5367 ( <i>ctpC</i> -Kpn-for)	5' - TTT GTT ACC GGG AAG TGG CTT GCC ACT TCC C - 3'	This study
CH4887 ( <i>ctpC</i> -Xho-rev)	5' - AAA CTC GAG CGA CAG TTA ATC GTT GCT CTC CTG TAT C - 3'	This study
CH4529 ( <i>puuP</i> -Nco-for)	5' - TTT CCA TGG CTA TTA ATT CAC CAC TGA ATA TTG C - 3'	This study
CH5085 ( <i>puuP</i> -Xba-rev)	5' - TTT TCT AGA CTA TTA CGT TTC ACT CAC CGG C - 3'	This study
CH5095 ( <i>plaP</i> -Kpn-for)	5' - TTT GGT ACC ATG TCG CAT AAC GTT ACT CCA AAC ACC - 3'	This study
CH5096 ( <i>plaP</i> -Xho-rev)	5' - TTT CTC GAG TTA GC TAC GTC TTC GTA CTG CGG - 3'	This study

*Ch. 4 primers, cont'd.*

# Chapter 5

## Conclusion

**The big picture.** Bacteria are capable of inhabiting nearly every niche on Earth. The result of such dramatic microbial diversity is represented first by an array of metabolic capabilities, but is also reflected in the multiplicity of small molecules and proteins used to mediate interactions between bacteria and their surroundings. Examples include the many nonessential secretion systems bacteria encode for adaptation to specific lifestyles (see section 1.4) as well as diffusible quorum-sensing molecules used in communication to control population density [181]. Produced by so-called "accessory genes", these proteins and molecules are not essential for growth, but their benefit clearly outweighs the cost of replicating and producing them. Indeed, pathogenic bacteria acquire virulence capabilities specifically by expressing proteins associated with pathogenicity islands, which are by definition large regions of disposable genomic content [182]. Thus, one over-arching goal of investigating bacterial physiology is to better understand what role all of these nonessential accessory genes are playing in communities where bacteria are constantly competing, yet thriving. Ultimately, these findings will both help us to better understand the pathogens that cause us harm and also introduce us to new genes and proteins that may prove useful for microbial engineering in the future.

This thesis explores one particular genetic locus that is often associated with pathogenicity islands in the Proteobacteria - termed contact-dependent growth inhibition

(*cdiBAI*). Although CDI systems are dispensable for growth, when present in a mixed bacterial community, they exert pressure on neighboring bacteria through the delivery of toxic proteins (CdiA-CT is the toxin itself). Indeed, due to the strong selection pressure they pose for CDI-resistant (i.e., *cdiI*-containing) bacteria in the community, *cdiBAI* loci act like plasmid stabilization systems, killing off any cells that have lost the locus and associated genetic content and thus immunity to CdiA-CT [93]. Therefore, it is thought that CDI systems might be selfish genetic elements, but also confer a competitive advantage on the pathogens in which they are found. Although there is work to be done on the role of CDI *in vivo* as well as the transcriptional regulation of *cdiBAI* loci, it is conceivable that CDI is deployed to interfere with the growth of commensals during the initial stages of colonization, since CdiA also initiates biofilm formation, is proximity-dependent, and its activity is apparently restricted to solid surfaces [183, 158] (see Ch. 3). Indeed, T6SSs are another toxin-delivery system used by pathogens (see section 1.4) which are known to facilitate commensal invasion by *Shigella sonnei*, *Vibrio cholerae*, and *Listeria monocytogenes*, to name a few [184]. Ch. 2 and Ch. 3 introduce *Citrobacter rodentium* as a potential mouse infection model for the study of CDI *in vivo*, which not only has its own CDI systems that are likely repressed under laboratory conditions but is also a target for the Class 4 system (section 3). It will be exciting to study CDI in a natural host-pathogen model in the future to determine when these systems are expressed and what their true role inside the host is. ruhe2013bama Furthermore, the study of CDI necessitates a host-pathogen model not only to investigate the possibility of its role in pathogen colonization, but also because CDI systems may not actually mediate interference competition when they are naturally deployed. Indeed, many lines of evidence may indicate CDI toxins regulate growth under stressful conditions much like toxin-antitoxin (TA) systems, which are internally expressed toxins that inhibit bacterial growth when the antitoxin/immunity protein is selectively degraded, leading to a persis-

tent state. Persister cells are known to be more antibiotic tolerant and present in biofilms [185], both of which are also associated with CDI activity [59, 90, 157, 158]. Like TA systems, CdiA-CTs are genetically paired with a cognate immunity gene that prevents a CDI+ cell from self-intoxication. Importantly, the range of targets to which any CdiA protein can deliver toxin is quite small due to the receptor-dependent nature of CdiA-CT delivery: not only does CdiA require an OM protein to initiate toxin translocation, but CdiA-CT is incapable of transport across the IM without the aid of a membrane protein [79, 83] (also see Ch. 4). Moreover, tRNA-degrading CDI toxins can either target a single species of tRNA, or require a third target cell protein in the cytoplasm for stability [162, 80]. Thus, CdiA-CTs may require up to 3 checkpoints to intoxicate a cell. Therefore, if there is a benefit to CDI intoxication, only closely-related bacteria can receive it. It is generally accepted that the reason TA systems work is due to selective degradation of the antitoxin protein under stressful conditions, which leads to free toxin and eventually growth arrest and persistence. Nothing is known of the regulation of *cdiI* expression even in rich media, though it is possible we will find that regulated internal expression of CdiA-CT/CdiI pairs in addition to surface expression of the full CdiA protein plays a role in CDI physiology. Interestingly, a recent study by Ghosh et al. revealed that CdiI- cells do become antibiotic tolerant upon receipt of CdiA-CT [90], suggesting that CDI toxins may also cause persister formation like TA modules. How this changes in the presence of immunity will be important to understand, especially since previous studies on a CDI DNase toxin reveal that when bound to its cognate immunity, the toxin-immunity complex has affinity for DNA [91]. These data present the intriguing possibility that CDI systems may discriminate between CDI+/- cells and induce gene expression changes accordingly. Indeed, we have much to learn from CDI systems and how they mediate cell-cell interactions. This thesis provides a framework for future studies to build on, in the hopes of improving our understanding of CDI.

**Implications of class 4 CDI.** In Chapter 2, I identify a novel CdiA protein (class 4 CdiA) which undergoes lipidation to bind target bacteria at the core of lipopolysaccharide. In Ch. 3, I use this CdiA protein to explore how O-antigen might affect CDI in general. Due to its affinity for the conserved LPS core, the identification of CdiA<sub>4</sub> not only offers a new tool for synthetic biology but also allows us to investigate CDI in more natural isolates like *Salmonella* and *Citrobacter*. Lastly, the class 4 CDI locus also introduces a new family of bacterial acyltransferases whose mechanism and diversity begs to be explored.

LPS is the first non-protein receptor identified for a CdiA protein, meaning class 4 CdiA is less discriminatory than previously identified CDI systems. Additionally, CdiA<sub>4</sub> activity can be tuned by replacement of Lys1467 or removal of CdiC (Fig. 2.11). Therefore, CdiA<sub>4</sub> is an intriguing candidate for synthetic biology applications that seek to target important pathogens of *Enterobacteriales*. Indeed, we have demonstrated that both the receptor-binding domain and toxin domains are modular. The RBD, for example, could be used for targeted delivery of cargo such as has been done using the receptor-binding protein of phage T5 [186]. It is important to note, however, that class II CdiA was also recently demonstrated to have some affinity for OmpC receptors from other species [116], and CdiA from *Burkholderia* appears to rely on LPS as well but perhaps not as a sole receptor. In contrast with Class 2 CdiA, though, target cells are much less likely to gain resistance to Class 4 CdiA since it binds directly to the core of LPS. However, resistance could arise through receptor-independent means as well, such as alternative cell surface changes that block receptor access. Target cell resistance, though, is an issue for any synthetic biology application which aims to inhibit cell growth. The second attribute of Class 4 CDI that makes it a tempting target for engineering purposes is the presence of an accessory acyltransferase (CdiC), whose role in CDI is to increase the affinity of CdiA for the LPS core. Lipidation of CdiA<sub>4</sub> may be exploited for modulating LPS affinity,

since the removal or inactivation of CdiC results in 100-fold reduction in growth inhibition in the lab, which may actually have a greater effect in a host environment (see 2.3.3 and 3.3.3). Future work on CdiC and its homologues may reveal new opportunities for engineering CdiA, perhaps through the addition of alternative fatty acids. Finally, since we have mapped the receptor-binding activity to the resolution of a single amino acid, receptor affinity can also be modulated by making modifications to CdiA itself (Fig. 2.7). Thus, taken together, this work provides numerous approaches for using the LPS RBD or full CdiA<sub>4</sub> protein in applications where modulation of binding affinity of the LPS from several important bacterial genera is needed.

By identifying LPS as a CDI receptor, I also became interested in the potential effect O-antigen might have on LPS binding, especially since this CdiA protein can inhibit several more "wild-type" lab isolates (see Fig. 3.5). Using a lab strain restored for O-antigen biosynthesis, I found that, perhaps unsurprisingly, LPS binding is mitigated in the presence of O-antigen (Fig. 3.3). In fact, in shaking liquid broth, O-antigen appears to completely shield targets from any CdiA protein. Thus, the natural question is whether this phenomenon translates to natural isolates. Using an insertional mutagenesis approach to disrupt O-antigen ligase (*waaL*), we succeeded in removing O-antigen from the surface of two clinically relevant target species (*Salmonella enterica* and *Citrobacter rodentium*) to test against CdiA<sub>4</sub> (Fig. 3.5). However, there appears to be selection against our insertion since both *waaL* deficient strains have unexpected phenotypes in addition to loss of O-side chains that might be interfering with the CdiA-LPS interaction. Interestingly, one of the phenotypes we observed in a *waaL* deletion strain appears to be upregulation of capsule polysaccharide since the colonies are dense and more opaque (in *S. enterica*), which results in even more CDI-resistance. Thus, if *S. enterica* is upregulating capsule in response to removal of *waaL*, this is further evidence that surface polysaccharides do indeed shield natural isolates from CDI systems. Future studies should



explore this interaction further in the isolates in which CDI systems are found. Indeed, gaining a better understanding of CdiA's interactions with the complex cell envelope of natural isolates will shed light on the physiology of CDI and how it can shape the sessile biofilm communities in which it is most likely deployed.

In addition to identifying a new CDI receptor, Chapter 2 also introduces a new accessory lysine acyltransferase: CdiC. CdiC proteins are associated with many CDI loci in *Enterobacteriales*, all of which appear to be related to the class 4 LPS-binding CdiA protein. Here, we investigate the activity of a single CdiC protein isolated from *E. coli* STEC O31 to understand its role in CDI. However, the identification of this new enzyme opens up many new avenues of research into modified CdiA proteins and their cognate acyltransferases. We show that CdiC modifies the receptor-binding domain of CdiA at lysine 1467 with 3-hydroxydecanoate (Fig. 2.7). Thus, CdiC's role in CDI is to increase the affinity of CdiA for LPS. CdiC therefore shares both sequence and functional homology with the toxin-activating acyltransferase (TAAT) family of enzymes, which modify hemolysin toxins with fatty acids also to increase their affinity for erythrocyte membranes [28]. Remarkably, the addition of 3-hydroxydecanoate appears to mimic the Gram-negative outer membrane bilayer composition, which contains N-linked 3-hydroxytetradecanoyl chains at the glucosamine residues of lipid A. Other TAAT homologues such as HlyC from *E. coli* UTI89 add 14-, 15-, or 16-carbon saturated fatty acids to their substrates [29], which mimic the phospholipid composition of the erythrocytes into which they insert. Indeed, hemolysins are often nontoxic in the absence of lipidation [123]. It makes sense, then, that a protein destined for the diderm outer membrane would undergo modification with a fatty acid that more closely resembles the bacterial envelope.

As a first step in the study of diverse CdiC proteins, we tried to complement the CdiC-deficient class 4 locus from *E. coli* STEC O31 with two CdiC homologues from other species that encode class 4 systems. Interestingly, we found that neither non-

cognate CdiC allele could substitute for the cognate acyltransferase (Fig. 2.12). By contrast, TAAT proteins can cross-activate non-cognate substrates [187]. Additionally, hemolysins are Type 1 secretion systems and are thus exported across both membranes via a C-terminal signal sequence by a dedicated transporter (HlyB) [188], whereas CdiA is predicted to cross the IM by the Sec translocon using an N-terminal signal sequence. Unique to CdiA<sub>4</sub> is the presence of an extended signal peptide ~ 60 amino acids long. These so-called ESPRs are imperfect signals for post-translational IM translocation, and therefore delay export [189]. We anticipate that the CDI ESPR may provide time for CdiC to access its substrate in the cytosol. Future work on modified CdiA proteins should explore the mechanism by which CdiC activates CdiA<sub>4</sub>, and investigate the potential diversity of modifications throughout *Enterobacteriales*.

**Future directions for CDI pore-forming toxins.** Chapters 2 & 3 investigate the interaction between class 4 CdiA and LPS. Chapter 4, however, focuses on the process of toxin translocation following OM receptor-binding. In Ch. 4, I identify four inner-membrane proteins required for the activity of two ionophore CDI toxins, and propose possible mechanisms by which CDI ionophores could exploit these proteins for pore formation. The findings I present in Ch. 4 help pave the way for more mechanistic investigations of CDI ionophores but, in the meantime, this study reveals some important insights into the behavior of CDI ionophore toxin domains.

To determine which proteins are required for the delivery of the two ionophore toxins introduced in Ch.4, we conducted genetic selections on UV and *mariner* transposon-mutagenized pools of target cells to find mutations rendering them CDI-resistant. These experiments revealed that both toxins uniquely exploit two IM nutrient transporters interchangeably to exert toxicity. In contrast, all previously characterized CdiA-CTs have evolved affinity for a single IM protein. The question that arises is: why do both of these

toxins have the capability of exploiting two receptor/cytoplasmic-entry proteins? As the process of obtaining CDI-resistant mutants reveals very clearly, redundancy in receptor selection can ensure targeted cells do not easily evade toxin activity through spontaneous mutations. It's possible that other CDI toxins may have even evaded characterization in the lab due to the difficulty in enriching for CDI-resistance because of redundant receptor dependencies. Thus, future studies should consider this when uncovering genes involved in the CDI delivery pathway.

In Ch. 4, we also demonstrate that both newly-characterized CdiA-CTs dissipate the proton-motive force in target bacteria (see Fig. 4.4). Two other toxins have previously been described which also have this effect on targets, and both are thought to do so by forming holes in the IM to allow protons through. However, the channel-forming colicins (see 1.3), which serve as a model for monomeric bactericidal pore-forming toxins, insert into the bilayer independent of an IM receptor. Why CdiA-CT ionophores require a protein partner has yet to be understood. However, we do know that the endonuclease CdiA-CTs can share almost identical structural homology with non-CDI bactericidal toxins while evolving CDI-specific features, such as disulfides for providing structure to an otherwise molten globule domain [83]. It's possible that CDI ionophores have also evolved receptor dependence to initiate or aid in folding when in the periplasm, and this will be an exciting topic for future investigations to explore using the toxin-receptor pairs identified here.

Interestingly, one clue as to how pore forming CDI toxins achieve membrane depolarization comes from the presence of two putative glycine zipper domains in their C-terminal region (see 4.14). Additionally, a close examination of primary sequence between both NI1076 CdiA-CTs reveals a short N-terminal putative cytoplasmic entry domain (Fig. 4.20), responsible for binding the IM receptor, and a much larger C-terminal domain that would contain the pore-forming activity. The glycine zippers

found in the C-terminal region are short: they contain only 2 GxxxG motifs rather than the 3 typically associated with glycine zipper proteins [30] (Fig. 4.14). However, one of two identified motifs appears to be conserved in all four ionophores (Fig. 4.14). Glycine zippers mediate helix-helix packing of transmembrane alpha helices within a membrane, and could mediate pore formation as has been observed with the vacuolating toxin from *Helicobacter pylori* [33]. Therefore, it is tempting to speculate that the imperfect glycine zippers found in CDI toxins may have evolved to prevent spontaneous bilayer insertion, such as in the periplasm of the inhibitor cell. During delivery into a target cell, then, the process of CdiA-CT cleavage would reveal the N-terminal cytoplasmic-entry domain which might lead to structural changes upon receptor binding.

Even if CDI ionophores use proteins to insert into the membrane, the mystery remains of how a single toxin containing at most two glycine zipper motifs would be capable of forming an ion channel. Perhaps an additional role for the IM protein, after enabling CdiA-CT bilayer entry, is to provide a scaffold for pore formation. One reason this hypothesis is enticing is because of the behavior of the ionophore immunity proteins; in contrast to their cognate toxins, these proteins are highly hydrophobic (Fig. 4.21) and therefore are likely pre-localized to the IM. Indeed, ectopic over-expression of pore-former immunity proteins but not other CdiI proteins is toxic (data not shown). In order to inactivate the toxin through direct binding, pre-localized CdiI would then rely on random diffusion in the bilayer or, alternatively, by directly binding an IM receptor, CdiI would be poised to block the toxin-receptor binding interaction. To determine how ionophores disrupt the pmf, then, future work may find that studying their immunity proteins will reveal useful insights into the ionophore mechanism itself.

# Bibliography

- [1] M. A. Hassani, P. Durán, and S. Hacquard, *Microbial interactions within the plant holobiont*, *Microbiome* **6** (Mar., 2018).
- [2] J. Lloyd-Price, G. Abu-Ali, and C. Huttenhower, *The healthy human microbiome*, *Genome Medicine* **8** (Apr., 2016) 51.
- [3] M. A. Fischbach and J. A. Segre, *Signaling in Host-Associated Microbial Communities*, *Cell* **164** (Mar., 2016) 1288–1300.
- [4] J. M. Pickard, M. Y. Zeng, R. Caruso, and G. Núñez, *Gut Microbiota: Role in Pathogen Colonization, Immune Responses and Inflammatory Disease*, *Immunological reviews* **279** (Sept., 2017) 70–89.
- [5] A. Zipperer, M. C. Konnerth, C. Laux, A. Berscheid, D. Janek, C. Weidenmaier, M. Burian, N. A. Schilling, C. Slavetinsky, M. Marschal, *et. al.*, *Human commensals producing a novel antibiotic impair pathogen colonization*, *Nature* **535** (2016), no. 7613 511–516.
- [6] A. L. Byrd, Y. Belkaid, and J. A. Segre, *The human skin microbiome*, *Nature Reviews Microbiology* **16** (Mar., 2018) 143–155.
- [7] B. Wang, M. Yao, L. Lv, Z. Ling, and L. Li, *The Human Microbiota in Health and Disease*, *Engineering* **3** (Feb., 2017) 71–82.
- [8] D. Ribet and P. Cossart, *How bacterial pathogens colonize their hosts and invade deeper tissues*, *Microbes and Infection* **17** (Mar., 2015) 173–183.
- [9] M. Yang, S. Ren, D. Shen, N. Yang, B. Wang, S. Han, X. Shen, S.-H. Chou, and G. Qian, *An intrinsic mechanism for coordinated production of the contact-dependent and contact-independent weapon systems in a soil bacterium*, *PLoS pathogens* **16** (2020), no. 10 e1008967.
- [10] K. R. V. Thappeta, K. Ciezki, N. Morales-Soto, S. Wesener, H. Goodrich-Blair, S. P. Stock, and S. Forst, *R-type bacteriocins of xenorhabdus bovienii determine the outcome of interspecies competition in a natural host environment*, *Microbiology* (2020) micro000981.

- [11] R. B. Sarma-Rupavtarm, Z. Ge, D. B. Schauer, J. G. Fox, and M. F. Polz, *Spatial Distribution and Stability of the Eight Microbial Species of the Altered Schaedler Flora in the Mouse Gastrointestinal Tract*, *Applied and Environmental Microbiology* **70** (May, 2004) 2791–2800.
- [12] J. L. Mark Welch, Y. Hasegawa, N. P. McNulty, J. I. Gordon, and G. G. Borisy, *Spatial organization of a model 15-member human gut microbiota established in gnotobiotic mice*, *Proceedings of the National Academy of Sciences* **114** (Oct., 2017) E9105–E9114.
- [13] J. Pizarro-Cerdá and P. Cossart, *Bacterial Adhesion and Entry into Host Cells*, *Cell* **124** (Feb., 2006) 715–727.
- [14] C. Belzer, L. W. Chia, S. Aalvink, B. Chamlagain, V. Piironen, J. Knol, and W. M. de Vos, *Microbial Metabolic Networks at the Mucus Layer Lead to Diet-Independent Butyrate and Vitamin B<sub>12</sub> Production by Intestinal Symbionts*, *mBio* **8** (Nov., 2017).
- [15] G. A. Hedblom, H. A. Reiland, M. J. Sylte, T. J. Johnson, and D. J. Baumler, *Segmented Filamentous Bacteria – Metabolism Meets Immunity*, *Frontiers in Microbiology* **9** (2018).
- [16] E. Cascales, S. K. Buchanan, D. Duche, C. Kleanthous, R. Lloubes, K. Postle, M. Riley, S. Slatin, and D. Cavard, *Colicin Biology*, *Microbiology and Molecular Biology Reviews* **71** (Mar., 2007) 158–229.
- [17] H. Ridleya, C. L. Johnson, and J. H. Lakey, *Interfacial interactions of pore-forming colicins*, in *Proteins Membrane Binding and Pore Formation*, pp. 81–90. Springer, 2010.
- [18] C. Kleanthous, *Swimming against the tide: progress and challenges in our understanding of colicin translocation*, *Nature Reviews Microbiology* **8** (2010), no. 12 843.
- [19] M. Dal Peraro and F. G. Van Der Goot, *Pore-forming toxins: ancient, but never really out of fashion*, *Nature reviews microbiology* **14** (2016), no. 2 77.
- [20] M. Parker, F. Pattus, A. Tucker, and D. Tsernoglou, *Structure of the membrane-pore-forming fragment of colicin a*, *Nature* **337** (1989), no. 6202 93.
- [21] I. R. Vetter, M. W. Parker, A. D. Tucker, J. H. Lakey, F. Pattus, and D. Tsernoglou, *Crystal structure of a colicin n fragment suggests a model for toxicity*, *Structure* **6** (1998), no. 7 863–874.

- [22] N. Galitsky, V. Cody, A. Wojtczak, D. Ghosh, J. R. Luft, W. Pangborn, and L. English, *Structure of the insecticidal bacterial  $\delta$ -endotoxin cry3bb1 of bacillus thuringiensis*, *Acta Crystallographica Section D: Biological Crystallography* **57** (2001), no. 8 1101–1109.
- [23] J. L. Hilsenbeck, H. Park, G. Chen, B. Youn, K. Postle, and C. Kang, *Crystal structure of the cytotoxic bacterial protein colicin b at 2.5 Å resolution*, *Molecular microbiology* **51** (2004), no. 3 711–720.
- [24] S. J. Tilley and H. R. Saibil, *The mechanism of pore formation by bacterial toxins*, *Current opinion in structural biology* **16** (2006), no. 2 230–236.
- [25] M. W. Parker, J. P. Postma, F. Pattus, A. D. Tucker, and D. Tsernoglou, *Refined structure of the pore-forming domain of colicin a at 2.4 Å resolution*, *Journal of molecular biology* **224** (1992), no. 3 639–657.
- [26] D. W. Hilbert, T. E. Paulish-Miller, C. K. Tan, A. J. Carey, G. C. Ulett, E. Mordechai, M. E. Adelson, S. E. Gygax, and J. P. Trama, *Clinical escherichia coli isolates utilize alpha-hemolysin to inhibit in vitro epithelial cytokine production*, *Microbes and infection* **14** (2012), no. 7-8 628–638.
- [27] B. E. Ragle and J. B. Wardenburg, *Anti-alpha-hemolysin monoclonal antibodies mediate protection against staphylococcus aureus pneumonia*, *Infection and immunity* **77** (2009), no. 7 2712–2718.
- [28] C. Hughes, J.-P. Issartel, K. Hardie, P. Stanley, E. Koronakis, and V. Koronakis, *Activation of escherichia coli prohemolysin to the membrane-targeted toxin by hlyc-directed acp-dependent fatty acylation*, *FEMS microbiology immunology* **5** (1992), no. 1-3 37–43.
- [29] K. B. Lim, C. R. B. Walker, L. Guo, S. Pellett, J. Shabanowitz, D. F. Hunt, E. L. Hewlett, A. Ludwig, W. Goebel, R. A. Welch, et. al., *Escherichia coli  $\alpha$ -hemolysin (hlya) is heterogeneously acylated in vivo with 14-, 15-, and 17-carbon fatty acids*, *Journal of Biological Chemistry* **275** (2000), no. 47 36698–36702.
- [30] W. P. Russ and D. M. Engelman, *The gxxxg motif: a framework for transmembrane helix-helix association*, *Journal of molecular biology* **296** (2000), no. 3 911–919.
- [31] S. Kim, T.-J. Jeon, A. Oberai, D. Yang, J. J. Schmidt, and J. U. Bowie, *Transmembrane glycine zippers: physiological and pathological roles in membrane proteins*, *Proceedings of the National Academy of Sciences* **102** (2005), no. 40 14278–14283.
- [32] R. E. Dalbey, P. Wang, and A. Kuhn, *Assembly of bacterial inner membrane proteins*, *Annual review of biochemistry* **80** (2011) 161–187.

- [33] S. Kim, A. K. Chamberlain, and J. U. Bowie, *Membrane channel structure of helicobacter pylori vacuolating toxin: role of multiple gxxxg motifs in cylindrical channels*, *Proceedings of the National Academy of Sciences* **101** (2004), no. 16 5988–5991.
- [34] R. E. Dalbey and A. Kuhn, *Protein traffic in gram-negative bacteria—how exported and secreted proteins find their way*, *FEMS microbiology reviews* **36** (2012), no. 6 1023–1045.
- [35] P. J. Bakkes, S. Jenewein, S. H. Smits, I. B. Holland, and L. Schmitt, *The rate of folding dictates substrate secretion by the escherichia coli hemolysin type 1 secretion system*, *Journal of Biological Chemistry* **285** (2010), no. 52 40573–40580.
- [36] D. L. Baldi, E. E. Higginson, D. M. Hocking, J. Praszquier, R. Cavaliere, C. E. James, V. Bennett-Wood, K. I. Azzopardi, L. Turnbull, T. Lithgow, *et. al.*, *The type ii secretion system and its ubiquitous lipoprotein substrate, ssle, are required for biofilm formation and virulence of enteropathogenic escherichia coli*, *Infection and immunity* **80** (2012), no. 6 2042–2052.
- [37] G. Ball, É. Durand, A. Lazdunski, and A. Filloux, *A novel type ii secretion system in pseudomonas aeruginosa*, *Molecular microbiology* **43** (2002), no. 2 475–485.
- [38] A. P. Pugsley, *The complete general secretory pathway in gram-negative bacteria.*, *Microbiology and Molecular Biology Reviews* **57** (1993), no. 1 50–108.
- [39] B. Py, L. Loiseau, and F. Barras, *Assembly of the type ii secretion machinery of erwinia chrysanthemi: direct interaction and associated conformational change between oute, the putative atp-binding component and the membrane protein outl*, *Journal of molecular biology* **289** (1999), no. 3 659–670.
- [40] D. Ghosal, K. W. Kim, H. Zheng, M. Kaplan, H. K. Truchan, A. E. Lopez, I. E. McIntire, J. P. Vogel, N. P. Cianciotto, and G. J. Jensen, *In vivo structure of the legionella type ii secretion system by electron cryotomography*, *Nature microbiology* **4** (2019), no. 12 2101–2108.
- [41] P. Ghosh, *Process of protein transport by the type iii secretion system*, *Microbiol. Mol. Biol. Rev.* **68** (2004), no. 4 771–795.
- [42] J. E. Galán and H. Wolf-Watz, *Protein delivery into eukaryotic cells by type iii secretion machines*, *Nature* **444** (2006), no. 7119 567–573.
- [43] A. Loquet, N. G. Sgourakis, R. Gupta, K. Giller, D. Riedel, C. Goosmann, C. Griesinger, M. Kolbe, D. Baker, S. Becker, *et. al.*, *Atomic model of the type iii secretion system needle*, *Nature* **486** (2012), no. 7402 276–279.



- [44] H.-J. Yeo and G. Waksman, *Unveiling molecular scaffolds of the type iv secretion system*, *Journal of bacteriology* **186** (2004), no. 7 1919–1926.
- [45] D. Hofreuter, S. Odenbreit, and R. Haas, *Natural transformation competence in helicobacter pylori is mediated by the basic components of a type iv secretion system*, *Molecular microbiology* **41** (2001), no. 2 379–391.
- [46] A. Seubert, R. Hiestand, F. De La Cruz, and C. Dehio, *A bacterial conjugation machinery recruited for pathogenesis*, *Molecular microbiology* **49** (2003), no. 5 1253–1266.
- [47] C. Locht, L. Coutte, and N. Mielcarek, *The ins and outs of pertussis toxin*, *The FEBS journal* **278** (2011), no. 23 4668–4682.
- [48] E. Bayer-Santos, W. Cenens, B. Y. Matsuyama, G. U. Oka, G. Di Sessa, I. D. V. Mininel, T. L. Alves, and C. S. Farah, *The opportunistic pathogen stenotrophomonas maltophilia utilizes a type iv secretion system for interbacterial killing*, *PLoS pathogens* **15** (2019), no. 9 e1007651.
- [49] G. G. Sgro, G. U. Oka, D. P. Souza, W. Cenens, E. Bayer-Santos, B. Matsuyama, N. F. Bueno, T. R. Dos Santos, C. E. Alvarez-Martinez, R. K. Salinas, *et. al.*, *Bacteria-killing type iv secretion systems*, *Frontiers in microbiology* **10** (2019) 1078.
- [50] J. Ghrayeb and M. Inouye, *Nine amino acid residues at the nh<sub>2</sub>-terminal of lipoprotein are sufficient for its modification, processing, and localization in the outer membrane of escherichia coli.*, *Journal of Biological Chemistry* **259** (1984), no. 1 463–467.
- [51] V. Roussel-Jazédé, J. Grijpstra, V. van Dam, J. Tommassen, and P. van Ulsen, *Lipidation of the autotransporter nalp of neisseria meningitidis is required for its function in the release of cell-surface-exposed proteins*, *Microbiology* **159** (2013), no. 2 286–295.
- [52] J. H. Peterson, R. L. Szabady, and H. D. Bernstein, *An unusual signal peptide extension inhibits the binding of bacterial presecretory proteins to the signal recognition particle, trigger factor, and the secyeg complex*, *Journal of Biological Chemistry* **281** (2006), no. 14 9038–9048.
- [53] S. Reidl, A. Lehmann, R. Schiller, A. S. Khan, and U. Dobrindt, *Impact of o-glycosylation on the molecular and cellular adhesion properties of the escherichia coli autotransporter protein ag43*, *International Journal of Medical Microbiology* **299** (2009), no. 6 389–401.

- [54] S. Jain and M. B. Goldberg, *Requirement for *yaet* in the outer membrane assembly of autotransporter proteins*, *Journal of bacteriology* **189** (2007), no. 14 5393–5398.
- [55] J. Selkrig, K. Mosbahi, C. T. Webb, M. J. Belousoff, A. J. Perry, T. J. Wells, F. Morris, D. L. Leyton, M. Totsika, M.-D. Phan, *et. al.*, *Discovery of an archetypal protein transport system in bacterial outer membranes*, *Nature structural & molecular biology* **19** (2012), no. 5 506–510.
- [56] C. M. Rojas, J. H. Ham, W.-L. Deng, J. J. Doyle, and A. Collmer, *Heca, a member of a class of adhesins produced by diverse pathogenic bacteria, contributes to the attachment, aggregation, epidermal cell killing, and virulence phenotypes of erwinia chrysanthemi ec16 on nicotiana clelandii seedlings*, *Proceedings of the National Academy of Sciences* **99** (2002), no. 20 13142–13147.
- [57] L. D. Cope, R. Yogev, U. Muller-Eberhard, and E. J. Hansen, *A gene cluster involved in the utilization of both free heme and heme: hemopepin by haemophilus influenzae type b.*, *Journal of bacteriology* **177** (1995), no. 10 2644–2653.
- [58] M. Vakevainen, S. Greenberg, and E. J. Hansen, *Inhibition of phagocytosis by haemophilus ducreyi requires expression of the *lspa1* and *lspa2* proteins*, *Infection and immunity* **71** (2003), no. 10 5994–6003.
- [59] D. O. Serra, M. S. Conover, L. Arnal, G. P. Sloan, M. E. Rodriguez, O. M. Yantorno, and R. Deora, *Fha-mediated cell-substrate and cell-cell adhesions are critical for bordetella pertussis biofilm formation on abiotic surfaces and in the mouse nose and the trachea*, *PloS one* **6** (2011), no. 12.
- [60] C. Baud, H. Hodak, E. Willery, H. Drobecq, C. Locht, M. Jamin, and F. Jacob-Dubuisson, *Role of *degp* for two-partner secretion in bordetella*, *Molecular microbiology* **74** (2009), no. 2 315–329.
- [61] A. V. Kajava and A. C. Steven, *The turn of the screw: variations of the abundant  $\beta$ -solenoid motif in passenger domains of type v secretory proteins*, *Journal of structural biology* **155** (2006), no. 2 306–315.
- [62] Z. C. Ruhe, D. A. Low, and C. S. Hayes, *Bacterial contact-dependent growth inhibition*, *Trends in microbiology* **21** (2013), no. 5 230–237.
- [63] S. K. Aoki, R. Pamma, A. D. Hernday, J. E. Bickham, B. A. Braaten, and D. A. Low, *Contact-dependent inhibition of growth in escherichia coli*, *Science* **309** (2005), no. 5738 1245–1248.
- [64] S. K. Aoki, E. J. Diner, C. t. de Roodenbeke, B. R. Burgess, S. J. Poole, B. A. Braaten, A. M. Jones, J. S. Webb, C. S. Hayes, P. A. Cotter, *et. al.*, *A widespread*

- family of polymorphic contact-dependent toxin delivery systems in bacteria*, *Nature* **468** (2010), no. 7322 439.
- [65] M. S. Anderson, E. C. Garcia, and P. A. Cotter, *The burkholderia bcpaiob genes define unique classes of two-partner secretion and contact dependent growth inhibition systems*, *PLoS genetics* **8** (2012), no. 8 e1002877.
- [66] J.-C. Ogier, B. Duvic, A. Lanois, A. Givaudan, and S. Gaudriault, *A new member of the growing family of contact-dependent growth inhibition systems in xenorhabdus doucetiae*, *PLoS One* **11** (2016), no. 12 e0167443.
- [67] E. De Gregorio, R. Zarrilli, and P. P. Di Nocera, *Contact-dependent growth inhibition systems in acinetobacter*, *Scientific reports* **9** (2019), no. 1 154.
- [68] S. Aoki, J. Webb, B. Braaten, and D. Low, *Contact-dependent growth inhibition causes reversible metabolic downregulation in escherichia coli*, *Journal of bacteriology* **191** (2009), no. 6 1777–1786.
- [69] M. Roussin, S. Rabarioelina, L. Cluzeau, J. Cayron, C. Lesterlin, S. P. Salcedo, and S. Bigot, *Identification of a contact-dependent growth inhibition (cdi) system that reduces biofilm formation and host cell adhesion of acinetobacter baumannii dsm30011 strain*, *Frontiers in microbiology* **10** (2019) 2450.
- [70] Z. C. Ruhe, P. Subramanian, K. Song, J. Y. Nguyen, T. A. Stevens, D. A. Low, G. J. Jensen, and C. S. Hayes, *Programmed secretion arrest and receptor-triggered toxin export during antibacterial contact-dependent growth inhibition*, *Cell* **175** (2018), no. 4 921–933.
- [71] Z. C. Ruhe, J. Y. Nguyen, J. Xiong, S. Koskiniemi, C. M. Beck, B. R. Perkins, D. A. Low, and C. S. Hayes, *Cdia effectors use modular receptor-binding domains to recognize target bacteria*, *MBio* **8** (2017), no. 2 e00290–17.
- [72] Z. C. Ruhe, A. B. Wallace, D. A. Low, and C. S. Hayes, *Receptor polymorphism restricts contact-dependent growth inhibition to members of the same species*, *MBio* **4** (2013), no. 4 e00480–13.
- [73] C. M. Beck, J. L. Willett, D. A. Cunningham, J. J. Kim, D. A. Low, and C. S. Hayes, *Cdia effectors from uropathogenic escherichia coli use heterotrimeric osmoporins as receptors to recognize target bacteria*, *PLoS pathogens* **12** (2016), no. 10 e1005925.
- [74] J. S. Webb, K. C. Nikolakakis, J. L. Willett, S. K. Aoki, C. S. Hayes, and D. A. Low, *Delivery of cdia nuclease toxins into target cells during contact-dependent growth inhibition*, *PloS one* **8** (2013), no. 2 e57609.

- [75] R. Krasauskas, J. Skerniškytė, J. Martinkus, J. Armalytė, and E. Sužiedėlienė, *Capsule protects acinetobacter baumannii from inter-bacterial competition mediated by cdiA toxin*, *Frontiers in microbiology* **11** (2020) 1493.
- [76] K. Nikolakakis, S. Amber, J. S. Wilbur, E. J. Diner, S. K. Aoki, S. J. Poole, A. Tuanyok, P. S. Keim, S. Peacock, C. S. Hayes, *et. al.*, *The toxin/immunity network of burkholderia pseudomallei contact-dependent growth inhibition (cdi) systems*, *Molecular microbiology* **84** (2012), no. 3 516–529.
- [77] R. P. Morse, K. C. Nikolakakis, J. L. Willett, E. Gerrick, D. A. Low, C. S. Hayes, and C. W. Goulding, *Structural basis of toxicity and immunity in contact-dependent growth inhibition (cdi) systems*, *Proceedings of the National Academy of Sciences* **109** (2012), no. 52 21480–21485.
- [78] A. M. Jones, F. Garza-Sánchez, J. So, C. S. Hayes, and D. A. Low, *Activation of contact-dependent antibacterial trnase toxins by translation elongation factors*, *Proceedings of the National Academy of Sciences* **114** (2017), no. 10 E1951–E1957.
- [79] J. L. Willett, G. C. Gucinski, J. P. Fatherree, D. A. Low, and C. S. Hayes, *Contact-dependent growth inhibition toxins exploit multiple independent cell-entry pathways*, *Proceedings of the National Academy of Sciences* **112** (2015), no. 36 11341–11346.
- [80] K. Michalska, G. C. Gucinski, F. Garza-Sánchez, P. M. Johnson, L. M. Stols, W. H. Eschenfeldt, G. Babnigg, D. A. Low, C. W. Goulding, A. Joachimiak, *et. al.*, *Structure of a novel antibacterial toxin that exploits elongation factor tu to cleave specific transfer rnas*, *Nucleic acids research* **45** (2017), no. 17 10306–10320.
- [81] C. M. Beck, R. P. Morse, D. A. Cunningham, A. Iniguez, D. A. Low, C. W. Goulding, and C. S. Hayes, *CdiA from enterobacter cloacae delivers a toxic ribosomal rnaase into target bacteria*, *Structure* **22** (2014), no. 5 707–718.
- [82] G. Batot, K. Michalska, G. Ekberg, E. M. Irimpan, G. Joachimiak, R. Jedrzejczak, G. Babnigg, C. S. Hayes, A. Joachimiak, and C. W. Goulding, *The cdi toxin of yersinia kristensenii is a novel bacterial member of the rnaase a superfamily*, *Nucleic acids research* **45** (2017), no. 9 5013–5025.
- [83] N. L. Bartelli, S. Sun, G. C. Gucinski, H. Zhou, K. Song, C. S. Hayes, and F. W. Dahlquist, *The cytoplasm-entry domain of antibacterial cdiA is a dynamic  $\alpha$ -helical bundle with disulfide-dependent structural features*, *Journal of molecular biology* **431** (2019), no. 17 3203–3216.
- [84] A. Mychack, R. Amrutha, C. Chung, K. Cardenas Arevalo, M. Reddy, and A. Janakiraman, *A synergistic role for two predicted inner membrane proteins of escherichia coli in cell envelope integrity*, *Molecular microbiology* **111** (2019), no. 2 317–337.

- [85] S. K. Aoki, J. C. Malinverni, K. Jacoby, B. Thomas, R. Pamma, B. N. Trinh, S. Remers, J. Webb, B. A. Braaten, T. J. Silhavy, *et. al.*, *Contact-dependent growth inhibition requires the essential outer membrane protein bama (yaet) as the receptor and the inner membrane transport protein acrb*, *Molecular microbiology* **70** (2008), no. 2 323–340.
- [86] M. Wäneskog, *Too close for comfort: The role of Contact-Dependent growth Inhibition (CDI) in interbacterial competition and cooperation*. PhD thesis, Acta Universitatis Upsaliensis, 2020.
- [87] E. J. Diner, C. M. Beck, J. S. Webb, D. A. Low, and C. S. Hayes, *Identification of a target cell permissive factor required for contact-dependent growth inhibition (cdi)*, *Genes & development* **26** (2012), no. 5 515–525.
- [88] P. M. Johnson, C. M. Beck, R. P. Morse, F. Garza-Sánchez, D. A. Low, C. S. Hayes, and C. W. Goulding, *Unraveling the essential role of cysk in cdi toxin activation*, *Proceedings of the National Academy of Sciences* **113** (2016), no. 35 9792–9797.
- [89] E. C. Garcia, A. I. Perault, S. A. Marlatt, and P. A. Cotter, *Interbacterial signaling via burkholderia contact-dependent growth inhibition system proteins*, *Proceedings of the National Academy of Sciences* **113** (2016), no. 29 8296–8301.
- [90] A. Ghosh, Ö. Baltekin, M. Wäneskog, D. Elkhalfa, D. L. Hammarlöf, J. Elf, and S. Koskiniemi, *Contact-dependent growth inhibition induces high levels of antibiotic-tolerant persister cells in clonal bacterial populations*, *The EMBO journal* **37** (2018), no. 9.
- [91] J. L. E. Willett, *Delivery and activity of toxic effector domains from contact-dependent growth inhibition systems in Escherichia coli*. PhD thesis, UC Santa Barbara, 2016.
- [92] A. B. Ocasio and P. A. Cotter, *Cdi/cds system-encoding genes of burkholderia thailandensis are located in a mobile genetic element that defines a new class of transposon*, *PLoS genetics* **15** (2019), no. 1 e1007883.
- [93] Z. C. Ruhe, J. Y. Nguyen, A. J. Chen, N. Y. Leung, C. S. Hayes, and D. A. Low, *Cdi systems are stably maintained by a cell-contact mediated surveillance mechanism*, *PLoS genetics* **12** (2016), no. 6 e1006145.
- [94] B. T. Ho, T. G. Dong, and J. J. Mekalanos, *A View to a Kill: The Bacterial Type VI Secretion System*, *Cell Host & Microbe* **15** (Jan., 2014) 9–21.
- [95] Y. Fu, M. K. Waldor, and J. J. Mekalanos, *Tn-Seq analysis of vibrio cholerae intestinal colonization reveals a role for T6SS-mediated antibacterial activity in the host*, *Cell host & microbe* **14** (2013), no. 6 652–663.

- [96] P. G. Leiman, M. Basler, U. A. Ramagopal, J. B. Bonanno, J. M. Sauder, S. Pukatzki, S. K. Burley, S. C. Almo, and J. J. Mekalanos, *type VI secretion apparatus and phage tail-associated protein complexes share a common evolutionary origin*, *Proceedings of the National Academy of Sciences* **106** (2009), no. 11 4154–4159.
- [97] M. Brackmann, S. Nazarov, J. Wang, and M. Basler, *Using force to punch holes: mechanics of contractile nanomachines*, *Trends in cell biology* **27** (2017), no. 9 623–632.
- [98] á. Basler and J. Mekalanos, *Type 6 secretion dynamics within and between bacterial cells*, *Science* **337** (2012), no. 6096 815–815.
- [99] á. Basler, á. Pilhofer, G. Henderson, G. Jensen, and J. Mekalanos, *Type VI secretion requires a dynamic contractile phage tail-like structure*, *Nature* **483** (2012), no. 7388 182.
- [100] A. B. Russell, S. B. Peterson, and J. D. Mougous, *Type VI secretion system effectors: poisons with a purpose*, *Nature reviews microbiology* **12** (2014), no. 2 137–148.
- [101] J. Alcoforado Diniz, Y.-C. Liu, and S. J. Coulthurst, *Molecular weaponry: diverse effectors delivered by the type vi secretion system*, *Cellular microbiology* **17** (2015), no. 12 1742–1751.
- [102] F. R. Cianfanelli, J. A. Diniz, M. Guo, V. De Cesare, M. Trost, and S. J. Coulthurst, *Vgrg and paar proteins define distinct versions of a functional type vi secretion system*, *PLoS pathogens* **12** (2016), no. 6 e1005735.
- [103] X. Liang, F. Kamal, T.-T. Pei, P. Xu, J. J. Mekalanos, and T. G. Dong, *An onboard checking mechanism ensures effector delivery of the type vi secretion system in vibrio cholerae*, *Proceedings of the National Academy of Sciences* **116** (2019), no. 46 23292–23298.
- [104] S. L. Murdoch, K. Trunk, G. English, M. J. Fritsch, E. Pourkarimi, and S. J. Coulthurst, *The opportunistic pathogen serratia marcescens utilizes type vi secretion to target bacterial competitors*, *Journal of bacteriology* **193** (2011), no. 21 6057–6069.
- [105] E. Gueguen and E. Cascales, *Promoter swapping unveils the role of the citrobacter rodentium cts1 type vi secretion system in interbacterial competition*, *Appl. Environ. Microbiol.* **79** (2013), no. 1 32–38.
- [106] M. D. Carruthers, P. A. Nicholson, E. N. Tracy, and R. S. Munson Jr, *Acinetobacter baumannii utilizes a type vi secretion system for bacterial competition*, *PloS one* **8** (2013), no. 3 e59388.

- [107] L. Speare, A. G. Cecere, K. R. Guckes, S. Smith, M. S. Wollenberg, M. J. Mandel, T. Miyashiro, and A. N. Septer, *Bacterial symbionts use a type vi secretion system to eliminate competitors in their natural host*, *Proceedings of the National Academy of Sciences* **115** (2018), no. 36 E8528–E8537.
- [108] M. Bauer, M. Kube, H. Teeling, M. Richter, T. Lombardot, E. Allers, C. A. Würdemann, C. Quast, H. Kuhl, F. Knaust, *et. al.*, *Whole genome analysis of the marine bacteroidetes ‘gramella forsetii’ reveals adaptations to degradation of polymeric organic matter*, *Environmental Microbiology* **8** (2006), no. 12 2201–2213.
- [109] D. L. Kirchman, *The ecology of cytophaga–flavobacteria in aquatic environments*, *FEMS microbiology ecology* **39** (2002), no. 2 91–100.
- [110] P. D. Veith, N. A. Nor Muhammad, S. G. Dashper, V. A. Likic, D. G. Gorasia, D. Chen, S. J. Byrne, D. V. Catmull, and E. C. Reynolds, *Protein substrates of a novel secretion system are numerous in the bacteroidetes phylum and have in common a cleavable c-terminal secretion signal, extensive post-translational modification, and cell-surface attachment*, *Journal of Proteome Research* **12** (2013), no. 10 4449–4461.
- [111] T. Yang, X. Bu, Q. Han, X. Wang, H. Zhou, G. Chen, W. Zhang, and W. Liu, *A small periplasmic protein essential for cytophaga hutchinsonii cellulose digestion*, *Applied microbiology and biotechnology* **100** (2016), no. 4 1935–1944.
- [112] A. M. Lasica, M. Ksiazek, M. Madej, and J. Potempa, *The type ix secretion system (t9ss): highlights and recent insights into its structure and function*, *Frontiers in cellular and infection microbiology* **7** (2017) 215.
- [113] N. O’Brien-Simpson, P. Veith, S. Dashper, and E. Reynolds, *Porphyromonas gingivalis gingipains: the molecular teeth of a microbial vampire*, *Current Protein and Peptide Science* **4** (2003), no. 6 409–426.
- [114] F. Lauber, J. C. Deme, S. M. Lea, and B. C. Berks, *Type 9 secretion system structures reveal a new protein transport mechanism*, *Nature* **564** (2018), no. 7734 77–82.
- [115] C. Mercy, B. Ize, S. P. Salcedo, S. de Bentzmann, and S. Bigot, *Functional characterization of pseudomonas contact dependent growth inhibition (cdi) systems*, *PloS one* **11** (2016), no. 1.
- [116] P. Virtanen, M. Wäneskog, and S. Koskiniemi, *Class ii contact-dependent growth inhibition (cdi) systems allow for broad-range cross-species toxin delivery within the enterobacteriaceae family*, *Molecular microbiology* **111** (2019), no. 4 1109–1125.

- [117] W. Brabetz, S. Muller-Loennies, O. Holst, and H. Brade, *Deletion of the heptosyltransferase genes rfac and rfaf in escherichia coli k-12 results in an re-type lipopolysaccharide with a high degree of 2-aminoethanol phosphate substitution*, *European journal of biochemistry* **247** (1997), no. 2 716–724.
- [118] C. Parker, A. Kloser, C. Schnaitman, M. Stein, S. Gottesman, and B. Gibson, *Role of the rfag and rfap genes in determining the lipopolysaccharide core structure and cell surface properties of escherichia coli k-12.*, *Journal of Bacteriology* **174** (1992), no. 8 2525–2538.
- [119] S. Gronow, W. Brabetz, and H. Brade, *Comparative functional characterization in vitro of heptosyltransferase i (waac) and ii (waaf) from escherichia coli*, *European journal of biochemistry* **267** (2000), no. 22 6602–6611.
- [120] J. A. Yethon and C. Whitfield, *Purification and characterization of waap from escherichia coli, a lipopolysaccharide kinase essential for outer membrane stability*, *Journal of Biological Chemistry* **276** (2001), no. 8 5498–5504.
- [121] C. Pagnout, B. Sohm, A. Razafitianamaharavo, C. Caillet, M. Offroy, M. Leduc, H. Gendre, S. Jomini, A. Beaussart, P. Bauda, *et. al.*, *Pleiotropic effects of rfa-gene mutations on escherichia coli envelope properties*, *Scientific reports* **9** (2019), no. 1 1–16.
- [122] A. Ludwig, F. Garcia, S. Bauer, T. Jarchau, R. Benz, J. Hoppe, and W. Goebel, *Analysis of the in vivo activation of hemolysin (hlya) from escherichia coli.*, *Journal of bacteriology* **178** (1996), no. 18 5422–5430.
- [123] P. Stanley, L. C. Packman, V. Koronakis, and C. Hughes, *Fatty acylation of two internal lysine residues required for the toxic activity of escherichia coli hemolysin*, *Science* **266** (1994), no. 5193 1992–1996.
- [124] N. P. Greene, A. Crow, C. Hughes, and V. Koronakis, *Structure of a bacterial toxin-activating acyltransferase*, *Proceedings of the National Academy of Sciences* **112** (2015), no. 23 E3058–E3066.
- [125] T. Myers-Morales, A. E. Oates, M. S. Byrd, and E. C. Garcia, *Burkholderia cepacia complex contact-dependent growth inhibition systems mediate interbacterial competition*, *Journal of bacteriology* **201** (2019), no. 12 e00012–19.
- [126] S. Koskiniemi, F. Garza-Sánchez, N. Edman, S. Chaudhuri, S. J. Poole, C. Manoil, C. S. Hayes, and D. A. Low, *Genetic analysis of the cdi pathway from burkholderia pseudomallei 1026b*, *PLoS One* **10** (2015), no. 3.
- [127] A. Khondker, A. K. Dhaliwal, S. Saem, A. Mahmood, C. Fradin, J. Moran-Mirabal, and M. C. Rheinstädter, *Membrane charge and lipid packing*



- determine polymyxin-induced membrane damage, *Communications biology* **2** (2019), no. 1 1–11.
- [128] P. Viljanen and M. Vaara, *Susceptibility of gram-negative bacteria to polymyxin b nonapeptide.*, *Antimicrobial agents and chemotherapy* **25** (1984), no. 6 701–705.
- [129] I. Ofek, S. Cohen, R. Rahmani, K. Kabha, D. Tamarkin, Y. Herzig, and E. Rubinstein, *Antibacterial synergism of polymyxin b nonapeptide and hydrophobic antibiotics in experimental gram-negative infections in mice.*, *Antimicrobial agents and chemotherapy* **38** (1994), no. 2 374–377.
- [130] M. Vaara, J. Fox, G. Loidl, O. Siikanen, J. Apajalahti, F. Hansen, N. Frimodt-Møller, J. Nagai, M. Takano, and T. Vaara, *Novel polymyxin derivatives carrying only three positive charges are effective antibacterial agents*, *Antimicrobial agents and chemotherapy* **52** (2008), no. 9 3229–3236.
- [131] J. Fantini and N. Yahi, *Molecular basis for the glycosphingolipid-binding specificity of  $\alpha$ -synuclein: key role of tyrosine 39 in membrane insertion*, *Journal of molecular biology* **408** (2011), no. 4 654–669.
- [132] C. Xu, E. Gagnon, M. E. Call, J. R. Schnell, C. D. Schwieters, C. V. Carman, J. J. Chou, and K. W. Wucherpfennig, *Regulation of t cell receptor activation by dynamic membrane binding of the cd3 cytoplasmic tyrosine-based motif*, *Cell* **135** (2008), no. 4 702–713.
- [133] M. E. Bauer and R. A. Welch, *Association of rtx toxins with erythrocytes.*, *Infection and immunity* **64** (1996), no. 11 4665–4672.
- [134] M. Hackett, L. Guo, J. Shabanowitz, D. F. Hunt, and E. L. Hewlett, *Internal lysine palmitoylation in adenylate cyclase toxin from bordetella pertussis*, *Science* **266** (1994), no. 5184 433–435.
- [135] E. M. Barry, A. Weiss, I. Ehrmann, M. Gray, E. Hewlett, and M. Goodwin, *Bordetella pertussis adenylate cyclase toxin and hemolytic activities require a second gene, cyac, for activation.*, *Journal of Bacteriology* **173** (1991), no. 2 720–726.
- [136] N. Chevalier, M. Moser, H.-G. Koch, K.-L. Schimz, E. Willery, C. Loch, F. Jacob-Dubuisson, and M. Müller, *Membrane targeting of a bacterial virulence factor harbouring an extended signal peptide*, *Journal of molecular microbiology and biotechnology* **8** (2004), no. 1 7–18.
- [137] R. L. Szabady, J. H. Peterson, K. M. Skillman, and H. D. Bernstein, *An unusual signal peptide facilitates late steps in the biogenesis of a bacterial autotransporter*, *Proceedings of the National Academy of Sciences* **102** (2005), no. 1 221–226.

- [138] S. Datta, N. Costantino, and D. L. Court, *A set of recombinering plasmids for gram-negative bacteria*, *Gene* **379** (2006) 109–115.
- [139] T. Baba, T. Ara, M. Hasegawa, Y. Takai, Y. Okumura, M. Baba, K. A. Datsenko, M. Tomita, B. L. Wanner, and H. Mori, *Construction of escherichia coli k-12 in-frame, single-gene knockout mutants: the keio collection*, *Molecular systems biology* **2** (2006), no. 1 2006–0008.
- [140] K.-H. Choi, J. B. Gaynor, K. G. White, C. Lopez, C. M. Bosio, R. R. Karkhoff-Schweizer, and H. P. Schweizer, *A *tn* 7-based broad-range bacterial cloning and expression system*, *Nature methods* **2** (2005), no. 6 443–448.
- [141] S. L. Chiang and E. J. Rubin, *Construction of a mariner-based transposon for epitope-tagging and genomic targeting*, *Gene* **296** (2002), no. 1-2 179–185.
- [142] L. Ferrieres, G. Hémerly, T. Nham, A.-M. Guérout, D. Mazel, C. Beloin, and J.-M. Ghigo, *Silent mischief: bacteriophage *mu* insertions contaminate products of escherichia coli random mutagenesis performed using suicidal transposon delivery plasmids mobilized by broad-host-range *rp4* conjugative machinery*, *Journal of bacteriology* **192** (2010), no. 24 6418–6427.
- [143] F. Garza-Sánchez, B. D. Janssen, and C. S. Hayes, *Prolyl-trn<sup>apro</sup> in the a-site of secM-arrested ribosomes inhibits the recruitment of transfer-messenger rna*, *Journal of Biological Chemistry* **281** (2006), no. 45 34258–34268.
- [144] M. F. Feldman, C. L. Marolda, M. A. Monteiro, M. B. Perry, A. J. Parodi, and M. A. Valvano, *The activity of a putative polyisoprenol-linked sugar translocase (*wzx*) involved in escherichia coli o antigen assembly is independent of the chemical structure of the o repeat*, *Journal of Biological Chemistry* **274** (1999), no. 49 35129–35138.
- [145] H. Chen, Q. Fang, Q. Tu, C. Liu, J. Yin, Y. Yin, L. Xia, X. Bian, and Y. Zhang, *Identification of a contact-dependent growth inhibition system in the probiotic escherichia coli nissle 1917*, *FEMS microbiology letters* **365** (2018), no. 11 fny102.
- [146] A. Peschel and H.-G. Sahl, *The co-evolution of host cationic antimicrobial peptides and microbial resistance*, *Nature Reviews Microbiology* **4** (2006), no. 7 529–536.
- [147] M. M. Mwangi, S. W. Wu, Y. Zhou, K. Sieradzki, H. de Lencastre, P. Richardson, D. Bruce, E. Rubin, E. Myers, E. D. Siggia, *et. al.*, *Tracking the in vivo evolution of multidrug resistance in staphylococcus aureus by whole-genome sequencing*, *Proceedings of the National Academy of Sciences* **104** (2007), no. 22 9451–9456.
- [148] I. Lerouge and J. Vanderleyden, *O-antigen structural variation: mechanisms and possible roles in animal/plant–microbe interactions*, *FEMS microbiology reviews* **26** (2002), no. 1 17–47.

- [149] D. M. Post, L. Yu, B. C. Krasity, B. Choudhury, M. J. Mandel, C. A. Brennan, E. G. Ruby, M. J. McFall-Ngai, B. W. Gibson, and M. A. Apicella, *O-antigen and core carbohydrate of vibrio fischeri lipopolysaccharide composition and analysis of their role in euprymna scolopes light organ colonization*, *Journal of Biological Chemistry* **287** (2012), no. 11 8515–8530.
- [150] V. C. Burns, E. J. Pishko, A. Preston, D. J. Maskell, and E. T. Harvill, *Role of bordetella o antigen in respiratory tract infection*, *Infection and immunity* **71** (2003), no. 1 86–94.
- [151] C. Chaput, E. Spindler, R. T. Gill, and A. Zychlinsky, *O-antigen protects gram-negative bacteria from histone killing*, *PloS one* **8** (2013), no. 8.
- [152] J. A. Bengoechea, H. Najdenski, and M. Skurnik, *Lipopolysaccharide o antigen status of yersinia enterocolitica o: 8 is essential for virulence and absence of o antigen affects the expression of other yersinia virulence factors*, *Molecular microbiology* **52** (2004), no. 2 451–469.
- [153] P. Van der Ley, P. De Graaff, and J. Tommassen, *Shielding of escherichia coli outer membrane proteins as receptors for bacteriophages and colicins by o-antigenic chains of lipopolysaccharide.*, *Journal of bacteriology* **168** (1986), no. 1 449–451.
- [154] P. van der Ley, O. Kuipers, J. Tommassen, and B. Lugtenberg, *O-antigenic chains of lipopolysaccharide prevent binding of antibody molecules to an outer membrane pore protein in enterobacteriaceae*, *Microbial pathogenesis* **1** (1986), no. 1 43–49.
- [155] C. Sharp, C. Boinett, A. Cain, N. G. Housden, S. Kumar, K. Turner, J. Parkhill, and C. Kleanthous, *O-antigen-dependent colicin insensitivity of uropathogenic escherichia coli*, *Journal of bacteriology* **201** (2019), no. 4 e00545–18.
- [156] Y. Shifrin, A. Peleg, O. Ilan, C. Nadler, S. Kobi, K. Baruch, G. Yerushalmi, T. Berdichevsky, S. Altuvia, M. Elgrably-Weiss, *et. al.*, *Transient shielding of intimin and the type iii secretion system of enterohemorrhagic and enteropathogenic escherichia coli by a group 4 capsule*, *Journal of bacteriology* **190** (2008), no. 14 5063–5074.
- [157] E. C. Garcia, M. S. Anderson, J. A. Hagar, and P. A. Cotter, *B urkholderia bcpa mediates biofilm formation independently of interbacterial contact-dependent growth inhibition*, *Molecular microbiology* **89** (2013), no. 6 1213–1225.
- [158] M. S. Anderson, E. C. Garcia, and P. A. Cotter, *Kind discrimination and competitive exclusion mediated by contact-dependent growth inhibition systems shape biofilm community structure*, *PLoS pathogens* **10** (2014), no. 4.

- [159] J. P. Allen and A. R. Hauser, *Diversity of contact-dependent growth inhibition systems of pseudomonas aeruginosa*, 2019.
- [160] M. J. Bottery, I. Passaris, C. Dytham, A. J. Wood, and M. W. van der Woude, *Spatial organization of expanding bacterial colonies is affected by contact-dependent growth inhibition*, *Current Biology* **29** (2019), no. 21 3622–3634.
- [161] C. S. Hayes, S. Koskiniemi, Z. C. Ruhe, S. J. Poole, and D. A. Low, *Mechanisms and biological roles of contact-dependent growth inhibition systems*, *Cold Spring Harbor perspectives in medicine* **4** (2014), no. 2 a010025.
- [162] G. C. Gucinski, K. Michalska, F. Garza-Sánchez, W. H. Eschenfeldt, L. Stols, J. Y. Nguyen, C. W. Goulding, A. Joachimiak, and C. S. Hayes, *Convergent evolution of the barnase/endou/colicin/rele (becr) fold in antibacterial trnase toxins*, *Structure* **27** (2019), no. 11 1660–1674.
- [163] G. D. Ekberg, *Characterization of a Novel Nuclease Domain Delivered by the Contact Dependent Inhibition System of Yersinia kristensenii*. PhD thesis, University of California, Santa Barbara, 2020.
- [164] J. D. te Winkel, D. A. Gray, K. H. Seistrup, L. W. Hamoen, and H. Strahl, *Analysis of antimicrobial-triggered membrane depolarization using voltage sensitive dyes*, *Frontiers in cell and developmental biology* **4** (2016) 29.
- [165] S. Kurihara, Y. Tsuboi, S. Oda, H. G. Kim, H. Kumagai, and H. Suzuki, *The putrescine importer puup of escherichia coli k-12*, *Journal of bacteriology* **191** (2009), no. 8 2776–2782.
- [166] S.-S. Jiang, T.-Y. Lin, W.-B. Wang, M.-C. Liu, P.-R. Hsueh, and S.-J. Liaw, *Characterization of udp-glucose dehydrogenase and udp-glucose pyrophosphorylase mutants of proteus mirabilis: defectiveness in polymyxin b resistance, swarming, and virulence*, *Antimicrobial Agents and Chemotherapy* **54** (2010), no. 5 2000–2009.
- [167] S. Lacour, E. Bechet, A. J. Cozzone, I. Mijakovic, and C. Grangeasse, *Tyrosine phosphorylation of the udp-glucose dehydrogenase of escherichia coli is at the crossroads of colanic acid synthesis and polymyxin resistance*, *PLoS One* **3** (2008), no. 8 e3053.
- [168] D. Harder, J. Stolz, F. Casagrande, P. Obrdlik, D. Weitz, D. Fotiadis, and H. Daniel, *Dtpb (yhip) and dtpa (tppb, ydgr) are prototypical proton-dependent peptide transporters of escherichia coli*, *The FEBS journal* **275** (2008), no. 13 3290–3298.

- [169] Y. Ural-Blimke, A. Flayhan, J. Strauss, V. Rantos, K. Bartels, R. Nielsen, E. Pardon, J. Steyaert, J. Kosinski, E. M. Quistgaard, *et. al.*, *Structure of prototypic peptide transporter dtpa from e. coli in complex with valganciclovir provides insights into drug binding of human pept1*, *Journal of the American Chemical Society* **141** (2019), no. 6 2404–2412.
- [170] E. Malle, H. Zhou, J. Neuhold, B. Spitzenberger, F. Klepsch, T. Pollak, O. Bergner, G. F. Ecker, and P. C. Stolt-Bergner, *Random mutagenesis of the prokaryotic peptide transporter ydgr identifies potential periplasmic gating residues*, *Journal of Biological Chemistry* **286** (2011), no. 26 23121–23131.
- [171] S. Kurihara, Y. Sakai, H. Suzuki, A. Muth, O. Phanstiel, and P. N. Rather, *Putrescine importer plap contributes to swarming motility and urothelial cell invasion in proteus mirabilis*, *Journal of Biological Chemistry* **288** (2013), no. 22 15668–15676.
- [172] Z. Shi, Q. Wang, Y. Li, Z. Liang, X. L. HUI, J. Zhou, Z.-N. Cui, and L.-H. Zhang, *Putrescine is an intraspecies and interkingdom cell-cell communication signal modulating the virulence of dickeya zaeae*, *Frontiers in Microbiology* **10** (2019) 1950.
- [173] S. Kurihara, H. Suzuki, M. Oshida, and Y. Benno, *A novel putrescine importer required for type 1 pili-driven surface motility induced by extracellular putrescine in escherichia coli k-12*, *Journal of Biological Chemistry* **286** (2011), no. 12 10185–10192.
- [174] S. D. Zakharov, E. A. Kotova, Y. N. Antonenko, and W. A. Cramer, *On the role of lipid in colicin pore formation*, *Biochimica et Biophysica Acta (BBA)-Biomembranes* **1666** (2004), no. 1-2 239–249.
- [175] S. D. Zakharov, M. Lindeberg, and W. A. Cramer, *Kinetic description of structural changes linked to membrane import of the colicin e1 channel protein*, *Biochemistry* **38** (1999), no. 35 11325–11332.
- [176] M. S. McClain, H. Iwamoto, P. Cao, A. D. Vinion-Dubiel, Y. Li, G. Szabo, Z. Shao, and T. L. Cover, *Essential role of a gxxxg motif for membrane channel formation by helicobacter pylori vacuolating toxin*, *Journal of Biological Chemistry* **278** (2003), no. 14 12101–12108.
- [177] B. K. Mueller, S. Subramaniam, and A. Senes, *A frequent, gxxxg-mediated, transmembrane association motif is optimized for the formation of interhelical  $\alpha$ -h hydrogen bonds*, *Proceedings of the National Academy of Sciences* **111** (2014), no. 10 E888–E895.
- [178] X. Robert and P. Gouet, *Deciphering key features in protein structures with the new endscrip server*, *Nucleic acids research* **42** (2014), no. W1 W320–W324.

- [179] C. S. Hayes and R. T. Sauer, *Cleavage of the a site mrna codon during ribosome pausing provides a mechanism for translational quality control*, *Molecular cell* **12** (2003), no. 4 903–911.
- [180] P. P. Cherepanov and W. Wackernagel, *Gene disruption in escherichia coli: Tcr and kmr cassettes with the option of flp-catalyzed excision of the antibiotic-resistance determinant*, *Gene* **158** (1995), no. 1 9–14.
- [181] S. Mukherjee and B. L. Bassler, *Bacterial quorum sensing in complex and dynamically changing environments*, *Nature Reviews Microbiology* **17** (2019), no. 6 371–382.
- [182] J. Hacker and J. B. Kaper, *Pathogenicity islands and the evolution of microbes*, *Annual Reviews in Microbiology* **54** (2000), no. 1 641–679.
- [183] Z. C. Ruhe, L. Townsley, A. B. Wallace, A. King, M. W. Van der Woude, D. A. Low, F. H. Yildiz, and C. S. Hayes, *Cdia promotes receptor-independent intercellular adhesion*, *Molecular microbiology* **98** (2015), no. 1 175–192.
- [184] L. García-Bayona and L. E. Comstock, *Bacterial antagonism in host-associated microbial communities*, *Science* **361** (2018), no. 6408.
- [185] K. Lewis, *Persister cells*, *Annual review of microbiology* **64** (2010) 357–372.
- [186] A. Zampara, M. C. H. Sørensen, D. Grimon, F. Antenucci, A. R. Vitt, V. Bortolaia, Y. Briers, and L. Brøndsted, *Exploiting phage receptor binding proteins to enable endolysins to kill gram-negative bacteria*, *Scientific reports* **10** (2020), no. 1 1–12.
- [187] C. Forestier and R. A. Welch, *Nonreciprocal complementation of the hlyc and lktc genes of the escherichia coli hemolysin and pasteurella haemolytica leukotoxin determinants.*, *Infection and immunity* **58** (1990), no. 3 828–832.
- [188] M. H. Lenders, S. Weidtkamp-Peters, D. Kleinschrodt, K.-E. Jaeger, S. H. Smits, and L. Schmitt, *Directionality of substrate translocation of the hemolysin a type i secretion system*, *Scientific reports* **5** (2015) 12470.
- [189] M. Desvaux, A. Scott-Tucker, S. M. Turner, L. M. Cooper, D. Huber, J. P. Nataro, and I. R. Henderson, *A conserved extended signal peptide region directs posttranslational protein translocation via a novel mechanism*, *Microbiology* **153** (2007), no. 1 59–70.
- [190] J. L. Willett, Z. C. Ruhe, C. W. Goulding, D. A. Low, and C. S. Hayes, *Contact-dependent growth inhibition (cdi) and cdib/cdia two-partner secretion proteins*, *Journal of molecular biology* **427** (2015), no. 23 3754–3765.

- [191] S. J. Poole, E. J. Diner, S. K. Aoki, B. A. Braaten, C. t. de Roodenbeke, D. A. Low, and C. S. Hayes, *Identification of functional toxin/immunity genes linked to contact-dependent growth inhibition (cdi) and rearrangement hotspot (rhs) systems*, *PLoS genetics* **7** (2011), no. 8.
- [192] H. A. Ernst, A. Pham, H. Hald, J. S. Kastrup, M. Rahman, and O. Mirza, *Ligand binding analyses of the putative peptide transporter yjdl from e. coli display a significant selectivity towards dipeptides*, *Biochemical and biophysical research communications* **389** (2009), no. 1 112–116.
- [193] L. Song, M. R. Hobaugh, C. Shustak, S. Cheley, H. Bayley, and J. E. Gouaux, *Structure of staphylococcal  $\alpha$ -hemolysin, a heptameric transmembrane pore*, *Science* **274** (1996), no. 5294 1859–1865.
- [194] T. Eicher, M. A. Seeger, C. Anselmi, W. Zhou, L. Brandstätter, F. Verrey, K. Diederichs, J. D. Faraldo-Gómez, and K. M. Pos, *Coupling of remote alternating-access transport mechanisms for protons and substrates in the multidrug efflux pump acrb*, *Elife* **3** (2014) e03145.
- [195] F. Husain and H. Nikaido, *Substrate path in the acrb multidrug efflux pump of escherichia coli*, *Molecular microbiology* **78** (2010), no. 2 320–330.